

## ABSTRACT

Title of Document: THE ROLE OF INTRACELLULAR CALCIUM  
PERTURBATIONS IN MUSCLE DAMAGE AND  
DYSFUNCTION IN MOUSE MODELS OF MUSCULAR  
DYSTROPHY

Davi Augusto Garcia Mázala

Directed by: Assistant Professor, Eva R. Chin, Ph.D. Department of  
Kinesiology

Duchenne muscular dystrophy (DMD) is a neuromuscular disease caused by mutations in the dystrophin gene. DMD is clinically characterized by severe, progressive and irreversible loss of muscle function, in which most patients lose the ability to walk by their early teens and die by their early 20's. Impaired intracellular calcium ( $\text{Ca}^{2+}$ ) regulation and activation of cell degradation pathways have been proposed as key contributors to DMD disease progression. This dissertation research consists of three studies investigating the role of intracellular  $\text{Ca}^{2+}$  in skeletal muscle dysfunction in different mouse models of DMD. Study one evaluated the role of  $\text{Ca}^{2+}$ -activated enzymes (proteases) that activate protein degradation in excitation-contraction (E-C) coupling failure following repeated contractions in *mdx* and dystrophin-utrophin null (*mdx/utr<sup>-/-</sup>*) mice. Single muscle fibers from *mdx/utr<sup>-/-</sup>* mice had greater E-C coupling failure following

repeated contractions compared to fibers from *mdx* mice. Moreover, protease inhibition during these contractions was sufficient to attenuate E-C coupling failure in muscle fibers from both *mdx* and *mdx/utr<sup>-/-</sup>* mice. Study two evaluated the effects of overexpressing the Ca<sup>2+</sup> buffering protein sarcoplasmic/endoplasmic reticulum Ca<sup>2+</sup>-ATPase 1 (SERCA1) in skeletal muscles from *mdx* and *mdx/utr<sup>-/-</sup>* mice. Overall, SERCA1 overexpression decreased muscle damage and protected the muscle from contraction-induced injury in *mdx* and *mdx/utr<sup>-/-</sup>* mice. In study three, the cellular mechanisms underlying the beneficial effects of SERCA1 overexpression in *mdx* and *mdx/utr<sup>-/-</sup>* mice were investigated. SERCA1 overexpression attenuated calpain activation in *mdx* muscle only, while partially attenuating the degradation of the calpain target desmin in *mdx/utr<sup>-/-</sup>* mice. Additionally, SERCA1 overexpression decreased the SERCA-inhibitory protein sarcolipin in *mdx* muscle but did not alter levels of Ca<sup>2+</sup> regulatory proteins (parvalbumin and calsequestrin) in either dystrophic model. Lastly, SERCA1 overexpression blunted the increase in endoplasmic reticulum stress markers Grp78/BiP in *mdx* mice and C/EBP homologous protein (CHOP) in *mdx* and *mdx/utr<sup>-/-</sup>* mice. Overall, findings from the studies presented in this dissertation provide new insight into the role of Ca<sup>2+</sup> in muscle dysfunction and damage in different dystrophic mouse models. Further, these findings support the overall strategy for improving intracellular Ca<sup>2+</sup> control for the development of novel therapies for DMD.

THE ROLE OF INTRACELLULAR CALCIUM PERTURBATIONS IN MUSCLE  
DAMAGE AND DYSFUNCTION IN MOUSE MODELS OF MUSCULAR  
DYSTROPHY

By

Davi Augusto Garcia Mázala

Dissertation submitted to the Faculty of the Graduate School of the  
University of Maryland, College Park in partial fulfillment  
of the requirements for the degree of  
Doctor of Philosophy

2016

Advisory Committee:

Assistant Professor Eva R. Chin, Ph.D., Chair

Professor James M. Hagberg, Ph.D.

Professor Stephen Roth, Ph.D.

Associate Professor Robert W. Grange, Ph.D.

Professor Norma W. Andrews, Ph. D. (Dean's Representative)

© Copyright by  
Davi Augusto Garcia Mázala  
2016

## **Dedication**

I dedicate this work to all individuals affected by neuromuscular diseases, especially to those affected by Duchenne Muscular Dystrophy and their families.

## Acknowledgements

Being here today is due to the support and encouragement of many individuals, including family members, friends, teachers, neighbors, coaches, and many other individuals, so I apologize for not including all the names that should have been included in this section.

I would like to first thank my parents, Carlos Roberto Mázala and Elisabete Victor Garcia Mázala, for all the support during the past years. I couldn't have asked for better parents, and I'm grateful every day for having you both in my life. The values I learned from you, such as hard work, diligence, commitment, and perseverance were key in helping me achieve my goals. Also, the moral, financial, and overall support from both of you have greatly helped me to get to this point in my life. Thank you for your patience in moments that I had to work during vacations, holidays, birthdays, and other occasions. I love you both a lot.

I would also like to thank my amazing fiancé/future wife Molly Evans, for all the support and for understanding the hectic life of a graduate student. You have been there for me any time I needed you, and I'm forever thankful for your support. Your encouragement, positive attitude, and patience during the last few years were critical for me to get here today. You are my rock, and I love you very much! I would also like to thank the Evans family (Gerry, Kathy, Hayley, Michael, Jesse, and Shannon) for your support and encouragement, as well as for providing me a place that feels like home away from home.

I would also like to thank my advisor, Dr. Eva Chin, for all the support, mentoring, guidance, patience, and friendship. You have been a role model for me in so many aspects

that I feel like I have learned enough for a lifetime during the past 6 years. I would also like my committee members, Dr. James Hagberg, Dr. Stephen Roth, Dr. Robert Grange, and Dr. Norma Andrews for taking the time to provide insightful feedback on my research and future career. Also, to previous committee members, Dr. Espen Spangenburg and Dr. Richard Lovering, who have also contributed to my education and research. Additionally, to all faculty/staff who have been there for me during these past years (in special to Dr. Marcio Oliveira, Dr. Jane Clark, and Dr. Coke Farmer – you all have a special place in my heart).

A very special thanks to all current and previous KNES graduate students. You guys were/are amazing, and without you this experience would have been much harder! Special thanks to Dr. Dapeng Chen, for your mentoring, patience, and friendship; I really appreciate your help during the past years! Also, thanks to Du Yue, Dr. Rian Landers-Ramos, Andrew Venezia, Harry Li, Sam English, Alicia DeRusso, Adam, Drew, Fonzo, Farzie, Lauren, Stef, Shawn, and many others. To my little KNES familia, including Regina Clary, Jessica Duque, and Bianca Garcia (thank you for all your patience and for being there for me!).

## Tables of Contents

Dedication.....	ii
Acknowledgements.....	iii
List of Tables.....	vii
List of Figures.....	viii
Chapter 1: Introduction and Specific Aims.....	1
Background.....	1
Specific Aim 1.....	3
Specific Aim 2.....	5
Specific Aim 3.....	6
Specific Aim 4.....	9
Specific Aim 5.....	13
Chapter 2: Review of Literature.....	16
Skeletal muscle.....	16
Overview of skeletal muscle development and mature skeletal muscle components.....	16
Skeletal muscle contraction (E-C coupling).....	19
Sarcoplasmic/endoplasmic reticulum Ca <sup>2+</sup> -ATPases (SERCAs).....	20
Duchenne muscular dystrophy.....	21
DMD disease characteristics.....	21
Dystrophin glycoprotein complex.....	24
Dystrophin gene structure and mutations.....	28
Mouse models for DMD.....	31
Intracellular calcium handling in dystrophic muscles.....	34
Resting intracellular Ca <sup>2+</sup> and E-C coupling in DMD.....	34
Alterations in calcium handling proteins in DMD.....	37
Stretch and store operated Ca <sup>2+</sup> entry in dystrophic muscles.....	40
Background and structure of skeletal muscle calpains.....	42
Functional role, activity, and substrates of calpain-1.....	43
Functional role, activity, and substrates of calpain-3.....	45
Evidence of increased calpain activity in DMD.....	46
Oxidative stress.....	48
Evidence of increased oxidative stress in DMD.....	49
Sources of ROS in DMD: mitochondria, monoamine oxidases, and NADPH oxidases.....	51
Endoplasmic reticulum stress.....	52
Grp78/BiP.....	54
CHOP.....	55
Evidence of ER stress in DMD.....	55
Chapter 3: The role of proteases in excitation-contraction coupling failure in muscular dystrophy.....	57
Abstract.....	59
Introduction.....	61
Methods.....	64



Results.....	70
Discussion.....	73
Chapter 4: SERCA1 overexpression minimizes skeletal muscle damage in dystrophic mouse models.....	87
Abstract.....	89
Introduction.....	91
Methods.....	94
Results.....	102
Discussion.....	108
Chapter 5: Investigating the mechanism of reduced muscle damage with SERCA1 overexpression in mouse models of Duchenne muscular dystrophy.....	125
Abstract.....	127
Introduction.....	128
Methods.....	132
Results.....	137
Discussion.....	143
Chapter 6: Summary and Future Directions.....	165
Literature cited.....	173
Appendices.....	195

## List of Tables

Table 2.1.....	30
Table 2.2.....	33
Table 3.1.....	81
Table 3.2.....	82
Table 3.3.....	83
Table 4.1.....	118

## List of Figures

Figure 2.1.....	17
Figure 2.2.....	18
Figure 2.3.....	19
Figure 2.4.....	24
Figure 2.5.....	25
Figure 2.6.....	29
Figure 2.7.....	43
Figure 3.1.....	84
Figure 3.2.....	85
Figure 3.3.....	86
Figure 4.1.....	119
Figure 4.2.....	120
Figure 4.3.....	121
Figure 4.4.....	122
Figure 4.5.....	123
Figure 4.6.....	124
Figure 5.1.....	158
Figure 5.2.....	159
Figure 5.3.....	160
Figure 5.4.....	161
Figure 5.5.....	162
Figure 5.6.....	163
Figure 5.7.....	164
Figure 6.1.....	171

## Chapter 1: Background and Specific Aims

### Background

Duchenne muscular dystrophy (DMD) is a neuromuscular disease that was first described over a century ago (37). DMD is an X-linked disease caused by mutations in the dystrophin gene, and affects 1 in 3600 - 6000 males at birth (53, 62, 63). Overall, patients with DMD have progressive muscle weakness and degeneration, with a loss of 75% of muscle mass by the age of 10 (204). The repetitive cycles of degeneration/regeneration induces the exhaustion of muscular regenerative capacity, thus leading to substitution of muscle fibers by connective and adipose tissue (93). Consequently, DMD patients become wheelchair bound by the age of 11, and die in their early to mid-twenties due to respiratory and/or cardiac failure (62).

Although the cause of DMD has been known for almost 30 years, the mechanisms responsible for increased muscle damage and limited repair remain unclear. Different theories have been proposed in an attempt to explain the cellular events leading to the continuous muscle degeneration in dystrophic muscles. While the mechanical instability theory proposes that the lack of dystrophin leads to mechanical muscle weakness which leads to increased susceptibility of muscle damage during eccentric muscle contractions, the cell signaling alteration theory suggests that secondary events that take place due to the lack of dystrophin are key factors leading to the increased muscle damage in DMD (117). More specifically, the presence of increased inflammation, oxidative stress, and calcium ( $\text{Ca}^{2+}$ ) dysregulation have been shown to play a key role in the disease pathophysiology (170, 287, 342).

Intracellular  $\text{Ca}^{2+}$  dysregulation and further activation of cell degradative pathways has been proposed as a key contributor to DMD disease progression. Overall, intracellular  $\text{Ca}^{2+}$  ions are involved in the regulation of a variety of cellular processes, such as excitation-contraction (E-C) coupling (i.e., muscle contraction) and the activation of different intracellular mechanisms (e.g., cell death), thus having a direct role in controlling the expression on a wide range of cellular processes in both health and disease (30). Over 30 years ago, Bodensteiner & Engel demonstrated that muscle biopsies from DMD patients have increased  $\text{Ca}^{2+}$  accumulation in pre-necrotic fibers (43). Subsequently, many different investigations demonstrated that dystrophic cells (e.g., muscle fibers and myotubes) have elevated intracellular  $\text{Ca}^{2+}$  levels and abnormal  $\text{Ca}^{2+}$  regulation (170, 172, 239, 255). More recently,  $\text{Ca}^{2+}$  dysregulation, per se, was shown to be sufficient to induce changes in muscles that mimic the dystrophic phenotype (236).

Since its discovery, the *mdx* mouse model has been used in the majority of studies investigating underlying mechanisms (134, 374) and potential treatments (92, 305) for DMD. However, *mdx* mice only show a mild disease progression compared with DMD patients. The milder phenotype from *mdx* mice is also due, at least in part, to overexpression of utrophin (*utr*), a protein with a similar role as dystrophin in muscles (357). In an attempt to aggravate the pathophysiology of the *mdx* mouse model, *utr* null mice were crossed with *mdx* mice to generate the double KO mouse model (*mdx/utr<sup>-/-</sup>*) (95). In contrast from the *mdx* mouse, the *mdx/utr<sup>-/-</sup>* model has altered neuromuscular and myotendinous junctions, early onset of damage in the diaphragm (as early as 6 days after birth), joint contractures, kyphosis, and premature death between 4 to 20 weeks (95, 366). To our knowledge, one clinical case of a boy missing both dystrophin and *utr* has been

reported to date (76). The patient had early onset DMD and died at the age of 15 due to acute intestinal occlusion and bleeding, respiratory failure, and cardiac arrhythmia (76).

*The overall purpose of this dissertation is to evaluate the role of intracellular Ca<sup>2+</sup> in the disease progression of the mdx/utr<sup>-/-</sup> mouse model. More specifically, we sought to evaluate the role of intracellular Ca<sup>2+</sup> dysregulations in muscle function, damage, and overall phenotype of the mdx/utr<sup>-/-</sup> mouse model.* Overall, findings presented in this dissertation further support the view of Ca<sup>2+</sup> as a key contributor to the dystrophic phenotype, and that therapeutic strategies targeting intracellular Ca<sup>2+</sup> control could be beneficial for DMD patients.

**Specific aim #1:** The purpose of this aim was twofold: 1) to determine if prolonged E-C coupling failure following repeated contractions was greater in mice lacking both dystrophin and utr (*mdx/utr<sup>-/-</sup>*) compared with mice only lacking dystrophin (*mdx*); and 2) to assess whether protease inhibition would prevent E-C coupling failure following repeated tetani in different dystrophic mouse models (255).

*Hypothesis 1.1:* The disruption of E-C coupling following repeated contractions is greater in single muscle fibers from *mdx/utr<sup>-/-</sup>* compared with single muscle fibers from *mdx* mice.

*Hypothesis 1.2:* protease inhibition during repeated contractions attenuates the prolonged decrease in E-C coupling failure in single muscle fibers from different dystrophic mouse models.

In brief, to test our hypotheses, single muscle fibers from the flexor digitorum brevis (FDB) muscle were stimulated across different frequencies (10, 30, 50, 70, 100, 120, and 150Hz) to assess peak Fura-2 ratios as an indirect measurement of free intracellular

Ca<sup>2+</sup> levels. After resting for 10 min, single muscle fibers were subsequently exposed to repeated contractions while perfused in solution either containing a pan-protease inhibitor [*N*-acetyl-L-leucyl-L-leucyl-L-norleucinal (ALLN) - 1μM] or vehicle (ethanol - 1μM). Peak Fura-2 ratios were reassessed one hour post repeated contractions at the same stimulation frequencies to evaluate any deficits in E-C coupling.

Our findings demonstrated that resting Fura-2 ratios were higher in single muscle fibers from *mdx*, *mdx/utr<sup>+/-</sup>*, and *mdx/utr<sup>-/-</sup>* compared with WT fibers (255). We found no differences in peak Fura-2 ratios in response to electrical stimulation between dystrophic compared with WT fibers (255). One hour after repeated tetani, 73% of fibers from *mdx/utr<sup>-/-</sup>* mice were either unable to respond to stimuli or demonstrated abnormal Fura-2 transients (255). While there were fibers from both *mdx* and *mdx/utr<sup>+/-</sup>* mice that either failed to maintain the peak Fura-2 ratios or did not respond to stimuli after the repeated tetani, the percent failing fibers was highest for *mdx/utr<sup>-/-</sup>* mice (255). This finding suggests that *mdx/utr<sup>-/-</sup>* muscle fibers have greater E-C uncoupling following repeated contractions, which supports our initial hypothesis. Muscle fibers from all three dystrophic groups demonstrated deficits in peak Fura-2 ratios one hour post-repeated contractions, which did not occur in WT fibers (255). Thus, deficits in peak Fura-2 ratio one hour post-repeated contractions in all three dystrophic groups demonstrates that dystrophic fibers have greater E-C coupling failure after repeated contractions. Furthermore, the greater incidence of E-C coupling failure in dystrophic fibers appeared to be due to protease activation because such decrease was mitigated in the presence of ALLN (255). These findings support our hypothesis that protease inhibition during repeated contractions would attenuate the prolonged decrease in E-C coupling failure in different dystrophic animal models (255).

**Specific aim #2:** to assess the effects of SERCA1 overexpression in decreasing muscle damage and rescuing defects in muscle function in the *mdx/utr<sup>-/-</sup>* mouse model of DMD (256).

*Hypothesis 2.1:* *mdx/utr<sup>-/-</sup>* mice overexpressing SERCA1 (*mdx/utr<sup>-/-</sup>/+SERCA1*) would have less muscle damage (i.e., centrally nucleated fibers, necrosis, and serum creatine kinase levels) compared with *mdx/utr<sup>-/-</sup>* mice.

*Hypothesis 2.2:* *mdx/utr<sup>-/-</sup>* mice overexpressing SERCA1 (*mdx/utr<sup>-/-</sup>/+SERCA1*) would have improved muscle function in response to repetitive eccentric contractions compared with *mdx/utr<sup>-/-</sup>* mice.

In this study, we used two sub-sets of mice to evaluate the effects of SERCA1 overexpression on body and muscle mass, protein expression, SR-Ca<sup>2+</sup> ATPase activity, intracellular Ca<sup>2+</sup> levels in single muscle fibers, quadriceps muscle function, and markers of muscle damage (256). Overall, we hypothesized that *mdx/utr<sup>-/-</sup>/+SERCA1* would have decreased muscle damage and improved muscle function compared with *mdx/utr<sup>-/-</sup>* mice.

Overall, our data showed that overexpression of SERCA1 in skeletal muscles of dystrophic mice led to a 2 to 3-fold increase in SR-Ca<sup>2+</sup> ATPase activity and this increase was sufficient to: 1) alter body and muscle mass to more closely resemble that of healthy animals; 2) decrease markers of muscle damage; and 3) protect the muscle from contraction-induced injury (256). Thus, our findings partially support our initial hypothesis since SERCA1 overexpression decreased muscle damage, but did not rescue the deficit in muscle function in the *mdx/utr<sup>-/-</sup>* mouse model of DMD. Nevertheless, SERCA1 overexpression in *mdx/utr<sup>-/-</sup>* mice protected the muscle from contraction-induced



injury. We hypothesize that this is due to the increased capacity of SERCA1 to remove cytosolic  $\text{Ca}^{2+}$  following influx with eccentric contractions. This is the first report to demonstrate that this approach can mitigate the disease phenotype in the *mdx/utr<sup>-/-</sup>* mouse, a model with a more similar disease progression to that of DMD patients than the *mdx* mouse. These data support the notion that increased SERCA1 expression, or activity, could have therapeutic utility in DMD.

**Specific aim #3:** the purpose of this study was to evaluate the effects of SERCA1 overexpression in the activation of  $\text{Ca}^{2+}$ -activated proteases (i.e., calpains) in gastrocnemius muscles from *mdx* and *mdx/utr<sup>-/-</sup>* mice.

Hypothesis 3.1: gastrocnemius muscles from *mdx/+SERCA1* mice have lower levels of autolyzed calpain-1 compared with muscles from *mdx* mice. Also, gastrocnemius muscles from *mdx/utr<sup>-/-</sup>+SERCA1* have lower levels of autolyzed calpain-1 compared with gastrocnemius muscles from *mdx/utr<sup>-/-</sup>* mice.

Hypothesis 3.2: gastrocnemius muscles from *mdx/+SERCA1* mice have lower levels of calpain enzymatic activity compared with gastrocnemius muscles from *mdx* mice. Also, gastrocnemius muscles from *mdx/utr<sup>-/-</sup>+SERCA1* have lower levels of calpain enzymatic activity compared with gastrocnemius muscles from *mdx/utr<sup>-/-</sup>* mice.

Calpains are  $\text{Ca}^{2+}$ -dependent cysteine proteinases that, when activated, perform the proteolysis or breakdown of proteins. Although the extent of calpain activity is not fully understood, calpains participate in a variety of cellular processes including different signal transduction pathways, remodeling of cytoskeletal/membrane attachments, and apoptosis

(142). Over 14 types of calpains have been identified, and skeletal muscle contains calpain-1, calpain-2, and the muscle specific calpain-3. Calpain-1, also known as  $\mu$ -calpain, and calpain-2, also known as m-calpain, received their names based on the amount of  $\text{Ca}^{2+}$  necessary for their activation (142). Calpain-3, on the other hand, requires much lower levels of  $\text{Ca}^{2+}$  for activation and is much less stable compared with calpain-1 and -2 (115). Numerous studies have demonstrated that calpain activity is increased in different dystrophic mouse models (8, 134, 255) as well as muscle samples from DMD patients (185, 290). Furthermore, studies evaluating the effectiveness of calpain inhibitors in the *mdx* mouse model in vivo might appear controversial, but overall they provide proof of concept for calpain inhibition attenuating muscle damage and improving muscle function (8, 19, 52, 321). We hypothesize that SERCA1 overexpression in both *mdx* and *mdx/utr<sup>-/-</sup>* mice increased intracellular  $\text{Ca}^{2+}$  buffering capacity, thus decreasing the activation of calpains.

Hypothesis 3.3: SERCA1 overexpression will attenuate the degradation of downstream protein targets of calpains in diaphragm muscles from *mdx* and *mdx/utr<sup>-/-</sup>* mice.

Hypothesis 3.3.1: diaphragm muscles from *mdx/+SERCA1* mice have higher levels of full-length junctophilin-1 (JP1) compared with diaphragm muscles from *mdx* mice. Also, diaphragm muscles from *mdx/utr<sup>-/-</sup>+SERCA1* have higher levels of full-length JP1 compared with diaphragm muscles from *mdx/utr<sup>-/-</sup>* mice.

Exploratory hypothesis 3.3.2: diaphragm muscles from *mdx/+SERCA1* mice have higher levels of full-length desmin compared with diaphragm muscles from *mdx* mice. Also, diaphragm muscles from *mdx/utr<sup>-/-</sup>+SERCA1* have higher levels of full-length desmin compared with diaphragm muscles from *mdx/utr<sup>-/-</sup>* mice.

Skeletal muscle calpains are known to proteolyse multiple sarcomeric and cytoskeletal proteins (e.g., desmin) as well as proteins responsible for maintaining proper triad junction structure [e.g., junctophilin-1 (JP1)] (249, 349, 380). Desmin is a 53 kDa protein located at the periphery of the Z-disk of skeletal muscles that plays a critical role in maintaining the integrity of the muscle's contractile apparatus (268). It has been previously shown that muscle sections from DMD patients have decreased desmin staining, which suggests increased breakdown of the protein (88). JP1 is a 90 kDa protein localized at the triad junction of skeletal muscles which interacts with the dihydropyridine receptor (an L-type calcium channel) and inserts into the SR membrane through a transmembrane region in their C-terminus (140, 273, 332). Recent evidence demonstrates that JP1 undergoes marked proteolysis in the diaphragm muscle of *mdx* mice, and that this correlates with increased autolysis of calpain-1 (249).

In summary, the presence of increased calpain activity with concomitant breakdown of desmin and JP1 in dystrophic muscles suggests that  $\text{Ca}^{2+}$  is a key player in activating this detrimental mechanism. Therefore, we hypothesize that our reported reduction in muscle damage and protection from contraction-induced injury in *mdx* and *mdx/utr<sup>-/-</sup>* mice by SERCA1 overexpression was due, at least in part, to decreased activation of calpains, thus leading to attenuation in the breakdown of desmin and JP1.

**Specific aim #4:** the purpose of this study was to evaluate the effects of SERCA1 overexpression on markers of protein oxidation (carbonyl formation) and ER stress in skeletal muscles from *mdx* and *mdx/utr<sup>-/-</sup>* mice.

Hypothesis 4.1: gastrocnemius muscles from *mdx*/+SERCA1 mice have lower levels of protein carbonyls compared with gastrocnemius muscles from *mdx* mice. Also, gastrocnemius muscles from *mdx*/utr<sup>-/+</sup>SERCA1 have lower levels of protein carbonyls compared with gastrocnemius muscles from *mdx*/utr<sup>-/-</sup> mice.

Reactive oxygen species (ROS) are generally defined as molecules or ions formed by the incomplete reduction of oxygen (125). Generally, ROS include free radicals (e.g., superoxide and hydroxyl radical) as well as non-radical species (e.g., hydrogen peroxide) (125). Under normal physiological conditions cells maintain homeostasis by keeping the balance between the production and scavenging of ROS. However, when ROS scavenging is incomplete, oxidative stress takes place leading to the damage of cellular components such as proteins, lipids, and nucleic acids, which can culminate in cell death (125). Elevation in markers of oxidative stress has been reported in samples from both DMD patients (160, 298) as well as *mdx* mice (159, 182, 286). Protein carbonyl levels were found markedly higher in muscle samples from DMD patients compared with control subjects (160). Rodriguez *et al.* (298) reported higher levels of 8-hydroxy-2'-deoxyguanosine, a marker of oxidative damage to DNA, in urine samples from DMD patients compared with healthy controls. Skeletal muscles from *mdx* mice have increased lipid peroxidation and higher values for oxidoreductase of nicotinamide adenine dinucleotide (NADH) O<sub>2</sub> and cytochrome C compared with skeletal muscles from control mice (159, 286). Furthermore, free radical-mediated injury is thought to contribute to DMD pathogenesis since oxidative stress has been shown to be increased in the stages preceding the onset of muscle death in *mdx* mice (97). In summary, findings from the

studies listed above support the idea that that oxidative stress could play a vital role in the pathogenesis of DMD.

Mitochondrial  $\text{Ca}^{2+}$  overload is one of the proposed mechanisms contributing to increases in oxidative stress in dystrophic muscles. Mitochondria is a major organelle for  $\text{Ca}^{2+}$  buffering which helps to maintain cellular homeostasis (125). Under normal physiological conditions,  $\text{Ca}^{2+}$  can stimulate oxidative phosphorylation and adenosine triphosphate synthesis, thus being beneficial for mitochondrial function (125). However, in pathological conditions, greater amounts of  $\text{Ca}^{2+}$  might be taken up by mitochondria, thus leading to detrimental effects to cell function (125). Theoretically,  $\text{Ca}^{2+}$  might increase mitochondrial ROS production by the following mechanisms: 1) stimulation of tricarboxylic acid cycle and oxidative phosphorylation; 2) stimulation of nitric oxide synthase and subsequent nitric oxide production; 3) induction of the dissociation of cytochrome c from the inner mitochondrial cardiolipin, which can lead to mitochondrial permeability transition pore opening and cytochrome c release into the cytoplasm (54). Findings from Millay and colleagues demonstrated that dystrophic mitochondria are major recipients of the greater  $\text{Ca}^{2+}$  influx through the cell membrane (237). Moreover, this greater  $\text{Ca}^{2+}$  uptake by dystrophic mitochondria leads to mitochondrial permeability transition pore opening and cytochrome c release from mitochondria, which can effectively block the respiratory chain at complex III and enhance mitochondrial ROS generation (54, 151). We hypothesized that the beneficial effects of SERCA1 overexpression in both *mdx* and *mdx/utr<sup>-/-</sup>* mice was also due to a decrease in oxidative stress. More specifically, we hypothesized that the greater  $\text{Ca}^{2+}$  buffering capacity by SERCA1 in muscles from *mdx/+SERCA1* and *mdx/utr<sup>-/-</sup>/+SERCA1* mice potentially attenuated mitochondrial  $\text{Ca}^{2+}$

overload, and subsequently decreased mitochondrial ROS production, oxidative stress, and formation of protein carbonyls.

Hypothesis 4.2: diaphragm muscles from *mdx/+SERCA1* mice have lower levels of Grp78/BIP compared with diaphragm muscles from *mdx* mice. Also, diaphragm muscles from *mdx/utr<sup>-/-</sup>+SERCA1* have lower levels of Grp78/BIP compared with diaphragm muscles from *mdx/utr<sup>-/-</sup>* mice.

Hypothesis 4.3: diaphragm muscles from *mdx/+SERCA1* mice have lower levels of C/EBP homologous protein (CHOP) compared with diaphragm muscles from *mdx* mice. Also, diaphragm muscles from *mdx/utr<sup>-/-</sup>+SERCA1* have lower levels of CHOP compared with diaphragm muscles from *mdx/utr<sup>-/-</sup>* mice.

In order for properly synthesize and fold proteins, the ER requires high levels of  $\text{Ca}^{2+}$  and an appropriate redox balance (55, 202). The ER is a highly developed organelle responsible for several cellular processes, such as preserving intracellular  $\text{Ca}^{2+}$  homeostasis and protein synthesis (372). Thus,  $\text{Ca}^{2+}$  deficits and oxidative stress in the ER lumen can result in accumulation of a large quantity of misfolded and/or unfolded proteins in the ER, which is known to trigger ER stress (184). Moreover, proper  $\text{Ca}^{2+}$  uptake from the cytosol into the ER is critical for optimal function of the protein synthesis and folding machinery in cardiac muscle cells (202). ER stress occurs in most cells and is a natural mechanism for maintaining proper protein folding under cell stress conditions to maintain cell homeostasis (372). However, ER stress is detrimental to cells in instances where

prolonged cellular stress occurs, which ultimately leads to the activation of the ER stress-specific cell death pathway (372).

Grp78/BiP and CHOP are two proteins commonly upregulated in the presence of ER stress. Grp78/BiP is a member of the 70 kDa heat shock protein (Hsp70) family with ATP binding sequences that interacts with unfolded proteins (164). After post-translational modifications, newly synthesized proteins experience further folding in the ER lumen with the assistance of ER chaperones such as Grp78/BiP (164). CHOP, a member of the C/EBP family of proteins, is a specific ER stress-induced apoptotic mediator (372). Findings from a recent study demonstrated that both Grp78/BiP and CHOP are upregulated in dystrophic muscles. More specifically, Grp78/BiP protein levels were 2- to 40-fold higher in samples from DMD patients compared with healthy controls (242). Additionally, Grp78/BiP protein levels was found to be increased in the TA, EDL, and diaphragm muscles of *mdx* compared with WT mice, while the levels of CHOP were increased in the TA muscles of *mdx* vs. WT mice (242). Overall, these findings suggest that ER stress potentially contributes to DMD disease pathophysiology.

We propose that SERCA1 overexpression in *mdx* and *mdx/utr<sup>-/-</sup>* mice might have attenuated ER stress, thus inducing alterations in the expression of Grp78/BiP and CHOP. More specifically, we propose that the improved ability to cope with abnormal intracellular Ca<sup>2+</sup> levels in muscles from *mdx/+SERCA1* and *mdx/utr<sup>-/-</sup>/+SERCA1* potentially attenuated ER stress, thus leading to decreases in cell death.

**Specific aim #5:** to evaluate the effects of SERCA1 overexpression on the levels of SERCA-regulatory and other  $\text{Ca}^{2+}$  handling proteins in diaphragm muscles from *mdx* and *mdx/utr<sup>-/-</sup>* mice.

Hypothesis 5.1: diaphragm muscles from *mdx/+SERCA1* mice have lower levels of sarcolipin (SLN), a SERCA inhibitory protein, compared with diaphragm muscles from *mdx* mice. Also, diaphragm muscles from *mdx/utr<sup>-/-</sup>+SERCA1* have lower levels of SLN compared with diaphragm muscles from *mdx/utr<sup>-/-</sup>* mice.

Hypothesis 5.2: diaphragm muscles from *mdx/+SERCA1* mice have lower levels of phospholamban (PLN), a SERCA inhibitory protein, compared with diaphragm muscles from *mdx* mice. Also, diaphragm muscles from *mdx/utr<sup>-/-</sup>+SERCA1* have lower levels of PLN compared with diaphragm muscles from *mdx/utr<sup>-/-</sup>* mice.

Hypothesis 5.3: diaphragm muscles from *mdx/+SERCA1* mice have higher levels of the  $\text{Ca}^{2+}$  buffering protein parvalbumin (PV) compared with diaphragm muscles from *mdx* mice. Also, diaphragm muscles from *mdx/utr<sup>-/-</sup>+SERCA1* have higher levels of PV compared with diaphragm muscles from *mdx/utr<sup>-/-</sup>* mice.

Hypothesis 5.4: diaphragm muscles from *mdx/+SERCA1* mice have higher levels of the  $\text{Ca}^{2+}$ -binding protein calsequestrin compared with diaphragm muscles from *mdx* mice. Also, diaphragm muscles from *mdx/utr<sup>-/-</sup>+SERCA1* have higher levels of calsequestrin compared with diaphragm muscles from *mdx/utr<sup>-/-</sup>* mice.

The regulation of intracellular  $\text{Ca}^{2+}$  homeostasis relies on 1) the activity of  $\text{Ca}^{2+}$ -ATPases, such as the plasma membrane  $\text{Ca}^{2+}$ -ATPase, the  $\text{Na}^+/\text{Ca}^{2+}$  exchanger, or the sarco(endo)plasmic reticulum pumps (SERCA1 and SERCA2a), and 2) on a large array of



Ca<sup>2+</sup> binding proteins, including troponin and PV (225). Additionally, other proteins like SLN and PLN, which inhibit SERCA activity by lowering the apparent Ca<sup>2+</sup> affinity of the pump, also play a role in intracellular Ca<sup>2+</sup> homeostasis (348). Studies have shown that dystrophic muscles have altered levels of Ca<sup>2+</sup> handling proteins (89, 261, 262, 304, 306). Most of the Ca<sup>2+</sup> located within the SR is bound to calsequestrin, and studies have reported inconsistent results regarding calsequestrin levels in muscles from dystrophic mice. While one study reported lower levels of calsequestrin-like proteins in muscles from *mdx* compared with control mice (89), others reported higher levels of calsequestrin in muscles from *mdx* and *mdx/utr*<sup>-/-</sup> compared with controls (306). Nevertheless, only the quadriceps muscle from *mdx* and *mdx/utr*<sup>-/-</sup> had higher levels of calsequestrin compared with controls, while no differences were found in soleus and diaphragm (306). The rate of muscle relaxation in fast twitch muscles is influenced by the levels of PV, and studies have shown that both DMD patients and *mdx* mice have lower levels of PV compared with controls (262, 304). The SR-Ca<sup>2+</sup> ATPases, SERCA1 and SERCA2a, play a key role in controlling muscle contraction and relaxation. Diaphragm muscles from both *mdx* and *mdx/utr*<sup>-/-</sup> mice have lower levels of SERCA1 compared with control mice; however, SERCA1 levels in soleus and quadriceps is similar between both dystrophic groups and control mice (256, 306). The slower SR-Ca<sup>2+</sup> uptake in dystrophic muscles was shown to be correlated with higher levels of SLN (306). Increased SLN protein and/or mRNA levels have been reported as pathological markers across different myopathies (66, 208, 257) and findings in the *mdx* mouse and *mdx/utr*<sup>-/-</sup> mouse suggest that its expression may be directly proportional to disease severity (306). Not much is known about the expression of PLN in DMD and other myopathies. In its dephosphorylated form, PLN is known to tightly interact

with SERCA2a, thus inhibiting its activity (216). Masseter muscles from *mdx* mice have higher levels of PLN compared with control mice (195), which is potentially another factor contributing to the decreased SR-Ca<sup>2+</sup> uptake in dystrophic muscles.

The changes in Ca<sup>2+</sup>-regulatory and -binding proteins in dystrophic muscles are thought to be compensatory mechanisms to cope with the increases in intracellular Ca<sup>2+</sup> levels. We propose that the beneficial effects of SERCA1 overexpression in *mdx* and *mdx/utr*<sup>-/-</sup> mice reported in our previous study were partially due to, at least in part, alterations in intracellular Ca<sup>2+</sup> handling proteins. Therefore, findings from this aim will allow us to understand additional changes in Ca<sup>2+</sup>-regulatory and -binding proteins that might help explain our previous results.

## Chapter 2: Review of literature

### Skeletal muscle

#### Overview of skeletal muscle development and mature skeletal muscle components

Skeletal muscle comprises 40–50% of total body mass and is necessary for movement, whole-body energy metabolism, and substrate storage and utilization (128). Skeletal muscle cells are composed of many organelles commonly found in other cell types such as mitochondria, endoplasmic/sarcoplasmic reticulum (ER/SR), lysosomes, and nucleus. However, while most cell types are mononucleated, muscle cells are multinucleated. Over 60 years ago Huxley & Hanson described the essential force transmitting properties of striated skeletal muscles, and since then much has been learned about the complexity and importance of this organ (175).

Skeletal muscle fibers are multi-nucleated cells formed from the fusion of multiple myoblasts during development. During pre-natal muscle development, most myocytes are derived from the somites of the embryo (266). The somite can be divided into two parts, epaxial and hypaxial, according to an anatomical division of the body and its musculature (56). The epaxial dermomyotome gives rise to the deep back muscles whereas the rest of the musculature derives from the hypaxial extremity of the dermomyotome (56). The delamination and migration of muscle progenitor cells depend on the activation and deactivation of specific transcription factors (Figure 2.1). Formation of the myoblasts is characterized by the downregulation of the transcriptional factors *Pax3* and *Pax7*, and the action of the myogenic regulatory factors (MRFs), a family of basic helix-hoop-helix transcription factors that orchestrate muscle development and differentiation (266). Briefly, cells that migrate from the somite activate the myogenic determination genes *MyoD* and *Myf5*, which will turn on the developmental program, thus enabling stem cells

to become myoblasts (330). One of the first steps in myogenesis is the aggregation of myoblasts into clusters. Further development of myoblasts, through differentiation and maturation, is accompanied by the expression of *mrf4* and *myogenin* (330). Clusters of myoblasts fuse and form small multinucleated myotubes; then other myoblasts fuse at the end of myotubes to increase their length (330). The earlier myotubes are known as primary myotubes. With further development, primary myotubes separate from other primary myotubes into clusters that are surrounded by a basal lamina (330). At this point, more myotubes begin to fuse and aggregate beneath the primary myotube's basal lamina. The subsequent myoblasts also fuse into myotubes, known as secondary myotubes (300). Now the cell cluster is composed of primary myotubes, secondary myotubes, and unfused myoblasts known as *satellite cells*. With further development, the primary myotube starts to look more like a mature muscle fiber, with the nuclei being forced out of the center of the fiber because of progressive filling with contractile proteins (300).

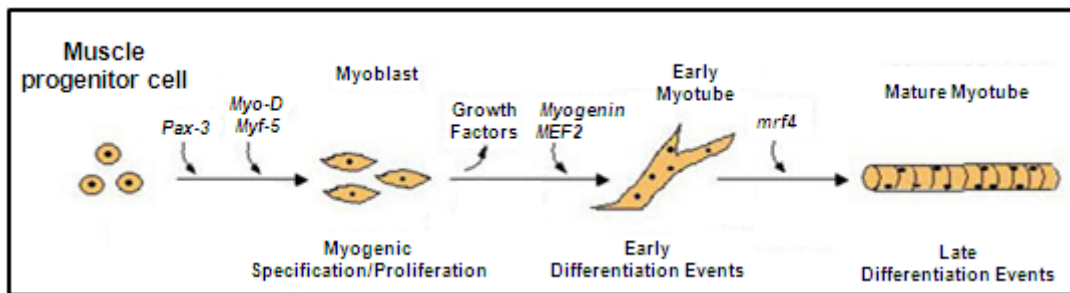


**Figure 2.1 – Myogenesis during development.** The delamination and migration of muscle progenitor cells depend on the activation and deactivation of specific factors, such as *Pax3*, *Myo-D*, and *Myf-5*. The action of myogenic regulatory factors will further coordinate muscle development and differentiation. Adapted from <https://www.bio.purdue.edu/>

As the name suggests, the majority of skeletal muscles are attached to bones via tendons (Figure 2.2). Although muscles differ in size and shape, their overall anatomy is very similar (Figure 2.2). A muscle is covered by a layer of connective tissue known as epimysium, which holds the muscle together and give its shape (276). Bundles of muscle

fibers, called fascicles, are wrapped by a layer of connective tissue known as perimysium (276). A layer of connective tissue, named endomysium, further covers each individual muscle fiber (276). The membrane that surrounds each muscle fiber is called sarcolemma. Beneath the sarcolemma lies the sarcoplasm, which contains all different cell components, including the myofibrils. The myofibrils are made up of numerous sarcomeres with actin (thin filaments) and myosin filaments (thick filaments), the two main protein filaments responsible for muscle contraction (Figure 2.2). Moreover, actin filaments also have the proteins troponin and tropomyosin, which play a role in regulating muscle contraction.

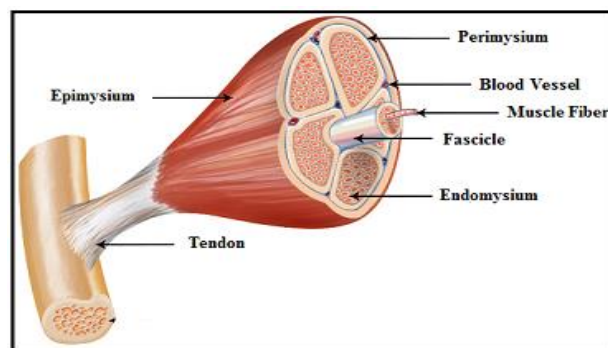


**Figure 2.2 – Skeletal muscle.** Skeletal muscles are composed of blood vessels, nerves, and various types of connective tissue. Generally, skeletal muscles are attached to bones via tendons. A whole muscle is covered by a layer of connective tissue known as epimysium. Fascicles are composed of bundles of muscle fibers and are covered by the perimysium. Lastly, individual muscle fibers are surrounded by connective tissue called endomysium. Adapted from <http://training.seer.cancer.gov/>

Myofibrils can be further subdivided into segments called sarcomeres (Figure 2.3). The sarcomeres are composed of different parts including I band, H zone, and A band, and are divided by the Z line, which is a thin sheet of connective tissue. Myosin filaments are located at the A band (the dark portion of the sarcomere), while actin filaments are located at the I bands (the lighter region of the sarcomere). Nevertheless, actin filaments overlap with myosin filaments, and therefore are also found in the A band. The H zone is located at the center of the sarcomere, and is only composed of myosin filaments.

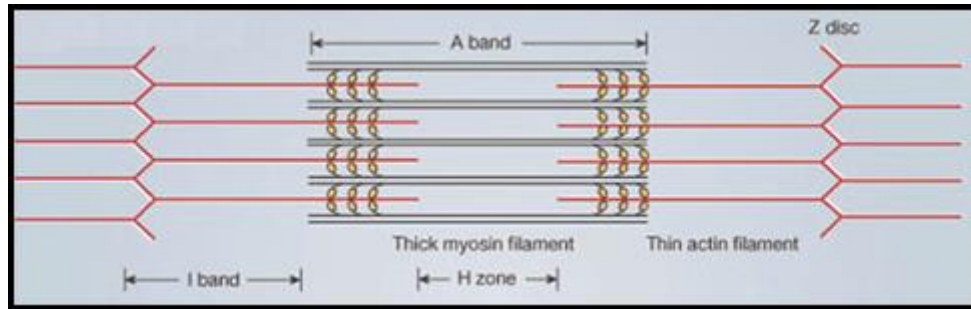


**Figure 2.3 – Sarcomere and myofibrils.** **A)** Myofibrils are subdivided into sarcomeres, which are located within two Z lines, and divided in the middle by the M line. **B)** The filaments between two consecutive Z lines. Actin filaments are located in the I band and in the A band (overlapping with myosin). Myosin filaments are located in the A band. The H zone is only composed of myosin filaments. Adapted from (194)

### Skeletal muscle contraction (E-C coupling)

The sequence of excitation-contraction coupling (E-C coupling) leading to muscle contraction and relaxation is initiated by an action potential derived from the brain or spinal cord (e.g., reflex). Briefly, when the action potential arrives at the axon terminals, it stimulates the release of acetylcholine, which travels through the synaptic cleft and binds to specific receptors on the muscle cell membrane. The binding of acetylcholine to its receptor stimulates the opening of its voltage-dependent sodium ( $\text{Na}^+$ ) channels in the muscle cell membrane to allow  $\text{Na}^+$  to enter and initiate the depolarization of the plasma membrane. The depolarization of the plasma membrane is actively conducted down the transverse tubules (t-tubules), which will then induce the conformational change of the voltage-sensitive L-type  $\text{Ca}^{2+}$  channels, the dihydropyridine receptors (DHPRs), resulting in a charge movement (31, 308). The charge movement will then stimulate the opening of the SR- $\text{Ca}^{2+}$  release channels also known as ryanodine receptors (RyR). Calcium will then be released from the SR, leading to a transient increase in intracellular free  $\text{Ca}^{2+}$  ( $[\text{Ca}^{2+}]_i$ ). The magnitude of the increases in intracellular  $\text{Ca}^{2+}$  transients depends on the net SR- $\text{Ca}^{2+}$  release and proteins that bind  $\text{Ca}^{2+}$ . The later include troponin C, parvalbumin (PV), the

SR- $\text{Ca}^{2+}$  ATPase (SERCA), calmodulin, and ATP (24). Part of the intracellular free  $\text{Ca}^{2+}$  will bind to troponin C, initiating the movement of tropomyosin, which will allow the binding of actin to myosin (18). When the strong association between actin and myosin is formed, the myosin head tilts and drags the thin filament toward the center of the sarcomere, which is often referred as the “power stroke” (194). The pulling of the thin filament toward the center of the sarcomere shortens the sarcomere, thus generating force. At the end of muscle contraction  $\text{Ca}^{2+}$  is pumped back into the SR by SERCA pumps, and this allows troponin and tropomyosin to return to their resting conformation. One single contraction cycle or “power stroke” of all the cross-bridges in a muscle only shortens the muscle by 1% of its resting length; thus, repeated cycles of attachment and detachment after the “power stroke” must occur to allow the muscles to shorten at its full capacity (some muscles are able to shorten up to 60% of their resting length).

#### Sarcoplasmic/endoplasmic reticulum $\text{Ca}^{2+}$ -ATPases (SERCAs)

Sarcoplasmic/endoplasmic reticulum  $\text{Ca}^{2+}$ -ATPases (SERCAs) are 110 kDa transmembrane proteins belonging to the P-type family of cation transporters (339). SERCAs regulate intracellular free  $\text{Ca}^{2+}$  in muscle cells by using free energy released from the hydrolysis of ATP to transport  $\text{Ca}^{2+}$  ions from the cytosol into the lumen of the SR/ER (two  $\text{Ca}^{2+}$  ions per ATP hydrolyzed) (339). There are three distinct genes producing more than ten isoforms of SERCA through alternative splicing in vertebrates (269). However, in adult skeletal muscle, only two SERCA isoforms predominate, SERCA1a and SERCA2a (269). Furthermore, SERCA1a and SERCA2a are differentially expressed in different muscle fiber types (269). Whole SERCA1a is expressed in fast-twitch skeletal

muscle fibers, SERCA2 is expressed predominantly in cardiac and slow-twitch skeletal muscle fibers (49, 217). Although differentially expressed in different muscle types, the primary structure of SERCAs is highly conserved (SERCA1a and SERCA2a are 84% identical), and due to this high conservation, all SERCA isoforms have identical transmembrane geometric and tertiary structures (269). Overall, skeletal muscle SERCAs have a dual function: (i) to induce muscle relaxation by decreasing cytosolic  $\text{Ca}^{2+}$ , and (ii) to restore SR- $\text{Ca}^{2+}$  stores for muscle contraction (269).

During the process of  $\text{Ca}^{2+}$  transport from the cytoplasm to the SR/ER, the SERCA pump transitions through multiple steps (269). The first step involves the binding of  $\text{Ca}^{2+}$  to the high-affinity sites on the cytoplasmic face of the SERCA pump (269). Subsequently, ATP hydrolysis occurs, the enzyme is phosphorylated, and several conformational changes in the enzyme will induce the transport of  $\text{Ca}^{2+}$  into the SR/ER (269). Due to the high quantity of SERCA pumps in each ER/SR,  $\text{Ca}^{2+}$  reuptake occurs quickly (only a few milliseconds), allowing fast rates of muscle relaxation (269).

## **Duchenne muscular dystrophy (DMD)**

### *DMD disease characteristics*

Muscular dystrophies (MD) are a group of over 30 genetic and heterogeneous neuromuscular disorders characterized by muscle loss and weakness (93). Duchenne muscular dystrophy (DMD), the most frequent and lethal form of MD, is named after the French scientist Duchenne de Boulogne, who reported the first case of cognitive problems in a child with DMD during the second half of the 19<sup>th</sup> century (37). Although DMD has been known for over a century, the main cause of the disease was not known until the



1980's (168). DMD is an X-linked disease that occurs as a result of mutations in the dystrophin gene, and affects 1 in 3600 - 6000 males at birth (53, 62, 63). Dystrophin is one of the largest genes in the human genome with more than 2.5 million base pairs (bp), with at least 7 promoters and 86 exons (247). Furthermore, dystrophin is expressed in skeletal, cardiac, and smooth muscle, and brain (247). Overall, patients with DMD have progressive muscle weakness and wasting, with a loss of 75% of muscle mass by the age of 10 (204). Ultimately this induces the exhaustion of muscular regenerative capacity, thus leading to substitution of muscle fibers by connective and adipose tissue (93).

Patients with DMD display symptoms of muscle weakness in early childhood and their physical ability diverges markedly from that of their peers (62). For instance, DMD patients display abnormal walking, difficulty rising from the floor, are usually unable to run, and have difficulty climbing stairs (222). Untreated patients might become wheelchair bound before reaching their teens, and die in their early to mid-twenties (62). Generally, the diaphragm is the most impaired muscle in DMD patients, and its deterioration is responsible for respiratory failure and early death of patients (123, 244). Moreover, more than 90% of DMD patients have cardiac complications, which causes a progressive reduction in cardiac function (e.g., reduced ejection fraction), and may lead to heart failure (123, 181, 244). Currently, DMD is incurable and the most used treatment option include the use of glucocorticoids (deflazacort or prednisone) which delay disease progression due to its anti-inflammatory benefits. Nevertheless, long term use of glucocorticoids leads to adverse side effects (e.g., immunosuppression, glucose intolerance, osteoporosis, and others) which limit their clinical utility.

Over the past 50 years the lifespan of patients has greatly increased. Not many patients survived beyond their teenage years in the 1960's, but nowadays treated patients live into their 20s and 30s (110). The increased lifespan is due to a combination of scientific discoveries in the DMD research area, and improved care from a team of specialists. In addition, factors such as routine flu and pneumococcal vaccinations, physical therapy, early use of antibiotics, improved nocturnal ventilation, early cardiac management, and the use of corticosteroids play an important role in improving the patients' lifespan (351). A multidisciplinary management is generally necessary due to complications faced by patients, such as respiratory, digestive, cardiovascular, and psychological problems (Figure 2.4). Several different locations in the US and other countries have multidisciplinary clinics with a range of medical professionals, including cardiologists, pulmonologists, neurologists, dietitians, nurses, rehabilitation specialists, orthopedists, physical therapists, and geneticists (62, 63). This multidisciplinary team is crucial as patients with DMD and their families need expert advice regarding diagnosis and managing of disease progression (62, 63).

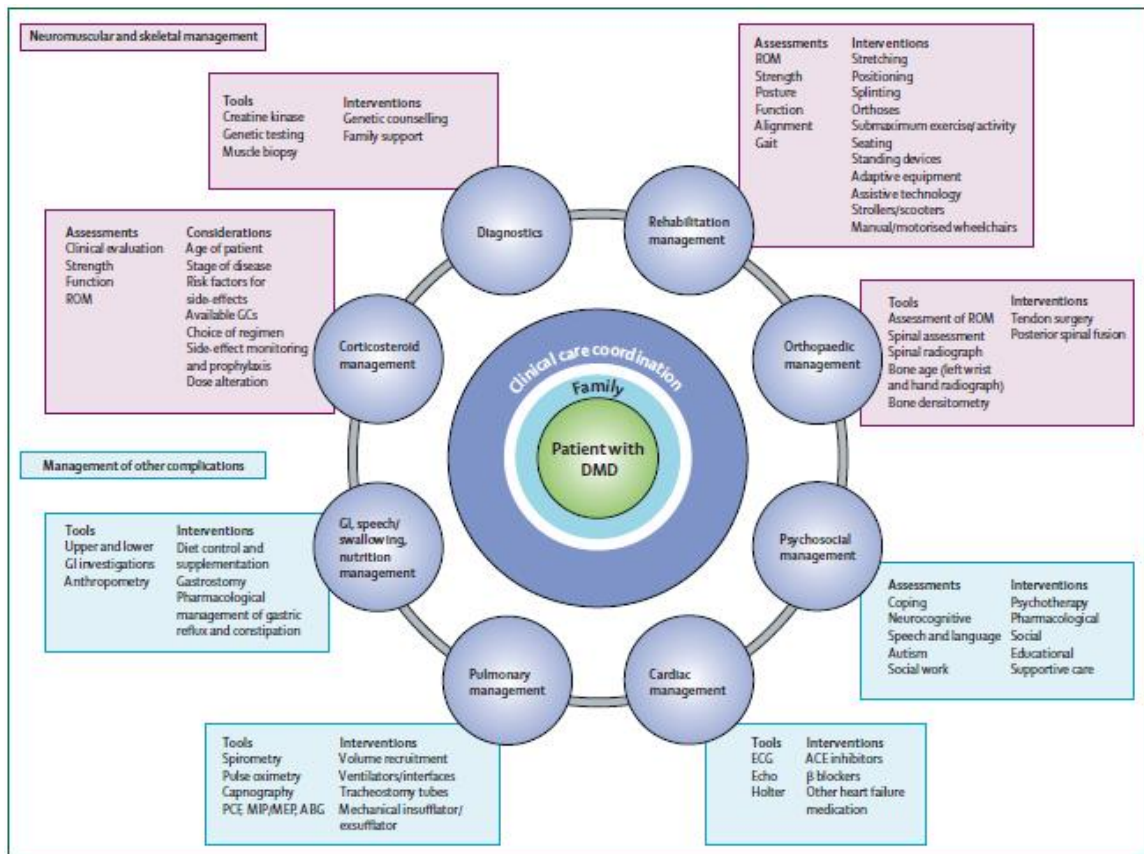


**Figure 2.4 – Multidisciplinary management of DMD.** Multidisciplinary management is generally necessary due to complications faced by DMD patients. The team of specialists have the expertise to support patients and families in a collaborative effort. Briefly, monitoring and treating neuromuscular and skeletal complications is critical for delaying decrements in muscle function, but management of other complications such as cardiovascular, pulmonary, digestive, and psychological problems have greatly added to the increased lifespan of patients. Adapted from (62).

### Dystrophin glycoprotein complex

The dystrophin-glycoprotein complex (DGC) is composed of at least 13 different proteins forming a bridge connecting the extracellular matrix to the muscle cytoskeleton (36). Some of the proteins comprising the DGC are dystrophin,  $\alpha$ -dystrobrevin, syntrophins ( $\alpha$ -1, and  $\beta$ -1), dystroglycans ( $\alpha$ , and  $\beta$ ), sarcoglycans ( $\alpha$ ,  $\beta$ ,  $\gamma$ , and  $\delta$ ), and sarcospan (Figure 2.5). Overall, the main role of the DGC is to stabilize the sarcolemma, thus preventing damage during muscle contractions and muscle necrosis (327). Yet, in addition to its mechanical function, the DGC acts as a transmembrane signaling complex,

hence playing a role in cellular communication (288). Mutations in some members of the DGC are deleterious to muscle fiber function and might disrupt intracellular mechanisms, thus leading to a MD phenotype.

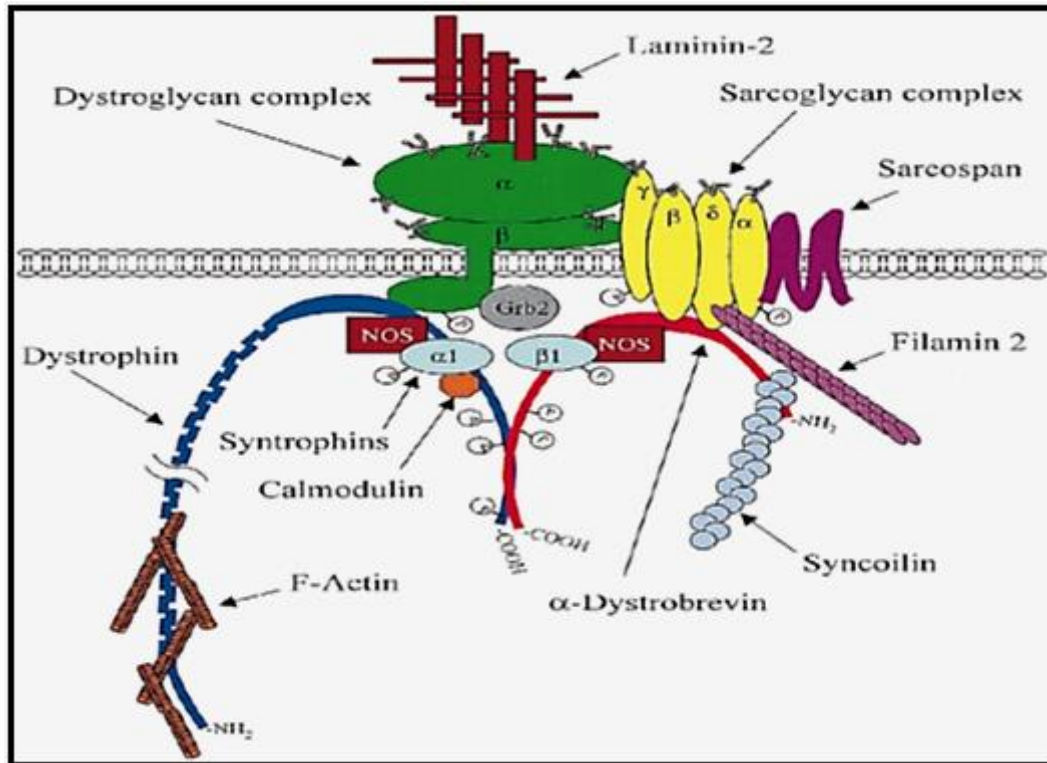


**Figure 2.5 – Schematic figure of the dystrophin-glycoprotein complex (DGC).** The DGC is composed of dystrophin,  $\alpha$ -dystrobrevin, syntrophins ( $\alpha$ -1, and  $\beta$ -1), dystroglycans ( $\alpha$ , and  $\beta$ ), sarcoglycans ( $\alpha$ ,  $\beta$ ,  $\gamma$ , and  $\delta$ ), and sarcospan. The DGC connects to the extracellular matrix through its binding to laminin, while it connects to the intracellular environment via binding to F-actin, filamin-2, and syncoilin. Signaling molecules such as calmodulin, Grb2, and nNOS are also associated with the DGC. Adapted from (288).

Dystroglycan is a heterodimer with  $\alpha$ - and  $\beta$ -subunits translated from a single gene (176, 177) (Figure 2.5). Both subunits are generally subjected to extensive co- and post-translational modifications, including proteolysis, glycosylation, and phosphorylation (7, 118). Such post-translational modifications are known to play a role in pathogenic processes, since aberrant glycosylation is a hallmark of dystroglycanopathies (e.g., hypoglycosylation of  $\alpha$ -dystroglycan is a hallmark of dystroglycanopathies), and both aberrant

glycosylation and proteolysis of dystroglycan are present in many tumors (240, 315). In addition, post-translational phosphorylation of dystroglycan has a profound effect on its function (118). The glycosylation of the extracellular  $\alpha$ -subunit is also vital for its interaction with laminin while phosphorylation of the cytoplasmic domain modulates its association with the cytoskeleton and other binding partners (241). Dystroglycan expression is essential for embryonic development as gene disruption is lethal for mouse embryos (365).

The sarcoglycan complex is composed of four transmembrane glycoproteins ( $\alpha$ -,  $\beta$ -,  $\gamma$ -, and  $\delta$ -sarcoglycan) only expressed in skeletal and cardiac muscle (296, 297) (Figure 2.5). Each sarcoglycan has a large extracellular domain, a single transmembrane domain, and a small intracellular domain. Generally, mutations in any sarcoglycan leads to the partial or total loss of other sarcoglycans from the DGC. In addition, mutations in sarcoglycans lead to a MD phenotype, as seen in humans with severe childhood autosomal recessive MD who lack  $\alpha$ -sarcoglycan, and transgenic mouse models lacking either  $\alpha$ -,  $\beta$ -, or  $\delta$ -sarcoglycan (85, 103, 108, 145, 297). Interestingly, absence or reduction in the levels of sarcoglycans does not lead to the full disappearance of dystrophin, which supports the role of intracellular modifications in inducing the MD phenotype.

Sarcospan is a transmembrane protein that is an integral part of the sarcoglycan complex, and also member of the DGC (200) (Figure 2.5). The expression of sarcospan is highly dependent on the expression of sarcoglycans, since  $\alpha$ -,  $\beta$ -, or  $\delta$ -sarcoglycan knockout mice do not express sarcospan (14, 85, 103, 108). Although sarcospan is a member of the sarcoglycan complex, the absence of the protein does not lead to changes in the expression of DGC proteins or to a MD phenotype (200). On the other hand, mice

overexpressing sarcospan exhibit a severe phenotype (e.g., severe kyphosis and premature death) that is similar to mouse models of laminin-deficient congenital MD (270).

Another important component of the DGC is dystrobrevin (Figure 2.5). Dystrobrevin is thought to have a role in intracellular signal transduction in muscles, and its absence leads to MD and NMJ defects (36, 51, 288). Two different genes encode the mammalian dystrobrevin family of proteins, and skeletal and cardiac muscles have three different isoforms of dystrobrevin, including  $\alpha$ -dystrobrevin-1, -2 and -3 (13, 38). However, only the two larger isoforms,  $\alpha$ -dystrobrevin-1 and -2, contain the syntrophin and dystrophin binding sites (259). Studies have demonstrated that  $\alpha$ -dystrobrevin has a dual role in the pathogenesis of MD and in acetylcholine receptor stabilization at the NMJ (147, 149). Mice lacking  $\alpha$ -dystrobrevin develop a very mild MD phenotype, and are much less severely affected than *mdx* mice (147). Moreover, very few muscle fibers appear damaged when compared with fibers from *mdx* mice, suggesting that the sarcolemma is more stable (147). Overall, although the lack of dystrobrevin does not lead to a severe MD phenotype, studies have shown that the protein is still important for proper DGC stability and NMJ function.

The DGC is also composed of syntrophins, which are proteins known to interact with dystrophin, utrophin, and dystrobrevin (5, 109, 192, 219, 271). There are five different isoforms of syntrophins ( $\alpha$ 1,  $\beta$ 1,  $\beta$ 2,  $\gamma$ 1, and  $\gamma$ 2), but only three isoforms ( $\alpha$ 1,  $\beta$ 1, and  $\gamma$ 2) are highly expressed in skeletal muscles (3, 6, 274). The interaction between syntrophin and dystrophin is regulated by the  $\text{Ca}^{2+}$  binding protein calmodulin, and by phosphorylation and dephosphorylation events in the dystrophin protein (212, 218, 235, 260). To date, no known human MD cases has been caused by mutations in any of the

syntrophins. The role of syntrophins in DMD has been evaluated since muscles from both DMD patients and dystrophic mouse models lack expression of  $\alpha 1$ -syntrophin (4). Mice lacking  $\alpha 1$ -syntrophin have no decrements in force production or increased muscle damage (183). Nevertheless, recent evidence demonstrates that  $\alpha 1$ -syntrophin null mice have impaired muscle force recovery after osmotic shock and impaired recovery of endurance capacity after endurance exercise (375). This is partially explained by the concomitant loss in expression of the water channel aquaporin-4 (AQP4), which is known to interact with  $\alpha 1$ -syntrophin (375). Although the function of aquaporins is not fully understood in muscle, aquaporins are known to be involved in regulatory volume increase or decrease against osmotic shocks in other tissues (169). The reduced force production due to osmotic shock was not associated with membrane damage, which further supports of role of alterations in signaling pathways other than membrane fragility, per se, in DMD disease pathogenesis.

#### *Dystrophin gene structure and mutations*

The dystrophin gene is the largest gene in humans. The gene has more than 2.5 million bp, which corresponds to 0.1% of the total human genome, and 1.5% of the total X-chromosome (247). Full-length dystrophin is a very large rod-shaped protein comprised of four domains with a molecular weight of 427 kDa (Figure 2.6) (247). Dystrophin is anchored to the plasma membrane by the interaction of its carboxy-terminal (C-terminus) with  $\beta$ -dystroglycan and to the cytoskeleton by the connection of its amino-terminal (N-terminal) with F-actin (see Figure 2.6) (116). Dystrophin is also composed of central rod

domain with 25 triple-helical repeats containing roughly 3000 residues, and a cysteine rich domain with 280 residues (Figure PP) (303).

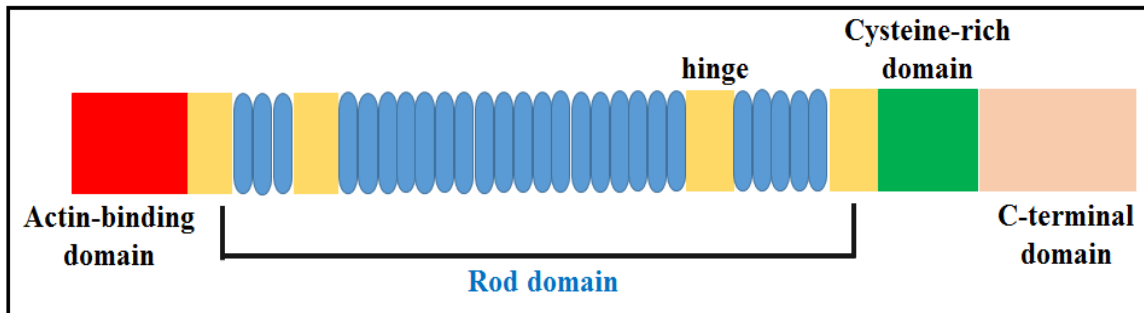


**Figure 2.6 – Full length dystrophin.** Dystrophin gene has four domains: 1) the N-terminal domain which binds  $\alpha$ -actin; 2) the rod-like domain; 3) the cysteine rich domain; and 4) the C-terminus domain which binds  $\beta$ -dystroglycan.

The dystrophin gene is susceptible to genetic alterations due to its size. Generally, there is no simple relation between deletion size and the resultant clinical phenotype of MD. For instance, deletion of exon 44, a small exon, results in classic DMD phenotype, while large deletions (nearly 50% of the gene) have been found in patients with the milder type of MD known as Becker muscle dystrophy (114, 209, 210). Deletions in the central and distal rod domains are only associated with myalgia and muscle cramps, but no general muscle weakness (247). Furthermore, changes in phenotype depend on if the deletion disrupts the reading frame of the gene (247). For example, in-frame mutations generally lead to a partially functional dystrophin protein, thus leading to BMD (247). On the other hand, frameshift mutations (deletions and duplications), usually results in unstable RNA which leads to the synthesis of a truncated form of dystrophin, which is nearly undetectable (247). Deletions are the most common mutations in the dystrophin gene, comprising 65% of all mutations (247). Such deletions can happen in any location of the gene, and the two most common hotspots are located at the central part of the gene (between exons 45-55) and at the 5' end (between exons 2-19) (247).



Although one in three cases of DMD are due to a new mutations and most patients have unique mutations, 60%-65% of all DMD patients carry a deletion of one or more exons, usually between exons 45-55 (1, 340). This idea was further supported by a recent study evaluating dystrophin mutations in more than 7,000 DMD patients (35). Briefly, results demonstrated that large mutations ( $\geq 1$  exon) were found in 5,684 cases (79%), of which 4,894 (86%) were deletions and 784 (14%) were duplications (Table 2.1) (35). The majority of the large deletions (80% of all large deletions) were found between exons 45-55 and exons 2-20 while the most common duplication was found in exon 2 (11% of duplications) (35). There were 1,445 small mutations of less than 1 exon (20% of all mutations), which included deletions (358 cases; 25% of all small mutations) and duplications (132 cases; 9% of all small mutations) (35). There were also 756 point mutations (10% of all mutations) including 726 nonsense mutations (10% of all mutations, 50% of small mutations) and 3 missense mutations (less than 1% of all mutations) (35).

<b>Type and frequency of mutations held within the TREAT-NMD DMD Global Database</b>		
		<b>% of total mutations</b>
<b>Total</b>	<b>7,149</b>	
Large mutations	5,682	79
Large deletions ( $\geq 1$ exon)	4,894	68
Large duplications ( $\geq 1$ exon)	784	11
Small mutations	1,445	20
Small deletions ( $< 1$ exon)	358	5
Small insertions ( $< 1$ exon)	132	2
Slice sites ( $< 10$ bp from exon)	199	3
Point mutations	756	11
Nonsense	726	10
Missense	30	0.4
Mid-intronic mutations	20	0.3

**Table 2.1 – Type and frequency of DMD mutations from over 7,000 cases.** Adapted from (35).

### Mouse models for DMD

Up until the discovery of *mdx* mice, the most used mouse models for muscle degeneration studies were the *dy* and *dy<sup>2J</sup>* mutants (58). However, these mouse models had great limitations due to phenotypic differences compared with MD patients. For instance, it was not known if these animals were either myogenic or neurogenic in origin, and some of their disease symptoms were fairly different from those found in MD patients (58). The *mdx* mice was first described in 1984 in a colony of C57BL/10 mice (C57BL/10ScSnJ) (58). Dystrophin is fully absent in *mdx* mice due to a point mutation in exon 23 which yields a premature stop codon (366). The *mdx* mouse model shares some phenotypic changes with DMD patients, including high CK levels, muscle degeneration, increased macrophage accumulation, and increased fibrosis with aging (72, 187, 256). Moreover, although some studies have shown that *mdx* mice have no decrements in absolute muscle force of limb muscles comparable to unaffected mice, the relative force (normalized to body mass) decreases by approximately 50% at the age of 4 mos (84, 234, 289). Others have also shown that *mdx* mice have increased muscle damage and force deficit during lengthening contractions (238, 374).

Although *mdx* mice shares many disease similarities in DMD patients, these mice have a relatively mild phenotype compared with the patient population [this was first noted in the original study describing the phenotype of *mdx* mice (58)]. Additionally, the only muscle demonstrating similar disease progression as seen in humans, with progressive degeneration and detectable muscle weakness, is the diaphragm (215, 326). For instance, the relative force and power generation of adult *mdx* diaphragm (4-6 mo old) is 40 and 54% lower compared with WT mice (215). Additionally, the relative force and power

generation of older *mdx* diaphragm (24-mo old) is 52 and 69% lower compared with age – matched WT mice (215). The normal lifespan of the *mdx* mice is partially due to continued satellite cell function, which is known to be limited in DMD patients (41, 42, 45, 165). Briefly, the constant activation and use of satellite cells in muscles from DMD patients, due to repetitive cycles of muscle damage and repair, depletes the satellite cell pool, which ultimately leads to the failure of muscle repair (41, 42, 165). In contrast, this is not the case in muscles from *mdx* mice (45). Furthermore, *mdx* mice lacking the RNA component of telomerase presented limited satellite cell availability as their aged, and this corresponded to the amount of muscle wasting (45).

The milder phenotype from *mdx* mice is also due, at least in part, to overexpression of utrophin (*utr*), a protein with similar role as dystrophin in muscles (357). Muscles from *mdx* mice have ~5 fold increase in *utr* levels compared with muscle from WT mice (357). In an attempt to aggravate the pathophysiology of the *mdx* mouse model, *utr* null mice were crossed with *mdx* mice to generate the double KO mouse model (*mdx/utr<sup>-/-</sup>*) (95). In contrast from the *mdx* mouse, the *mdx/utr<sup>-/-</sup>* model has altered neuromuscular and myotendinous junctions, early onset of damage in the diaphragm (as early as 6 days after birth), joint contractures, kyphosis, and premature death between 4 to 20 weeks (95, 366). To our knowledge, one clinical case of a boy missing both dystrophin and *utr* has been reported to date (76). The patient had early onset DMD and died at the age of 15 due to acute intestinal occlusion and bleeding, respiratory failure, and cardiac arrhythmia (76) .

Other mouse models have also been developed trying to recapitulate the disease phenotype of DMD patients. For example, the *mdx<sup>Cv</sup>* mice (i.e., *mdx<sup>2Cv</sup>*, *mdx<sup>3Cv</sup>*, *mdx<sup>4Cv</sup>*, and *mdx<sup>5Cv</sup>*) were recovered from male mice treated with a chemical mutagen that were

crossed with female *mdx* mice (74). Overall, *mdx<sup>Cv</sup>* mice display similar muscle pathophysiology and CK levels as *mdx* mice (366). In another model, exon 52 was disrupted on a C57BL/6J background to generate the *mdx52* mouse model (15). Although the *mdx52* model has muscle damage, necrosis, and fibrosis, these mice do not show skeletal muscle weakness or behavioral changes until 18 mos of age (366). Different mouse models with mutations in different DGC proteins have also been engineered, and these mice have different disease phenotypes/severity based on the specific mutation (see table 2.2) (107). Overall, findings from studies evaluating mice with specific DGC mutations have helped scientists to better understand the role of the DGC members in DMD disease phenotype (Table 2.2) (107).

Genotype (protein absent)	Lifespan	Skeletal dystrophy	Cardiac phenotype
<i>Sgca</i> <sup>-/-</sup> ( $\alpha$ -sarcoglycan)	>1 year	Moderate	None
<i>Sgcb</i> <sup>-/-</sup> ( $\beta$ -sarcoglycan)	>1 year	Severe	Severe
<i>Sgcg</i> <sup>-/-</sup> ( $\gamma$ -sarcoglycan)	20 weeks	Severe	Severe
<i>Sgcd</i> <sup>-/-</sup> ( $\delta$ -sarcoglycan)	>1 year	Severe	Severe
<i>Sspn</i> <sup>-/-</sup> (sarcospan)	>1 year	None	None
<i>DG</i> <sup>-/-</sup> (dystroglycan)	Embryonic lethal	NA	NA
DG chimeric (skeletal & cardiac dystroglycan KO)	>1 year	Moderate?	Severe
<i>Myd</i> (large)	Reduced	Moderate	None
<i>NNOS</i> <sup>-/-</sup> (neuronal nitric oxide synthase)	>1 year	None	None
<i>Adbn</i> <sup>-/-</sup> ( $\alpha$ -dystrobrevin)	8 - 10 mos	Mild	Mild
$\alpha$ 1-syntrophin <sup>-/-</sup>	>1 year	None	None
<i>Cav-3</i> <sup>-/-</sup> (caveolin-3)	>30 weeks	Mild	None

NA: not applicable

**Table 2.2 – Summary of DGC-associated mouse models (not including dystrophin).** Adapted from (107).

### **Intracellular calcium handling in dystrophic muscles**

Intracellular calcium ( $\text{Ca}^{2+}$ ) is a master regulator of a plethora of mechanisms in muscle cells, from E-C coupling to the activation of many downstream factors. Generally, intracellular  $\text{Ca}^{2+}$  is tightly regulated by  $\text{Ca}^{2+}$ -binding proteins (e.g., calmodulin and PV), organelles (e.g., SR/ER and mitochondria), and pumps (e.g., SERCA and plasma membrane  $\text{Ca}^{2+}$  ATPase). However, several of these mechanisms of intracellular  $\text{Ca}^{2+}$  control are disrupted in muscle lacking dystrophin. Dystrophic muscles have altered E-C coupling, higher resting free intracellular  $\text{Ca}^{2+}$ , impaired SR- $\text{Ca}^{2+}$  control (i.e., release and reuptake), mitochondrial  $\text{Ca}^{2+}$  overload, and increased  $\text{Ca}^{2+}$  influx through membrane channels. The purpose of this section is to discuss the current knowledge on  $\text{Ca}^{2+}$  handling in muscles lacking dystrophin.

#### **Resting intracellular $\text{Ca}^{2+}$ and E-C coupling in DMD**

Early studies had already shown that  $\text{Ca}^{2+}$  levels were higher in muscles from DMD patients prior to the creation of specific fluorescent  $\text{Ca}^{2+}$ -indicator dyes (43, 180, 229). Briefly, muscle samples from DMD patients stained via the von Kossa method, with alizarin red, and with glyoxalbis-(o-hydroxyanil), a method used to evaluate  $\text{Ca}^{2+}$  positive fibers, had higher  $\text{Ca}^{2+}$  positive stained muscle fibers compared with muscle samples from individuals with other myopathies (43). Other studies using different techniques, such as X-ray fluorescence (229) and atomic absorption spectrophotometry (180), also showed higher  $\text{Ca}^{2+}$  levels in muscles from DMD patients. Later studies using fluorescent  $\text{Ca}^{2+}$ -indicator dyes (e.g., Fura-2 and Indo-1) were able to better evaluate  $\text{Ca}^{2+}$  levels in dystrophic muscle fibers and cells (239). Mongini and colleagues demonstrated that both

resting and peak free  $[Ca^{2+}]_i$  were higher in dystrophic cells compared with controls (239). Their findings were further confirmed in single muscle fibers from *mdx* mice (170, 172, 370). However, other studies reported no differences in resting  $[Ca^{2+}]_i$  levels between *mdx* and control muscle fibers (133, 203, 280). Most of the discrepancies in findings have been linked to a) differences in the methods applied to evaluate  $[Ca^{2+}]_i$  levels (i.e., type of fluorescent dye and dye loading conditions), b) age of the animals, and c) different muscles assessed. Nevertheless, later studies with arguably more definitive technical approaches (i.e.,  $Ca^{2+}$  sensitive microelectrodes) have demonstrated that resting  $[Ca^{2+}]_i$  levels are truly elevated in dystrophic muscles (11, 12, 60). For instance, Altamirano *et al.* used  $Ca^{2+}$  microelectrodes to show that resting  $[Ca^{2+}]_i$  was approximately 3 fold higher in *mdx* myotubes compared with WT myotubes (11). Furthermore, the same group demonstrated that in vivo resting  $[Ca^{2+}]_i$  in the gastrocnemius muscle of *mdx* mice was also approximately 3 fold higher compared with WT (12). Others also observed a 3 fold elevation in resting  $[Ca^{2+}]_i$  in gastrocnemius muscle from *mdx* mice compared with WT using microelectrode technique (60).

Alterations in E-C coupling have also been reported in DMD. Interestingly, E-C coupling problems were already known to be present in DMD muscles prior to evaluating intracellular  $Ca^{2+}$  levels (368). For instance, mothers of boys with DMD containing one functional dystrophin gene might not show muscle weakness, but their muscles take longer to relax after contraction compared with normal controls (368). Studies evaluating intracellular  $Ca^{2+}$  dynamics in *mdx* muscle fibers further observed a longer decay phase in  $Ca^{2+}$  tails, suggesting a longer/delayed relaxation phase (145, 344). The slower relaxation rate and increased resting  $[Ca^{2+}]_i$  suggested a potential impairment in  $Ca^{2+}$  handling by the

sarcoplasmic/endoplasmic reticulum (SR/ER) in DMD. More specifically, this mechanism appeared to be due to decreased activity of the SR-Ca<sup>2+</sup> ATPase (SERCA). Indeed, Leberer *et al.* (201) reported an age-dependent reduction in SR-Ca<sup>2+</sup> pump function in diseased muscle from the mouse strain C7BL/6J(dy<sup>2J</sup>/dy<sup>2J</sup>), which was further supported in *mdx* mice (98, 186, 306). Briefly, isolated SR vesicles from *mdx* mice had lower maximum velocity of Ca<sup>2+</sup> uptake compared with vesicles from control mice (186). More recently, both the rate of Ca<sup>2+</sup> dependent Ca<sup>2+</sup> uptake and maximal velocity of SR-Ca<sup>2+</sup> uptake have been shown to be decreased in soleus, quadriceps, and diaphragm muscles from both *mdx* and *mdx/utr*<sup>-/-</sup> mice compared with WT (306).

Abnormal Ca<sup>2+</sup> release has also been reported in dystrophic mouse models and such changes have been linked to alterations in ryanodine receptor (RyR) function, a protein responsible for the release of Ca<sup>2+</sup> from the SR. Alterations in RyR function were first reported by Takagi and colleagues (331), who demonstrated that skinned muscle fibers from *mdx* mice had increased leakiness of Ca<sup>2+</sup> from the SR. Later, Bellinger and colleagues (29) demonstrated that muscle fibers from *mdx* mice have an age-dependent increase in RyR S-nitrosylation, and that this coincided with dystrophic changes in muscle. In the same study the authors also reported that RyR S-nitrosylation led to depletion of the channel complex of calstabin 1 (calcium channel stabilizing binding protein) (29). More recent evidence has shown that Ca<sup>2+</sup> sparks can be readily observed in muscle fibers from dystrophic mice, and that such Ca<sup>2+</sup> sparks are attributed to unregulated opening of RyRs, further supporting the leakage of Ca<sup>2+</sup> through RyR (354). The inositol (1,4,5)-triphosphate receptor (IP3R) is an SR membrane glycoprotein that also plays a role in SR-Ca<sup>2+</sup> release, yet much less studied than the RyR complex. Recent evidence demonstrated

that  $\text{Ca}^{2+}$  leak through IP3R in dystrophic myotubes also contributes to the increased intracellular  $\text{Ca}^{2+}$  levels (11). Other previous studies showed increased IP3R and IP3 levels, and greater IP3R-dependent  $\text{Ca}^{2+}$  transients in myotubes from both DMD patients and *mdx* mice (22, 69, 206).

#### Alterations in calcium handling proteins in DMD

Calsequestrin is a 63 KDa protein that functions to maintain low levels of free intracellular  $\text{Ca}^{2+}$  in skeletal muscle fibers and is the most abundant  $\text{Ca}^{2+}$ -binding protein located in the SR (25). Studies have demonstrated that calsequestrin levels vary in different muscles from dystrophic mice (223). While some groups reported no differences or lower levels of calsequestrin-like proteins in muscles from *mdx* compared with control mice (89, 223), others reported higher levels of calsequestrin in muscles from *mdx* and *mdx/utr<sup>-/-</sup>* compared with controls (306). Overall, differences in the findings are related to the muscle group evaluated. While the quadriceps muscle from *mdx* and *mdx/utr<sup>-/-</sup>* had higher levels of calsequestrin compared with controls (223), no differences were found in soleus or diaphragm (223, 306). Moreover, the spared laryngeal and extraocular muscles from *mdx* mice were shown to have higher levels of calsequestrin compared with controls (127, 188, 378).

Parvalbumin acts as a fast  $\text{Ca}^{2+}$ -buffering protein in the cytoplasm of fast-twitch muscle fibers, thus playing a key role in muscle relaxation. Although studies have shown that both DMD patients and *mdx* mice have lower PV protein levels compared with controls (196, 262, 304), others have demonstrated that PV mRNA levels were higher in muscles from *mdx* vs. control mice (135). More specifically, Niebrój-Dobosz and colleagues



showed that PV protein levels were decreased in muscles from DMD patients across different ages (262). The fast twitch muscles, TA and gastrocnemius, from *mdx* mice were found to contain significantly lower levels of PV compared with controls (304). Additionally, PV levels were shown to be significantly decreased in *mdx* tongue and masseter muscles (196). The lower levels of PV might contribute to the elevations in intracellular  $\text{Ca}^{2+}$  levels in dystrophic muscles.

The SR- $\text{Ca}^{2+}$  ATPases (SERCA1 and SERCA2) play a key role in controlling muscle contraction and relaxation. Several studies have demonstrated that the fast twitch muscle  $\text{Ca}^{2+}$ -ATPase isoform SERCA1 is differentially expressed in dystrophic muscles (127, 196, 306). While SERCA1 protein levels have been shown to be lower in diaphragms from both *mdx* and *mdx/utr<sup>-/-</sup>* mice compared with WT, no differences were reported for soleus or quadriceps (306). In addition, others have found no differences in SERCA1 protein levels in the masseter, tongue, and temporalis muscles from *mdx* vs. WT (196). Studies have also evaluate SERCA2a mRNA and protein levels in muscles from dystrophic mouse models (99, 305, 306). Although some investigations reported higher SERCA2a transcript and protein levels in EDL muscles from *mdx* mice (99, 306), others have found no differences (305). Moreover, SERCA2a protein levels were shown to be increased in muscles from *mdx/utr<sup>-/-</sup>* mice compared with controls (306).

The activity of the SERCA pump is regulated by phospholamban (PLN) and sarcolipin (SLN) (32, 269). Only a few studies have evaluated PLN levels in DMD or other myopathies (196, 334). PLN mRNA expression was shown to be downregulated in samples from DMD patients (334), while PLN protein levels were significantly upregulated in the masseter muscles but not altered in the tongue or temporalis muscles of

*mdx* mice compared with controls (196). Collectively, these data suggests that, in response to DMD, PLN expression varies across different muscles. More recently, Fajardo and colleagues demonstrated that PLN overexpression in WT mice leads to features of centronuclear myopathy – a congenital myopathy characterized by central nuclei, type I fiber predominance, atrophy, and central aggregation of oxidative activity (121). These findings suggest that PLN overexpression might alter intracellular  $\text{Ca}^{2+}$  control by decreasing SR- $\text{Ca}^{2+}$  reuptake, thus leading to an accumulation of  $\text{Ca}^{2+}$  in the cytoplasm and potential activation of  $\text{Ca}^{2+}$ -induced damage. Due to its role in SERCA inhibition and subsequent modification in SR- $\text{Ca}^{2+}$  uptake, SLN has also been proposed as an important protein in intracellular  $\text{Ca}^{2+}$  kinetics. Indeed, increased SLN protein and/or mRNA levels are becoming widely known as a common pathological marker across many myopathies (66, 208, 257, 264). In dystrophic muscles, SLN mRNA levels were shown to be upregulated in the hindlimb muscles (301, 338) and medial gastrocnemius (224). More recently, Schneider and colleagues reported a several fold upregulation in SLN protein levels in quadriceps, soleus, and diaphragm muscles from *mdx* and *mdx/utr<sup>-/-</sup>* mice (306). Further, SLN protein levels in quadriceps, soleus, and diaphragm muscles from *mdx/utr<sup>-/-</sup>* mice were higher compared with *mdx* (306). These findings between *mdx* and *mdx/utr<sup>-/-</sup>* mice suggest that SLN expression may be directly proportional to disease severity (306). The increased SLN upregulation also correlated with decreased maximum velocity of SR- $\text{Ca}^{2+}$  uptake in *mdx* and *mdx/utr<sup>-/-</sup>* mice, which indicates that increased SLN levels could lead to SERCA inhibition, thus contributing to the abnormal elevation of  $\text{Ca}^{2+}$  concentration in DMD (306).

Stretch and store operated  $Ca^{2+}$  entry in dystrophic muscles

High cytosolic  $Ca^{2+}$  levels may result from increased  $Ca^{2+}$  influx through the plasma membrane in DMD. Indeed, the higher resting intracellular  $Ca^{2+}$  levels in DMD have been associated with increased  $Ca^{2+}$  influx through the plasma membrane since the 1980's (343). Turner and colleagues were the first to demonstrate an abnormal  $Ca^{2+}$  entry through the plasma membrane in *mdx* single fibers (343). Similar results were also reported in dystrophic myotubes, but such increased  $Ca^{2+}$  influx was inhibited by  $Ca^{2+}$  channel blockers (8). A number of potential candidate channels that could mediate the entry of  $Ca^{2+}$  into dystrophic fibers, such as stretch-activated channels, store-operated channels, leak channels, and/or growth factor-regulated channels, have been suggested in the literature. Another feasible hypothesis proposes that the greater  $Ca^{2+}$  influx in dystrophic muscles is caused by membrane lesions, which occurs often in dystrophic muscles. However, findings from Yeung and colleagues demonstrated that  $Ca^{2+}$  entry in isolated muscle fibers from *mdx* mice occurs via channels rather than membrane tears (374). Briefly, dystrophic fibers exposed to eccentric contractions in the presence of stretch-activated  $Ca^{2+}$  channel blockers (i.e., streptomycin or the spider venom toxin GsMTx4) had lower increases in resting  $[Ca^{2+}]_i$  compared with dystrophic fibers exposed to eccentric contractions alone (374). Additionally, stretch-activated  $Ca^{2+}$  channel blockers partially suppressed the decline in tetanic  $[Ca^{2+}]_i$  and force following eccentric contractions (374).

Increased mechanosensitive channel activity is another suggested mechanism for the increased  $Ca^{2+}$  influx in DMD. Resting activity of mechanosensitive ion channels is elevated in dystrophin-deficient muscle compared with controls (131). These mechanosensitive channels are store-operated channels belonging to the transient receptor

potential canonical (TRPC) channel family, and such channels are known to play a role in the increased  $\text{Ca}^{2+}$  influx in DMD (347). While some have shown that antisense based inhibition of TRPCs (i.e., TRPC 1, 3, and 6) decreased  $\text{Ca}^{2+}$  influx in dystrophic fibers by 90% (347), others demonstrated that, in dystrophin-deficient fibers, TRPC1 binds to caveolin-3 and subsequently increases  $\text{Ca}^{2+}$  entry through the plasma membrane (138). The role of TRPCs in increasing membrane  $\text{Ca}^{2+}$  influx and contributing to the dystrophic phenotype was further supported by genetic manipulation (236). Briefly, overexpression of TRPC3 channels in skeletal muscles from normal mice enhanced  $\text{Ca}^{2+}$  influx and resulted in a phenotype that closely resembled DMD (236). Stretch-activated channels have also been shown to be activated by ROS, since ROS scavengers were shown to decrease its activity (152, 275). In addition to being mechanosensitive, TRPC channels are known to function as store-operated channels, thus being involved in store-operated  $\text{Ca}^{2+}$  entry (SOCE). This increased SOCE associated with TRPC1 channels has been shown in dystrophic fibers, and remarkably, it was restored to normal levels by inducing expression of minidystrophin (346).

In addition to TRPC channels, other proteins have also been shown to play a role in the increased SOCE in DMD. For instance, the stromal interaction molecule 1 (STIM1), which acts as an SR- $\text{Ca}^{2+}$  sensor that translocates from the ER/SR membrane to regions close to the plasma membrane following depletion of the intracellular  $\text{Ca}^{2+}$  stores, can trigger SOCE through both TRPCs and Orai1 channels (371, 381). Recent evidence demonstrated that the expression levels of Orai1 are significantly elevated in dystrophic muscles, and that this paralleled with increases in SOCE activity (381). Moreover,

knockdown of Orai1 eliminated the differences in SOCE activity between *mdx* and WT muscle fibers (381).

### **Background and structure of skeletal muscle calpains**

Protein turnover is determined by the balance between protein synthesis and break-down, and refers to the continual renewal of proteins. When the rate of protein break-down surpasses protein synthesis, muscle cells enter a catabolic state; on the other hand, when protein synthesis is greater than protein break-down, muscle cells enter an anabolic state. The rate of protein turnover is controlled by a set of specific proteolytic machinery, and the two most important cell proteolytic systems are the ubiquitin-proteasome and the autophagy-lysosome systems (47). The ubiquitin-proteasome system degrades specific substrate proteins tagged with ubiquitin, while the autophagy-lysosome system primarily degrades nonspecific cell components (e.g., proteins and microorganisms) (319). Although calpains have also been implicated in muscle protein turnover, calpains primarily performs the proteolytic processing of proteins, rather than degradation, to modulate and/or modify substrate activity, specificity, and structure (319).

Calpains are calcium-dependent non-lysosomal cysteine proteases that were first described over 50 years ago (142, 155). Over 15 calpain genes have been identified, some being ubiquitous whereas others are tissue specific (316, 319). It is generally assumed that ubiquitous calpains have basic roles in different cell types, while tissue-specific calpains are involved in specific functions in the cell they are located. Skeletal muscle contains calpain-1, calpain-2, and the muscle specific calpain-3 (316, 319). For instance, calpain-3 mRNA levels in skeletal muscle are 10-fold greater compared with calpain-1 or -2, which

suggests an important role of calpain-3 in skeletal muscles (318). Calpain-1, also known as  $\mu$ -calpain, and calpain-2, also known as m-calpain, have received their names based on the amount of  $\text{Ca}^{2+}$  necessary for their activation (142). Calpain-3, on the other hand, requires much lower levels of  $\text{Ca}^{2+}$  for activation and is much less stable compared with calpain-1 and -2 (115).

While calpain-1 and -2 are heterodimers containing a large subunit (80 KDa) and a small subunit (30kDa), calpain-3 has a monomeric structure of 94kDa (142, 248). All three calpains have similar structure by possessing four domains: i) the N-terminal domain containing the site for autolysis; ii) the proteolytic domain; iii) a C2-like region involved in membrane phospholipid interaction; iv) the  $\text{Ca}^{2+}$ -binding site which contains five EF-hand domains (248, 318) (Figure 2.7). In addition of the four domains, calpain-3 also has three unique sequences not found in the other calpains, including the NS (N-terminal sequence), and the IS1 and IS2 (inserted sequences 1 and 2) sequences (319) (Figure 2.7). Calpastatin, the only known endogenous inhibitor of both calpain-1 and -2, contains four different calpain inhibitory units, each one with different inhibitory efficiency (113, 220, 221). Calpastatin does not inhibit calpain-3, but instead is proteolysed by calpain-3, which implies that calpain-3 assists in the regulation of calpains in skeletal muscle (263).

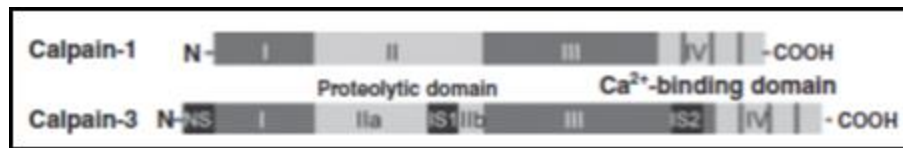


**Figure 2.7. Schematic figure demonstrating the domains of calpain-1 and calpain-3.** Both calpain-1 and calpain-3 have four domains in common: 1) N-terminal domain containing the site for autolysis; 2) the proteolytic domain; 3) C2-like region involved in membrane phospholipid interaction; and 4)  $\text{Ca}^{2+}$ -binding site which contains five EF-hand domains. Calpain-3 also has three unique sequences, the NS (N-terminal sequence), and the IS1 and IS2 (inserted sequences 1 and 2). Adapted from (248).

### Functional role, activity, and substrates of calpain-1

Although the physiological role of calpain-1 is not very well understood, studies have shown that calpain-1 participates in cellular functions such as apoptosis, myogenesis, cell signaling and cell differentiation (141). Calpain-1 has also been shown to be required for proper  $\text{Ca}^{2+}$ -mediated membrane repair after damage (231, 232). Briefly, by utilizing siRNAs to decrease expression of calpain-1 in mouse embryonic fibroblast cell lines, Mellgren and colleagues showed that loss of calpain-1 activity compromises  $\text{Ca}^{2+}$ -mediated survival after cell damage (231). Calpain-1 also plays a role in E-C coupling. More specifically, calpain-1 is known to proteolyse JP1 (a protein connecting DHPRs with RyRs), thus leading to E-C uncoupling and decreased force production (249). Although proteolysis of JP1 by calpain-1 is detrimental to muscle function, this mechanism is also thought to be protective since it avoids greater  $\text{Ca}^{2+}$ -dependent damage to muscle fibers (248).

While in its inactive state, calpain-1 is freely diffusible in the cytoplasm, but once activated it moves closer to specific substrates (248). Activation of calpain-1 is dependent on the presence of  $\text{Ca}^{2+}$ . In vitro assays have shown that calpain-1 becomes autolyzed between  $[\text{Ca}^{2+}]_i$  of 3-50 $\mu\text{M}$  (142). Moreover, other findings have shown that autolysis of calpain-1 happens when  $[\text{Ca}^{2+}]$  is raised to  $\geq 2\mu\text{M}$  for  $\geq 1$  min (254). The binding of  $\text{Ca}^{2+}$  to calpain-1 triggers an autolytic process in which calpain-1 cleaves its own NH<sub>2</sub>-terminal domain, reducing its size from 80 to 78 kDa and then to 76 kDa, thus increasing its proteolytic activity against other substrates and also its  $\text{Ca}^{2+}$  sensitivity (e.g., after initial autolysis calpain-1 can remain active even when  $[\text{Ca}^{2+}]$  is as low as 300nM) (142, 254).

In vitro studies have shown that the most well-known substrates of calpain-1 are cytoskeletal proteins, including the troponin complex,  $\alpha$ -actinin, titin, and the Z-disc proteins fodrin and desmin (28, 142). Moreover, recent evidence demonstrates that JP1 and JP2 are substrates of calpain-1 in skeletal and cardiac muscle (249). The junctophilin family of proteins are responsible for mediating the close contact between the SR and t-tubules in both skeletal and cardiac muscles (167, 179, 189, 332). Skeletal muscles contain both JP1 and JP2, while cardiac muscles only contains JP2 (179, 332). Recent findings demonstrated that JP1 and JP2 undergo proteolysis in tissues from humans and mice when exposed to increasing  $[Ca^{2+}]$ , and that this was associated with autolytic activation of calpain-1 (249).

### *Functional role, activity, and substrates of calpain-3*

Although the physiological roles of calpain-3 in skeletal muscle are not fully understood, calpain-3 is known to have a crucial for adult skeletal muscle homeostasis, since its absence leads to MD (294). More specifically, mutations in calpain-3 are linked to limb-girdle MD type 2A (LGMD2A), and this was further supported by transgenic mouse models lacking calpain-3 (193, 294, 295). Calpain-3 also plays a role in skeletal muscle repair and maintenance (e.g., sarcomere turnover), and this has been the subject of many reviews [e.g., (27, 105)]. Calpain 3 is mainly expressed in skeletal muscle (very low levels in cardiac muscle), and it localizes at several regions of the sarcomere through binding to the I-band and M-line regions of titin (27, 130). It has been proposed that the anchoring of calpain-3 to titin has three purposes: 1) to keep calpain-3 from degrading



itself; 2) to maintain calpain-3 in a proteolytically inactive state; and 3) to place calpain-3 near its substrates (27).

Calpain-3 is only proteolytically active after it first autolyzes itself in a  $\text{Ca}^{2+}$ -dependent process, removing its IS1 region and producing 60 to 55 kDa products, and a small fragment of 30 kDa (105, 293). In vitro assays have shown that calpain-3 becomes autolyzed when exposed to  $[\text{Ca}^{2+}]$  as low as 500 nM (48). Moreover, recent evidence demonstrated that the  $\text{Ca}^{2+}$ -binding protein calmodulin binds at two different sites on calpain-3, thus enhancing calpain-3 autolytic activation (115). Coexpression experiments and in vitro studies have led to the identification of many different proteins that can be cleaved by calpain-3, including titin, filamin C, vinexin, ezrin and talin (156, 193, 333).

#### *Evidence of increased calpain activity in DMD*

Earlier studies demonstrated that calpain activity is increased in muscle samples from DMD patients (185, 290). However, one of the first studies showing direct evidence between calpains and DMD pathophysiology was only published in the 1990's (320). Briefly, calpain levels were shown to be regulated differently during the necrotic and regenerated phases in muscles from dystrophic mice (320). At peak necrosis, levels of full length calpain-2 were increased, while no changes were found in levels of the autolyzed isoform (320). In contrast, levels of full length calpain-1 were not increased during necrosis, but the amount of the autolyzed isoform was greater (320). During the regenerated phase, levels of autolyzed calpain-1 and calpain-2 were unchanged (320). Subsequently, the same group demonstrated that intracellular localization of calpains change as dystrophic muscles undergoes cycles of degeneration and regeneration (322).

Although, the distribution of calpains in muscle fibers was shown to be similar between *mdx* and control mice in the pre-necrotic stage, higher amount of calpains were associated with the plasma membrane in *mdx* fibers (322). Furthermore, majority of the calpains were found in the cytoplasm in dystrophic fibers during the necrotic stage (322).

Several studies have also reported higher levels of calpain activity in different dystrophic animal models (77, 255, 309), which further suggested a potential therapeutic benefit of calpain inhibition in DMD. Studies have evaluated the potential of calpain inhibition in improving the phenotype of dystrophic mouse models, but results have been inconsistent (19, 52, 77, 309, 321). Although calpain inhibition decreased markers of muscle damage in muscles from *mdx* mice in some studies (19, 321), others reported no improvements (52, 309). Briefly, daily intramuscular injections of the calpain inhibitor leupeptin for 30 days led to decreases in markers of muscle, while long term (6 mos) treatment with leupeptin (intraperitoneal injections) did not attenuate muscle fibrosis or necrosis (19, 309). A different type leupeptin-based drug, C101, has also been tested in dystrophic animal models (309). Short-term treatment (4 weeks) and long-term treatment (6 mos) of *mdx* mice with C101 failed to improve muscle function or markers of muscle damage (309). Moreover, muscles from C101 treated *mdx* mice demonstrated a compensatory increased activation of calpain as well as increased activation of proteasome activity (309). The potential benefit of C101 was also evaluated in dystrophic dogs (77). Although C101 treated dogs were able to maintain muscle strength in cranial pelvic limb muscles, the compound failed to maintain the strength in the posterior pelvic limb muscle (77). Additionally, C101 failed to attenuate force decrements following eccentric contractions or mitigate muscle necrosis in dystrophic dogs (77). Overexpression of

calpastatin, the endogenous calpain inhibitor, in *mdx* mice has also been evaluated (52, 321). Briefly, *mdx* mice overexpressing calpastatin had reduced muscle necrosis, regenerating areas, and membrane damage compared with *mdx* mice (321). Nevertheless, others reported no differences in the markers of muscle damage between *mdx* mice overexpressing calpastatin compared with *mdx* mice (52).

### **Oxidative stress**

Oxidative stress refers to a state of imbalance between reactive oxygen species (ROS) production and removal, which can either occur as a result of increased ROS formation or reduced antioxidant defense (67). Oxidative stress is known to play a role in several different pathological conditions, including inflammatory disorders, cancer, muscle wasting, atherosclerosis, and MD (17, 287, 310, 345). Under normal cellular conditions, the primary source of ROS is derived from the leakage of superoxide anions from complex I and III of the respiratory chain (54). A series of linked enzymatic reactions take place for the detoxification of superoxide, with the initial step being its conversion to hydrogen peroxide by superoxide dismutase (287). Subsequently, hydrogen peroxide is metabolized to oxygen and water by glutathione peroxidase (287). Hydrogen peroxide can also react with metal ions to produce the highly reactive hydroxyl radical (158), while superoxide can react with nitric oxide and produce peroxynitrite (26). Both hydroxyl radical and peroxynitrite are capable of oxidizing DNA, proteins, lipids, and carbohydrates in the cell (287).

Protein carbonylation is a major hallmark of oxidative stress and is known as one of the most harmful irreversible oxidative protein modifications (90, 373). Generally,

protein carbonylation is defined as an irreversible post-translational modification that yields a reactive carbonyl moiety in a protein (e.g., aldehyde, ketone, or lactam) (124). In the Fenton reaction, transition metal ions are reduced by hydrogen peroxide, thus generating highly reactive hydroxyl radicals (325). These hydroxyl radicals can oxidize amino acid side chains or cleave the backbone of proteins, thus leading to numerous modifications in proteins (324). Carbonylated proteins are not repaired by cellular enzymes, and if not eliminated (usually proteins are degraded by either the 26S proteasome or by the 20S proteasome) they tend to aggregate and this might result in cell death (124). Studies have shown that certain tissues and organs have specific carbonylation, and this has allowed oxidative stress to be linked with several diseases (20, 101, 124, 146). For example, skeletal muscle proteins have been intensively studied in many different pathological conditions (e.g., sepsis, diabetes, ischemia reperfusion injury) (20, 101, 146), and protein oxidation and particularly carbonylation were proposed as main contributors for MD (20).

#### *Evidence of increased oxidative stress in DMD*

The first evidence suggesting the potential contribution of oxidative stress to DMD was proposed in 1965 (33). Briefly, the study demonstrated that dystrophic muscles showed phenotypic changes that were very similar to muscles from individuals with vitamin E deficiency (33). Further studies demonstrated that oxidative stress was increased in muscles from both DMD patients (160, 298) and *mdx* mice (159, 286). Protein carbonyl levels (160) and 8-hydroxy-2'-deoxyguanosine (298), a marker of DNA damage, were found to be higher in muscle samples from DMD patients compared with samples from

heathy subjects. Moreover, levels of O-tyrosine (159), a marker of hydroxide radical damage, and lipid peroxidation (286) were shown to be greater in skeletal muscles from *mdx* mice compared with control mice. ROS accumulation has been described as a causative event rather than a consequence of muscle degeneration in the *mdx* mouse model, since oxidative stress was found to be elevated in skeletal muscles from *mdx* mice during the pre-necrotic phase (<20 days old), which precedes the onset of inflammation and necrosis (97).

To further support the role of oxidative stress in DMD pathophysiology, studies have evaluated the effects of antioxidant treatment in both DMD patients and dystrophic animal models (57, 102, 119, 126, 299, 352); however, results have been inconsistent. For example, green tea extract (GTE) (57, 102, 119), and N-acetylcysteine (NAC) (360) were shown to protect the muscle against damage in *mdx* mice. Treatment of *mdx* mice with GTE for 4 weeks led to a dose dependent reduction in EDL necrosis and regeneration compared with non-treated *mdx* mice (57). In another study, *mdx* mice treated with GTE for 6 weeks exhibited ~15 % fewer regenerating fibers and reduction in NF- $\kappa$ B levels compared with non-treated *mdx* mice (119). Dystrophic mice treated with NAC for 6 weeks had lower incidence of central nuclei, macrophage invasion, and weakness in the EDL muscle compared with non-treated dystrophic mice (360). Furthermore, NAC treatment increased protein levels of  $\beta$ -dystroglycan and utrophin, suggesting increased stability of the muscle membrane, while decreasing caveolin-3 and NF- $\kappa$ B activation (360). While antioxidant treatment has shown great benefits in *mdx* mice, earlier clinical trials in DMD patients did not report similar beneficial outcomes (126, 299, 352). Briefly, DMD patients treated with penicillamine and vitamin E for 18 mos did not show any

improvement in muscle strength or cardio-pulmonary function (126). Moreover, DMD patients treated with vitamin B3 and vitamin E did not have any improvement in muscle function or motor behavior (352).

*Sources of ROS in DMD: mitochondria, monoamine oxidases, and NADPH oxidases*

Recent studies have focused on evaluating the source of ROS in dystrophic muscles as a potential therapeutic target for clinical trials (233, 363). As previously stated, mitochondria are the major producers of ROS in cells, and mitochondrial ROS production is augmented in pathological conditions (67). The link between intracellular  $\text{Ca}^{2+}$  dysregulation and mitochondria  $\text{Ca}^{2+}$  overload has been proposed as one of the mechanisms leading to the increased ROS production in dystrophic muscles (125). Theoretically,  $\text{Ca}^{2+}$  might increase mitochondrial ROS production by the following mechanisms: 1) stimulation of tricarboxylic acid cycle and oxidative phosphorylation; 2) stimulation of nitric oxide synthase and subsequent nitric oxide production; 3) induction of the dissociation of cytochrome c from the inner mitochondrial cardiolipin, which can lead to mitochondrial permeability transition pore opening and cytochrome c release into the cytoplasm (54). Dystrophic mitochondria are major recipients of the greater  $\text{Ca}^{2+}$  influx through the cell membrane, and this greater  $\text{Ca}^{2+}$  uptake by dystrophic mitochondria leads to mitochondrial permeability transition pore opening and cytochrome c release from mitochondria, which can effectively block the respiratory chain at complex III and enhance mitochondrial ROS generation (54, 151, 237).

Another potential source of ROS in dystrophic muscles might be derived from monoamine oxidases (MAO) (233). MAO are flavoproteins located at the outer

mitochondrial membrane known to catalyze the oxidative deamination of neurotransmitters and dietary amines (376). Generally, increased levels or activity of MAO are known to increase ROS production in cells (67). Both protein levels and enzymatic activity of MAO were found to be increased in *mdx* mice (233). Treatment of *mdx* mice with MAO inhibitor (pargyline), significantly improved the dystrophic phenotype, which suggested the role of MAO as a key source of ROS in DMD (233). Another relevant source of ROS in dystrophic muscles are NADPH oxidases (NOX). These multiprotein enzyme complexes use NADPH as a substrate to convert oxygen into superoxide or hydrogen peroxide (67). Studies have shown that NOX expression and activity are increased in muscles from *mdx* mice (323, 363, 364). More importantly, NOX-dependent ROS increases were reported in muscles of *mdx* mice at the pre-necrotic stage, suggesting that NOX activation with concomitant ROS production is a causative event rather than a consequence in dystrophic muscles.

### **Endoplasmic reticulum stress**

The endoplasmic reticulum (ER) is a highly developed organelle responsible for several cellular processes (372). Overall, the ER is a major site of protein synthesis and cellular  $\text{Ca}^{2+}$  stores, while it also responds to cellular stress conditions and serves to maintain homeostasis of the cell (164). In order for properly synthesize and fold proteins, the ER requires high levels of  $\text{Ca}^{2+}$  and an appropriate redox balance (55, 202). Increased oxidative stress and/or  $\text{Ca}^{2+}$  deficits in the ER lumen can result in accumulation of a large quantity of misfolded and/or unfolded proteins in the ER, which triggers a process called ER stress (184). For instance, inhibition of the SERCA pumps by specific inhibitors (e.g.,

thapsigargin and A23187) lowers ER  $\text{Ca}^{2+}$  levels and potently activates ER stress (36). Thus, this demonstrates that secretory pathway proteins require the high ER  $\text{Ca}^{2+}$  levels to properly fold (Hendershot 2004). ER stress occurs in most cells and is a natural mechanism for maintaining proper protein folding under conditions of cell stress (372). Although several ER stress pathway participants have been described in the literature, little is known about which specific protein is key for this process (372).

The lumen of the ER contains the highest concentration of  $\text{Ca}^{2+}$  within the cell due to the active transport of  $\text{Ca}^{2+}$  ions by  $\text{Ca}^{2+}$  ATPases (i.e., SERCA pumps) (372). Moreover, the ER lumen contains the right oxidizing environment which promotes disulfide bond formation between cysteine residues and the proper folding of proteins (164, 372). Due to its role in protein folding and transport, the ER lumen is also rich in molecular chaperones (e.g., Grp78/BiP, Grp94, and calreticulin) which stabilize protein folding intermediates (372). While the vast majority of proteins entering the ER fold quickly and accurately, some proteins fail to properly fold (e.g., these are protein subunits produced in excess, mutant proteins, and/or even occasionally normal proteins that fail to mature properly) (164). A major function of the ER is to detect these "abnormal" proteins (i.e., misfolded/unfolded proteins) and remove them in a process called ER-associated degradation (230). Under normal cellular conditions, activation of ER stress is an essential mechanism for maintaining normal cellular function via upregulation of ER chaperones (e.g., Grp78/BiP), repression of protein synthesis, and removal of abnormal proteins (230). However, if the ER stress response is not able to cope with the accumulation of misfolded and unfolded proteins, the ER stress-specific cell death pathway is activated through the upregulation of the pro-apoptotic transcription factor C/EBP homologous protein (CHOP),



c-jun N-terminal kinase (JNK), and/or caspase-12 (murine caspase-12 is the equivalent of human caspase-4) (166). Importantly, both CHOP and caspase-12 are activated specifically by ER stress, but not by other apoptotic stimuli (258).

### Grp78/BiP

Mammalian Grp78/BiP is a stress-inducible protein initially identified in cells depleted of glucose (82, 91), and was the first ER chaperone identified due to its association with the incompletely assembled subunits of antibody molecules (46, 157). Grp78/BiP is a member of the heat shock protein 70 family, and has ATP binding sequences that interact with unfolded proteins. Under normal cellular conditions, Grp78/BiP is bound to ER stress sensors [e.g., inositol-requiring kinase 1 (IRE1 $\alpha$ ), protein kinase RNA-like endoplasmic reticulum kinase (PERK), and activating transcription factor 6 (ATF6)] on the ER membrane, thus inhibiting their aggregation and ER stress activation (372). These ER stress sensor proteins have their N-terminus in the ER lumen while their C-terminus is in the cytosol, providing a bridge that connects these 2 compartments (372). Normally, Grp78/BiP is bound to the N-termini of these transmembrane ER proteins (372). Once misfolded or unfolded proteins accumulate in the ER, Grp78/BiP moves away from ER stress sensor proteins to bind to abnormal proteins (372). This allows the aggregation of these transmembrane signaling proteins, and activation of ER stress (372). Grp78/BiP is also known to play a role as a Ca<sup>2+</sup> buffer in the ER (207, 329). Overexpression of Grp78/BiP in HeLa cells was shown to directly increase ER Ca<sup>2+</sup> levels, and this increase was due to Grp78/BiP's ability to bind to Ca<sup>2+</sup> and not to its chaperoning of another ER protein (207). Moreover, association between Grp78/BiP and nascent polypeptides is

stabilized by high  $\text{Ca}^{2+}$  concentrations in the ER (329). Grp78/BiP has also been proposed to be involved in  $\text{Ca}^{2+}$  transport from the ER to the mitochondria (104).

### CHOP

The protein CHOP is a member of the C/EBP family of proteins, and is a specific ER stress-induced apoptotic mediator (372). The CHOP gene was initially identified in a search for genes induced by genotoxic stress (e.g., ultraviolet irradiation and alkylating agents methyl methanesulfonate), and was also reported in cells undergoing glucose deprivation and amino-acid starvation (129). The CHOP gene promoter has binding sites for major inducers of ER stress activation, such as ATF4, ATF6, and X box protein-1 (XBP-1) (372). All these factors, ATF4, ATF6, and XBP-1, have been shown to induce CHOP gene transcription (372). Activation of ER stress-induced cell death is partially dependent on CHOP. Briefly, studies have shown that CHOP KO mice have lower apoptosis in response to ER stress (265, 382).

### Evidence of ER stress in DMD

To our knowledge only a limited number of studies has evaluated specific ER stress markers in dystrophic muscles. Recently, Moorwood and Barton showed an upregulation of ER stress in the skeletal muscles of both DMD patients and *mdx* mice (242). In 5 mo old *mdx* mice, the levels of Grp78/BiP, pro- and active caspase-12, CHOP and P-JNK in the TA, EDL and diaphragm muscles were higher compared with controls (242). Moreover, in DMD patients, the levels of Grp78/BiP and caspase-4 were also elevated compared with controls (242). The increase in caspase-12 has been previously shown in

the masseter of young *mdx* mice (171). Due to the heightened ER stress in dystrophic muscles, Moorwood and Barton evaluated the effects of blocking caspase-12 in the *mdx* mice (242). Caspase-12 null mice were crossed with *mdx* mice to generate dystrophin-deficient, caspase-12 null mice (*mdx/cas*) (242). Results demonstrated that muscles from *mdx/cas* had similar levels of CHOP, Grp78/BiP, and P-JNK compared with *mdx* mice (242). Nevertheless, *mdx/cas* had improved specific force production and decreased susceptibility of force loss following eccentric contractions compared with *mdx* mice (242). The authors further demonstrated that the pseudo-hypertrophy commonly found in *mdx* was attenuated by caspase-12 ablation in *mdx/cas* mice (242). Lastly, although markers of muscle damage were not changed (e.g., CK levels and percentage of CNFs) between *mdx* vs. *mdx/cas* mice, muscle fiber degeneration in *mdx/cas* was almost reduced to WT levels (242).

**Chapter 3: The role of proteases in excitation-contraction coupling failure in  
muscular dystrophy**

The following study has been published in the *American Journal of Physiology-Cell  
Physiology*, 308 (1) C33-C40; 2014; (doi:10.1152/ajpcell.00267.2013)

**The role of proteases in excitation-contraction coupling failure  
in muscular dystrophy**

Davi A G Mázala<sup>1</sup>, Robert W Grange<sup>2</sup>, Eva R Chin<sup>1</sup>

<sup>1</sup>Department of Kinesiology, School of Public Health, University of Maryland, College Park, MD 20742, USA.

<sup>2</sup>Department of Human Nutrition, Foods and Exercise, Virginia Polytechnic Institute and State University, Blacksburg, VA 24061, USA.

**Running head:** Proteases and E-C coupling failure in DMD

**Correspondence:** Eva R. Chin, Ph.D.

Department of Kinesiology, School of Public Health

University of Maryland, College Park, Maryland 20742

e-mail: [erchin@umd.edu](mailto:erchin@umd.edu)

Phone: 301- 404-2478

## Abstract

Duchenne muscular dystrophy (DMD) is one of the most frequent types of muscular dystrophy. Alterations in intracellular calcium ( $\text{Ca}^{2+}$ ) handling are thought to contribute to the disease severity in DMD, possibly due to the activation of  $\text{Ca}^{2+}$ -activated proteases. The purpose of this study was two-fold: 1) to determine if prolonged excitation-contraction (E-C) coupling disruption following repeated contractions is greater in animals lacking both dystrophin and utrophin (*mdx/Utr<sup>-/-</sup>*) compared with mice lacking only dystrophin (*mdx*); and 2) to assess whether protease inhibition can prevent E-C coupling failure following repeated tetani in these dystrophic mouse models. Excitation-contraction coupling was assessed using Fura-2 ratio, as an index of intracellular free  $\text{Ca}^{2+}$  concentration, in response to electrical stimulation of single muscle fibers from the flexor digitorum brevis muscle. Resting Fura-2 ratio was higher in dystrophic compared with control (CON) fibers, but peak Fura-2 ratios during stimulation were similar in dystrophic and CON fibers. One hour after a series of repeated tetani, peak Fura-2 ratios were reduced by  $30 \pm 5.6\%$ ,  $23 \pm 2\%$  and  $36 \pm 3.1\%$  in *mdx*, *mdx/Utr<sup>+/-</sup>* and *mdx/Utr<sup>-/-</sup>*, respectively, with the greatest reduction in *mdx/Utr<sup>-/-</sup>* fibers ( $p < 0.05$ ). Protease inhibition attenuated this decrease in peak Fura-2 ratio. These data indicate that E-C coupling impairment after repeated contractions is greatest in fibers lacking both dystrophin and utrophin and that prevention of protease activation can mitigate the prolonged E-C coupling impairment. These data further suggest that acute protease inhibition may be useful in reducing muscle weakness in DMD.

**Keywords:** Duchenne muscular dystrophy; intracellular  $\text{Ca}^{2+}$ ; excitation-contraction coupling; protease(s)

## Introduction

Duchenne muscular dystrophy (DMD) is one of the most frequently occurring and devastating types of muscular dystrophy (10). Skeletal muscles of patients with DMD lack dystrophin (168), a protein that contributes to membrane stability during muscle contractions (39, 283). The absence of dystrophin increases the susceptibility of muscle to stretch-induced damage (374), and disrupts intracellular signaling pathways (198). Disruptions in membrane integrity and/or intracellular homeostasis (i.e. increased oxidative stress) result in increased intracellular free calcium concentration ( $[Ca^{2+}]_i$ ) in dystrophic muscle (172) and alterations in  $Ca^{2+}$ -dependent signaling. In particular, elevated resting  $Ca^{2+}$  levels may contribute to increased activation of the  $Ca^{2+}$ -activated proteases (i.e. calpains) and the ubiquitin proteasome pathway and thus may accelerate proteolysis in response to contractile activity.

Repeated tetanic contractions result in muscle fatigue. Force recovery after repeated contractions occurs in two phases: a rapid phase which is related to metabolic recovery (80) and a slow phase related to the elevation in  $[Ca^{2+}]_i$  during contractions (79, 80, 197). In an *in vitro* single muscle fiber model, slow recovery from fatigue was shown to be due to prolonged failure of mechanisms of excitation-contraction (E-C) coupling leading to reduced  $Ca^{2+}$  release. This prolonged reduction in E-C coupling can also be induced without contractions by exposing muscle fibers to high  $Ca^{2+}$  concentrations (197, 350).

Activation of calpains is thought to be a mechanism contributing to the prolonged disruption of E-C coupling following repeated tetanic contractions (197, 350). Elevations in  $[Ca^{2+}]_i$  in the physiological range of muscle contractions (0.5 – 3.0 $\mu$ M) can lead to



activation of the two major calpains, calpain-3 and  $\mu$ -calpain (48, 250, 252). Calpains can then degrade proteins involved in E-C coupling such as ryanodine receptor (139) or junctophilin-1 (249). Contraction-induced impairments of E-C coupling are also observed in dystrophic muscle, with greater impairments in dystrophic branched fibers compared with control and “non-branched” dystrophic fibers (162). The dysfunctional  $\text{Ca}^{2+}$  handling combined with evidence of increased proteolytic activity in dystrophic muscle (134) suggests a potential role for calpains in DMD disease progression (239, 343).

Studies that investigate underlying mechanisms (134, 374) and potential treatments (92, 305) for DMD have largely been conducted in *mdx* mice. However, under normal physiological conditions, the diaphragm is the only muscle in *mdx* mice demonstrating similar disease progression to DMD patients, with progressive degeneration and detectable muscle weakness (326). Other muscles appear to be protected because utrophin, a protein with a similar function in muscle to dystrophin, is upregulated in these animals (228, 357). Thus, a double mutant model lacking both dystrophin and utrophin (*mdx/Utr<sup>-/-</sup>*) is thought to be more suitable for studies of the intracellular mechanisms altered in DMD (148). In response to repeated tetanic contractions, muscle fibers from the *mdx/Utr<sup>-/-</sup>* mice had a greater decay in  $\text{Ca}^{2+}$  transients compared with the *mdx* and control mice (68) suggesting greater E-C coupling impairment with repeated contractions in fibers lacking both dystrophin and utrophin. However, it is not known whether the prolonged reductions in E-C coupling following muscle fatigue, which contribute to muscle weakness, are exacerbated in the muscle fibers from the *mdx/Utr<sup>-/-</sup>* mice.

The evidence for poor  $[\text{Ca}^{2+}]_i$  handling during repeated muscle contractions in dystrophic muscle and the impaired E-C coupling due to protease (i.e. calpain) activation

with repeated tetani, suggest that proteases play a role in prolonged E-C coupling impairment in dystrophic muscle. Due to the more severe disease pathophysiology in the *mdx/Utr<sup>-/-</sup>* mice [i.e. reduced lifespan, early onset of damage in the diaphragm, joint contractures, and kyphosis (95)], we hypothesized that prolonged E-C coupling disruption following repeated contractions would be greater in muscles that lack both dystrophin and utrophin. We also hypothesized that protease inhibition would attenuate the decrease in E-C coupling failure following repeated contractions in both dystrophic animal models.

## Methods

Ethical Approval: All procedures were conducted under a protocol approved by the Institutional Animal Care and Use Committee of the University of Maryland, College Park.

Animals: Three control (CON) mice (C57BL/10ScSn) were obtained from Jackson laboratories. Three *mdx/Utr*<sup>+/-</sup> breeders (two females and one male) were obtained from Dr. Diego Fraidenraich of the University of Medicine and Dentistry, New Jersey, and in collaboration with Dr. Robert Grange of Virginia Tech University. Colonies of *mdx/Utr*<sup>+/-</sup> mice were bred at the University of Maryland Central Animal Research Facility according to previously published breeding schemes (95). Once females appeared pregnant, they were removed from the males and housed separately until pups were born and weaned. Offspring were weaned at age 21 days, sorted by gender and then genotyped. Genotyping of animals was performed using a primer sequence and polymerase chain reaction conditions generously provided by Dr. Dawn A. Lowe from the University of Minnesota, Department of Physical Medicine & Rehabilitation. It was expected that 25% of the pups born would be *mdx/Utr*<sup>+/+</sup> (will be referred to as *mdx*) and 25% would be *mdx/Utr*<sup>-/-</sup>, while the other 50% would be *mdx/Utr*<sup>+/-</sup>. However, based on offspring from several generations, the percentages of mice per genotype was greater for *mdx/Utr*<sup>+/-</sup> (~60%), than *mdx* (~30%) and *mdx/Utr*<sup>-/-</sup> (~10%). This is consistent with the findings of others (Dr. Robert Grange, personal communication) and indicates some *in utero* loss of the *mdx/Utr*<sup>-/-</sup> mice. Moreover, not all animals born lacking both dystrophin and utrophin survived for 2 mos. At approximately two mos of age, mice were used for assessment of E-C coupling in single muscle fibers. This age was chosen based on the shortened lifespan (100% lethality by 90-

100d) of the *mdx/Utr<sup>-/-</sup>* mice (95) and previous reports by Capote *et al.* (68) which is a comparative data set. All mice were kept in the same room (typical ambient conditions 20.9% O<sub>2</sub> and 22±1°C) and had the same access to food and water, bedding, and light cycle (12h light/12h dark) until used for analyses. At time of use, animals were euthanized by cervical dislocation and tissues were rapidly dissected. Extensor digitorum longus (EDL) and plantaris muscles were quickly excised and frozen in liquid nitrogen and stored at -80°C for subsequent analysis. Single muscle fibers were obtained immediately after dissection from the flexor digitorum brevis (FDB) muscle.

Single muscle fiber isolation: The FDB single muscle fibers were obtained by collagenase digestion with Type 2 Collagenase (Worthington) in Minimal Essential Medium (MEM) with 10% fetal bovine serum (FBS) and 1% Penicillin/Streptomycin (Invitrogen) according to the protocol described by Bischoff (34). After incubation at 37°C in 95% O<sub>2</sub>/5% CO<sub>2</sub>, single muscle fibers were obtained by trituration. Subsequently, fibers were maintained in MEM solution with 10% FBS at 37°C, 95% O<sub>2</sub>/5% CO<sub>2</sub> until used for E-C coupling assessment. All single muscle fibers were evaluated at room temperature.

Intracellular Ca<sup>2+</sup> measurements: One day after dissection, fibers were loaded with Fura-2AM for 15 min. The Fura-2 ratio was assessed in response to varying stimuli (see protocol below) as an index of [Ca<sup>2+</sup>]<sub>i</sub> and the E-C coupling response. Fibers loaded with Fura-2AM were placed in a stimulation chamber containing parallel electrodes that was positioned on a Nikon TiU microscope stage. Intracellular Ca<sup>2+</sup> levels were assessed by the Fura-2 fluorescence ratio using an IonOptix Hyperswitch system with dual excitation, single emission filter set for Fura-2 (Excitation 340nm and 380nm; Emission 510nm). Signals were captured and analyzed using the IonWizard software (IonOptix).

Single muscle fiber stimulation protocol: Muscle fibers were continuously perfused with a stimulating tyrode solution (units in mM - NaCl, 121.0; KCl, 5.0; CaCl<sub>2</sub>, 1.8; MgCl<sub>2</sub>, 0.5; NaH<sub>2</sub>PO<sub>4</sub>, 0.4; NaHCO<sub>3</sub>, 24.0; and glucose, 5.5) with 0.2 % FBS (78). This solution was bubbled with 95% O<sub>2</sub>/5% CO<sub>2</sub> to maintain a pH of 7.3 (78). The muscle fibers used for assessment were selected based on 3 criteria: i) normal shape (non-branched); ii) initial response to 15Hz stimuli; and iii) normal contractile behavior when exposed to six 100Hz tetani (2s between each). Fibers that elicited robust contractions in response to the 100Hz stimuli were deemed suitable for repeated tetanic contractions to induce E-C coupling failure and thus used for subsequent analyses. This represented ~90% of CON and 60%, 50% and 20% of *mdx*, *mdx/Utr<sup>+/-</sup>* and *mdx/Utr<sup>-/-</sup>* fibers, respectively. Although branched fibers show greater deficits in Ca<sup>2+</sup> release in response to electrical stimulation (73, 211), we chose non-branched fibers due to the high rate of failure for fibers to complete the entire stimulation protocol (described below) and the inability to image specific regions of the branched fibers (i.e. branch bifurcation vs. trunk region).

Global Fura-2 ratio was assessed in muscle fibers using trains of stimuli at 10, 30, 50, 70, 100, 120, and 150Hz for 350ms. Fibers rested 1 min between frequencies, and then rested for 10 min before assessment at all frequencies again. After the first set of stimuli, fibers were either perfused with the calpain inhibitor ALLN (N-Acetyl-L-leucyl-L-leucyl-L-norleucinal (EMD Biosciences) at 1μM in ethanol (ETOH) or the vehicle ETOH (Veh) to test for acute exposure effects. Subsequently, fibers rested for 10 min before being stimulated by repeated 100Hz tetani to induce E-C coupling failure. Fibers were evaluated again 1 hr after repeated tetani at the same 7 stimulation frequencies to evaluate the prolonged decrease in E-C coupling. Fibers that did not continue to respond to stimuli

throughout this protocol were counted as “fibers not responding to stimuli” and the percent of fibers failing to respond relative to total fibers assessed were recorded.

Peak Fura-2 ratios at each frequency were determined by the average ratio in the last 100ms of the 350ms tetanus, when  $\text{Ca}^{2+}$ -Fura-2 should be at a steady state. For fibers where the peak Fura-2 levels were not maintained for 350msec, separate analyses were completed to determine the percent of fibers failing to maintain peak  $\text{Ca}^{2+}$  levels (i.e. failing fibers) at each stimulation frequency. The number of failing fibers, relative to the number of fibers assessed (% failing), was also determined for each genotype.

Assessment of E-C coupling failure: Fibers were exposed to intermittent 100Hz tetani (350ms duration) starting at 1 contraction every 4 sec for 2 min, then 1 contraction every 3 sec for 2 min, then 1 contraction every 2 sec for 2 min, and then 1 contraction every sec for 2 min (79). We used an indirect assessment of muscle fatigue, the time for Fura-2 signal to decline, because we were not able to measure force production in our single muscle fiber preparation. Using this same protocol for repeated tetanic contractions, it was previously shown that the point of fatigue, defined as a 70% decrease in force, corresponded with a 50% reduction in  $[\text{Ca}^{2+}]_i$  and induced prolonged impairments in E-C coupling (79, 359). Thus, we used time to 50% decline in Fura-2 peak as the criterion for “fatigue” and induction of E-C coupling failure, and discontinued the repetitive 100Hz tetani at that point. One hour after inducing E-C coupling failure, single fiber Fura-2 ratios were re-assessed in the same fiber using the same stimulation protocol (10, 30, 50, 70, 100, 120, and 150Hz) to determine the prolonged decrease in E-C coupling as an index of muscle weakness (80).

Determining the role of proteases in prolonged E-C coupling failure: To evaluate the role of proteases in the prolonged decrease in E-C coupling, muscle fibers were continuously perfused with a protease inhibitor (ALLN) or Veh after the first set of stimulation frequencies and throughout the entire protocol. Changes in Fura-2 ratios pre- vs. post- E-C coupling failure were compared between fibers exposed to ALLN and those exposed to Veh. The pan-protease inhibitor (ALLN) used is a potent inhibitor of the Ca<sup>2+</sup> activated proteases  $\mu$ -calpain (Ki 190nM) and calpain-2 (Ki 220nM) compared with other proteases (cysteine proteases and proteasome, Ki 6 $\mu$ M), although it also potently inhibits Cathepsin B (Ki 150nM) and Cathepsin L (Ki 500pM).

Assessment of maximal calpain activity in dystrophic muscle: Extensor digitorum longus (EDL) and plantaris (PLT) muscles were used to determine maximum calpain activity. Based on the sample size needed to achieve 80% power to detect a p<0.05 difference (n=7), we used muscle from the cohort of mice used in the present study combined with samples obtained in a similar fashion from subsequent studies which were stored at -80°C. Maximal calpain activity was determined using a calpain assay kit (Calbiochem Cat. No. QIA120) as described by the manufacturer. Muscles were homogenized in lysis buffer (20 mM Hepes, pH 7.5, 100 mM NaCl, 1.5 mM MgCl<sub>2</sub>, 0.1% Triton X-100, 20% Glycerol) containing 1 mM DTT and protease inhibitor cocktail (complete mini EDTA-free Protease Inhibitor Cocktail, Roche). The cytosolic fraction was obtained by centrifugation (20000g for 5 min). Calpain distribution in CON muscle is diffused throughout the cytoplasm and slightly enriched in the cell membrane (322). Further, calpain localization changes slightly in dystrophic mice at different stages of the disease. At the age we evaluated the animals (~8 wks old), most of the calpain is localized

in the cytoplasmic portion of the muscle (322). Maximal calpain activity was determined by the amount of AMC released by its cleavage from the substrate Suc-LLVY-AMC in the presence of tissue lysate. Several studies have used a similar protocol to assess maximal calpain activity in muscle homogenates (52, 75, 190). AMC cleavage was measured using a fluorescence plate reader (Perkin Elmer Wallac Victor 1420) with Excitation of 340nm and Emission of 460nm. Calpain activity is expressed as relative fluorescence units (RFU) of AMC per gram (g) tissue. Muscle lysates were incubated with either activation (10mM  $\text{Ca}^{2+}$ ) or inhibition (5mM BAPTA) buffer, and calpain activity determined as the difference between the activation and inhibition buffers. To assess the efficacy of ALLN to inhibit calpain specifically, we also evaluated calpain activity in muscle lysates with activation buffer in the presence of 1 $\mu$ M ALLN (15 min exposure).

*Statistical Analysis:* SPSS software (version 18.0; IBM Somers, NY) was used to calculate between and within genotypes differences in Fura-2 ratio for resting Fura-2 and peak Fura-2 at each stimulation frequency, time to E-C coupling failure, increase in resting Fura-2 ratio during repeated tetani, Fura-2 ratios at each frequency pre- vs. post E-C coupling failure, and maximal calpain activity. One way Analysis of Variance (ANOVA) was used for group comparisons, with the Scheffe test for post-hoc analyses. For changes in Fura-2 ratio pre- vs. post E-C coupling failure, a paired t-test was performed. For comparing maximum calpain activity between CON and dystrophic genotypes, and between +/- ALLN treatment in vitro, unpaired t-tests were used. To compare the percentage of failed fibers between groups, a chi square test was used. The statistical significance was accepted at  $p < 0.05$ . Values shown represent the mean  $\pm$  standard error of the mean (SEM) as specified.



## Results

### Animals and single muscle fibers

The characteristics of animals and number of fibers analyzed in the current study are shown in Table 1. Body mass of *mdx/Utr<sup>-/-</sup>* mice was significantly lower than the other genotypes ( $p < 0.05$ ), consistent with previous reports (68, 95, 148). The diameter of fibers was also significantly smaller for *mdx/Utr<sup>-/-</sup>* mice compared with fibers from all other genotypes ( $p < 0.05$ ; see Table 3.1). There were no differences in fiber length between groups (data not shown).

### Ca<sup>2+</sup> handling

Resting Fura-2 ratio, representing resting  $[Ca^{2+}]_i$ , was higher in all dystrophic phenotypes compared with CON fibers ( $p < 0.05$ ; Table 3.1) with no differences between *mdx*, *mdx/Utr<sup>+/-</sup>*, *mdx/Utr<sup>-/-</sup>*. The peak Fura-2 ratio during stimulation was similar in all fibers from the various genotypes across all stimulation frequencies (data not shown). Acute (10min) exposure to ALLN or Veh did not alter the Fura-2 levels in response to stimulation at any of the frequencies measured (data not shown).

### E-C coupling failure

Excitation-contraction coupling failure was induced by subjecting single muscle fibers to repeated 100Hz tetani with gradually decreasing rest intervals between tetani until Fura-2 peak reached 50% of the initial level. A representative trace for the change in Fura-2 ratio with repeated tetani from an *mdx* fiber is shown in Figure 3.1. There were no differences in time to E-C coupling failure (i.e. 50% initial Fura-2 peak) between fibers from CON and dystrophic mice (Table 3.2). During repeated tetani there is a characteristic

increase in resting  $[Ca^{2+}]_i$  (358). In all groups, there was an increase in resting Fura-2 ratio at the end of the contractions, but the magnitude of increase in resting Fura-2 ratio in response to repeated tetani was not different between CON and dystrophic fibers (Table 3.2). Therefore, all fibers were exposed to the same number of tetani (~90 tetani) and the same magnitude of increase in resting  $Ca^{2+}$  during the repeated tetani.

Although all fibers from the CON and dystrophic mice were exposed to the same number of tetani, there was a large discrepancy in the ability of fibers to respond to the test contractions following the 1hr recovery. After repeated tetani, eight of eleven fibers (73%) from *mdx/Utr<sup>-/-</sup>* mice were either unable to respond to stimuli (n=6) or demonstrated abnormal  $Ca^{2+}$  transients (n=2) (Table 3.3). While there were fibers from both *mdx* and *mdx/Utr<sup>+/-</sup>* mice that either failed to maintain the Fura-2 peak during the 350ms stimulus or did not respond to stimuli after the repeated tetani, the % failing fibers was highest for *mdx/Utr<sup>-/-</sup>* mice (Table 3.3;  $p < 0.05$ ). These data indicate that *mdx/Utr<sup>-/-</sup>* muscle fibers are more severely impaired by repetitive contractile activity.

#### Effect of protease inhibition on E-C coupling failure

There were no differences in time to reach 50% initial  $[Ca^{2+}]_i$  between treatment conditions (Veh and ALLN), for fibers from CON and dystrophic mice (Table 2). Also, there were no differences in resting Fura-2 ratio increase during repeated contractions in Veh compared with ALLN treated fibers for any of the genotypes (Table 3.2). Thus, protease inhibition did not alter the level of  $[Ca^{2+}]_i$  that enzymes such as proteases were exposed to during the repeated tetani.

As shown in Figure 3.2, there were no differences in peak Fura-2 ratios pre vs. post repeated tetani for CON fibers exposed to Veh or ALLN (Fig. 3.2A & 3.2B). This outcome

indicates that there was no long-lasting decrease in E-C coupling in response to repeated tetanic contractions in non-dystrophic fibers and no effect of ALLN treatment. In contrast, there were differential effects of the repeated tetani on peak Fura-2 ratio in dystrophic fibers in the absence and presence of ALLN. In fibers from *mdx* and *mdx/Utr<sup>+/-</sup>* there was an average  $30 \pm 5.6\%$  and  $23 \pm 2.0\%$  decrease, respectively, in peak Fura-2 ratio, in response to the tetani when treated with Veh (Figures 3.2C & 3.2E;  $p < 0.05$ ). This decrease, however, was not observed in fibers treated with ALLN (Figures 3.2D & 3.2F). Fibers from *mdx/Utr<sup>-/-</sup>* (Veh) had lower Fura-2 ratios after repeated tetani at some but not all stimulation frequencies (100 and 120Hz,  $p < 0.05$ ; Figure 3.2G). On average Fura-2 ratio decreased  $36 \pm 3.1\%$  across all stimulation frequencies in Veh treated fibers from *mdx/Utr<sup>-/-</sup>* mice ( $p < 0.01$ ), a greater decrease compared with *mdx* and *mdx/Utr<sup>+/-</sup>* ( $p < 0.05$ ), indicating greater E-C coupling failure in fibers lacking both dystrophin and utrophin. This deficit was not observed in fibers treated with ALLN (Figure 3.2H). Given that only 5 out of 11 (45%) of *mdx/Utr<sup>-/-</sup>* fibers responded to stimuli after repeated tetani, this assessment underestimates the true impairment of E-C coupling failure in these mice.

#### Maximal calpain activity in control and dystrophic muscles

To assess the potential for elevations in  $[Ca^{2+}]_i$  to activate calpain-dependent proteolysis, maximal calpain activity was measured *ex vivo* in muscle homogenates. Maximal calpain activity under maximal  $Ca^{2+}$ -activating conditions was significantly higher in *mdx* (2.8-fold), *mdx/Utr<sup>+/-</sup>* (2.1 -fold) and *mdx/Utr<sup>-/-</sup>* (2.9 -fold) compared with CON muscle ( $p < 0.05$ ) (Figure 3.3A). We also confirmed that ALLN, under the conditions used in the single fibers (1  $\mu$ M and 15 min exposure), could inhibit maximal calpain activity (95% decrease) in dystrophic muscle *ex vivo* (Figure 3B,  $p < 0.05$ ).

## Discussion

We examined the changes in E-C coupling in response to repeated tetanic contractions in single muscle fibers from three mouse models of DMD. We found that peak  $\text{Ca}^{2+}$  in response to electrical stimulation was not different between fibers from dystrophic and CON mice before repeated tetani but that intracellular  $\text{Ca}^{2+}$  was reduced in response to electrical activation after the repeated tetani in dystrophic mice indicating E-C coupling failure. This pattern was observed in fibers from *mdx*, *mdx/Utr<sup>+/-</sup>*, and *mdx/Utr<sup>-/-</sup>* mice but not in CON fibers. In fibers lacking both dystrophin and utrophin, there was a lower probability of the fibers being able to respond to electrical activation after repetitive contractions. The impairment appears to be due to protease activation because the decrease was mitigated in the presence of a protease inhibitor. Overall, these data suggest that repetitive activation of dystrophic muscle leads to protease activation which would be manifest as prolonged muscle weakness after a bout of activity.

Although the primary cause of DMD is due to the lack of dystrophin (168), many of the downstream mechanisms contributing to the muscle pathophysiology have not been fully elucidated. Weakening of the muscle membrane is one of the mechanisms that contribute to disease severity (23). It is known that dystrophic muscle has greater susceptibility to damage during eccentric contractions compared with normal muscle (374). Another mechanism that contributes to disease severity is related to intracellular modifications within dystrophic muscle. Studies have shown that muscles lacking dystrophin have increased oxidative stress, decreased antioxidant capacity and poor  $\text{Ca}^{2+}$  handling (137, 170, 287). A novel finding from this investigation is related to the role of proteases in the prolonged E-C coupling defects that would lead to muscle weakness in

dystrophic muscle. Dystrophin-deficient fibers treated with a pan-protease inhibitor could maintain stimulation-induced  $\text{Ca}^{2+}$  peaks after repeated contractions, whereas fibers treated with vehicle showed prolonged reductions in peak  $\text{Ca}^{2+}$  after a bout of repeated tetani (Figure 3.2).

### *Ca<sup>2+</sup> handling in dystrophic vs. normal muscle*

In the current study, we show that elevations in resting  $[\text{Ca}^{2+}]_i$  are similar in all three models of muscular dystrophy (Table 1). These data suggest that the lack of utrophin does not augment the increase in  $[\text{Ca}^{2+}]_i$  found in muscle fibers that lack only dystrophin. This outcome is consistent with previous reports of increased intracellular free  $\text{Ca}^{2+}$  concentration in fibers from *mdx* mice (170, 369, 370). However, other studies reported no difference in resting  $[\text{Ca}^{2+}]_i$  between CON fibers and muscle fibers from dystrophic *mdx* mice (83, 133, 203, 211, 280).

We reported no differences in peak tetanic  $\text{Ca}^{2+}$  at any of the stimulation frequencies assessed between CON, *mdx*, *mdx/Utr<sup>+/-</sup>* and *mdx/Utr<sup>-/-</sup>* fibers prior to repeated tetani, suggesting that there are no differences in E-C coupling and  $\text{Ca}^{2+}$  release mechanisms under normal physiological conditions. Previous studies evaluating differences in peak  $\text{Ca}^{2+}$  between *mdx* and CON fibers have shown inconsistent results with some studies reporting no differences between *mdx* and CON muscle (83, 163, 341, 343), and others showing lower  $\text{Ca}^{2+}$  release in dystrophic muscle (170, 211, 369, 370). Capote et al. (68) reported that both *mdx* and *mdx/Utr<sup>-/-</sup>* fibers have peak  $\text{Ca}^{2+}$  release that is reduced compared with CON fibers, but that there is no further reduction in the absence of utrophin (i.e. peak  $\text{Ca}^{2+}$  release from *mdx/Utr<sup>-/-</sup>* fibers were similar to *mdx* fibers). In the current study we did not observe these differences in peak  $\text{Ca}^{2+}$  between fibers lacking dystrophin

or both dystrophin and utrophin and CON fibers. This discrepancy may be due to a number of technical differences, such as the type of muscle fiber preparation, the dye form used to assess intracellular  $\text{Ca}^{2+}$  and/or the resting tension of the fibers during assessment of  $\text{Ca}^{2+}$  transients.

#### *$\text{Ca}^{2+}$ -induced disruption of excitation-contraction coupling*

Previous studies have demonstrated the role of increased intracellular  $\text{Ca}^{2+}$  during repeated muscle contractions in the prolonged reduction in E-C coupling following a bout of activity (79, 80, 249). This inability to release  $\text{Ca}^{2+}$  in response to membrane depolarization is also seen in skinned muscle fibers exposed to high  $\text{Ca}^{2+}$  concentrations (197, 349, 350) and was shown to be due, at least in part, to calpain activation (252, 349, 350). Recently, Murphy et al. (249) showed that increases in  $[\text{Ca}^{2+}]_i$  in intact muscle fibers via repeated contractions in the presence of caffeine leads to E-C coupling disruption due to selective proteolysis of junctophilin-1 (249). Given the role of junctophilin-1 in the proper formation and maintenance of mature skeletal muscle triad junction (179, 189), these data suggest that junctophilin proteolysis contributes to prolonged impairments in E-C coupling. The proteolysis of junctophilin-1 and corresponding autolytic activation of calpain-1 (249) further suggest that  $\text{Ca}^{2+}$ -activated proteases contribute to prolonged disruption of the skeletal muscle triads and thus E-C coupling failure. Although we did not measure proteolysis of these target proteins in the current study, our data are consistent with this mechanism of E-C coupling failure being due to protease activation.

In the current study, we assessed intracellular  $\text{Ca}^{2+}$  in non-branched fibers. Others have shown that force production, and peak intracellular  $\text{Ca}^{2+}$  are reduced and that susceptibility to damage is increased in branched compared with non-branched dystrophic

fibers (73). Furthermore, when specific regions within a fiber are assessed using confocal microscopy, greater reductions in electrically-induced  $\text{Ca}^{2+}$  transients are observed in the branch of the bifurcated fiber compared with the linear trunk region of the same fiber (211). Our imaging technique only allowed us to measure average intracellular  $\text{Ca}^{2+}$  across a fiber and therefore we were not able to address differences in branched vs. unbranched regions. Therefore we focused on the unbranched fibers. As a result, our findings likely underestimate the magnitude of change in E-C coupling failure that may occur in dystrophic muscle *in vivo* where there are both branched and unbranched fibers.

In the current study we have only measured the average intracellular  $\text{Ca}^{2+}$  in response to electrical activation. We have not directly assessed whether a ryanodine receptor agonist (i.e. caffeine) could overcome the reduction in  $\text{Ca}^{2+}$  transient nor have we assessed the role of  $\text{Ca}^{2+}$  stores in this reduction. Thus, we cannot infer that the cause was a true impairment in electrical activation of  $\text{Ca}^{2+}$  release from SR  $\text{Ca}^{2+}$  stores. Rather our data show only a deficit in the  $\text{Ca}^{2+}$  transient in response to electrical activation after repetitive stimuli and that this reduction is mitigated with a protease inhibitor in all 3 models of muscular dystrophy.

#### *Effects of protease inhibition on E-C coupling in dystrophic muscle*

Calpains are non-lysosomal  $\text{Ca}^{2+}$ -activated proteases that, when activated, participate in the breakdown of muscle proteins. We hypothesized that impaired intracellular  $\text{Ca}^{2+}$  regulation in dystrophic muscle would be exacerbated during repeated tetani and this would contribute to greater E-C coupling disruption in single muscle fibers lacking both dystrophin and utrophin. In dystrophic muscles, there was a 2.1 to 2.9 –fold increase in maximal calpain activity measured *ex vivo*. This, combined with the finding

that ALLN eliminated the reduction in peak  $\text{Ca}^{2+}$  following tetanic contractions in single fibers from the dystrophic mice, support the notion that proteases play an important role in prolonged E-C coupling failure. Since ALLN is also a potent inhibitor of other proteases it is possible that other proteolytic enzymes contributed to the E-C coupling impairment. The primary target of ALLN is calpain-1, however calpain-2 and Cathepsin B are also inhibited by ALLN with similar potency, while Cathepsin L is inhibited at a greater potency (~400-fold more potent for Cathepsin L). We did confirm in our *ex vivo* assay that ALLN effectively inhibits calpain activity in muscle tissue lysates (Figure 3.3B).

The repeated tetani that reduce tetanic  $[\text{Ca}^{2+}]_i$  post-contraction are expected to increase calpain activity and result in prolonged reductions in muscle force (i.e. muscle weakness) (79, 359) in dystrophic muscle. Further, bouts of contractile activity are expected to increase calpain activity to a similar extent in both dystrophin null (*mdx*) and dystrophin/utrophin null (*mdx/Utr<sup>-/-</sup>*) fibers. A limitation of the current study is that we did not measure the acute increase in calpain activity with stimulation. However previous studies have shown increased calpain activity of ~26% during exercise (16) and 13-25% (291) with resistive loading of the diaphragm and thus we expect a similar increase with the repeated contractions used in this study. Given that ALLN blunted the prolonged E-C coupling failure, our data suggests that a pan-protease inhibitor would protect against the contractile-induced impairments in  $\text{Ca}^{2+}$  release (and thus muscle weakness) in dystrophic muscle by preventing this acute activation of calpain activity. In the present study we have not identified the specific targets of calpain/protease activation. While this is a limitation of the present study, others have shown that elevations in  $\text{Ca}^{2+}$  are associated with key calpain-induced alterations of proteins involved in E-C coupling (i.e. ryanodine receptors,



junctophilin-1) (139, 249). Thus, alterations in these proteins may explain the calpain-dependent impairment in E-C coupling and the protection we observed with ALLN.

Studies evaluating the effectiveness of calpain inhibitors for improving muscle function in the *mdx* mouse model *in vivo* appear controversial but overall provide proof of concept for calpain inhibition attenuating muscle damage and improving muscle function (19, 52, 191, 309, 321). While some studies show a decrease in necrosis and regenerating areas (central nucleated fibers) within the muscle (19, 321), others show no differences in regenerating areas or in muscle necrosis (52, 309). In *mdx* mice treated for 30d with daily intramuscular injections of the calpain inhibitor leupeptin, there was a decrease in muscle fibrosis and necrosis (19). However, with long-term (6 mos.) leupeptin treatment by intraperitoneal (*ip*) injection there was no attenuation of fibrosis or necrosis; moreover, these mice had an increase in  $\mu$ -calpain and proteasome activity (309). Thus, short term rather than long-term chronic treatment may be beneficial. Mode of administration (direct muscle versus *ip* injections), may also be critical, leading to differences in efficacy in skeletal muscle.

A potentially more effective and less toxic calpain inhibitor, C101, did not reduce muscle necrotic area when animals were treated with daily injections from 8 to 12 weeks of age (309). The compound C101 was also examined in a canine model of DMD and although it showed some efficacy in maintaining muscle strength in cranial pelvic limb muscles, it failed to maintain strength in posterior pelvic limb muscle (77). Moreover, C101 did not attenuate the decrease in force following eccentric contractions or mitigate the muscle necrosis observed in the dystrophic dogs (77). Others have shown that inhibition of both  $\text{Ca}^{2+}$ -dependent ubiquitin proteasome as well as calpain inhibition using

a small molecule inhibitor is more beneficial in reducing muscle damage (52). Combined with data from the current study, broader spectrum protease inhibitors targeting other proteolytic enzymes may be most effective in mitigating muscle damage, impaired contractile function and prolonged E-C coupling defects in dystrophic muscle. Future studies need to address *in vivo* dosing strategies to optimize the benefits of calpain and other protease/proteasome inhibition acutely after repetitive contractile activity while not suppressing the beneficial role of proteolysis in normal turnover of muscle proteins.

In conclusion, this study is the first to demonstrate the role of proteases in the prolonged E-C coupling failure following repeated muscle contractions in multiple dystrophic mouse models. Dystrophic single muscle fibers are less likely to respond to electrical stimulation after fatigue-inducing contractions, and this failure is greater in fibers lacking both dystrophin and utrophin. However, the prolonged E-C coupling failure can be prevented by a potent pan-protease inhibitor. Protease inhibition may therefore be beneficial in protecting against prolonged weakness in dystrophic muscle after an acute bout of activity, rather than as a long term treatment to reduce protease activity.

### **Author contributions**

D.A.G.M.: contributed to the design of the experiments, data collection, analysis and interpretation, and drafting and revising the manuscript. R.W.G.: contributed to data interpretation, critically reviewed and made important intellectual contributions to the manuscript. E.R.C.: contributed to the conception and design of the experiments, interpretation of data, and revising the manuscript.

\*All authors gave final approval of the version to be published.

### **Acknowledgments**

This work was supported by the University of Maryland, College Park new investigator funds to ERC. Additional grant support was provided by the Department of Kinesiology Graduate Research Initiative Project (GRIP) and the National Institute on Aging Predoctoral Training Grant T32AG-00268 to DAGM. We wish to thank Dr. Diego Fraidenraich and Joel Schneider from the University of Medicine and Dentistry, New Jersey for advice on breeding and maintaining the *mdx/Utr<sup>+/-</sup>* colony and establishing the genotyping protocols. We also thank Dapeng Chen and Samuel Andrew English from the Department of Kinesiology, University of Maryland, for technical contributions to the project.

**Table 3.1 - Body mass and single muscle fiber characteristics for each genotype**

	<b>Number of mice</b>	<b>Body mass (g)</b>	<b>Number of fibers</b>	<b>Fiber diameter (<math>\mu\text{m}</math>)</b>	<b>Resting Fura-2 ratio</b>
<b>CON</b>	3	26 $\pm$ 0.3	13	31 $\pm$ 1.7	0.34 $\pm$ 0.02
<i>mdx</i>	5	28 $\pm$ 2.5	23	31 $\pm$ 1.4	0.37 $\pm$ 0.03**
<i>mdx/Utr</i> <sup>+/-</sup>	5	28 $\pm$ 1.2	28	30 $\pm$ 1.5	0.37 $\pm$ 0.03**
<i>mdx/Utr</i> <sup>-/-</sup>	4	14 $\pm$ 3.0*	21	23 $\pm$ 1.6*	0.36 $\pm$ 0.02**

All values are mean  $\pm$  SEM.

\* p < 0.05 vs. CON, *mdx*, and *mdx/Utr*<sup>+/-</sup>

\*\*p < 0.05 vs. CON

**Table 3.2 - Time to excitation-contraction coupling failure and change in resting Fura-2 ratio at failure**

	Time to 50% of initial Fura-2 peak		Increase in resting Fura-2 ratio	
	Veh	ALLN	Veh	ALLN
<b>CON</b>	395 ± 56sec	301 ± 21sec	0.11 ± 0.02	0.15 ± 0.05
<i>mdx</i>	352 ± 66sec	320 ± 84sec	0.16 ± 0.06	0.14 ± 0.03
<i>mdx/Utr<sup>+/-</sup></i>	260 ± 93sec	340 ± 55sec	0.08 ± 0.03	0.11 ± 0.03
<i>mdx/Utr<sup>-/-</sup></i>	238 ± 40sec	276 ± 76sec	0.10 ± 0.04	0.11 ± 0.04

All values are mean ± SEM.

**Table 3.3 - Summary of fibers unable to respond to stimuli or demonstrating failing peaks**

	Fibers failing to maintain peak		Fibers not responding to stimuli	
	Before fatigue	After fatigue	Before fatigue	After fatigue
<b>CON</b>	0/13 (0%)	1/13 (8%)	0/13 (0%)	1/13 (8%)
<i>mdx</i>	8/23 (35%)	2/13 (15%)	2/23 (9%)	1/13 (8%)
<i>mdx/Utr<sup>+/-</sup></i>	11/28 (39%)	4/14 (29%)	3/28 (11%)	1/14 (7%)
<i>mdx/Utr<sup>-/-</sup></i>	9/21 (43%)	2/11 (18%)	1/21 (5%)	6/11 (54%) *

All values are mean  $\pm$  SEM.

\*  $p < 0.05$  vs. CON, *mdx* and *mdx/Utr<sup>+/-</sup>*.

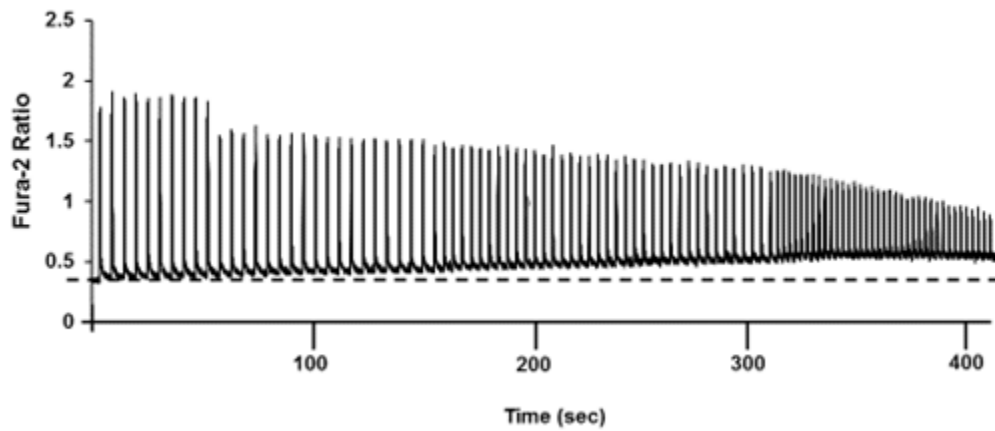


**Figure 3.1 – Raw data figure demonstrating changes in Fura-2 ratio during repeated contractions.** Time to E-C coupling failure was determined by the time to a 50% decrease in peak Fura-2 ratio relative to the initial peak. In this figure, each individual upward trace is a single Fura-2 peak. Note the progressive increase in the resting Fura-2 ratio during the fatigue protocol (dashed line corresponds to the initial Fura-2 ratio resting value) which is observed when peak Fura-2 is falling.

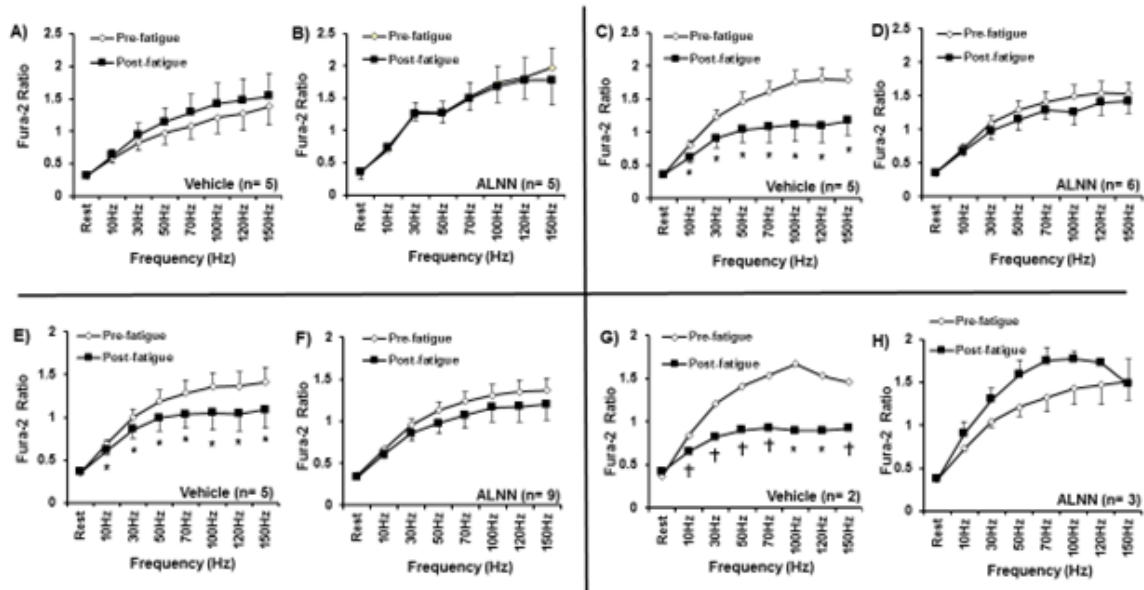


**Figure 3.2 – Peak Fura-2 ratio in single muscle fibers before after inducing excitation-contraction coupling failure with repetitive tetanic contractions.** Peak Fura-2 ratios are shown across the range of stimulation frequencies assessed before and one hour after recovery from repeated tetani. **A)** Vehicle treated fibers (n=5) and **B)** ALLN treated fibers (n=5) from CON mice; **C)** Vehicle treated fibers (n=6) and **D)** ALLN treated fibers (n=6) from *mdx* mice; **E)** Vehicle treated fibers (n=5) and **F)** ALLN treated fibers (n=9) from *mdx/Utr<sup>+/-</sup>* mice; and **G)** Vehicle treated fibers (n=2) and **H)** ALLN treated fibers (n=3) from *mdx/Utr<sup>-/-</sup>* mice. Data shown are mean  $\pm$  SEM. †  $P < 0.10$ ; \*  $P < 0.05$ .



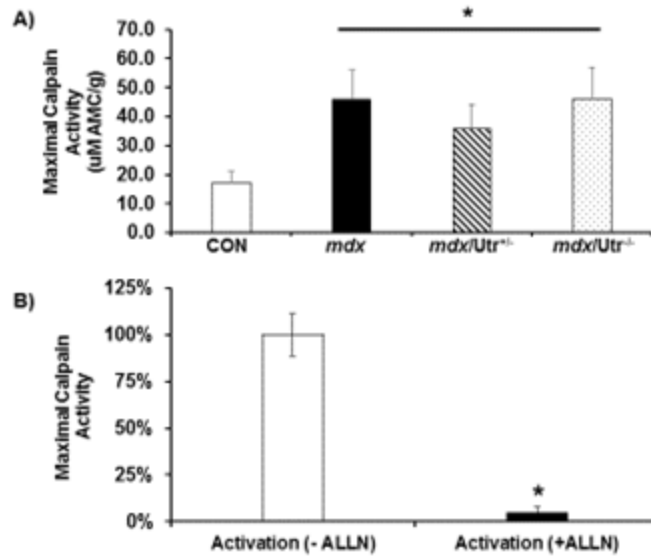


**Figure 3.3 – Maximal calpain activity in dystrophic and control muscle samples in the absence and presence of ALLN.** **A)** Maximal  $\text{Ca}^{2+}$ -induced calpain activation in extensor digitorum longus muscle from control (CON; n=9), *mdx* (n=12), *mdx/Utr<sup>+/-</sup>* (n=6), and *mdx/Utr<sup>-/-</sup>* (n=9) mice. **B)** Exposing muscle homogenates from plantaris muscle to  $1\mu\text{M}$  ALLN for 15 min greatly reduced  $\text{Ca}^{2+}$ -activated calpain activity in dystrophic muscle. White bar represents calpain activity in muscle homogenate exposed to activation buffer containing  $10\text{mM}$   $\text{Ca}^{2+}$  without ALLN (n=3); black bar shows calpain activity (expressed relative to white bar) under the same conditions but with addition of  $1\mu\text{M}$  ALLN (n=3). Bars represent percentage. Data shown are mean  $\pm$  SEM. \* $P < 0.05$ .

**Chapter 4: SERCA1 overexpression minimizes skeletal muscle damage in dystrophic mouse models**

The following study has been published in the *American Journal of Physiology-Cell Physiology*, 308: C699–C709, 2015; (doi:10.1152/ajpcell.00341.2014)

**SERCA1 overexpression minimizes skeletal muscle damage in  
dystrophic mouse models**

Davi A. G. Mázala<sup>1</sup>, Stephen J. P. Pratt<sup>2</sup>, Dapeng Chen<sup>1</sup>, Jeffery D Molkenin<sup>3</sup>, Richard M. Lovering<sup>2</sup> and Eva R. Chin<sup>1</sup>

Department of Kinesiology<sup>1</sup>, School of Public Health, University of Maryland,

Department of Orthopaedics<sup>2</sup>, University of Maryland School of Medicine and

<sup>3</sup>Department of Pediatrics, University of Cincinnati, Cincinnati Children's Hospital  
Medical Center.

**Correspondence to:** Dr. Eva Chin, School of Public Health, University of Maryland,  
2134b SPH Building, College Park, MD 20742 USA, [erchin@umd.edu](mailto:erchin@umd.edu)

**Running Title:** SERCA1 rescue of dystrophic muscle damage

**Key words:** Duchenne muscular dystrophy, *mdx*, *mdx/Utr<sup>-/-</sup>*, calcium, SERCA1, injury

## Abstract

Duchenne muscular dystrophy (DMD) is characterized by progressive muscle wasting secondary to repeated muscle damage and inadequate repair. Elevations in intracellular free  $\text{Ca}^{2+}$  have been implicated in disease progression and SERCA1 overexpression has been shown to ameliorate the dystrophic phenotype in *mdx* mice. The purpose of this study was to assess the effects of SERCA1 overexpression in the more severe *mdx/Utr<sup>-/-</sup>* mouse model of DMD. Mice overexpressing SERCA1 were crossed with *mdx/Utr<sup>+/-</sup>* mice to generate *mdx/Utr<sup>-/+</sup>*+SERCA1 mice and compared with wild-type (WT), WT/+SERCA1, *mdx*/+SERCA1 and genotype controls. Mice were assessed at ~12 weeks of age for changes in  $\text{Ca}^{2+}$ -handling, muscle mass, quadriceps torque, markers of muscle damage and response to repeated eccentric contractions. SERCA1 overexpressing mice had a 2- to 3-fold increase in maximal SR  $\text{Ca}^{2+}$  ATPase activity which was associated with an improvement in body mass for both *mdx*/+SERCA1 and *mdx/Utr<sup>-/+</sup>*+SERCA1 back to WT levels. . Torque deficit in the quadriceps after eccentric injury was 2.7-fold greater in *mdx/Utr<sup>-/-</sup>* vs. WT mice, but only 1.5-fold greater in *mdx/Utr<sup>-/+</sup>*+SERCA1 vs. WT mice, an attenuation of 44%. Markers of muscle damage (% central nucleated fibers, necrotic area, and serum creatine kinase) were higher in both *mdx* and *mdx/Utr<sup>-/-</sup>* vs. WT and all were attenuated by overexpression of SERCA1. These data indicate that SERCA1 overexpression ameliorates functional impairments and cellular markers of damage in a more severe mouse model of DMD. These findings support targeting intracellular  $\text{Ca}^{2+}$  control as a therapeutic approach for DMD.

Abbreviations: Duchenne muscular dystrophy (DMD), calcium ( $\text{Ca}^{2+}$ ), Sarcoplasmic/Endoplasmic Reticulum ATPase 1 (SERCA1), utrophin (Utr), wild-type (WT), tibialis anterior (TA), extensor digitorum longus (EDL), quadriceps (QUAD), centrally nucleated fibers (CNFs), serum creatine kinase (CK), Newton-millimeters (Nmm), Analysis of Variance (ANOVA), standard error of the mean (SEM), intracellular free  $\text{Ca}^{2+}$  [ $\text{Ca}^{2+}$ ]<sub>i</sub>.

## **Introduction**

Duchenne muscular dystrophy (DMD), the most common form of muscular dystrophy, is an X-linked disorder that was first described over a century ago (154). DMD is caused by the absence of dystrophin, a structural protein found on the cytoplasmic surface of the sarcolemma (168) and is characterized clinically by severe, progressive and irreversible loss of muscle function. While the genetic basis for DMD has been known since 1987 (168), the mechanism(s) responsible for the progressive muscle damage and decrease in muscle specific force production that occur secondary to the lack of dystrophin remain unclear. Two main theories have been proposed to explain the cellular basis for the marked and progressive muscle degeneration: i) a mechanical instability theory; and ii) an alteration in cell signaling theory (211). The mechanical instability hypothesis (117) suggests that, in the absence of dystrophin, the resulting mechanical weakness of either the sarcolemma or the cytoskeletal-sarcolemmal interface triggers a pathway of cellular damage, degeneration and repair (213, 336). An increase in myofiber damage observed secondary to stress, such as after forceful lengthening (“eccentric”) contractions, supports the concept of mechanical instability as the initial cause of symptoms associated with dystrophic skeletal muscle (272). The second hypothesis focuses on alterations in molecular signaling processes within dystrophic myofibers. Specifically, alterations in myofiber calcium ( $\text{Ca}^{2+}$ ), nitric oxide, and reactive oxygen species have been identified in dystrophic myofibers.

Elevations in intracellular free  $\text{Ca}^{2+}$  ( $[\text{Ca}^{2+}]_i$ ) and the downstream activation of protein degrading or necrotic pathways have been implicated in DMD disease progression (71, 132, 203). Although the precise mechanisms remain unclear, there is evidence to

support increased activation of membrane  $\text{Ca}^{2+}$  influx channels in the activation of  $\text{Ca}^{2+}$ -dependent proteases (i.e. calpains) (10, 52, 251, 335) and either cell necrosis or apoptosis (21, 100, 292, 317). Furthermore, there is evidence of impaired  $\text{Ca}^{2+}$  removal from the sarcoplasm due to reduced levels of the Sarcoplasmic/Endoplasmic Reticulum ATPase 1 (SERCA1) expression or impaired  $\text{Ca}^{2+}$  pumping capacity of SERCA1 (98, 186, 306). Investigations targeting SERCA1 upregulation supports the notion that increased levels of SERCA1 can mitigate the dystrophic pathophysiology as well as contraction-induced muscle damage in *mdx* mice (145, 243).

One challenge in understanding the cellular basis of DMD as well as developing effective therapeutic strategies is that not all animal models closely mimic the disease. The most universally used laboratory animal model of DMD, the *mdx* mouse, has an X-linked recessive mutation in the dystrophin gene that resembles that seen in boys with DMD (58). This mouse model lacks dystrophin (313) and shows some hallmark features of the DMD pathophysiology (58, 326). However, *mdx* mice live a near normal lifespan and the phenotype is transient and much less severe than that seen in patients with DMD, casting doubt on the *mdx* mouse as the most appropriate model of DMD (9). One reason that *mdx* mice do not display an equivalent pathophysiology to DMD may be due to utrophin (Utr) (357), a homologue of dystrophin, that in mice is up-regulated in the absence of dystrophin. This idea has been supported by the observation that mice lacking both dystrophin and utrophin (*mdx/Utr*<sup>-/-</sup>) have a much more severe myopathy (96, 148).

Based on studies demonstrating the role of impaired  $\text{Ca}^{2+}$  homeostasis and impaired SERCA1 in the dystrophic phenotype, we hypothesized that SERCA1 overexpression would mitigate the severe muscle pathophysiology observed in *mdx/Utr*<sup>-/-</sup> mice. The

purpose of this study was to compare changes in  $\text{Ca}^{2+}$  handling, muscle size and histology, contractile function and susceptibility to contraction-induced injury in wild-type (WT), *mdx*, and *mdx/Utr<sup>-/-</sup>* mice with or without overexpression of SERCA1. Our results show that overexpression of SERCA1 in dystrophic mouse models not only decreases markers of muscle damage, but also attenuates force loss after maximal eccentric contractions. This is the first report to show significant changes in the *mdx/Utr<sup>-/-</sup>* mouse from SERCA1 overexpression. These novel findings suggest that improvements in control of  $[\text{Ca}^{2+}]_i$  may be of importance in the development of therapies for DMD.



## Materials and methods

Ethical Approval: All procedures were conducted under a protocol approved by the Institutional Animal Care and Use Committee of the University of Maryland, College Park.

Animal breeding and genotyping: A breeding pair of SERCA1 overexpressing (+SERCA1) mice were obtained from the Cincinnati Children's Hospital Medical Center. Briefly, +SERCA1 mice were generated using a modified human skeletal muscle  $\alpha$ -actinin promoter to selectively overexpress the fast muscle isoform SERCA1 (145) in skeletal muscle. Breeders were then used to establish a colony of +SERCA1 mice at the University of Maryland Central Animal Research Facility. Animals were genotyped using the following forward and reverse primer sequences: 5'-CGA GAG TAG CAG TTG TAG CTA -3' (forward) and 5'-ACA AAG GCA GTG ACA GT -3' (reverse). The thermocycler polymerase chain reaction (PCR) conditions consisted of 5 min at 94°C followed by 34 cycles of 94°C for 30 sec, 58°C for 30 sec, 72°C for 60 sec, and a final extension at 72°C for 5 min. Breeding pairs of *mdx/Utr*<sup>+/-</sup> were previously obtained from Dr. Diego Fraidenaich of the University of Medicine and Dentistry, New Jersey in collaboration with Dr. Robert Grange of Virginia Tech University. Offspring from *mdx/Utr*<sup>+/-</sup> mice were genotyped for Utr using a primer sequence and PCR conditions generously provided by Dr. Dawn A. Lowe from the University of Minnesota, Department of Physical Medicine & Rehabilitation. Genotyping for dystrophin was performed according to a protocol previously published (311).

To establish the +SERCA1 dystrophic mice, +SERCA1 mice were bred with *mdx/Utr*<sup>+/-</sup> mice. Offspring from +SERCA1 x *mdx/Utr*<sup>+/-</sup> were genotyped and used to

produce breeding pairs to generate *mdx/+SERCA1* and *mdx/Utr<sup>-/-</sup>/+SERCA1* mice. All animals, including WT, WT/+SERCA1, *mdx*, *mdx/+SERCA1*, *mdx/Utr<sup>-/-</sup>*, and *mdx/Utr<sup>-/-</sup>/+SERCA1* used in the present study were derived from our in-house animal colony. All mice were kept in the same room (typical ambient conditions 20.9% O<sub>2</sub> and 22 ± 1°C) with equal access to food and water, bedding, and light cycles (12 h light/12 h dark). For all evaluations, we used animals at 3 mo of age based on previous work by Goonasekera *et al.* (145).

*Experimental Procedures:* Two sub-sets of mice were used in the current study: i) mice used to analyze muscle mass, protein expression, SR Ca<sup>2+</sup> ATPase activity and [Ca<sup>2+</sup>]<sub>i</sub> levels in single muscle fibers; ii) mice used to evaluate quadriceps muscle function (torque and response to eccentric contractions) and muscle histology. In the sub-set of mice used to evaluate the effect of SERCA1 overexpression on muscle mass, [Ca<sup>2+</sup>]<sub>i</sub> handling and protein expression, animals were euthanized by cervical dislocation and the tibialis anterior (TA), extensor digitorum longus (EDL), soleus, plantaris, heart, and quadriceps (QUAD) were quickly dissected, weighed, and snap frozen in liquid nitrogen and stored at -80 °C. At time of sacrifice, the flexor digitorum brevis (FDB) muscle was removed and single muscle fibers isolated for assessing [Ca<sup>2+</sup>]<sub>i</sub> levels. In the subset of mice used to perform functional assessments, mice were anaesthetized with isoflurane and maintained under anesthesia throughout the duration of the assessment for muscle torque and injury (details below). At the end of the experiment, animals were sacrificed by cervical dislocation and muscles were obtained for histological assessments.

Single muscle fiber isolation and free  $[Ca^{2+}]_i$  measurements: Detailed methods for single muscle fiber isolation and  $[Ca^{2+}]_i$  measurements have been previously described (255). Briefly, single muscle fibers were obtained from the FDB muscle by collagenase digestion with type 2 collagenase (Worthington) in minimal essential medium (MEM) with 10% fetal bovine serum (FBS) and 1% penicillin-streptomycin (Invitrogen). After incubation at 37°C in 95% O<sub>2</sub>-5% CO<sub>2</sub>, single muscle fibers were obtained by trituration. Subsequently, fibers were maintained in MEM solution with 10% FBS at 37°C, 95% O<sub>2</sub>-5% CO<sub>2</sub> until used for  $[Ca^{2+}]_i$  assessment.

One day after dissection, fibers were loaded with Fura-2AM for 15 min. The Fura-2 ratio was measured in response to varying stimuli (see protocol below) as an index of  $[Ca^{2+}]_i$ . Fibers loaded with Fura-2AM were placed in a stimulation chamber containing parallel electrodes and the chamber was positioned on a Nikon TiU microscope stage. Muscle fibers were continuously perfused with a stimulating Tyrode solution (121.0 mM NaCl, 5.0 mM KCl, 1.8 mM CaCl<sub>2</sub>, 0.5 mM MgCl<sub>2</sub>, 0.4 mM NaH<sub>2</sub>PO<sub>4</sub>, 24.0 mM NaHCO<sub>3</sub>, and 5.5 mM glucose) with 0.2% FBS (78). This solution was bubbled with 95% O<sub>2</sub>-5% CO<sub>2</sub> to maintain a pH of 7.3 (78). Levels of  $[Ca^{2+}]_i$  were assessed by the Fura-2 fluorescence ratio using an IonOptix Hyperswitch system with dual excitation, single emission filter set for Fura-2 (excitation 340 nm and 380 nm; emission 510 nm). Signals were captured and analyzed using the IonWizard software (IonOptix). Global Fura-2 ratio was measured in muscle fibers using trains of stimuli at 10, 30, 50, 70, 100, 120, and 150 Hz for 350 ms with fibers resting 1 min between frequencies. Peak Fura-2 ratios at each frequency were determined by the average ratio in the last 100 ms of the 350 ms tetanus,

when  $\text{Ca}^{2+}$  Fura-2 should be at a steady state. All single muscle fibers were evaluated at room temperature.

Maximal  $\text{Ca}^{2+}$ -ATPase activity: Quadriceps muscles were homogenized and used to measure maximal SR  $\text{Ca}^{2+}$  ATPase activity in whole muscle homogenates as described by Chin *et al.* 1994 (81). Briefly, frozen muscles were weighted and homogenized in 200 mM Sucrose, 10 mM  $\text{NaN}_3$ , 1mM EDTA, and 40 mM L-histidine (pH 7.8), with a polytron at 60% maximal power for three 10 s intervals, separated by at least 30 s (81). Aliquots of the initial homogenate were frozen for analysis of maximal SR  $\text{Ca}^{2+}$ -ATPase activity. Maximal SR  $\text{Ca}^{2+}$ -ATPase activity was measured as described (81, 314) with assay modified for a 96 well plate. Briefly, the ATPase reaction was measured in buffer containing 20 mM HEPES, 200 mM KCl, 15 mM  $\text{MgCl}_2$ , 10 mM  $\text{NaN}_3$ , 1 mM EGTA, 0.3 mM NADH, 10 mM phosphoenolpyruvate (PEP), 5 mM ATP, 2  $\mu\text{M}$  calcium ionophore A23187, and 18 U/ml of both lactate dehydrogenase and pyruvate kinase (pH 7.0) and either 1 mM  $\text{CaCl}_2$  or 1 mM  $\text{CaCl}_2$  + cyclopiazonic acid (CPA). CPA is a selective inhibitor of the SR  $\text{Ca}^{2+}$ -ATPase. SR  $\text{Ca}^{2+}$ -activated ATPase activity was measured in triplicates in a 96 well plate at 37°C and maximum activity determined as the difference between maximal activity (1 mM  $\text{CaCl}_2$ ) and basal activity (1 mM  $\text{CaCl}_2$  + CPA).

SERCA1 protein expression: Total protein was isolated from QUAD by homogenization in lysis buffer (20 mM HEPES buffer, pH 7.5, 100 mM NaCl, 1.5 mM  $\text{MgCl}_2$ , 0.1 % Triton X-100, 20 % Glycerol) containing 1 mM DTT and protease inhibitor cocktail (cOmplete mini EDTA-free protease inhibitor cocktail, Roche Diagnostics, Indianapolis, IN). After 20 min incubation at 4°C, samples were centrifuged at 20,000g, supernatant collected and frozen at -80°C until analyzed. Total protein concentration was

determined using a BCA assay (Thermo Fisher Scientific Inc., Rockford, IL). Samples were solubilized in loading buffer and denatured by heating at 100°C for 5 min. For immunoblotting for SERCA1 expression, 10 µg total protein was loaded on bis-acrylamide gels, separated by SDS-PAGE electrophoresis then transferred to PVDF membrane (EMD Millipore, Billerica, MA). Membranes were blocked with 5% non-fat milk at room temperature for 1 h followed by over-night incubation at 4°C in anti-SERCA1 antibody (1:2500, Thermo Fisher Scientific Inc., Rockford, IL). GAPDH (1:2000, Thermo Fisher Scientific Inc., Rockford, IL) was used as a loading control. Proteins were detected with Clarity western ECL substrate (Bio-Rad Laboratories Inc., Hercules, CA) and imaged using Image Lab system (Bio-Rad Laboratories Inc., Hercules, CA) and protein levels quantified by densitometry. SERCA1 protein levels are expressed in arbitrary units (AU). Membranes were also stained with MemCode™ Reversible Protein Stain Kit (Thermo Fisher Scientific Inc., Rockford, IL) to confirm equal loading.

*Markers of Skeletal Muscle Damage:* Histological analysis was completed based on recommended standards from previously published protocols [TREAT-NMD - <http://www.treat-nmd.eu/research/preclinical/dmd-sops/>) and (282)]. For histological analysis, transverse sections were cut from frozen muscle on a cryostat (~8 µm thickness) and collected onto glass slides (Superfrost Plus; VWR, West Chester, PA). After fixation in methanol for 5 min followed by a 30 sec wash in H<sub>2</sub>O, samples were incubated in Harris modified hematoxylin solution for 3 min. After washing in H<sub>2</sub>O and Scott's tap water solution for 1 min each, slides were incubated in Eosin for 2 min. Samples were then washed in a series of ethanol solutions (50% x 30 sec, 75% x 30 sec, 95% x 2 min, 100% x 2 min) and then xylene (2 washes for 3 min each). Slides were mounted in Permount.

Sections were imaged using a Nikon Eclipse 50i microscope (20x objective) and Nikon's NIS-Elements Basic Research software. The percentage of centrally nucleated fibers (CNFs) was determined in a blinded fashion and was calculated as the number of fibers with central nuclei divided by the number of total fibers per muscle section. Muscle necrosis was determined by calculating the percentage area of the muscle with the presence of infiltrating inflammatory cells (basophilic staining), hypercontracted fibers, and degenerating fibers with scattered sarcoplasm (153) as a percentage (area) of the whole muscle section. For both percentage of CNFs and necrotic area, sections were randomized and viewed at 20X. Optical fields contained an average of  $183 \pm 19$  fibers and  $> 20$  fields were counted per muscle.

For assessment of creatine kinase (CK) activity, blood was collected from animals through heart puncture immediately prior to euthanasia. CK levels were determined using a Creatine Kinase Fluorometric Assay Kit (Cayman Cat. No. 700630) as described by the manufacturer. Briefly, blood was allowed to clot for 30 min at 25 °C and then spun at 2000 g for 15 min at 25 °C. The top yellow layer was then aspirated and saved in separate eppendorf tubes at -80 °C. The assay was run in triplicate and fluorescence was measured using an excitation wavelength of 370 nm and emission wavelength of 470 nm.

*Muscle torque and injury assessments:* Quadriceps torque measurements and injury induced by maximal lengthening contractions was performed *in vivo* as previously described (277, 278). With the animal anesthetized under isoflurane and placed in a supine position, the thigh and pelvis were stabilized and the ankle was secured onto a lever arm. The axis of the knee was aligned with the axis of the stepper motor and a torque sensor used to measure torque in Newton-millimeters (Nmm). The femoral nerve was stimulated

via subcutaneous needle electrodes (36BTP, Jari Electrode Supply, Gilroy, CA). Proper electrode position was determined by a series of isometric twitches and by observing isolated knee extension in the anesthetized animal. Length-tension and force-frequency curves were generated to ensure maximum isometric tension, and optimal length set prior to initiating lengthening contractions. For inducing lengthening contractions, a custom program, written on commercial software (LabVIEW version 8.5, National Instruments, Austin, TX), was used to synchronize contractile activation and the onset of forced knee flexion. Injury resulted from 15 maximal lengthening contractions (150Hz stimulation; 900°/sec) superimposed onto maximal quadriceps isometric contractions through a 40° - 100° arc of motion (full knee extension considered 0°) spaced 1 minute apart. Maximal isometric torque was measured before lengthening contractions and 5 minutes after the last lengthening contraction, and was used to calculate force deficits. Sham procedures (contractions without lengthening, or passive lengthening without contractions, both with knee immobilized) have been performed (277).

Radiography: Postural changes, such as excessive kyphosis, have been noted previously in the *mdx/Utr<sup>-/-</sup>* mice (59, 285, 353). To confirm those reports and assess any changes due to SERCA1 overexpression, radiographs (x-rays) were performed on a separate group of mice with a digital Faxitron radiography machine (Faxitron X-Ray LLC, Lincolnshire, IL). We used a previously established protocol to demonstrate the spine curvature of mice (the kyphotic index) by drawing two lines between the caudal margin of the last cervical vertebra and the caudal margin of the sixth lumbar vertebra (199).

Statistical Analysis: SPSS software (version 21.0; IBM Somers, NY) was used for statistical analyses of data. A one way Analysis of Variance (ANOVA) was used to

evaluate differences between all groups, with the Scheffe test for post-hoc analyses. In cases where two independent groups were compared (i.e. *mdx* vs. *mdx*/+SERCA1 or *mdx/Utr<sup>-/-</sup>* vs. *mdx/Utr<sup>-/-</sup>*/+SERCA1) we used a Student's t-test. The statistical significance was accepted at  $p < 0.05$ . Values shown represent the mean  $\pm$  standard error of the mean (SEM).



## Results

### Effect of SERCA1 overexpression on body mass, muscle mass, and intracellular calcium handling

The body and muscle mass of mice are shown in Table 4.1. The body mass of *mdx* mice was 13% greater than WT, while the body mass from *mdx/Utr<sup>-/-</sup>* was 35% lower than WT ( $p < 0.05$ ; Table 4.1). Body mass of dystrophic mice overexpressing SERCA1 (*mdx/+SERCA1* and *mdx/Utr<sup>-/-</sup>/+SERCA1*) was similar to WT mice, indicating that overexpression of SERCA1 was able to rescue the characteristic *greater* body mass of *mdx* mice and the *lower* body mass of *mdx/Utr<sup>-/-</sup>* model. Absolute muscle mass was higher in TA, plantaris, soleus and EDL of *mdx* mice compared with WT (Table 4.1) and this compensatory hypertrophy was attenuated with SERCA1 overexpression. Absolute muscle mass of QUAD and heart was significantly reduced in *mdx/Utr<sup>-/-</sup>* vs. WT, with the difference mitigated in *mdx/Utr<sup>-/-</sup>/+SERCA1* for QUAD, indicating rescue in the larger proximal skeletal muscle.

Since muscle hypertrophy is a known early response in dystrophic mice, we also evaluated changes in relative muscle mass (Figure 4.1). The relative mass of the TA, soleus, and plantaris from *mdx* was 22%, 27% and 25% greater, respectively, compared with WT ( $p < 0.05$ ; Figure 4.1). Moreover, the TA (37%), soleus (28%), plantaris (38%), and EDL (46%) had greater relative masses in *mdx/Utr<sup>-/-</sup>* vs. WT ( $p < 0.05$ ; Figure 4.1). Overexpression of SERCA1 in both *mdx* mice (*mdx/+SERCA1*) and *mdx/Utr<sup>-/-</sup>* (*mdx/Utr<sup>-/-</sup>/+SERCA1*) rescued this pseudo-hypertrophy in TA, soleus, plantaris, and EDL muscles. When expressed relative to body mass, we did not observe any differences in QUAD (Figure 4.1E) and heart muscle mass (Figure 4.1F) between *mdx* and *mdx/Utr<sup>-/-</sup>* relative to

WT. Interestingly, SERCA1 overexpression resulted in lower relative muscle mass for EDL and QUAD in WT mice ( $p < 0.05$ ; Figure 4.1), although no differences were found for TA, soleus, and plantaris. Similarly, hearts from WT/+SERCA1 mice had a greater muscle mass compared with WT mice ( $p < 0.05$ ; Figure 4.1F).

Aside from characterization of muscle mass, all experiments were performed using the QUAD muscle. This muscle was chosen since proximal muscles are affected earlier and to a greater extent in patients with DMD and the *mdx* mice (87, 226, 278). The QUAD muscle was also chosen because 1) it is a large muscle that allows for better assessment of differences in contractility; 2) is the only knee extensor; and 3) is more crucial for gait than the plantar flexors and dorsiflexors (279). We performed western blot analysis to determine the level of SERCA1 protein expression in the QUAD muscle of all genotypes (Figure 4.2A). SERCA1 content was higher in QUADs from WT/+SERCA1 vs. WT (77%;  $p < 0.05$ ), *mdx*/+SERCA1 vs. *mdx* (49%;  $p < 0.05$ ), and *mdx/Utr<sup>-/-</sup>*/+SERCA1 vs. *mdx/Utr<sup>-/-</sup>* (36%;  $p < 0.05$ ) (Figure 4.2A). This is consistent with previous characterization of the skeletal  $\alpha$ -actinin driven SERCA1 transgenic mouse showing increased expression of SERCA1 in QUAD, gastrocnemius, diaphragm and soleus muscle (145). There was no difference in SERCA1 content between WT, *mdx*, and *mdx/Utr<sup>-/-</sup>*, in agreement with previous findings for the QUAD muscle (306). To determine whether SERCA1 overexpression resulted in an increase in function (i.e. greater SERCA1 activity) we measured maximal SR  $\text{Ca}^{2+}$ -ATPase activity in QUAD muscle homogenates. Our results demonstrate that QUAD muscles from animals overexpressing SERCA1 had greater maximal  $\text{Ca}^{2+}$ -activated ATPase activity compared with genotype-matched animals (Figure 4.2B). Maximal  $\text{Ca}^{2+}$ -activated ATPase activity was 2.0 fold higher in

WT/+SERCA1 vs. WT ( $p < 0.05$ ), 1.8 fold higher in *mdx*/+SERCA1 vs. *mdx* ( $p < 0.05$ ), and 2.9 fold higher in *mdx*/Utr<sup>-/-</sup>/+SERCA1 vs. *mdx*/Utr<sup>-/-</sup> ( $p < 0.01$ ) indicating that SERCA1 overexpression resulted in an increase in total SR Ca<sup>2+</sup> ATPase enzyme in the muscle.

We also evaluated the effects of SERCA1 overexpression on [Ca<sup>2+</sup>]<sub>i</sub> levels in single muscle fibers isolated from the FDB muscle both under basal (resting) conditions and in response to electrical stimulation (Figure 4.3). Resting Fura-2 ratio was higher in *mdx* vs. WT fibers ( $p < 0.05$ ), although surprisingly was not higher in *mdx*/Utr<sup>-/-</sup> vs WT fibers. There were also no differences in resting Fura-2 ratios between WT vs. WT/+SERCA1 and *mdx*/Utr<sup>-/-</sup> vs. *mdx*/Utr<sup>-/-</sup>/+SERCA1. On the other hand, single muscle fibers from *mdx*/+SERCA1 had lower resting Fura-2 ratios compared with *mdx* fibers ( $p < 0.05$ ; Figure 4.3A). In response to electrical stimulation, single muscle fibers from WT/+SERCA1 had lower peak Fura-2 ratios compared with WT fibers ( $p < 0.05$  for 10, 30, 50, 70, 100, and 120Hz;  $p < 0.01$  for 150Hz – Fig. 3B). There were no differences in stimulation-evoked peak Fura-2 ratios between single muscle fibers from *mdx* vs. *mdx*/+SERCA1 and *mdx*/Utr<sup>-/-</sup> vs. *mdx*/Utr<sup>-/-</sup>/+SERCA1 (Figure 4.3C & 4.3D).

#### Effects of SERCA1 overexpression on markers of muscle damage

The effect of SERCA1 overexpression on muscle damage was evaluated by histology and circulating levels of CK. Skeletal muscles from WT/+SERCA1 mice did not show any pathological features compared with WT (see Figure 4.4A), consistent with a previous report by Goonasekera *et al.* (145). Muscle sections from *mdx* and *mdx*/Utr<sup>-/-</sup> mice had a greater number of CNFs compared with WT ( $p < 0.01$ ; Figure 4.4A & 4.4B) while *mdx*/+SERCA1 had 58% fewer CNFs compared with *mdx* mice ( $p < 0.05$ ; Figure 4.4A & 4.4B), and *mdx*/Utr<sup>-/-</sup>/+SERCA1 had 40% less CNFs compared with *mdx*/Utr<sup>-/-</sup> ( $p < 0.05$ ;

Figure 4.4A & 4.4B). Muscle necrosis was determined by the presence of basophilic staining (infiltrating inflammatory cells) and fibers with disrupted sarcoplasm (282). The percentage of necrosis in both *mdx* and *mdx/Utr<sup>-/-</sup>* was greater compared with WT ( $p < 0.05$  for *mdx* vs. WT, and  $p < 0.01$  for *mdx/Utr<sup>-/-</sup>* vs. WT Figure 4.4C). Muscle sections from *mdx/+SERCA1* had 50% less necrosis compared with *mdx* ( $p < 0.05$ ; Figure 4.4C), while muscle sections from *mdx/Utr<sup>-/-</sup>+SERCA1* had almost 90% less necrotic areas compared with *mdx/Utr<sup>-/-</sup>* ( $p < 0.01$ ; Figure 4.4C).

Creatine kinase is frequently used as an indirect measure of muscle damage in DMD (136, 144, 145, 153, 377). Both *mdx* and *mdx/Utr<sup>-/-</sup>* had greater CK levels compared with WT mice (86% greater for *mdx* and 76% for *mdx/Utr<sup>-/-</sup>*;  $p < 0.01$ ; Figure 4.4D). Overexpression of SERCA1 in *mdx* (*mdx/+SERCA1*) reduced CK levels by 60% compared with *mdx* mice ( $p < 0.05$ ; Figure 4.4D), results that support findings from Goonasekera *et al.* (145). The *mdx/Utr<sup>-/-</sup>+SERCA1* had a 50% reduction in blood CK levels compared with *mdx/Utr<sup>-/-</sup>* mice ( $p < 0.05$ ; Fig. Figure 4.4D).

#### Effects of SERCA1 overexpression on muscle torque and susceptibility to injury

To assess the effects of SERCA1 expression on skeletal muscle function, we used an *in vivo* model to assess QUAD muscle function before and after injury induced by repeated eccentric contractions. Without injury, muscle peak torque expressed relative to muscle mass (i.e., normalized peak torque) was ~43% lower in *mdx* compared with WT ( $p < 0.05$ , Figure 4.5A) indicating a reduction in muscle quality in *mdx* mice. In the QUAD of *mdx/Utr<sup>-/-</sup>* mice, normalized peak torque was 56% lower compared with WT ( $p < 0.05$ ; Figure 4.5A). We did not observe differences in normalized peak torque between *mdx* and *mdx/Utr<sup>-/-</sup>*, a finding different from previous studies that found differences in the posterior

crural muscles (gastrocnemius, soleus, and plantaris), EDL, and sternomastoid (65, 96, 148, 205). In WT mice with SERCA1 overexpression, there was no difference in normalized peak torque indicating that muscle quality was not altered in these mice ( $p = 0.14$ ). SERCA1 overexpression also did not alter normalized peak torque in *mdx* mice ( $p = 0.21$  vs. *mdx/+SERCA1*) or in *mdx/Utr<sup>-/-</sup>* mice ( $p = 0.19$  vs. *mdx/Utr<sup>-/-</sup>/+SERCA1*) compared with their genotype controls (Figure 4.5A). Overall, overexpression of SERCA1 did not rescue the deficit in normalized peak torque in either dystrophic mouse model.

To evaluate the possible protective effect of increased SERCA1 overexpression on the acute damage induced by eccentric contractions, we performed two different analyses to evaluate *in vivo* susceptibility to injury: 1) total percent loss in torque at the end of 15 eccentric contractions; and 2) average percent force loss during the 15 contractions (from rep 1 to rep 15). Lengthening contractions induced a greater deficit in torque in *mdx* and *mdx/Utr<sup>-/-</sup>* compared with WT mice ( $p < 0.05$ ; Figure 4.5B & 4.5C). Susceptibility to injury was reduced by the overexpression of SERCA1 in *mdx* mice (*mdx/+SERCA1*) and in *mdx/Utr<sup>-/-</sup>* mice (*mdx/Utr<sup>-/-</sup>/+SERCA1*). Our findings are in agreement with Morine *et al.* (243), in which overexpression of SERCA1 ameliorated *in vitro* contraction-induced damage in the diaphragm muscle of *mdx* mice.

#### Effects of SERCA1 overexpression on skeletal development in dystrophic mice

Muscle weakness is a key contributor to joint contractures, growth retardation and spinal curvature (i.e. kyphosis) in *mdx* and *mdx/Utr<sup>-/-</sup>* mice (199, 284). In *mdx/Utr<sup>-/-</sup>* mice the severe curvature (Fig. 6C) is reduced with SERCA1 overexpression (Figure 4.6B). This is consistent with the increased body mass in *mdx/Utr<sup>-/-</sup>/+SERCA1* mice, indicating

increased growth secondary to an improvement in muscle mass and attenuated muscle damage with contractile activity.

## Discussion

In the present study, we used two different mouse models of DMD with varying degrees of severity to show that overexpression of SERCA1 leading to a 2 to 3-fold increase in SR  $\text{Ca}^{2+}$  ATPase activity was sufficient to: 1) alter body and muscle mass to more closely resemble that of healthy animals; 2) decrease markers of muscle damage; and 3) protect the muscle from contraction-induced injury. More specifically, dystrophic mice overexpressing SERCA1 (*mdx/+SERCA1* and *mdx/Utr<sup>-/-</sup>+SERCA1*) had a lower incidence of CNFs and necrosis, and lower circulating CK levels compared with *mdx* and *mdx/Utr<sup>-/-</sup>*. While neither *mdx* nor *mdx/Utr<sup>-/-</sup>* dystrophic mice had any increase in relative peak torque or change in excitation-contraction (E-C) coupling with SERCA1 overexpression, both *mdx/+SERCA1* and *mdx/Utr<sup>-/-</sup>+SERCA1* were less susceptible to injury after eccentric contractions compared with *mdx* and *mdx/Utr<sup>-/-</sup>*. Overall, these results agree with and extend previous findings showing that SERCA1 overexpression can mitigate muscle damage in mouse models of DMD under both resting conditions and in response to eccentric contractions (145, 243). We hypothesize that this is due to the increased capacity of SERCA1 to remove cytosolic  $\text{Ca}^{2+}$  following influx with eccentric contractions. This is the first report to demonstrate that this approach can mitigate the disease phenotype in the *mdx/Utr<sup>-/-</sup>* mouse, a model with a more similar disease progression to that of DMD patients than the *mdx* mouse. These data support the notion that increased SERCA expression, or activity, could have therapeutic utility in DMD.

In the current study, we observed an attenuation of the pseudohypertrophy in limb muscles of *mdx* mice at 3 mos of age. Compared with WT, our observations of a 22-46% increase in muscle mass in *mdx* mice are consistent with previous reports showing a 20-

30% hypertrophy in soleus and EDL muscle (86) and a 20% (281) and 58% (267) increase in TA muscle in *mdx* mice under 6 mos of age. It is thought that this early hypertrophy is a compensatory effect, due to the muscle weakness and myocellular damage and consequent activation of satellite cells to induce new myofiber growth. The reduction in this hypertrophy with increased  $\text{Ca}^{2+}$  clearance capacity is consistent with the notion that  $\text{Ca}^{2+}$  -dependent pathways, including calcineurin activation, contribute to the adaptive hypertrophy early in the developmental stages of *mdx* mice (70, 328). The increased muscle size in *mdx* mice, however, does not result in an equivalent increase in force production per unit area, with both soleus and EDL muscle showing a decrease in specific force by 5 mos of age (214), indicating that these muscles are larger but weaker. Further, *mdx* muscles show evidence of cellular malformations including myofiber branching (120, 211) and altered E-C coupling (211). We also report pseudohypertrophy in the *mdx* and *mdx/Utr*<sup>-/-</sup> mice. In both disease models, SERCA1 overexpression rescued this pseudohypertrophy effect, bringing relative muscle mass down to WT levels.

Interestingly, SERCA1 overexpression also resulted in reduced muscle size in WT mice. It is possible that the increase in SR  $\text{Ca}^{2+}$  ATPase activity might result in increased energy expenditure and thus a smaller, less energy efficient muscle. It has recently been shown that treatment of muscle fibers with FK506 resulted in increased  $\text{Ca}^{2+}$  efflux from the ryanodine receptor with no significant increase in resting  $[\text{Ca}^{2+}]_i$  but rather an increase in energy expenditure (oxygen consumption) due to increased SR  $\text{Ca}^{2+}$  ATPase activation (50). Thus it is plausible that the increased energy expenditure from increased ATPase activity led to development of smaller, less efficient muscles. It was not the aim of the



current study to address this adaptation in WT muscle, but this issue warrants further investigation.

There was no improvement in QUAD normalized peak torque in either line of dystrophic mice indicating no improvement in specific tension (Figure 4.5A). This may be due to the fact that proximal muscles show an earlier and greater extent of damage in dystrophic mice (246), but this study also was not designed to detect a difference in normalized peak torque and thus was underpowered for this endpoint ( $\beta < 0.80$ ). This limitation is secondary to the challenges in breeding the *mdx/Utr<sup>-/-</sup>* mice (255). Although SERCA1 overexpression did not improve *mdx* and *mdx/Utr<sup>-/-</sup>* quadriceps torque production, the susceptibility to injury was attenuated in both dystrophic mouse models with SERCA1 overexpression. Morine *et al.* (243) previously showed an attenuation of eccentric-induced injury in diaphragm muscle with SERCA1 overexpression. However, we are the first to show a functional improvement in a hindlimb muscle group that is crucial to ambulatory activity. Overall, SERCA1 overexpression results in a relatively smaller but more durable muscle, capable of withstanding injury from repeated lengthening contractions.

Impaired  $\text{Ca}^{2+}$  homeostasis contributes to disease pathophysiology in dystrophic muscle (10, 138, 173, 236, 362). This appears to be due to both an increase in  $\text{Ca}^{2+}$  entry and reduced  $\text{Ca}^{2+}$  clearance. SERCA1 overexpression also reduced CNFs and necrotic area, indicating a less damaged, healthier muscle. Given the role of increased cytosolic  $\text{Ca}^{2+}$  in muscle degenerative/necrosis pathways (302), we postulate that increased expression of SERCA1 was critical in maintaining  $[\text{Ca}^{2+}]_i$  homeostasis and in reducing muscle damage in both *mdx* and *mdx/Utr<sup>-/-</sup>* during the described compensatory hypertrophy phase of 3 mo

old mice. One of the mechanisms that may contribute to increased sarcoplasmic  $\text{Ca}^{2+}$  entry in dystrophic muscle is store operated calcium entry (112, 236). Another source of  $\text{Ca}^{2+}$  influx in dystrophic muscle is through stretch-activated  $\text{Ca}^{2+}$  channels (361, 374). Isolated muscles from dystrophic mice treated with stretch-activated channel blockers (streptomycin or gadolinium) show improved muscle force production (361), while daily intraperitoneal injections of streptomycin decreased levels of blood CK and reduce cellular Evans blue dye uptake (227). Thus, current literature suggests multiple mechanisms that contribute to increased cytosolic  $\text{Ca}^{2+}$  levels in muscle of dystrophic mice and report evidence that inhibition of this  $\text{Ca}^{2+}$  influx attenuates the extent of muscle damage. Findings from the current study are consistent with these previous reports and reiterate the role of perturbations in  $[\text{Ca}^{2+}]_i$  in the disease pathophysiology in DMD and the ability of increased  $\text{Ca}^{2+}$  clearance mechanisms to attenuate muscle damage.

Dystrophic muscle has also been shown to have impairments in  $\text{Ca}^{2+}$  removal mechanisms such as the SERCA1 pump. Others (306) have shown that the expression of SERCA1 in the quadriceps does not differ between WT and dystrophic muscle, and is consistent with results from the present study. However, SERCA1 is decreased in diaphragm muscle (306) which also has a greater susceptibility to damage (106, 243). While SERCA1 protein levels may not be different in limb muscles, SR  $\text{Ca}^{2+}$  pump function is impaired, with both the rate of  $\text{Ca}^{2+}$ -dependent  $\text{Ca}^{2+}$  uptake and maximal velocity of SR- $\text{Ca}^{2+}$  uptake significantly decreased in dystrophic quadriceps muscle compared with WT (306). In the current study we did not observe any differences in resting  $[\text{Ca}^{2+}]_i$ , SERCA1 expression or maximum SR  $\text{Ca}^{2+}$  ATPase activity in *mdx* or *mdx/Utr<sup>-/-</sup>* muscle relative to WT. One possible reason is that SERCA1 regulatory proteins (i.e.

sarcolipin) are altered in *mdx* and *mdx/Utr<sup>-/-</sup>*, explaining the disconnect between SERCA1 expression level and SR Ca<sup>2+</sup> ATPase activity (306). It is known that sarcolipin, an SR membrane protein that inhibits SERCA1 and SERCA2 activities, is upregulated in dystrophic muscle and correlates with decreased SR Ca<sup>2+</sup> uptake velocity (306). A limitation in the current study is that we did not measure sarcolipin levels to determine whether it can explain the difference between our findings and those of Schneider and colleagues (306). We examined calsequestrin levels to see if there were any adaptive changes in SR Ca<sup>2+</sup> storage, and there was no difference between *mdx* and *mdx/Utr<sup>-/-</sup>* vs. WT or with SERCA1 overexpression (data not shown). Certainly, it is surprising that an ~100% increase in SERCA1 protein and a 2- to 3-fold increase in SR Ca<sup>2+</sup> ATPase lead to only minimal changes in muscle size and did not rescue pre-injury force production. Future studies are required to fully explore the SERCA1 regulatory proteins that effect sarcoplasmic Ca<sup>2+</sup> concentration in dystrophic muscle and cellular adaptations to increased SERCA1 levels.

A point of difference between the study from Schneider *et al.* (306) and the current study is that they observed a decrease in Ca<sup>2+</sup> uptake in dystrophic vs. WT mice but we did not detect a difference in SR Ca<sup>2+</sup> ATPase activity between these groups. Ca<sup>2+</sup> uptake, an *in vitro* assessment of Ca<sup>2+</sup> clearance capacity, was shown to be reduced in *mdx* (306) and  $\delta$ -sarcoglycan null mice (145) but SR Ca<sup>2+</sup> ATPase activity, an *in vitro* assessment of the maximum ATP catalytic rate of the SERCA pump, measured in the current study, was not reduced in *mdx* and *mdx/Utr<sup>-/-</sup>* vs. WT mice. SR Ca<sup>2+</sup> uptake *in vitro* could plausibly be altered without a decrease in SR Ca<sup>2+</sup> ATPase activity *in vitro* if membrane integrity is not maintained since Ca<sup>2+</sup> uptake measures require Ca<sup>2+</sup> to be sequestered and maintained in

membrane vesicles whereas this is not the case with ATPase activity measurement. Thus, membrane leakiness, which is thought to be a problem with dystrophic muscle, may be responsible for this difference between measurements of  $\text{Ca}^{2+}$  uptake *in vitro* versus *in vitro* SR  $\text{Ca}^{2+}$  ATPase activity per se.

Regardless of the cause, the inability to properly remove  $\text{Ca}^{2+}$  after contractions might be one of the factors contributing to increased sarcoplasmic  $\text{Ca}^{2+}$  levels, which leads to increased myofiber death through  $\text{Ca}^{2+}$ -dependent protease activation and mitochondrial  $\text{Ca}^{2+}$  overload in dystrophic muscle (10, 342, 362). Consistent with this notion, it was previously shown that SERCA1 overexpression attenuated muscle pathophysiology in both the *mdx* and the  $\delta$ -sarcoglycan null mouse models of DMD (145). In the current study we report a 2- to 3-fold increase in SR  $\text{Ca}^{2+}$  ATPase activity in SERCA1 overexpressing mice. This is similar to the 2- to 4-fold increase in SR  $\text{Ca}^{2+}$  uptake in SERCA1 overexpressing  $\delta$ -sarcoglycan null mice (145) which also show a rescue of the histopathology in their dystrophic mice. Reduced markers of muscle damage and improved function after lengthening contractions with increased SERCA1 further supports the idea that  $\text{Ca}^{2+}$  clearance mechanisms are rate-limiting for maintaining muscle health with repeated eccentric contractions in dystrophic muscle. There are reports now indicating that increased amount of SERCA1 protein and increasing total SR  $\text{Ca}^{2+}$  pump capacity can rescue some of the disease pathophysiology (145, 243). Future studies will be required to determine whether SERCA1 regulatory proteins are also altered when SERCA1 is overexpressed and what their functional consequences are on  $\text{Ca}^{2+}$  pumping capacity.

A striking finding in the current study is the attenuation of contraction-induced injury by overexpression of SERCA1. Although the traditional views was that eccentric

contraction induced injury was due to structural damage of the muscle, resulting in disruptions of the sarcomere, more recent evidence indicates that loss of force production following eccentric contraction is due to disruptions in excitation-contraction coupling (178, 355, 356). It has previously been shown that the acute decrease in force-producing capacity with eccentric contractions (i.e. within 1 hour) is both  $\text{Ca}^{2+}$ -dependent and dependent on the activation of  $\text{Ca}^{2+}$ -activated proteases (calpains) (380). This cellular change, following rupture of the plasma membrane, is due to an influx of  $\text{Ca}^{2+}$  through both stretch-activated and TRPC1 channels in the plasma membrane (379). Activated calpains are known to target components of the Z-disks, such as desmin and  $\alpha$ -actinin, as well as titin and proteins located at the triad junction responsible for E-C coupling, such as junctophilin-1 and -2 (249, 350, 380). Therefore, overexpression of SERCA1 may decrease the extent of muscle damage due to its ability to buffer intracellular calcium following influx from the extracellular space. This, in turn would minimize activation of calpains and the downstream degradation of proteins critical for E-C coupling, structural integrity of the muscle, and force production. This, in addition to healthier, less damaged muscle under rested conditions, would attenuate the damage due to eccentric contraction in *mdx/+SERCA1* and *mdx/Utr<sup>-/-</sup>+SERCA1* mice. Our data are consistent both with one previous report of reduced eccentric-induced force loss in diaphragm muscle from *mdx* mice with SERCA1 overexpression (243) and with the attenuation of eccentric-induced force loss in single fibers from *mdx* mice with inhibition of stretch-activated  $\text{Ca}^{2+}$  channels (361, 374).

In summary, we have shown that SERCA1 overexpression can mitigate the muscle hypertrophy, muscle damage and susceptibility to contraction-induced injury in two

models of DMD. These data indicate that increased SERCA1 can reduce the myocellular damage and improve functional outcomes in dystrophic mice. Further, these data support the validation of SERCA1 as a therapeutic target for new drug therapies in DMD.

## **Grants**

This work was supported by the University of Maryland, College Park new investigator funds to ERC. Grant support to DAGM was provided by the Department of Kinesiology Graduate Research Initiative Project (GRIP) and the National Institute on Aging Pre-doctoral Training Grant T32AG-00268. This work was also supported by grants to RML from the National Institutes of Health (1R01AR059179).

## **Disclosures**

Eva R. Chin is the Founder and Chief Scientific Officer of MyoTherapeutics. No other conflicts of interest, financial or otherwise, are declared by the authors.

## **Author contributions**

D.A.G.M.: contributed to the conception and design of the experiments, data collection, analysis and interpretation, and drafting and revising the manuscript. S.J.P.P.: contributed to data collection, analysis and interpretation, and drafting and revising the manuscript. D.C.: contributed to data collection, analysis and interpretation. J.D.M. contributed to the interpretation of data, and drafting and revising the manuscript. R.M.L.: contributed to the design of the experiments, interpretation of data, and drafting and revising the manuscript. E.R.C.: contributed to the conception and design of the experiments, interpretation of data, and drafting and revising the manuscript. \*All authors gave final approval of the version to be published.

## **Acknowledgments**

We wish to thank Dr. Diego Fraidenraich and Joel Schneider from the University of Medicine and Dentistry, New Jersey for advice on breeding and maintaining the *mdx/Utr<sup>+/-</sup>* colony and establishing the genotyping protocols. We also thank Mathew Liu and Pai Han Cheng from the University of Maryland, for technical contributions to the project.



**Table 1 – Effects of SERCA1 overexpression on body and muscle mass**

	Genotype					
	WT	WT/+SERCA1	<i>mdx</i>	<i>mdx</i> /+SERCA1	<i>mdx/Utr<sup>-/-</sup></i>	<i>mdx/Utr<sup>-/-</sup></i> /+SERCA1
Number of animals	20	16	14	16	5	8
Body mass (g)	29.6 ± 0.7	24.5 ± 1.6*	34.1 ± 1.1*	31.1 ± 0.7 <sup>&amp;</sup>	19.2 ± 3.6*	28.5 ± 1.2 <sup>¥</sup>
TA (mg)	44.3 ± 1.2	36.6 ± 3.7	67.4 ± 3.2*	44.4 ± 2.6	46.4 ± 8.5	54.5 ± 3.7
Plantaris (mg)	16.4 ± 0.4	12.9 ± 1.2	22.7 ± 0.8*	14.7 ± 1.3	14.9 ± 2.6	19.8 ± 0.3
Soleus (mg)	6.4 ± 0.2	6.4 ± 0.9	10.0 ± 0.5*	7.3 ± 0.4	6.4 ± 1.7	7.2 ± 1.1
EDL (mg)	9.0 ± 0.4	5.8 ± 0.6	12.7 ± 0.8*	6.8 ± 0.6	10.9 ± 1.9	7.4 ± 2.8
QUAD (mg)	271.5 ± 27.8	141.8 ± 31.0*	312.0 ± 16.8	219.0 ± 19.0	120.0 ± 28.2*	259.2 ± 33.9
Heart (mg)	136.2 ± 5.1	153.6 ± 18.6	156.6 ± 7.3	165.8 ± 4.7	100.9 ± 15.7*	153.0 ± 18.3

**Table 4.1 – Animal morphometric characteristics.** Total number of animals, body mass and muscle mass for mice of all genotypes used for all experiments. Muscles analyzed include tibialis anterior (TA), plantaris, soleus, extensor digitorum longus (EDL), quadriceps (QUAD) and heart [WT (n=9), WT/+SERCA1 (n=8), *mdx* (n=8), *mdx*/+SERCA1 (n=10), *mdx/Utr<sup>-/-</sup>* (n=5), and *mdx/Utr<sup>-/-</sup>*/+SERCA1 (n=5)]. \*p < 0.05 vs. WT; & p < 0.05 vs. *mdx*; ¥ p < 0.05 vs. *mdx/Utr<sup>-/-</sup>*. Data presented as mean ± SEM.

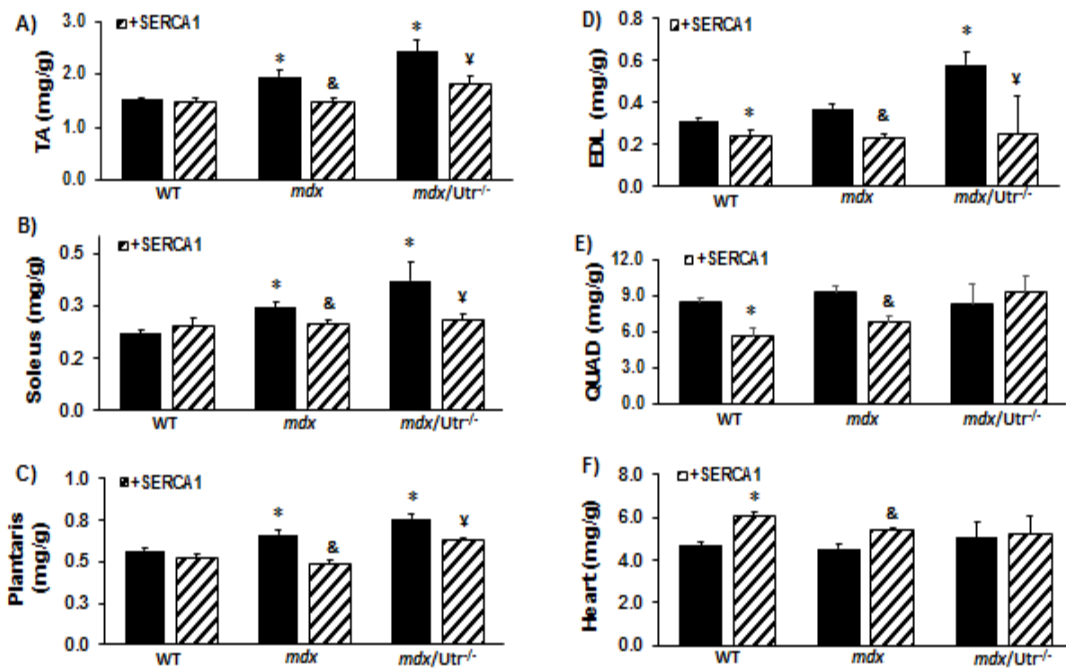


**Figure 4.1 – SERCA1 overexpression alters relative muscle mass in dystrophic mouse models.** Muscle mass is shown relative to body mass (mg/g) for tibialis anterior (TA), soleus, plantaris, extensor digitorum longus (EDL), quadriceps (QUAD), and heart [WT (n=15), WT/+SERCA1 (n=8), *mdx* (n=8), *mdx*/+SERCA1 (n=10), *mdx*/Utr<sup>-/-</sup> (n=5), and *mdx*/Utr<sup>-/-</sup>/+SERCA1 (n=5)]. \*p<0.05 vs. WT; & p<0.05 vs. *mdx*; Y p<0.05 vs. *mdx*/Utr<sup>-/-</sup>. Data presented as mean ± SEM.

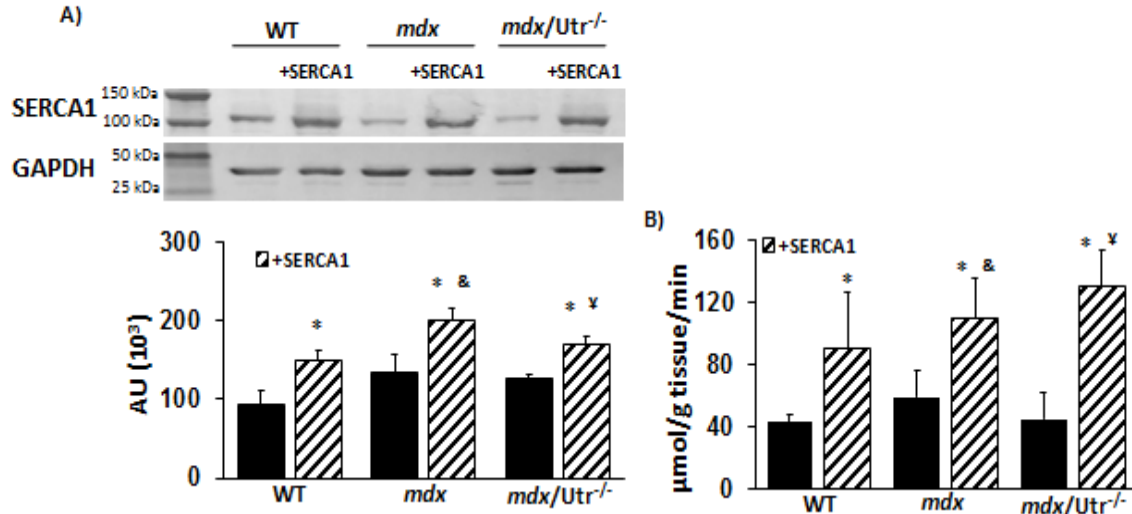


**Figure 4.2 – SERCA1 overexpression increases SERCA1 protein levels and maximal SR Ca<sup>2+</sup>-ATPase activity in QUAD muscle.** **A)** The top figure shows a representative western blot from WT, dystrophin deficient (*mdx*) and dystrophin and utrophin deficient (*mdx/Utr<sup>-/-</sup>*) mice with and without SERCA1 overexpression. Bottom figures shows densitometry values for WT (n=5), WT/+SERCA1 (n=5), *mdx* (n=3), *mdx*/+SERCA1 (n=3), *mdx/Utr<sup>-/-</sup>* (n=3), and *mdx/Utr<sup>-/-</sup>*/+SERCA1 (n=3). **B)** Maximal SR Ca<sup>2+</sup>-ATPase activity in QUAD muscle homogenates [WT (n=3), WT/+SERCA1 (n=3), *mdx* (n=3), *mdx*/+SERCA1 (n=3), *mdx/Utr<sup>-/-</sup>* (n=3), and *mdx/Utr<sup>-/-</sup>*/+SERCA1 (n=3)]. \*p<0.05 vs. WT; & p<0.05 vs. *mdx*; ¥ p<0.05 vs. *mdx/Utr<sup>-/-</sup>*. Data presented as mean ± SEM.

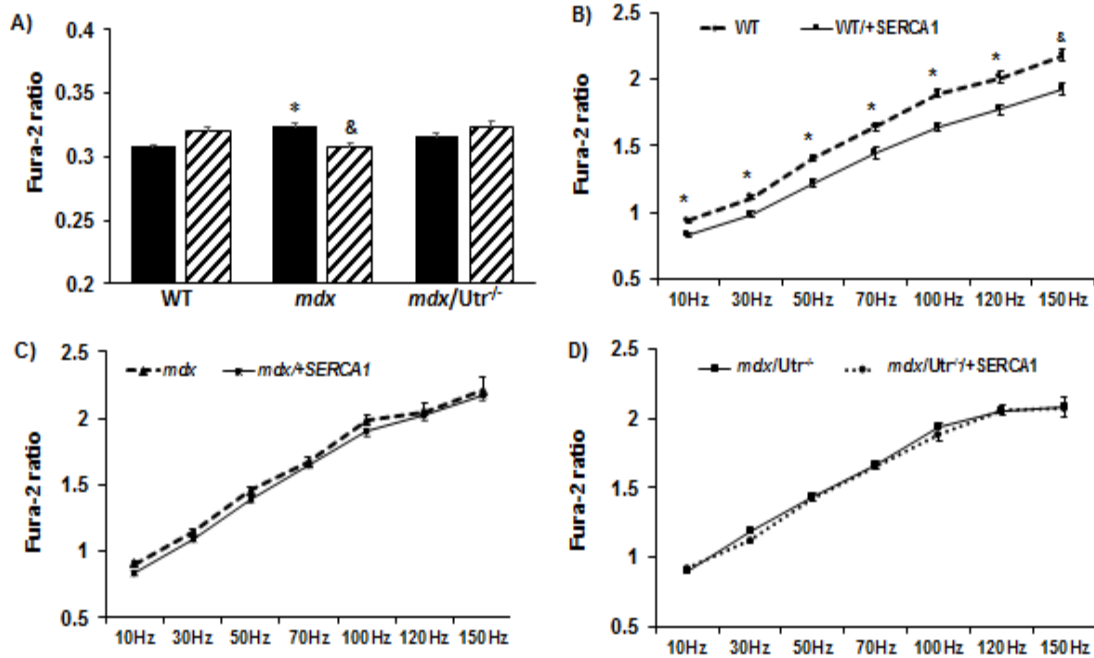


**Figure 4.3 – Effects of SERCA1 overexpression on resting and peak free  $[Ca^{2+}]_i$ .** Fura-2 ratios were used as an index of free  $[Ca^{2+}]_i$  as described in methods. **A)** Resting Fura-2 ratios from single muscle fibers from mouse genotypes [WT (n=74), WT/+SERCA1 (n=38), *mdx* (n=42), *mdx*/+SERCA1 (n=63), *mdx*/*Utr*<sup>-/-</sup> (n=46), and *mdx*/*Utr*<sup>-/-</sup>/+SERCA1 (n=33)]. **B)** Peak Fura-2 ratios from single muscle fibers from WT (n≥61 per frequency evaluated) and WT/+SERCA1 (n≥35 per frequency evaluated). **C)** Peak Fura-2 ratios from single muscle fibers from *mdx* (n≥26 per frequency evaluated) and *mdx*/+SERCA1 (n≥51 per frequency evaluated). **D)** Peak Fura-2 ratios from single muscle fibers from *mdx*/*Utr*<sup>-/-</sup> (n≥31 per frequency evaluated) and *mdx*/*Utr*<sup>-/-</sup>/+SERCA1 (n≥30 per frequency evaluated). Data presented as mean ± SEM.

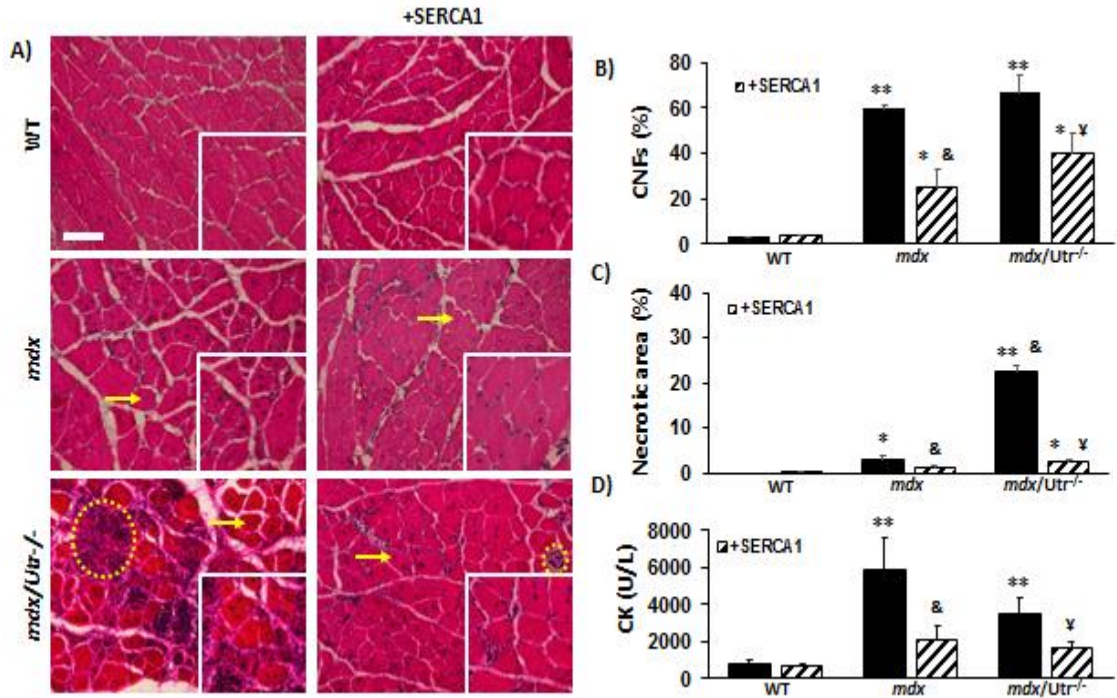


**Figure 4.4 – SERCA1 overexpression decreases markers of damage in dystrophic mouse models.** **A)** H&E staining of quadriceps muscle sections from different mouse genotypes (scale bar = 100 $\mu$ m). The yellow arrows indicate examples of central nuclei that were used for quantification of centrally nucleated fibers (CNFs). The yellow circles show examples of necrosis. **B)** Percent of CNFs in muscle sections from mouse genotypes [WT (n=4), WT/+SERCA1 (n=4), *mdx* (n=5), *mdx*/+SERCA1 (n=5), *mdx*/Utr<sup>-/-</sup> (n=4), *mdx*/Utr<sup>-/-</sup>/+SERCA1 (n=5)]. **C)** Percent of necrotic areas in mouse sections from different genotypes [WT (n=4), WT/+SERCA1 (n=4), *mdx* (n=5), *mdx*/+SERCA1 (n=5), *mdx*/Utr<sup>-/-</sup> (n=4), and *mdx*/Utr<sup>-/-</sup>/+SERCA1 (n=5)]. **D)** Levels of creatine kinase (CK) in different mouse groups [WT (n=4), WT/+SERCA1 (n=4), *mdx* (n=6), *mdx*/+SERCA1 (n=6), *mdx*/Utr<sup>-/-</sup> (n=3), and *mdx*/Utr<sup>-/-</sup>/+SERCA1 (n=3)]. \*p<0.05 vs. WT; \*\*p<0.01 vs. WT; & p<0.05 vs. *mdx*; Y p<0.05 vs. *mdx*/Utr<sup>-/-</sup>. Data presented as mean  $\pm$  SEM.

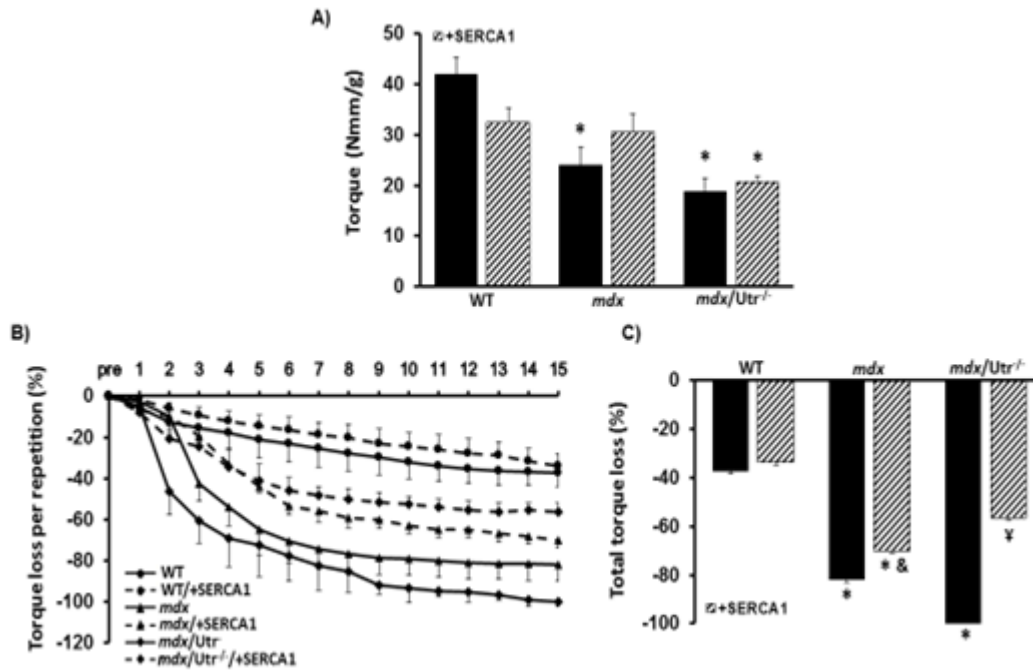


**Figure 4.5 – SERCA1 overexpression does not alter muscle torque production but protects DMD mouse models from eccentric contraction-induced injury.** **A)** Maximal isometric QUAD torque normalized to quadriceps mass in all genotypes [WT (n=5), WT/+SERCA1 (n=6), *mdx* (n=4), *mdx*/+SERCA1 (n=5), *mdx*/Utr<sup>-/-</sup> (n=3), and *mdx*/Utr<sup>-/-</sup>/+SERCA1 (n=7). **B)** Loss in maximal torque per lengthening contraction. A total of 15 repetitions were performed for each animal. **C)** Percent loss in torque throughout 15 lengthening contractions for all genotypes [WT (n=5), WT/+SERCA1 (n=6), *mdx* (n=4), *mdx*/+SERCA1 (n=5), *mdx*/Utr<sup>-/-</sup> (n=3), *mdx*/Utr<sup>-/-</sup>/+SERCA1 (n=7)]. \*p<0.05 vs. WT; & p<0.05 vs. *mdx*; ¥ p<0.05 vs. *mdx*/Utr<sup>-/-</sup>. Data presented as mean ± SEM.



**Figure 4.6 – Representative radiographs showing spinal curvature from A) WT mouse, B) *mdx/Utr<sup>-/+</sup>*+SERCA1, and C) *mdx/Utr<sup>-/-</sup>*.** The lines AB and CD are used to demonstrate the differences in spine curvature in different animal genotypes. Then, a line (Line CD) was drawn perpendicular from the dorsal edge of the vertebra at the point of greatest curvature. An increase in line CD indicates an increase in kyphosis.

**Chapter 5: Investigating the mechanism of reduced muscle damage with SERCA1 overexpression in mouse models of Duchenne muscular dystrophy**

The following is a manuscript in preparation based on my final dissertation research project.



**Investigating the mechanism of reduced muscle damage with SERCA1  
overexpression in mouse models of Duchenne muscular dystrophy**

Davi A G Mázala<sup>1</sup>, Dapeng Chen<sup>1</sup>, Val A Fajardo<sup>2</sup>, A. Russell  
Tupling<sup>2</sup> & Eva R Chin<sup>1</sup>

<sup>1</sup>Department of Kinesiology, School of Public Health, University of Maryland, College  
Park, MD 20742, USA.

<sup>2</sup>Department of Kinesiology, Faculty of Applied Health Sciences, University of  
Waterloo, Waterloo, ON N2L 3G1, Canada

**Correspondence to:** Dr. Eva Chin, School of Public Health, University of Maryland,  
2134b SPH Building, College Park, MD 20742 USA, [erchin@umd.edu](mailto:erchin@umd.edu)

**Running Title:** Underlying mechanisms behind SERCA1 benefits in different dystrophic  
mouse models

**Keywords:** Duchenne muscular dystrophy; SERCA1 overexpression; calpain; desmin;  
junctophilin-1; oxidative stress; ER stress; parvalbumin; calsequestrin; sarcolipin;  
phospholamban

## Abstract

Duchenne muscular dystrophy (DMD) is a devastating neuromuscular disease caused by mutations in the dystrophin gene. Loss of intracellular calcium ( $\text{Ca}^{2+}$ ) homeostasis has been proposed as one of the mechanisms playing an important role in DMD disease progression. Recent work from our lab and others have demonstrated that overexpression of the sarcoplasmic/endoplasmic reticulum  $\text{Ca}^{2+}$ -ATPase 1 (SERCA1) in skeletal muscle is sufficient to ameliorate disease phenotype in different DMD mouse models. In the present study we sought to evaluate the underlying mechanisms by which SERCA1 overexpression improved the disease phenotype in the *mdx* and *mdx/utr<sup>-/-</sup>* mouse models. We evaluated changes in calpain activation, degradation of calpain targets (desmin and junctophin-1), oxidative stress (protein carbonyls), ER stress [Grp78/BiP and C/EBP homologous protein (CHOP)], levels of SERCA inhibitory proteins [sarcolipin (SLN) and phospholamban], and  $\text{Ca}^{2+}$ -handling proteins (parvalbumin and calsequestrin). SERCA1 overexpression attenuated calpain activation in *mdx* muscle only, while partially attenuating the degradation of the calpain target desmin in *mdx/utr<sup>-/-</sup>* mice. Additionally, SERCA1 overexpression decreased the SERCA-inhibitory protein SLN in *mdx* muscle but did not alter levels of  $\text{Ca}^{2+}$  regulatory proteins in either dystrophic model. Lastly, SERCA1 overexpression blunted the increase in endoplasmic reticulum stress markers Grp78/BiP in *mdx* mice and CHOP in *mdx* and *mdx/utr<sup>-/-</sup>* mice. Overall, our findings provide a mechanistic insight into downstream alterations due to SERCA1 overexpression in *mdx* and *mdx/utr<sup>-/-</sup>* mice.

## **Introduction**

Duchenne muscular dystrophy (DMD) is a fatal neuromuscular disease affecting 1 in 3600 to 6000 newborn boys every year (62). DMD is an X-linked disease caused by mutations in the dystrophin gene, one of the largest genes in the human genome (247). Patients with DMD have progressive muscle weakness and wasting, with a loss of 75% of muscle mass by the age of 10 (204). The repetitive cycles of muscle degeneration and regeneration leads to the exhaustion of muscular regenerative capacity, thus leading to substitution of muscle fibers by connective and adipose tissue (93). Currently, the most common treatment option for DMD is the use of glucocorticoids (deflazacort or prednisone) which delay disease progression due to their anti-inflammatory actions. Nevertheless, long term use of glucocorticoids leads to adverse side effects (e.g., immunosuppression, glucose intolerance, osteoporosis, and others) which limit their clinical utility.

Dystrophin is a member of the dystrophin-glycoprotein complex (DGC) which connects the cytoskeleton of muscle fibers to proteins in its membrane. The lack of dystrophin leads to a functional instability of the DGC complex which is associated with increased mechanical stress during muscle contractions (272, 287). Moreover, muscles lacking dystrophin have increased susceptibility to contraction-induced damage, and numerous cellular and molecular alterations. Some of the intracellular modifications commonly found in dystrophic muscles are increased oxidative stress, increased intracellular free  $\text{Ca}^{2+}$  levels, increased inflammation, and increased proteolytic activity (170, 287, 342).

Loss of  $\text{Ca}^{2+}$  homeostasis has been proposed as one of the mechanisms playing an important role in DMD disease progression. Dystrophic muscle fibers have greater  $\text{Ca}^{2+}$  influx through the plasma membrane (361, 374), leakage of  $\text{Ca}^{2+}$  from the sarcoplasmic reticulum (SR) (29), and decreased SR- $\text{Ca}^{2+}$  reuptake (98). This abnormal  $\text{Ca}^{2+}$  control leads to mitochondrial  $\text{Ca}^{2+}$  overload, endoplasmic reticulum (ER) stress, increased oxidative stress, and activation of  $\text{Ca}^{2+}$ -activated proteases, which are known mechanisms to activate cell death pathways (19, 145, 237, 362). Altering mechanisms of intracellular  $\text{Ca}^{2+}$  control in dystrophic mouse models lessens the disease severity (145, 236, 243, 256). For instance, studies using genetic or pharmacological approaches to decrease  $\text{Ca}^{2+}$  overload either by: 1) decreasing  $\text{Ca}^{2+}$  influx through the plasma membrane (236); 2) increasing the amount of  $\text{Ca}^{2+}$  buffering proteins in muscle (145, 243, 256); or 3) inhibiting downstream targets of increased  $[\text{Ca}^{2+}]_i$  (237), have been effective in ameliorating disease progression in different mouse models of DMD. Further support for the role of  $[\text{Ca}^{2+}]_i$  in the progression of DMD was demonstrated in a study showing that unregulated  $\text{Ca}^{2+}$  influx due to overexpression of  $\text{Ca}^{2+}$  membrane channels in non-dystrophic mice was sufficient to induce the dystrophic phenotype independent of membrane instability (236). Overall, the evidence from various studies has provided overwhelming support that increased intracellular  $\text{Ca}^{2+}$  is one of the key contributors to disease progression in muscular dystrophy.

Since its discovery in 1984, the *mdx* mouse model has been used in the majority of studies evaluating the underlying mechanisms behind DMD disease progression (58). However, the only muscle in the *mdx* mice demonstrating similar disease progression to DMD patients, with progressive degeneration and detectable muscle weakness, is the

diaphragm (326). The milder phenotype in *mdx* mice is due, at least in part, to a ~5 fold increase in utrophin (*utr*) levels, a protein with similar role as dystrophin in muscles (357). Therefore, it has been suggested that animals lacking both proteins, dystrophin and *utr* (*mdx/utr<sup>-/-</sup>*), would be a better model to evaluate disease mechanisms and potential treatments for DMD. Briefly, the *mdx/utr<sup>-/-</sup>* mouse model has altered neuromuscular and myotendinous junctions, early onset of damage in the diaphragm, joint contractures, kyphosis, and premature death by the age of 20 weeks (94, 95).

Recent work from our lab (Chapter 4) and others have demonstrated that overexpression of the sarcoplasmic/endoplasmic reticulum  $\text{Ca}^{2+}$ -ATPase 1 (SERCA1) in skeletal muscle was sufficient to ameliorate disease phenotype in different DMD mouse models (145, 243, 256). Overexpression of SERCA1 altered body and muscle mass to more closely resemble that of healthy animals (256), decreased markers of muscle damage [e.g., serum creatine kinase (CK) levels and the percentage of centrally nucleated fibers (CNFs); (145, 256)], and protected the muscle from contraction-induced injury (243, 256). More importantly, we reported great benefits of SERCA1 overexpression in the *mdx/utr<sup>-/-</sup>* mouse model, which further supports the role of intracellular  $\text{Ca}^{2+}$  dysregulation in a mouse model with more similar disease progression to that of DMD patients than *mdx* mice (256).

Although we reported several benefits from SERCA1 overexpression in different dystrophic mouse models, we did not evaluate the underlying mechanisms behind such changes. Therefore, in the current study, we sought to evaluate the effects of SERCA1 overexpression in the common downstream targets of increased intracellular  $\text{Ca}^{2+}$  levels in different skeletal muscles from both *mdx* and *mdx/utr<sup>-/-</sup>* mouse models. More specifically, the purpose of this study was to evaluate changes in calpain activation and degradation of

calpain targets [desmin and junctophin-1 (JP1)], oxidative stress (protein carbonyls), and ER stress [Grp78/BiP and C/EBP homologous protein (CHOP)] in muscles from *mdx* and *mdx/utr<sup>-/-</sup>* mice with and without SERCA1 overexpression. Additionally, we evaluated the effects of SERCA1 overexpression in levels of SERCA inhibitory proteins [sarcolipin (SLN) and phospholamban (PLN)] and Ca<sup>2+</sup>-handling proteins [parvalbumin (PV) and calsequestrin]. Briefly, our findings demonstrated that SERCA1 overexpression attenuated calpain activation in *mdx* muscle only, while partially attenuating the degradation of the calpain target desmin in *mdx/utr<sup>-/-</sup>* mice. Additionally, SERCA1 overexpression decreased the SERCA-inhibitory protein sarcolipin in *mdx* muscle but did not alter levels of Ca<sup>2+</sup> regulatory proteins in either dystrophic model. Lastly, SERCA1 overexpression blunted the increase in endoplasmic reticulum stress markers Grp78/BiP in *mdx* mice and C/EBP homologous protein (CHOP) in *mdx* and *mdx/utr<sup>-/-</sup>* mice. Overall, our findings provide mechanistic insight into downstream alterations due to SERCA1 overexpression in *mdx* and *mdx/utr<sup>-/-</sup>* mice.

## Methods

Ethical approval: All procedures were conducted under a protocol approved by the Institutional Animal Care and Use Committee of the University of Maryland, College Park.

Animals and muscle samples: The muscle samples analyzed in the current study were harvested from mice used in study 2 (Chapter 4) (256). As previously explained in this document (Chapter 4), mice overexpressing SERCA1 (+SERCA1) were crossed with *mdx/utr<sup>+/-</sup>* mice to generate dystrophic mice overexpressing SERCA1 (*mdx/+SERCA1* and *mdx/utr<sup>-/+</sup>+SERCA1*). At approximately 3 mo of age, mice were euthanized by cervical dislocation and muscles were quickly dissected, weighed, and snap frozen in liquid nitrogen and stored at -80°C for further analysis.

Western blots: Unless specified differently, muscles were homogenized in lysis buffer (20 mM Hepes buffer, pH 7.5, 100 mM NaCl, 1.5 mM MgCl<sub>2</sub>, 0.1 % Triton X-100, and 20 % Glycerol) containing 1 mM DTT and protease inhibitor cocktail (cOmplete mini EDTA-free protease inhibitor cocktail, Roche Diagnostics). After homogenization, samples were kept on ice for 20 min and subsequently spun at 4°C at 20,000 g. The supernatant was subsequently collected and frozen at -80°C until analyzed. For all western blots samples were prepared with 5X loading buffer and denatured by incubation at 100°C for 5 min. Total protein was assessed using Pierce™ BCA Protein Assay Kit (Thermo Fisher Scientific – product #23225).

On the day of analysis, equal amounts of protein were loaded per gel following appropriate calibration with antibody. More specifically, optimal loading conditions were determined by performing western blots with different protein concentrations (e.g., 5, 10, 15, 20, and 30ug total protein) for each antibody. Samples with equal amounts of total

protein were separated on SDS-PAGE gels (8-15% - based on molecular weight of protein) and then transferred onto polyvinylidene difluoride (PVDF) membranes. After transferring, membranes were blocked with 5% (w/v) non-fat dry milk in Tris-buffered saline (pH 8.0) for 1 hr, and then incubated with primary antibodies at 4°C overnight. The primary antibodies used were the following: JP1 (1:250; rabbit IgG; Thermo Fisher Scientific #40-5100), desmin (1:100000; rabbit IgG; Abcam #ab32362), PV (1:1000; goat IgG; Swant #PVG214), CHOP (1:1000; mouse IgG2a; Cell Signaling Technology #L63F7), Grp78/BiP (1:1000; mouse IgG; Cell Signaling Technology #C50B12), and calsequestrin (1:1000; rabbit IgG; Santa Cruz Biotechnology #sc-28274). On the following day, membranes were washed and then probed with appropriate secondary antibodies [e.g., HRP-linked anti-rabbit IgG (Cell Signaling Technology #7074P); HRP-linked anti-mouse IgG (Cell Signaling Technology #7076S); and HRP-linked anti-goat (Novus Biologicals – NB710-H)] for 1 hr at room temperature. After incubation with secondary, membranes were washed and proteins will be detected with Clarity Western ECL Substrate (Bio-Rad Laboratories Inc.), and quantified by band densitometry using Bio-Rad ChemiDoc™ MP imaging system (Bio-Rad Laboratories Inc.). Protein expression levels were expressed in arbitrary units (AU). To confirm equal protein loading across samples, membranes were exposed to Pierce® Reversible Protein Stain Kit (Thermo Scientific #24585).

*Calpain-1 western blotting:* Western blotting conditions for assessing calpain-1 expression levels were adapted from Murphy and colleagues (249, 253). Briefly, muscles were homogenized (1:10 w/v) in lysis buffer (20 mM Hepes buffer, pH 7.5, 100 mM NaCl, 1.5 mM MgCl<sub>2</sub>, 0.1 % Triton X-100, 20 % Glycerol, and 50 mM EGTA) containing 1 mM



DTT. After homogenization, total protein was determined using Pierce™ BCA Protein Assay Kit (Thermo Fisher Scientific – product #23225).

On the day of analysis, samples with equal amounts of total protein were separated on SDS-PAGE gel (8%) and then transferred onto PVDF membranes. After transferring, membranes were blocked with 5% (w/v) non-fat dry milk in Tris-buffered saline (pH 8.0) for 1 hr, and then incubated with primary antibody (calpain-1 – 1:2000; mouse IgG; Thermo Fisher Scientific #MA1-124434) at 4°C overnight. On the following day membranes were washed and then probed with secondary (1:2000 – HRP-linked anti-mouse IgG; Cell Signaling Technology #7076S). After incubation with secondary, membranes were washed and proteins will be detected with Clarity Western ECL Substrate (Bio-Rad Laboratories Inc.), and quantified by band densitometry using Bio-Rad ChemiDoc™ MP imaging system (Bio-Rad Laboratories Inc.). Protein expression levels were expressed in arbitrary units (AU). To confirm equal protein loading across samples, membranes were stained with Pierce® Reversible Protein Stain Kit (Thermo Scientific #24585).

*Sarcolipin (SLN) and phospholamban (PLN) western blotting:* Western blotting to examine SLN and PLN content was performed as previously described (121). Briefly, lysates were placed into 1x solubilizing buffer and 25 µg of total protein were electrophoretically separated on 13% total acrylamide gels using a Tris-tricine-based system. For SLN proteins were transferred onto 0.1 µm Nitrocellulose membranes, whereas for PLN, proteins were transferred onto 0.2 µm PVDF membranes. Membranes were probed with the SLN antibody generated by Lampire Biologicals (122) and the PLN antibody (MA3-919) purchased from Pierce Thermo Fisher Scientific Inc. Antigen-

antibody complexes were detected using SuperSignal Femto West (Pierce Thermo) for SLN and Luminata Forte™ (Millipore) for PLN. Quantitation of optical densities was performed using GeneTools (Syngene). To confirm equal protein loading across samples, membranes were stained with Ponceau.

Calpain enzymatic activity assay: Calpain activity from gastrocnemius muscles was measured according to the manufacture's protocol (Abcam Calpain Activity Assay Kit; #ab65308). The fluorometric assay is based on the detection of cleavage of the calpain substrate Ac-LLY-AFC, which emits blue light (400 nm) in its native state but after calpain cleavage emits a yellow-green light (505 nm). Gastrocnemius muscles were homogenized in extraction buffer highly buffered with optimal concentrations of EGTA and EDTA, according to the manufacture, to chelate the Ca<sup>2+</sup> and avoid any further activation of calpains during the extraction procedure. Although the extraction buffer has a mild detergent concentration to ensure the extraction of activated calpains in the cytosol, 1% Triton X-100 was added to the buffer to also detect activated calpains associated with the plasma membrane. After homogenization, samples were spun at 20,000 g for 3 min and the supernatant was removed for analysis. Protein concentration was determined by BCA assay (Thermo Fisher Scientific, Rockford, IL) and 50 ug of protein incubated with calpain substrate for 1h at 37°C. Subsequently, samples were read in triplicates in a plate reader (Molecular Device, model StepraMax M5 - Exc=400 nm and Emm=505 nm). Positive and negative controls were assessed in the same plate with all the samples analyzed.

Protein carbonyl assessment: Protein carbonyl levels were assessed using a manufacturer-recommended protocol (Cayman Chemical - Protein Carbonyl Assay Kit # 10005020). Briefly, gastrocnemius muscles previously stored at -80°C were used to

evaluate protein carbonyl content. The assay uses the reaction between 2,4-Dinitrophenylhydrazine (DNPH) and protein carbonyls, to form a Schiff base and produce hydrazone, which was measured spectrophotometrically. Once ready for analysis, samples were read in duplicates in a plate reader (Abs 385 nm).

Statistical analysis: To evaluate differences between WT vs. WT/+SERCA1, WT vs. *mdx*, WT vs. *mdx/utr<sup>-/-</sup>*, *mdx* vs. *mdx/+SERCA1*, *mdx* vs. *mdx/utr<sup>-/-</sup>*, and *mdx/utr<sup>-/-</sup>* vs. *mdx/utr<sup>-/-</sup>/+SERCA1* we used Student's T-tests. The statistical significance was defined at  $P < 0.05$ . Values shown represent means  $\pm$  SE.

Power calculations: In order to achieve a minimum of 80% ( $\alpha < 0.05$ ) for the proposed evaluations, an  $n = 7$  samples was needed per group.

## Results

### Effects of SERCA1 overexpression in calpain activity levels

Calpain activation has been shown to be increased in dystrophic muscles (185, 255, 320). In order to evaluate calpain activation in *mdx* and *mdx/utr<sup>-/-</sup>* and whether it is attenuated with SERCA1 overexpression, we measured calpain-1 protein levels as well as calpain enzymatic activity in gastrocnemius muscles. Our results show that full length calpain-1 levels (80 kDa isoform) were similar between *mdx* and WT mice, as well as between *mdx/utr<sup>-/-</sup>* and WT ( $P > 0.05$ ; Figure 5.1). However, there was a greater incidence of the cleaved 78 kDa isoform of calpain-1 in both *mdx* and *mdx/utr<sup>-/-</sup>* that was not seen in WT mice (Figure 5.1). Dystrophin null mice overexpressing SERCA1 (*mdx/+SERCA1*) had lower levels of the 80 kDa calpain-1 isoform compared with WT mice ( $P < 0.05$ ; Figure 5.1). Moreover, the 78 kDa isoform of calpain-1 was not present in *mdx/+SERCA1*, which suggests a lower activation of calpain-1 in these mice compared with *mdx*. Lastly, there were no differences in calpain-1 levels, either the 78 or 80 kDa isoforms, between *mdx/utr<sup>-/-</sup>* and *mdx/utr<sup>-/-</sup>* mice ( $P > 0.05$ ; Figure 5.1), indicating no alteration in muscles lacking dystrophin and utrophin.

In addition to evaluating calpain-1 protein levels we also assessed calpain enzymatic activity in gastrocnemius muscle homogenates (Figure 5.2). The fluorometric assay used in the current study is based on the detection of cleavage of the calpain substrate Ac-LLY-AFC from muscle homogenates. To avoid further activation of calpains in muscle homogenates during sample preparation, we used an extraction buffer (lysis buffer) highly buffered with optimal concentrations of EGTA and EDTA to chelate free  $\text{Ca}^{2+}$ . Our results showed that calpain enzymatic activity was greater in dystrophic muscle (*mdx*,

*mdx/+SERCA1*, *mdx/utr<sup>-/-</sup>*, and *mdx/utr<sup>-/-</sup>/+SERCA1* mice) compared with WT ( $P < 0.05$ ; Figure 5.2). Calpain enzymatic activity was partially reduced (22 %) in *mdx/SERCA1* mice compared with *mdx* mice ( $P < 0.10$ ; Figure 5.2). In contrast, there was no difference in calpain enzymatic activity between *mdx/utr<sup>-/-</sup>/+SERCA1* and *mdx/utr<sup>-/-</sup>* mice ( $P > 0.05$ ; Figure 5.2).

#### Effects of SERCA1 overexpression on calpain targets

Activated calpains are known to proteolyse sarcomeric and cytoskeletal proteins (e.g., desmin) as well as proteins responsible for maintaining proper triad junction structure such as JP1 (249, 349, 380). We assessed desmin and JP1 expression levels to determine the downstream activities of calpain. Surprisingly, our findings show higher JP1 levels in diaphragm muscle from *mdx* mice compared with WT mice ( $P < 0.01$ ; Figure 5.3A & 5.3B). In contrast, there were no differences in JP1 content between *mdx/utr<sup>-/-</sup>* vs. WT mice ( $P > 0.05$ ; Figure 5.3A & 5.3B), while diaphragms from *mdx/utr<sup>-/-</sup>/+SERCA1* mice had higher levels of JP1 compared with WT mice ( $P < 0.01$ ; Figure 5.3A & 5.3B). Although not statistically significant, JP1 levels showed a trend towards being lower in *mdx/+SERCA1* vs. WT mice ( $P < 0.10$ ; Figure 5.3A & 5.3B), higher in *mdx/utr<sup>-/-</sup>/+SERCA1* vs. *mdx/utr<sup>-/-</sup>* mice ( $P < 0.10$ ; Figure 5.3A & 5.3B), and lower in *mdx/utr<sup>-/-</sup>* vs. *mdx* mice ( $P < 0.10$ ; Figure 5.3A & 5.3B).

We also evaluated expression of the calpain target, desmin. There were no differences in desmin protein levels in diaphragms from *mdx* vs. WT mice ( $P > 0.05$ ; Figure 5.3C & 5.3D). This agrees with a previous finding demonstrating equal amounts of desmin in diaphragms from *mdx* and WT controls (337). In contrast, desmin protein levels were

lower in diaphragms from *mdx/utr<sup>-/-</sup>* vs. WT mice ( $P < 0.05$ ; Figure 5.3C & 5.3D). SERCA1 overexpression did not alter desmin protein content in diaphragms from WT/+SERCA1 vs. WT or *mdx*/+SERCA1 vs. *mdx* mice ( $P > 0.05$ ; Figure 5.3C & 5.3D). However, diaphragm muscle from *mdx/utr<sup>-/-</sup>*/+SERCA1 mice had higher levels of desmin compared with *mdx/utr<sup>-/-</sup>* mice ( $P < 0.01$ ; Figure 5.3C & 5.3D).

#### Effects of SERCA1 overexpression in protein carbonyl levels

Due to the link between intracellular  $\text{Ca}^{2+}$  dysregulation and ROS production in dystrophic muscles, we hypothesized that SERCA1 overexpression would attenuate oxidative stress damage in different dystrophic mouse models. We evaluated protein carbonyl levels in gastrocnemius muscles from *mdx* and *mdx/utr<sup>-/-</sup>* with and without SERCA1 overexpression as an index of ROS-induced alterations in protein post-translational modification. Overexpression of SERCA1 in WT mice (WT/+SERCA1) did not change protein carbonyl levels ( $P > 0.05$ ; Figure 5.4). As expected, protein carbonyl levels were higher in *mdx* and *mdx/utr<sup>-/-</sup>* mice compared with WT mice ( $P < 0.05$  vs. WT; Figure 5.4). However, SERCA1 overexpression in *mdx* ( $P > 0.05$  for *mdx* vs. *mdx*/+SERCA1) and *mdx/utr<sup>-/-</sup>* (*mdx/utr<sup>-/-</sup>*/+SERCA1) mice did not attenuate the increases in protein carbonyl levels compared with WT ( $P < 0.05$  for *mdx*/+SERCA1 vs. WT; and  $P < 0.10$  for *mdx/utr<sup>-/-</sup>*/+SERCA1 vs. WT; Figure 5.4). Although not statistically significant, protein carbonyl levels had a tendency to be lower in gastrocnemius muscles from *mdx/utr<sup>-/-</sup>*/+SERCA1 vs. *mdx/utr<sup>-/-</sup>* ( $P < 0.10$ ; Figure 5.4) and between *mdx* vs. *mdx/utr<sup>-/-</sup>* ( $P < 0.10$ ; Figure 5.4).

### Effects of SERCA1 overexpression in ER stress markers

Based on the evidence of intracellular  $\text{Ca}^{2+}$  dysregulation and increased oxidative stress in dystrophic muscles, and the recent findings demonstrating an upregulation of ER stress in samples from DMD patients and *mdx* mice (242), the effect of SERCA1 overexpression in ER stress markers in different dystrophic mouse models was evaluated. The diaphragm from both *mdx* and *mdx/utr<sup>-/-</sup>* mice had higher levels of Grp78/BiP and CHOP compared with WT mice ( $P < 0.01$ ; Figure 5.5). Moreover, the protein levels of both Grp78/BiP and CHOP were also higher in diaphragms from WT/+SERCA1 compared with WT mice ( $P < 0.01$ ; Figure 5.5). Overexpression of SERCA1 in *mdx* mice (*mdx/+SERCA1*) partially attenuated the increases in Grp78/BiP and CHOP protein levels (to 68 and 59%, respectively;  $P < 0.10$  vs. *mdx*; Figure 5.5). Additionally, overexpression of SERCA1 in diaphragms from *mdx/utr<sup>-/-</sup>* mice did not reduce Grp78/BiP protein levels ( $P > 0.05$  for *mdx/utr<sup>-/-</sup>+SERCA1* vs. *mdx/utr<sup>-/-</sup>*; Figure 5.5). Nonetheless, diaphragms from *mdx/utr<sup>-/-</sup>+SERCA1* mice had lower levels of CHOP compared with *mdx/utr<sup>-/-</sup>* mice ( $P < 0.05$ ; Figure 5.5).

### Effects of SERCA1 overexpression on SERCA inhibitory proteins

SERCA activity is regulated by SLN and PLN (32, 269). SLN protein content has been previously shown to be upregulated in both *mdx* and *mdx/utr<sup>-/-</sup>* mice compared with WT controls (307) and thus may explain decreased SR  $\text{Ca}^{2+}$  clearance in these muscles. We also found significant elevations in SLN content in both the *mdx* and the *mdx/utr<sup>-/-</sup>* diaphragm compared with those from WT mice ( $P < 0.01$ ; Figure 5.6A & 5.6B) and in diaphragm from *mdx/utr<sup>-/-</sup>* vs. *mdx* mice ( $P < 0.01$ ; Figure 5.6A & 5.6B). Moreover, while

SERCA1 overexpression did not alter SLN levels in WT mice ( $P > 0.05$ ; Figure 5.6A & 5.6B), SLN content was reduced by 50% in diaphragm from *mdx*/+SERCA1 vs. *mdx* mice ( $P < 0.01$ ; Figure 5.6A & 5.6B), and by 40% in diaphragms from *mdx*/utr<sup>-/-</sup>/+SERCA1 vs. *mdx*/utr<sup>-/-</sup> mice ( $P < 0.01$ ; Figure 5.6A & 5.6B).

It was previously shown that PLN was downregulated in muscle from *mdx* mice (196). In the current study PLN content was similar in diaphragms from *mdx* compared with WT mice ( $P > 0.05$ ; Figure 5.6C & 5.6D). Contrarily, PLN content was significantly upregulated in *mdx*/utr<sup>-/-</sup> animals vs. WT mice ( $P < 0.01$ ; Figure 5.6C & 5.6D). Overexpression of SERCA1 did not alter PLN levels in either WT, *mdx*, or *mdx*/utr<sup>-/-</sup> mice ( $P > 0.05$ ; Figure 5.6C & 5.6D). Lastly, PLN was significantly upregulated in diaphragms from *mdx*/utr<sup>-/-</sup> vs. *mdx* mice ( $P < 0.05$ ; Figure 5.6C & 5.6D).

#### Effects of SERCA1 overexpression in levels of Ca<sup>2+</sup>-binding proteins

Calsequestrin functions to maintain low levels of free intracellular Ca<sup>2+</sup> in skeletal muscle fibers and is the most abundant Ca<sup>2+</sup>-binding protein located in the SR (25). We reported no differences in calsequestrin levels in diaphragm from *mdx* vs. WT or *mdx*/utr<sup>-/-</sup> vs. WT ( $P > 0.05$ ; Figure 5.7A & 5.7B). Thus, our findings agree with previous investigations that showed no differences in calsequestrin content in the diaphragm of *mdx* or *mdx*/utr<sup>-/-</sup> vs. WT (223, 307). We further evaluated the effects of SERCA1 overexpression on calsequestrin content. SERCA1 overexpression did not alter calsequestrin levels in diaphragm from either WT/+SERCA1 vs. WT, *mdx*/+SERCA1 vs. *mdx*, or *mdx*/utr<sup>-/-</sup>/+SERCA1 vs. *mdx*/utr<sup>-/-</sup> ( $P > 0.05$ ; Figure 5.7A & 5.7B).



PV is a  $\text{Ca}^{2+}$ -buffering protein located in the cytoplasm of fast-twitch muscle fibers that plays a key role in muscle relaxation. In the present study we observed lower PV levels in diaphragms from *mdx* vs. WT ( $P < 0.01$ ; Figure 5.7C & 5.7D) and from *mdx/utr<sup>-/-</sup>* vs. WT ( $P < 0.01$ ; Figure 5.7C & 5.7D). These findings agree with previous investigations which showed lower PV levels in both DMD patients and *mdx* mice compared to controls (196, 262, 304). We also evaluated the effects of SERCA1 overexpression in PV levels. SERCA1 overexpression did not alter PV content in diaphragm from WT/+SERCA1 vs. WT mice, or in *mdx*/+SERCA1 vs. *mdx* mice ( $P > 0.05$ ; Figure 5.7C & 5.7D). In contrast, PV levels were higher in diaphragm from *mdx/utr<sup>-/-</sup>* mice compared with *mdx/utr<sup>-/-</sup>*/+SERCA1 mice compared with *mdx/utr<sup>-/-</sup>* mice ( $P < 0.05$ ; Figure 5.7C & 5.7D).

## Discussion

Numerous studies have shown that loss of intracellular  $\text{Ca}^{2+}$  homeostasis is a key mechanism behind DMD disease progression (145, 236, 256, 320, 362). Abnormal  $\text{Ca}^{2+}$  control in dystrophic muscles leads to mitochondrial  $\text{Ca}^{2+}$  overload, endoplasmic reticulum (ER) stress, increased oxidative stress, and activation of  $\text{Ca}^{2+}$ -activated proteases, mechanisms known to activate cell death pathways (19, 145, 237, 362). Recent findings from our lab and others demonstrated that SERCA1 overexpression was sufficient to attenuate muscle damage and protect the muscle from contraction-induced injury in different dystrophic mouse models (145, 243, 256). In the present study we sought to evaluate common downstream targets of increased intracellular  $\text{Ca}^{2+}$  levels to understand the mechanisms by which SERCA1 overexpression attenuated the disease phenotype in different dystrophic mouse models. SERCA1 overexpression attenuated calpain activation in *mdx* muscle only, while partially attenuating the degradation of the calpain target desmin in *mdx/utr<sup>-/-</sup>* mice. Additionally, SERCA1 overexpression decreased the SERCA-inhibitory protein SLN in *mdx* muscle but did not alter levels of  $\text{Ca}^{2+}$  regulatory proteins in either dystrophic model. Lastly, SERCA1 overexpression blunted the increase in endoplasmic reticulum stress markers Grp78/BiP in *mdx* mice and CHOP in *mdx* and *mdx/utr<sup>-/-</sup>* mice. Overall our data provides a mechanistic insight into pathways altered by SERCA1 overexpression in different dystrophic mouse models.

### Effects of SERCA1 overexpression in activation of calpains

Calpains are  $\text{Ca}^{2+}$ -activated cysteine proteases responsible for the degradation or breakdown of proteins. Several studies reported higher levels of calpain activity in

different dystrophic animal models and DMD patients (77, 185, 255, 309). We evaluated calpain-1 protein levels in mice with and without SERCA1 overexpression. Levels of the 80 kDa calpain-1 isoform were not different between *mdx* vs. WT mice or between *mdx/utr<sup>-/-</sup>* vs. WT mice ( $P > 0.05$ ; Figure 5.1). On the other hand, *mdx/+SERCA1* had lower levels of calpain-1 (80 kDa isoform) compared with WT mice ( $P < 0.05$ ; Figure 5.1). Levels of calpain-1 were not different between *mdx/utr<sup>-/-</sup>+SERCA1* vs. *mdx/utr<sup>-/-</sup>* mice ( $P > 0.05$ ; Figure 5.1). Previous findings from Spencer and colleagues demonstrated that levels of calpain-1 and calpain-2 were similar between 14 week old *mdx* mice compared with WT mice (320). However, the combined levels of both calpain-1 and -2 were higher in muscles from 14 week old *mdx* mice compared with WT mice (320). Although we did not report greater calpain-1 levels in 12 week old *mdx* vs. WT mice, present findings show greater calpain enzymatic activity, which corresponds to the combined effects of different skeletal muscle calpains, in 12 week old *mdx* vs. WT mice.

Although calpain-1 levels (80 kDa isoform) were similar between WT and dystrophic mice, we reported a greater incidence of the cleaved 78 kDa isoform of calpain-1 in both *mdx* and *mdx/utr<sup>-/-</sup>* vs. WT mice, suggesting greater calpain-1 autolysis in dystrophic muscles (Figure 5.1). SERCA1 overexpression in *mdx* mice appeared to lower calpain-1 autolytic activity, since the 78 kDa isoform of calpain-1 was not commonly found in muscle homogenates of *mdx/+SERCA1* mice (Figure 5.1). In contrast, there were no differences in calpain-1 levels, either the 78 or 80 kDa isoforms, between *mdx/utr<sup>-/-</sup>+SERCA1* and *mdx/utr<sup>-/-</sup>* mice ( $P > 0.05$ ; Figure 5.1). Thus, it seems that SERCA1 overexpression does not attenuate increases in calpain-1 levels in *mdx/utr<sup>-/-</sup>* mice.

We also evaluated calpain enzymatic activity in addition to calpain-1 levels. Here we show that calpain enzymatic activity is greater in the gastrocnemius muscle from *mdx* and *mdx/utr<sup>-/-</sup>* mice compared with WT mice ( $P < 0.05$ ; Figure 5.2). Our findings agree with a previous study that showed greater calpain enzymatic activity in quadriceps muscle of sarcoglycan null mice compared with WT (145). We hypothesized that the increased  $\text{Ca}^{2+}$  buffering capacity in dystrophic mice by SERCA1 overexpression would decrease the activation of  $\text{Ca}^{2+}$  degrading pathways, including calpain enzymatic activity. Indeed, SERCA1 overexpression was previously shown to attenuate the increased calpain enzymatic activity in sarcoglycan null mice (145). Unexpectedly, SERCA1 overexpression only partially attenuated the increased calpain enzymatic activity in *mdx* mice ( $P < 0.10$ ; Figure 5.2), while not altering calpain enzymatic activity in *mdx/utr<sup>-/-</sup>* /+SERCA1 vs. *mdx/utr<sup>-/-</sup>* mice ( $P > 0.05$ ; Figure 5.2).

#### *Effects of SERCA1 overexpression in calpain activation and degradation of its targets*

Skeletal muscle calpains are known to proteolyse multiple sarcomeric and cytoskeletal proteins (e.g., desmin) as well as proteins responsible for maintaining proper triad junction structure (e.g., JP1) (249, 349, 380). Skeletal muscle fibers subjected to excessive activation, or stretched whilst contracting, display long-term reductions in force, apparently due in part to structural or molecular changes at the triad junction. Recent findings demonstrate that a key protein in triad junction structure and function are junctophilins-1 and -2 (JP1 and JP2) (249). JP1 is a 90 kDa protein localized at the triad junction of skeletal muscles which interacts with the dihydropyridine receptor (an L-type calcium channel) and inserts into the SR membrane through a transmembrane region in

their C-terminus (140, 273, 332). In normal muscles, supra-physiological muscle stimulation or increases in intracellular  $\text{Ca}^{2+}$  levels, causes activation of calpain-1 with concomitant proteolysis of JP1 (249). Proteolysis of JP1 is also seen in dystrophic muscles (249). For instance, in dystrophic diaphragm from 7 mo old *mdx* mice, JP1 undergoes marked proteolysis which is correlated with increased autolysis of calpain-1 (249). More specifically, diaphragm muscles from *mdx* mice have very low levels of the full length 90 kDa isoform of JP1, while having higher levels of the 15 kDa proteolysed isoform compared to WT mice (249).

Based on the findings from Murphy and colleagues, we proposed to evaluate the effects of SERCA1 overexpression in JP1 levels in diaphragm muscles from 3 mo old *mdx* and *mdx/utr<sup>-/-</sup>* mice. We hypothesized that the increased  $\text{Ca}^{2+}$  buffering capacity of dystrophic muscles overexpressing SERCA1 would decrease calpain activation tandem with JP1 proteolysis. However, our findings showed higher JP1 levels in diaphragm muscle from *mdx* mice compared with WT mice ( $P < 0.01$ ; Figure 5.3). In contrast, there were no differences in JP1 content between *mdx/utr<sup>-/-</sup>* vs. WT mice ( $P > 0.05$ ; Figure 5.3). Diaphragms from *mdx/utr<sup>-/-</sup>+SERCA1* mice had higher levels of JP1 compared with WT mice ( $P < 0.01$ ; Figure 5.3), while partially higher compared with *mdx/utr<sup>-/-</sup>* mice ( $P < 0.10$ ; Figure 5.3). We are not certain of the specific mechanism behind the changes in JP1 levels we reported in the diaphragm muscle from different dystrophic mice. A limitation of the current study is that we did not evaluate the levels of the 15 kDa isoform of JP1, hence not being able to fully determine the extent of breakdown of the protein. Moreover, Murphy and colleagues also reported marked proteolysis of JP1 in *mdx* mice with another antibody to the mid-region of JP1, which we were not able to purchase (product has been

discontinued). Lastly, we propose that changes in JP1 levels in *mdx* mice could be a compensatory mechanism due to a potential increased proteolysis of JP2, another junctophilin present at the triad junction of skeletal muscle fibers.

Desmin is a 53 kDa protein located at the periphery of the Z-disk of skeletal muscles that plays a critical role in maintaining the integrity of the muscle's contractile apparatus (268). It has been previously shown that muscle sections from DMD patients have decreased desmin staining, which suggests increased breakdown of the protein (88). Due to the role of calpains in desmin breakdown and evidence of lower desmin levels in muscles from dystrophic patients, we evaluated the effects of SERCA1 overexpression in desmin levels in different dystrophic mouse models. There were no differences in desmin protein levels in diaphragms from *mdx* vs. WT mice ( $P > 0.05$ ; Figure 5.3), which agrees with a previous finding demonstrating equal amounts of desmin in diaphragms from *mdx* and WT controls (337). In contrast, desmin protein levels were lower in diaphragms from *mdx/utr<sup>-/-</sup>* vs. WT mice ( $P < 0.05$ ; Figure 5.3). SERCA1 overexpression did not alter desmin protein content in diaphragms from *mdx/+SERCA1* vs. *mdx* mice ( $P > 0.05$ ; Figure 5.3). However, diaphragm muscle from *mdx/utr<sup>-/-</sup>+SERCA1* mice had higher levels of desmin compared with *mdx/utr<sup>-/-</sup>* mice ( $P < 0.01$ ; Figure 5.3). Overall, our findings suggest that SERCA1 overexpression in dystrophin/utrophin null muscles is sufficient to reduce desmin breakdown, which might help explain the protective effect of SERCA1 overexpression in attenuating eccentric contraction induced injury in *mdx/utr<sup>-/-</sup>* mice we reported in our previous study (256).

Effects of SERCA1 overexpression in protein carbonyl levels

Protein carbonylation is a major hallmark of oxidative stress and is known as one of the most harmful irreversible oxidative protein modifications (90, 373). Generally, protein carbonylation is defined as an irreversible post-translational modification that yields a reactive carbonyl moiety in a protein (e.g., aldehyde, ketone, or lactam) (124). Carbonylated proteins are not repaired by cellular enzymes, and if not eliminated (usually proteins are degraded by either the 26S proteasome or by the 20S proteasome) they tend to aggregate and this might result in cell death (124). Our present findings demonstrate that protein carbonyl levels were lower in gastrocnemius muscles from WT vs. *mdx* ( $P < 0.05$ ; Figure 5.4) and WT vs. *mdx/utr<sup>-/-</sup>* mice ( $P < 0.01$ ; Figure 5.4). Moreover, our findings agree with previous reports showing higher levels of oxidative stress in muscles from DMD patients (160, 298) and *mdx* mice (159, 286). Briefly, protein carbonyl levels (160) and 8-hydroxy-2'-deoxyguanosine (298), a marker of DNA damage, were found to be higher in muscle samples from DMD patients compared with samples from healthy subjects. Additionally, levels of O-tyrosine (159), a marker of hydroxide radical damage, and lipid peroxidation (286) were shown to be greater in skeletal muscles from *mdx* mice compared with control mice. ROS accumulation has been described as a causative event rather than a consequence of muscle degeneration in the *mdx* mouse model, since oxidative stress was found to be elevated in skeletal muscles from *mdx* mice during the pre-necrotic phase (<20 days old), which precedes the onset of inflammation and necrosis (97).

It has been previously shown that dystrophic fibers exposed to osmotic shock produce abnormal  $\text{Ca}^{2+}$  sparks, which results in mitochondrial  $\text{Ca}^{2+}$  accumulation and mitochondrial ROS production (312). Further results from Shkryl and colleagues indicated

that the excessive ROS production with concomitant activation of abnormal  $\text{Ca}^{2+}$  signals in dystrophic muscles amplify each other, and that this mechanism culminates in a vicious cycle of damaging events, which may contribute to the dystrophic phenotype (312). Dystrophic mitochondria have been shown to be major recipients of the greater  $\text{Ca}^{2+}$  influx through the cell membrane, which leads to mitochondrial permeability transition pore opening and cytochrome c release from mitochondria (237). Ultimately, this mechanism might effectively block the respiratory chain at complex III and enhance mitochondrial ROS generation (54, 151, 237). We hypothesized that the greater  $\text{Ca}^{2+}$  buffering capacity by SERCA1 in muscles from *mdx/+SERCA1* and *mdx/utr<sup>-/-</sup>+SERCA1* mice potentially attenuated mitochondrial  $\text{Ca}^{2+}$  overload, and subsequently decreased mitochondrial ROS production, oxidative stress, and protein carbonyl formation. Contrarily to our original hypothesis, SERCA1 overexpression did not alter protein carbonyl levels in the gastrocnemius muscle from *mdx* mice (Figure 5.4). Although protein carbonyl levels were 50% lower in the gastrocnemius muscle of *mdx/utr<sup>-/-</sup>+SERCA1* vs. *mdx/utr<sup>-/-</sup>* mice, this results did not reach statistical significance ( $P < 0.10$ ; Figure 5.4). We attribute the lack of differences to the small sample size and degree of variability of samples within each group. While protein carbonyl levels were not different between *mdx* vs. *mdx/+SERCA1* mice, we believe that further studies are required to evaluate if SERCA1 overexpression might have altered the levels of other markers of oxidative stress (e.g., lipid peroxidation or oxidative damage to DNA).



Effects of SERCA1 overexpression in levels of ER stress markers

In the current study we found elevations in Grp78/BiP and CHOP levels in diaphragms from both *mdx* and *mdx/utr<sup>-/-</sup>* mice compared with WT ( $P < 0.01$ ; Figure 5.5). To our knowledge, only two studies have evaluated specific ER stress markers in dystrophic muscles (171, 242). Honda and colleagues were the first to demonstrate that ER stress was higher in muscles from *mdx* mice (171). Briefly, Caspase-12 levels were upregulated in masseter muscles from 2-3 weeks old *mdx* mice (171). More recently, Moorwood and Barton showed an upregulation of ER stress in muscle samples of both DMD patients and *mdx* mice (242). Muscle samples from DMD patients had greater levels of Grp78/BiP and caspase-4 (the equivalent of murine caspase-12) compared to controls (242). Interestingly, although dystrophic muscle samples were collected from patients between 5 and 8 years of age, Grp78/BiP levels were upregulated from 2 to 40 fold compared to controls (242). Thus, this suggests great variability between patients for changes in Grp78/BiP levels. In 5 mo old *mdx* mice, levels of Grp78/BiP, pro- and active caspase-12, CHOP and P-JNK in the TA, EDL and diaphragm muscles were higher compared with controls (242). Due to the heightened ER stress in dystrophic muscles, Moorwood and Barton evaluated the effects of blocking caspase-12 in *mdx* mice (242). Caspase-12 null mice were crossed with *mdx* mice to generate dystrophin-deficient, caspase-12 null mice (*mdx/cas*) (242). Results demonstrated that muscles from *mdx/cas* had similar levels of CHOP, Grp78/BiP, and P-JNK compared with *mdx* mice (242). Nevertheless, *mdx/cas* had improved specific force production and decreased susceptibility of force loss following eccentric contractions compared to *mdx* mice (242). The authors further demonstrated that the pseudo-hypertrophy commonly found in *mdx* was attenuated

in *mdx/cas* mice (242). Lastly, although markers of muscle damage were not changed between *mdx* vs. *mdx/cas* mice (e.g., CK levels and percentage of CNFs), muscle fiber degeneration in *mdx/cas* was almost reduced to WT levels (242).

In order to properly synthesize and fold proteins, the ER requires high levels of  $\text{Ca}^{2+}$  and an appropriate redox balance (55, 202). Also, proper  $\text{Ca}^{2+}$  uptake from the cytosol into the ER has been shown to be critical for optimal function of the protein synthesis and folding machinery in cardiac muscle cells (202). Due to the role of SR- $\text{Ca}^{2+}$  in proper protein folding and ER/SR function, we hypothesized that SERCA1 overexpression would attenuate ER stress in both *mdx* and *mdx/utr<sup>-/-</sup>* mice. Surprisingly, although *mdx/+SERCA1* mice had an approximate 40% reduction in levels of Grp78/BiP and CHOP compared with *mdx* mice, this did not reach statistical significance ( $P < 0.10$ ; Figure 5.5). Thus, the lack of differences might be related to the degree of variability within groups, as seen with muscle samples from DMD patients (242), or due to technical limitations. Levels of Grp78/BiP were also similar between *mdx/utr<sup>-/-</sup>* and *mdx/utr<sup>-/-</sup>+SERCA1* mice, suggesting that SERCA1 overexpression in muscles from *mdx/utr<sup>-/-</sup>* mice does not attenuate elevations in Grp78/BiP (Figure 5.5). Based on the present findings we propose that increased levels of Grp78/BiP might be necessary due to the high protein turnover in muscles undergoing repeated cycles of degeneration/regeneration, as seen in dystrophic muscles. In contrast to our findings regarding Grp78/BiP, diaphragms from *mdx/utr<sup>-/-</sup>+SERCA1* mice had lower levels of CHOP compared with *mdx/utr<sup>-/-</sup>* mice ( $P < 0.05$ ; Figure 5.5). Thus, due to the role of CHOP in ER-mediated cell death, we propose that the decreased CHOP activation might explain some of the beneficial effects of SERCA1 overexpression in the *mdx/utr<sup>-/-</sup>* mouse model. Present findings partially agree with recent evidence from our lab

(unpublished data). Briefly, ALS-Tg mice were crossed with SERCA1 overexpressing mice to generate ALS-Tg/+SERCA1 mice, and levels of both Grp78/BiP and CHOP were evaluated. Overall, although ALS-Tg/+SERCA1 mice had an improved phenotype compared with ALS-Tg mice (e.g., improve skeletal muscle function, and delay disease progression), SERCA1 overexpression did not attenuate elevations in either Grp78/BiP or CHOP in ALS-Tg/+SERCA1 mice (unpublished data). Unexpectedly, SERCA1 overexpression increased the levels of Grp78/BiP and CHOP in WT mice in our study (Figure 5.5). Although we are not aware of the specific mechanism(s) behind this finding, we propose that SERCA1 overexpression could have prompt a temporary protein-overload in the SR/ER lumen, thus activating ER stress. Nevertheless, further studies should address the relationship between increased SERCA1 levels and ER/SR homeostasis in normal and dystrophic muscles.

#### Effects of SERCA1 overexpression in levels of SERCA inhibitory proteins

Upregulated SLN protein content has been previously found in muscle homogenates obtained from *mdx* and *mdx/utr<sup>-/-</sup>* mice compared with WT controls (306). In fact, increased SLN protein and/or mRNA is becoming widely known as a common pathological marker across many myopathies (66, 208, 257, 264) and findings in the *mdx* mouse and *mdx/utr<sup>-/-</sup>* mouse suggest that its expression may be directly proportional to disease severity (306). Here we observed significant elevations in SLN content in both *mdx* and the *mdx/utr<sup>-/-</sup>* diaphragms compared with those from WT and genotype controls overexpressing SERCA1 (Figure 5.6). Consistent with findings from Schneider and colleagues (2013) we found an approximate 7-fold increase in SLN content in the *mdx/utr<sup>-/-</sup>*

<sup>-/-</sup> diaphragm compared to *mdx* alone ( $P < 0.05$ ; Figure 5.6). Interestingly, as a result of SERCA1 overexpression, SLN content was reduced by 50% in the *mdx* diaphragm ( $P < 0.05$ ; Figure 5.6). A similar 40% reduction was found in the *mdx/utr<sup>-/+</sup>*+SERCA1 diaphragm compared with *mdx/utr<sup>-/-</sup>*, but this did not reach statistical significance ( $P < 0.10$ ; Figure 5.6), likely due to the degree of variability. Nevertheless, since SLN can be viewed as a marker of muscle pathophysiology, the reductions in SLN content are in agreement with the notion that SERCA1 overexpression normalizes Ca<sup>2+</sup> handling, thereby limiting myofiber necrosis and improving muscle structure and function in dystrophic mice (145, 256). In addition, the reduction in SLN content in both dystrophic mice could be beneficial by decreasing the SLN:SERCA ratio and thereby improving Ca<sup>2+</sup> handling at the SR level.

Conversely, there are fewer studies examining the expression of PLN, a well-known SLN homolog, in MD and other myopathies in general. Recently it was discovered that PLN overexpression in mice leads to features of centronuclear myopathy – a congenital myopathy characterized by central nuclei, type I fiber predominance and hypotrophy, and central aggregation of oxidative activity (121). With respect to MD, PLN mRNA expression was reportedly downregulated in DMD patients (334), whereas PLN protein was significantly upregulated in the masseter muscles but non-significantly altered in the tongue or temporalis muscles of *mdx* mice compared to controls (196). Collectively, these data could suggest that in response to MD, PLN expression varies across different muscles. Here, in the diaphragm muscles we found that PLN content is not different in *mdx* animals compared with WT and *mdx/+SERCA1* mice ( $P > 0.05$ ; Figure 5.6); however, PLN was significantly upregulated in *mdx/utr<sup>-/-</sup>* animals compared with WT mice ( $P < 0.01$ ; Figure

5.6). Lastly, we reported no differences in PLN levels between *mdx/utr<sup>-/-</sup>* and *mdx/utr<sup>-/-</sup>* /+SERCA1 mice ( $P > 0.05$ ; Figure 5.6).

#### Effects of SERCA1 overexpression on levels of calcium handling proteins

Calsequestrin is a 63 KDa protein that functions to maintain low levels of free intracellular  $\text{Ca}^{2+}$  in skeletal muscle fibers and is the most abundant  $\text{Ca}^{2+}$ -binding protein located in the SR (25). Here we reported equal levels of calsequestrin in diaphragms of WT and dystrophic mouse models (Figure 5.7). Thus, our results agree with recent findings that also did not report any differences in calsequestrin levels in diaphragms from WT, *mdx*, and *mdx/utr<sup>-/-</sup>* mice (306). Other studies have also evaluated calsequestrin levels in DMD mouse models (89, 127, 223, 306, 378). While some groups reported no differences or lower levels of calsequestrin-like proteins in muscles from *mdx* compared with control mice (89, 223), others reported higher levels of calsequestrin in muscles from *mdx* and *mdx/utr<sup>-/-</sup>* compared to controls (127, 306, 378). Overall, differences in findings are related to the muscle group evaluated. Briefly, calsequestrin levels were upregulated in quadriceps muscle from *mdx* and *mdx/utr<sup>-/-</sup>* compared to controls (223), while no differences were found in soleus or diaphragm (223, 306). Higher levels of calsequestrin were also shown in the spared laryngeal and extraocular muscles from *mdx* mice compared to controls (127, 188, 378). The expression of calsequestrin in the same muscle can also vary throughout disease progression in *mdx* mice. Findings from Maranhão and colleagues demonstrated that calsequestrin levels were higher in quadriceps muscles from 1 mo old *mdx* mice, whereas the levels of calsequestrin were similar at 4 and 9 mo of age (223). Overall,

muscles expressing higher levels of calsequestrin have better protection against myonecrosis due to the greater ability to buffer intracellular  $\text{Ca}^{2+}$ .

In the present study we hypothesized that SERCA1 overexpression would increase SR- $\text{Ca}^{2+}$  content and subsequently lead to increases in levels of SR- $\text{Ca}^{2+}$  binding proteins. More specifically, we hypothesized that SERCA1 overexpression would increase the levels of calsequestrin, the most abundant  $\text{Ca}^{2+}$ -binding protein located in the SR. However, SERCA1 overexpression did not alter calsequestrin levels in either WT vs. WT/+SERCA1, *mdx* vs. *mdx*/+SERCA1, or *mdx*/*utr*<sup>-/-</sup> vs. *mdx*/*utr*<sup>-/-</sup>/+SERCA1 mice ( $P > 0.05$ ; Figure 5.7). We propose that levels of other SR- $\text{Ca}^{2+}$  binding proteins, such as sarcalumenin, calsequestrin-like proteins, or calreticulin, could have been altered by SERCA1 overexpression. Thus, further studies will be needed to evaluate if SERCA1 overexpression induced changes in levels of other SR- $\text{Ca}^{2+}$  binding proteins.

PV acts as a fast binding  $\text{Ca}^{2+}$ -buffering protein in the cytoplasm of fast-twitch muscle fibers, thus playing a key role in muscle contraction/relaxation. Our results demonstrated that the diaphragm muscle from both *mdx* and *mdx*/*utr*<sup>-/-</sup> mice had lower levels of PV compared with controls ( $P < 0.01$ ; Figure 5.7). Indeed, our findings agree with previous investigations showing lower PV levels in both DMD patients and *mdx* mice compared to controls (196, 262, 304). More specifically, Niebrój-Dobosz and colleagues reported lower levels of PV in muscles from DMD patients across different ages compared to healthy controls (262). In *mdx* mice, the fast twitch muscles TA and gastrocnemius, were found to contain significantly lower levels of PV compared with controls (304). Additionally, others have shown that PV levels were significantly decreased in *mdx* tongue and masseter muscles compared with controls (196). In contrast, others have demonstrated

that PV mRNA levels were higher in muscles from *mdx* vs. control mice (135). Overall, the lower levels of PV in dystrophic muscles might contribute to the elevations in intracellular  $\text{Ca}^{2+}$  levels in dystrophic muscles.

We further evaluated the effects of SERCA1 overexpression in PV levels in diaphragms from WT and dystrophic mice. Briefly, SERCA1 overexpression did not alter PV levels in WT (WT/SERCA1) or *mdx* (*mdx*/SERCA1) mice ( $P > 0.05$ ; Figure 5.7). In contrast, diaphragms from *mdx/utr<sup>-/+</sup>*/SERCA1 had higher levels of PV compared with *mdx/utr<sup>-/-</sup>* mice ( $P < 0.05$ ; Figure 5.7). Yet, PV levels were still ~70% lower in diaphragms from *mdx/utr<sup>-/+</sup>*/SERCA1 mice vs. WT mice ( $P < 0.01$ ; Figure 5.7).

## Summary

In summary, present findings demonstrate that SERCA1 overexpression attenuated calpain activation in *mdx* muscle only, while partially attenuating the degradation of the calpain target desmin in *mdx/utr<sup>-/-</sup>* mice. Additionally, SERCA1 overexpression decreased the SERCA-inhibitory protein SLN in *mdx* muscle but did not alter levels of  $\text{Ca}^{2+}$  regulatory proteins (PV and calsequestrin) in either dystrophic model. Lastly, SERCA1 overexpression blunted the increase in ER stress markers Grp78/BiP in *mdx* mice and CHOP in *mdx* and *mdx/utr<sup>-/-</sup>* mice. Overall, these data provide a mechanistic evaluation demonstrating the downstream targets altered by SERCA1 overexpression in different dystrophic mouse models. Nevertheless, further studies will be required to evaluate additional mechanisms altered by SERCA1 overexpression in normal and dystrophic muscles.

## **Grants**

Grant support was provided by the Department of Kinesiology Graduate Research Initiative Project (GRIP), the National Institute on Aging Predoctoral Training Grant T32AG-00268, the University of Maryland Summer Research Fellowship, and by the University of Maryland Ann G. Wyllie Dissertation Fellowship to DAGM.

## **Author contributions**

D.A.G.M.: contributed to the design of the experiments, data collection, analysis and interpretation, and drafting and revising the manuscript. V.A.F.: contributed to data collection, analysis and interpretation, and drafting the manuscript. E.R.C.: contributed to the conception and design of the experiments, interpretation of data, and revising the manuscript.

## **Disclosures**

Eva R. Chin is the Founder and Chief Scientific Officer of MyoTherapeutics. No other conflicts of interest, financial or otherwise, are declared by the authors.

## **Acknowledgments**

We wish to thank Harry Li, Dr. Dapeng Chen, Patrick Solverson, Dr. Vladimir Ribeiro, Dr. Maria Fernanda Silva, and Dr. Tiago Castro-Gomes from the University of Maryland, for technical contributions to the project.



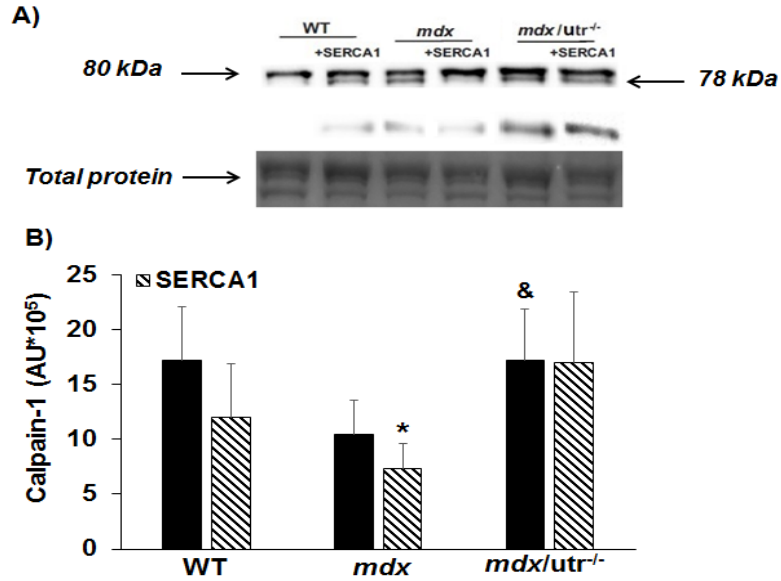


**Figure 5.1 – SERCA1 overexpression alters levels of autolyzed calpain-1 while not changing full-length calpain-1 in dystrophic muscles.** **A)** Representative western blot for calpain-1 from WT, *mdx* and *mdx/utr*<sup>-/-</sup> mice with and without SERCA1 overexpression. **B)** Densitometry values for calpain-1 from WT (n = 6), WT/+SERCA1 (n = 4), *mdx* (n = 5), *mdx*/+SERCA1 (n = 5), *mdx/utr*<sup>-/-</sup> (n = 3), and *mdx/utr*<sup>-/-</sup>/+SERCA1 (n = 3). \* indicates  $P < 0.05$  vs. WT; & indicates  $P < 0.10$  vs. *mdx*. Data presented as mean  $\pm$  SEM.

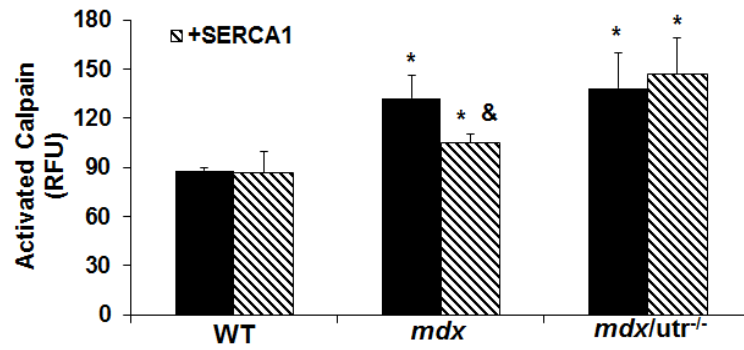


**Figure 5.2 – SERCA1 overexpression partially decreases calpain enzymatic activity in gastrocnemius muscles from *mdx* mice.** Calpain enzymatic activity in gastrocnemius muscles from WT (n = 3), WT/+SERCA1 (n = 3), *mdx* (n = 5), *mdx*/+SERCA1 (n = 5), *mdx/utr<sup>-/-</sup>* (n = 3), and *mdx/utr<sup>-/-</sup>*/+SERCA1 (n = 3). \* indicates  $P < 0.05$  vs. WT; & indicates  $P < 0.10$  vs. *mdx*. Data presented as mean  $\pm$  SEM.

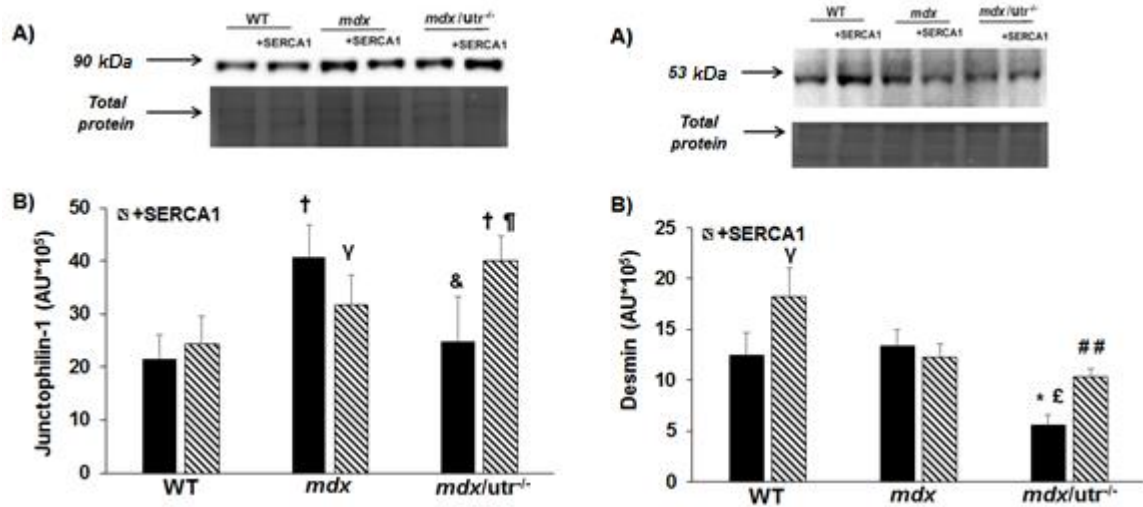


**Figure 5.3 – SERCA1 overexpression alters levels of desmin and junctophilin-1 in diaphragm muscles from different dystrophic mouse models.** **A)** Representative western blot for junctophilin-1 (JP1) from WT, *mdx* and *mdx/utr<sup>-/-</sup>* mice with and without SERCA1 overexpression. **B)** Densitometry values for JP1 from WT (n = 8), WT/+SERCA1 (n = 8), *mdx* (n = 8), *mdx*/+SERCA1 (n = 8), *mdx/utr<sup>-/-</sup>* (n = 5), and *mdx/utr<sup>-/-</sup>*/+SERCA1 (n = 3). **C)** Representative western blot for desmin from WT, *mdx* and *mdx/utr<sup>-/-</sup>* mice with and without SERCA1 overexpression. **D)** Densitometry values for desmin from WT (n = 9), WT/+SERCA1 (n = 7), *mdx* (n = 9), *mdx*/+SERCA1 (n = 9), *mdx/utr<sup>-/-</sup>* (n = 5), and *mdx/utr<sup>-/-</sup>*/+SERCA1 (n = 3). † indicates  $P < 0.01$  vs. WT; \* indicates  $P < 0.05$  vs. WT; γ indicates  $P < 0.10$  vs. WT; £ indicates  $P < 0.05$  vs. *mdx*; & indicates  $P < 0.10$  vs. *mdx*; ## indicates  $P < 0.01$  vs. *mdx/utr<sup>-/-</sup>*; ¶ indicates  $P < 0.10$  vs. *mdx/utr<sup>-/-</sup>*. Data presented as mean ± SEM.

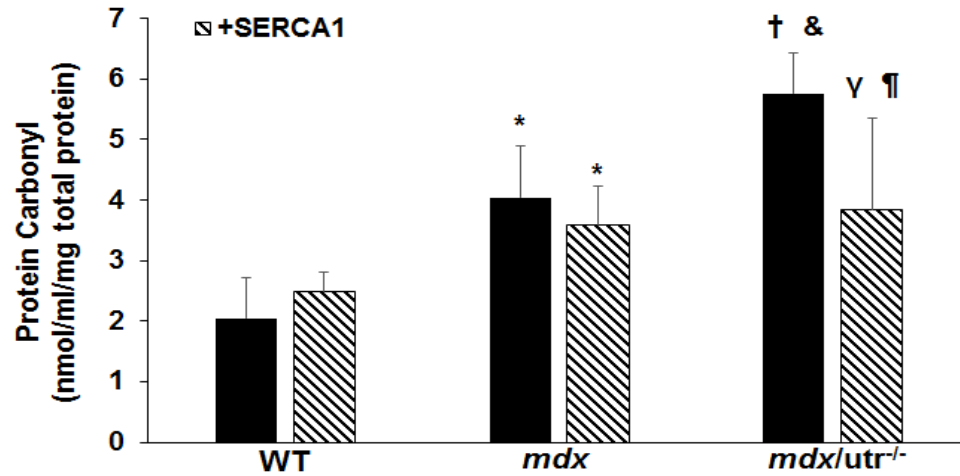


**Figure 5.4 – SERCA1 overexpression partially decreases protein carbonyl levels in gastrocnemius muscles from *mdx/utr*<sup>-/-</sup> mice.** Protein carbonyl levels were used as an indirect marker of oxidative stress. Briefly, gastrocnemius muscles from WT (n = 3), WT/+SERCA1 (n = 3), *mdx* (n = 3), *mdx*/+SERCA1 (n = 3), *mdx/utr*<sup>-/-</sup> (n = 4), and *mdx/utr*<sup>-/-</sup>/+SERCA1 (n = 3) were used to evaluate protein carbonyl levels. † indicates  $P < 0.01$  vs. WT; \* indicates  $P < 0.05$  vs. WT;  $\gamma$  indicates  $P < 0.10$  vs. WT; & indicates  $P < 0.10$  vs. *mdx*; ¶ indicates  $P < 0.10$  vs. *mdx/utr*<sup>-/-</sup>. Data presented as mean  $\pm$  SEM.

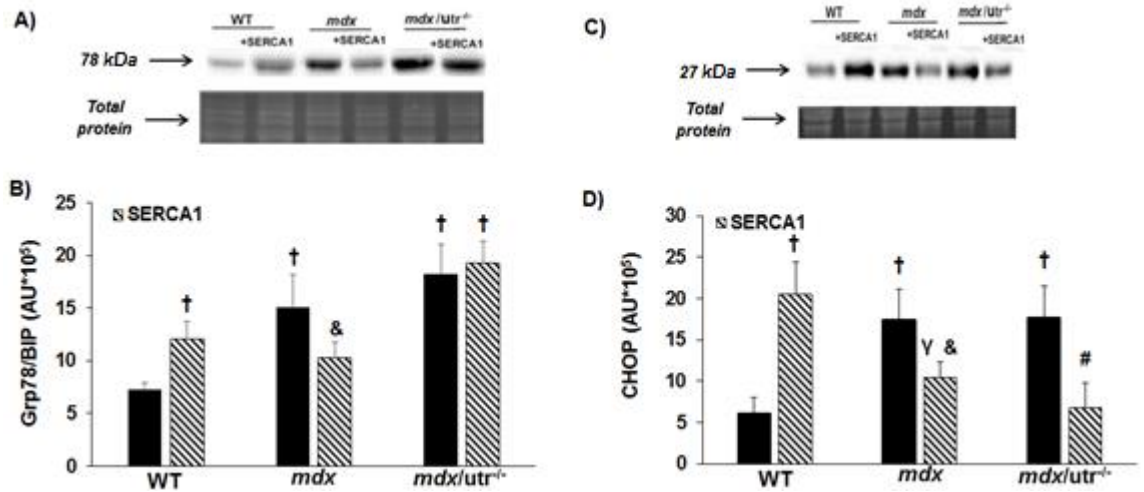


**Figure 5.5 – SERCA1 overexpression attenuates ER stress in diaphragms from different dystrophic mouse models.** **A)** Representative western blot for Grp78/BiP from WT, *mdx* and *mdx/utr<sup>-/-</sup>* mice with and without SERCA1 overexpression. **B)** Densitometry values for Grp78/BiP from WT (n = 9), WT/+SERCA1 (n = 8), *mdx* (n = 8), *mdx*/+SERCA1 (n = 8), *mdx/utr<sup>-/-</sup>* (n = 6), and *mdx/utr<sup>-/-</sup>*/+SERCA1 (n = 3). **C)** Representative western blot for CHOP from WT, *mdx* and *mdx/utr<sup>-/-</sup>* mice with and without SERCA1 overexpression. **D)** Densitometry values for CHOP from WT (n = 6), WT/+SERCA1 (n = 8), *mdx* (n = 9), *mdx*/+SERCA1 (n = 8), *mdx/utr<sup>-/-</sup>* (n = 5), and *mdx/utr<sup>-/-</sup>*/+SERCA1 (n = 3). † indicates  $P < 0.01$  vs. WT; γ indicates  $P < 0.10$  vs. WT; & indicates  $P < 0.10$  vs. *mdx*; # indicates  $P < 0.05$  vs. *mdx/utr<sup>-/-</sup>*. Data presented as mean ± SEM.

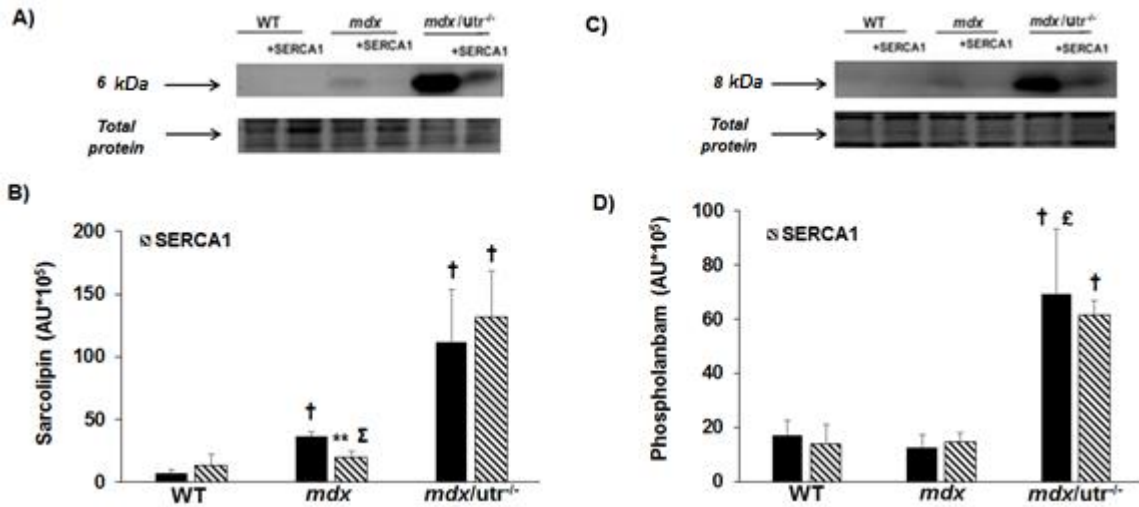


**Figure 5.6 – SERCA1 overexpression decreases levels of SERCA inhibitory proteins in diaphragm muscles from different dystrophic mouse models.** **A)** Representative western blot for sarcolipin (SLN) from WT, *mdx* and *mdx/utr<sup>-/-</sup>* mice with and without SERCA1 overexpression. **B)** Densitometry values for SLN from WT (n = 5), WT/+SERCA1 (n = 5), *mdx* (n = 9), *mdx*/+SERCA1 (n = 9), *mdx/utr<sup>-/-</sup>* (n = 5), and *mdx/utr<sup>-/-</sup>*/+SERCA1 (n = 3). **C)** Representative western blot for phospholamban (PLN) from WT, *mdx* and *mdx/utr<sup>-/-</sup>* mice with and without SERCA1 overexpression. **D)** Densitometry values for PLN from WT (n = 8), WT/+SERCA1 (n = 8), *mdx* (n = 9), *mdx*/+SERCA1 (n = 9), *mdx/utr<sup>-/-</sup>* (n = 6), and *mdx/utr<sup>-/-</sup>*/+SERCA1 (n = 3). † indicates  $P < 0.01$  vs. WT; \*\* indicates  $P = 0.05$  vs. WT; Σ indicates  $P < 0.01$  vs. *mdx*; £ indicates  $P < 0.05$  vs. *mdx*; # indicates  $P < 0.05$  vs. *mdx/utr<sup>-/-</sup>*. Data presented as mean ± SEM.

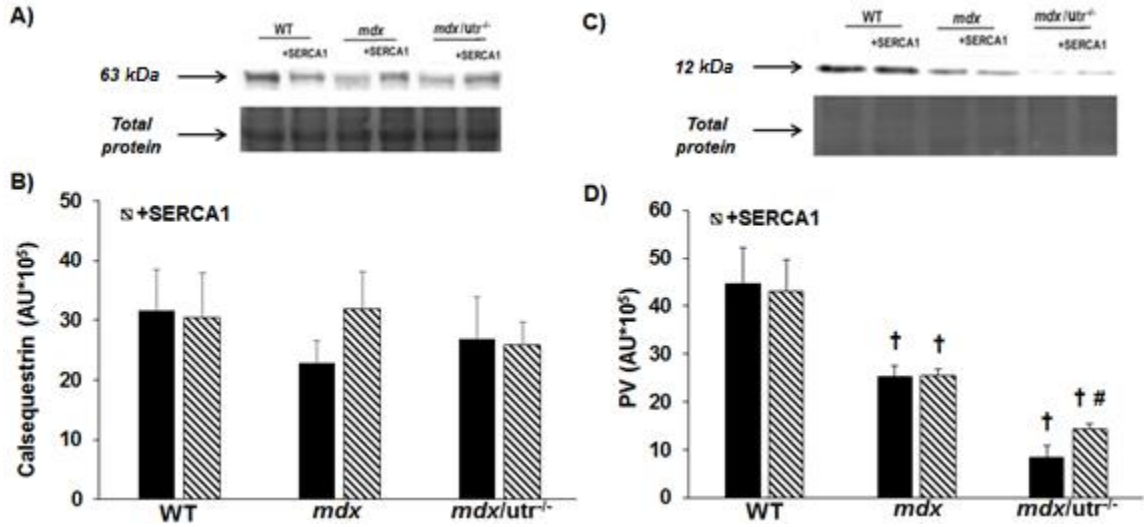


**Figure 5.7 – Effects of SERCA1 overexpression on Ca<sup>2+</sup> regulatory proteins.** **A)** Representative western blot for calsequestrin from WT, *mdx* and *mdx/utr<sup>-/-</sup>* mice with and without SERCA1 overexpression. **B)** Densitometry values for desmin from WT (n = 8), WT/+SERCA1 (n = 7), *mdx* (n = 7), *mdx*/+SERCA1 (n = 9), *mdx/utr<sup>-/-</sup>* (n = 4), and *mdx/utr<sup>-/-</sup>*/+SERCA1 (n = 3). **C)** Representative western blot for parvalbumin (PV) from WT, *mdx* and *mdx/utr<sup>-/-</sup>* mice with and without SERCA1 overexpression. **D)** Densitometry values for PV from WT (n = 5), WT/+SERCA1 (n = 7), *mdx* (n = 7), *mdx*/+SERCA1 (n = 8), *mdx/utr<sup>-/-</sup>* (n = 5), and *mdx/utr<sup>-/-</sup>*/+SERCA1 (n = 3). † indicates *P* < 0.01 vs. WT; # indicates *P* < 0.05 vs. *mdx/utr<sup>-/-</sup>*. Data presented as mean ± SEM.

## Chapter 6: Summary and Future Directions

### Summary

This dissertation is composed of three studies evaluating the role of intracellular  $\text{Ca}^{2+}$  in muscle dysfunction and damage in different mouse models of DMD. In study #1 we had two aims: the first aim was to evaluate if E-C coupling failure following repeated muscle contractions was greater in single muscle fibers from *mdx/utr<sup>-/-</sup>* mice compared with fibers from *mdx* mice, while in the second aim we determined whether protease inhibition could prevent E-C uncoupling following repeated tetani in single muscle fibers from different dystrophic mouse models. Our results demonstrated that E-C coupling failure following repeated contractions was greater in fibers from *mdx/utr<sup>-/-</sup>* mice compared with fibers from *mdx* mice, suggesting that lack of utr in dystrophic muscles further impairs muscle function following repeated contractions. Additionally, our data demonstrated that protease inhibition attenuated the prolonged E-C coupling impairment in muscle fibers from different dystrophic mice. This is the first study to demonstrate the role of proteases in the prolonged E-C coupling failure following repeated muscle contractions in multiple dystrophic mouse models. These data further suggest that acute protease inhibition may be useful in reducing muscle weakness in DMD.

In study #2 we evaluated the effects of SERCA1 overexpression in the more severe *mdx/utr<sup>-/-</sup>* mouse model of DMD. For this, we crossed SERCA1 overexpressing mice with *mdx/utr<sup>+/-</sup>* to generate *mdx/+SERCA1* and *mdx/utr<sup>-/-</sup>+SERCA1* mice. At ~3 mos of age, we used two subsets of mice to evaluate changes in body and muscle mass,  $\text{Ca}^{2+}$ -handling in single muscle fibers, quadriceps torque, markers of muscle damage and response to



repeated eccentric contractions. Overall, SERCA1 overexpression in dystrophic mice led to a 2 to ~3 fold increase in maximal SR-Ca<sup>2+</sup> ATPase activity, which was sufficient to alter body and muscle mass to more closely resemble that of healthy animals, decrease markers of muscle damage (i.e., lower CNFs, necrosis, and circulating CK levels), and protect the muscle from contraction-induced injury. This is the first report to demonstrate that SERCA1 overexpression can mitigate the disease phenotype in the *mdx/utr*<sup>-/-</sup> mouse, a model with a more similar disease progression to that of DMD patients than the *mdx* mouse. These data support the notion that increased SERCA1 expression, or activity, could have therapeutic utility in DMD.

In study #3 we evaluated the effects of SERCA1 overexpression on common downstream targets of increased intracellular Ca<sup>2+</sup> levels in different skeletal muscles from both *mdx* and *mdx/utr*<sup>-/-</sup> mouse models. More specifically, the purpose of this study was to evaluate changes in calpain activation, degradation of calpain targets [desmin and junctophin-1 (JP1)], oxidative stress (protein carbonyls), ER stress [Grp78/BiP and C/EBP homologous protein (CHOP)], levels of SERCA inhibitory proteins [sarcolipin (SLN) and phospholamban (PLN)], and Ca<sup>2+</sup>-handling proteins [parvalbumin (PV) and calsequestrin] in muscles from *mdx* and *mdx/utr*<sup>-/-</sup> mice with and without SERCA1 overexpression. Our findings demonstrated that SERCA1 overexpression decreased calpain activation in *mdx* muscle only, while partially attenuated the degradation of the calpain target desmin in *mdx/utr*<sup>-/-</sup> mice. Additionally, SERCA1 overexpression decreased the SERCA-inhibitory protein sarcolipin in *mdx* muscle but did not alter levels of Ca<sup>2+</sup> regulatory proteins in either dystrophic model. Lastly, SERCA1 overexpression blunted the increase in endoplasmic reticulum stress markers Grp78/BiP in *mdx* mice and CHOP in *mdx* and *mdx/utr*<sup>-/-</sup> mice.

Overall, our findings provide insight into downstream alterations due to SERCA1 overexpression in different dystrophic mouse models mice.

### **Limitations and Future Directions**

In study #3 we sought to evaluate the underlying mechanisms behind the benefits of SERCA1 overexpression in different dystrophic models. We evaluated samples previously collected from another study, thus limiting the amount of samples available for the proposed assays. For instance, we only had a small sample size for each muscle from animals from both *mdx/utr<sup>-/-</sup>* (n = 3-5) and *mdx/utr<sup>-/+</sup>+SERCA1* (n = 3) groups, which limited our ability to perform evaluations in at least 6-7 different samples in these groups. Moreover, although we originally proposed to evaluate multiple targets in the same muscle (i.e., diaphragm), we had to use a different muscle (i.e., gastrocnemius) to perform some of assays. This was not only due to the limited sample size, but also due to different conditions for sample preparation for different assays (e.g., lysis buffers for calpain activity, protein carbonyls, and western blot were not similar).

We were not able to assess targets that were previously proposed to be evaluated, such as SERCA2 levels or levels of titin, due to technical limitations and financial constraints (i.e., problems with antibody or limitations with our equipment). Although we evaluated several different pathways previously shown to be targeted by increased intracellular Ca<sup>2+</sup> levels, we did not address the contribution of other pathways or targets that could help explain the present findings. Briefly, while we used an assay to evaluate calpain enzymatic activity, which evaluates the activation of calpain-1, -2, and -3, we did not assess the levels of full length and autolyzed calpain-2 and -3. Additionally, we only

evaluated levels of protein carbonyls as a marker of oxidative stress, while not assessing the effects of SERCA1 overexpression on other markers of oxidative stress, such as carbohydrate oxidation, lipid peroxidation, and DNA oxidation. As previously mentioned in the discussion of chapter 5, another limitation of study #3 is that we did not evaluate the levels of the 15 kDa isoform of JP1, hence not being able to fully determine the extent of breakdown of the protein. Lastly, we did not evaluate levels of JP2, another junctophilin present at the triad junction of skeletal muscle fibers that has been shown to be proteolysed in *mdx* mice (249).

*Alternative pathways that could have been altered by SERCA1 overexpression: NF- $\kappa$ B, p38-MAPK, iNOS, & Bax*

Nuclear factor- $\kappa$ B (NF- $\kappa$ B) consists of a family of transcription factors that play critical roles in a variety of cellular processes (161). For instance, NF- $\kappa$ B has been shown to be one of the most important signaling pathways contributing to skeletal muscle loss (161). Genetic and pharmacological studies have provided evidence that specific modulation of NF- $\kappa$ B activity can prevent skeletal muscle loss in DMD mouse models, several types of cancer, and during muscle unloading (2, 64, 174). Increased activity of NF- $\kappa$ B leads to skeletal muscle atrophy through different mechanisms: 1) NF- $\kappa$ B can increase the expression of proteins in the ubiquitin-proteasome system involved in the breakdown of proteins during muscle wasting; and 2) NF- $\kappa$ B can increase the expression of inflammation-related molecules which can promote muscle wasting (161). The ubiquitin-proteasome system is a major regulator of muscle protein breakdown, and the key enzyme in this system is the E3 ubiquitin ligase. Two inducible E3 ubiquitin ligases,

atrogin-1 and muscle RING finger protein 1 (MuRF1), have been shown to play important roles in the degradation of skeletal muscle proteins (44, 143). Furthermore, reports in the literature have shown that inhibition of the NF- $\kappa$ B pathway leads to decreases in MuRF1 expression, thus attenuating muscle atrophy in response to nerve injury (64, 245).

Recent studies have demonstrated a link between increased intracellular Ca<sup>2+</sup> levels and activation of NF- $\kappa$ B in *mdx* myotubes (11, 12). Altamirano and colleagues showed that resting intracellular Ca<sup>2+</sup> levels and basal NF- $\kappa$ B activation were higher in dystrophic vs. WT myotubes (11). The increased NF- $\kappa$ B activity was associated with increased transcriptional activity and p65 nuclear localization, which were both reversed when resting intracellular Ca<sup>2+</sup> levels were lowered (11). Moreover, mRNA levels of nitric-oxide synthase (iNOS), an inducer of muscle oxidative damage through the production of nitric oxide and peroxynitrite, was 5 times greater in *mdx* vs. WT myotubes; yet, reducing resting intracellular Ca<sup>2+</sup> attenuated the increased iNOS expression in *mdx* myotubes (11). Although several different Ca<sup>2+</sup>-dependent pathways can modulate the NF- $\kappa$ B signaling pathway (e.g., JNK, ERK1/2, protein kinase C, etc.), Altamirano and colleagues demonstrated that *only* inhibition of p38 MAPK was able to attenuate the increases in NF- $\kappa$ B expression (11). Overall, these findings demonstrate that increased resting intracellular Ca<sup>2+</sup> levels in dystrophic myotubes modulate the activation of p38 MAPK, NF- $\kappa$ B, and iNOS. Wissing and colleagues have demonstrated that p38 MAPK, a widely recognized activator of apoptosis in different cells, induces myofiber death through a mitochondrial-dependent pathway that includes the activation of Bax (367). Briefly, in mitochondria-induced apoptosis, Bax migrates and releases cytochrome c from mitochondria. Once cytochrome c reaches the cytoplasm it binds Apaf-1, which results in the activation of

caspase-9. Activated caspase-9 will then activate caspase-3, which in turn will execute apoptosis (111). Treatment of *mdx* mice with nifedipine, an L-type Ca<sup>2+</sup> channel blocker, diminished the increased activation of Bax in *mdx* diaphragms (12).

Although intracellular Ca<sup>2+</sup> has been shown to contribute to the dystrophic phenotype through mechanisms such as the activation of calpains and opening of the mitochondrial permeability transition pore, newer evidence demonstrates that the underlying mechanisms behind the contribution of Ca<sup>2+</sup> to the increased muscle death in DMD are far more complex. Briefly, raises in intracellular Ca<sup>2+</sup> levels in dystrophic myotubes have been linked with the activation of NF- $\kappa$ B, p38-MAPK, iNOS, and Bax (Figure 6.1) (11, 12). Thus, activation of NF- $\kappa$ B, p38-MAPK, iNOS, and Bax are known to increase muscle wasting through the activation of apoptosis, oxidative stress, and the ubiquitin-proteasome system (11, 12). Therefore, we propose that the improvement in the disease pathophysiology of different dystrophic mouse models by SERCA1 overexpression could have also been due to the potential decrease in the activation of these pathways (Figure 6.1). Future studies should evaluate the role of SERCA1 overexpression in altering the activation of NF- $\kappa$ B, p38-MAPK, iNOS, and Bax in dystrophic muscles.

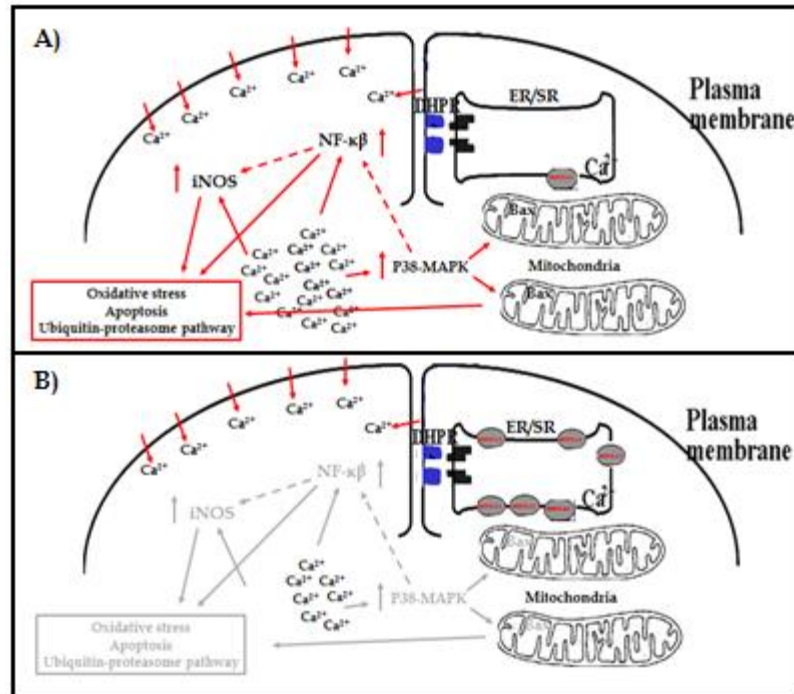


**Figure 6.1 – Proposed model of  $\text{Ca}^{2+}$  mediated activation of cell degradatory pathways.** **A)** Recent evidence demonstrates that elevated intracellular  $\text{Ca}^{2+}$  levels increases the expression of pro-apoptotic and pro-inflammatory genes (NF- $\kappa\beta$ , p38-MAPK, iNOS, and Bax), which leads to increased muscle damage in dystrophic skeletal muscle cells (11, 12). **B)** Suggested model demonstrating the role of SERCA1 overexpression in attenuating the activation of NF- $\kappa\beta$ , p38-MAPK, iNOS, and Bax in dystrophic muscles.

*Current therapeutic approaches in DMD – evidence of  $\text{Ca}^{2+}$  control as a therapeutic option*

The growing interest in therapies for rare diseases, combined with the lack of effective treatment for DMD, has triggered great interest from industry and academia in identifying potential treatments for the disease. Although DMD is a well-defined genetic disorder, translating the understanding of the molecular mechanisms underlying DMD pathophysiology to drug discovery and development has been challenging (40). One obstacle relates to the large size of dystrophin (427 kDa), which does not allow the use of common viral vectors, thus limiting the effectiveness of potential viral constructs for gene replacement approaches (40). Additionally, although the main cause of DMD is the lack of dystrophin, other intracellular alterations also contribute to disease progression (e.g.,

inflammation, oxidative stress, fibrosis, and  $\text{Ca}^{2+}$  dysregulation). Therefore, current therapies being evaluated focus on strategies to attenuate disease progression as well as dystrophin replacement. Such therapies include 1) dystrophin expression restoration (e.g., therapies targeting the suppression of nonsense mutations in the dystrophin gene); 2) expression of compensatory proteins (e.g., mini-dystrophin and utrophin); 3) improvement in intracellular  $\text{Ca}^{2+}$  (e.g., increase SERCA activity, L-type calcium channel blocker, or RyR stabilizer); 4) antioxidants (e.g., N-acetyl cysteine, coenzyme-Q10 and Idebenone); and 5) anti-inflammatory drugs (e.g., VBP15 and CAT-1004) (40).

In a recent review, Burr and Molckentin discussed the current state of knowledge of therapies focusing on the  $\text{Ca}^{2+}$  hypothesis as a potential treatment option for DMD (61). Briefly, studies using dystrophic mouse models have shown preclinical efficacy of several different compounds (e.g., Debio-025, cariporide, S107, BGP-15, streptomycin, and many others) that attenuate increases in intracellular  $\text{Ca}^{2+}$  levels and lead to improvements in disease pathophysiology [see reference (61)]. In addition to drug treatment, there is also a growing interest in gene therapy approaches (61). For example, human clinical trials with adeno-associated virus type 1 (AAV1)/SERCA2a demonstrated safety and increased coronary blood flow in patients with advanced heart failure (150). Additionally, SERCA gene therapy has also been efficacious in different dystrophic mouse models (145, 243).

Our findings presented in this dissertation provide further proof of concept that targeting intracellular  $\text{Ca}^{2+}$  control has therapeutic potential for DMD. More specifically, increased SERCA1 expression led to improvements in *mdx/utr<sup>-/-</sup>* mice, a mouse model with severe disease pathophysiology. Thus, our findings support the validation of SERCA1 as a therapeutic target for new drug treatments in DMD.

## Literature Cited

1. **Aartsma-Rus A, Van Deutekom JC, Fokkema IF, Van Ommen GJ, and Den Dunnen JT.** Entries in the Leiden Duchenne muscular dystrophy mutation database: an overview of mutation types and paradoxical cases that confirm the reading-frame rule. *Muscle Nerve* 34: 135-144, 2006.
2. **Acharyya S, Villalta SA, Bakkar N, Bupha-Intr T, Janssen PM, Carathers M, Li ZW, Beg AA, Ghosh S, Sahenk Z, Weinstein M, Gardner KL, Rafael-Fortney JA, Karin M, Tidball JG, Baldwin AS, and Guttridge DC.** Interplay of IKK/NF-kappaB signaling in macrophages and myofibers promotes muscle degeneration in Duchenne muscular dystrophy. *J Clin Invest* 117: 889-901, 2007.
3. **Adams ME, Butler MH, Dwyer TM, Peters MF, Murnane AA, and Froehner SC.** Two forms of mouse syntrophin, a 58 kd dystrophin-associated protein, differ in primary structure and tissue distribution. *Neuron* 11: 531-540, 1993.
4. **Adams ME, Dwyer TM, Dowler LL, White RA, and Froehner SC.** Mouse alpha 1- and beta 2-syntrophin gene structure, chromosome localization, and homology with a discs large domain. *J Biol Chem* 270: 25859-25865, 1995.
5. **Ahn AH, and Kunkel LM.** Syntrophin binds to an alternatively spliced exon of dystrophin. *J Cell Biol* 128: 363-371, 1995.
6. **Ahn AH, Yoshida M, Anderson MS, Feener CA, Selig S, Hagiwara Y, Ozawa E, and Kunkel LM.** Cloning of human basic A1, a distinct 59-kDa dystrophin-associated protein encoded on chromosome 8q23-24. *Proc Natl Acad Sci U S A* 91: 4446-4450, 1994.
7. **Akhavan A, Crivelli SN, Singh M, Lingappa VR, and Muschler JL.** SEA domain proteolysis determines the functional composition of dystroglycan. *Faseb j* 22: 612-621, 2008.
8. **Alderton JM, and Steinhardt RA.** Calcium influx through calcium leak channels is responsible for the elevated levels of calcium-dependent proteolysis in dystrophic myotubes. *J Biol Chem* 275: 9452-9460, 2000.
9. **Allamand V, and Campbell KP.** Animal models for muscular dystrophy: valuable tools for the development of therapies. *Hum Mol Genet* 9: 2459-2467, 2000.
10. **Allen DG, Gervasio OL, Yeung EW, and Whitehead NP.** Calcium and the damage pathways in muscular dystrophy. *Can J Physiol Pharmacol* 88: 83-91, 2010.
11. **Altamirano F, Lopez JR, Henriquez C, Molinski T, Allen PD, and Jaimovich E.** Increased resting intracellular calcium modulates NF-kappaB-dependent inducible nitric-oxide synthase gene expression in dystrophic mdx skeletal myotubes. *J Biol Chem* 287: 20876-20887, 2012.
12. **Altamirano F, Valladares D, Henriquez-Olguin C, Casas M, Lopez JR, Allen PD, and Jaimovich E.** Nifedipine treatment reduces resting calcium concentration, oxidative and apoptotic gene expression, and improves muscle function in dystrophic mdx mice. *PLoS One* 8: e81222, 2013.
13. **Ambrose HJ, Blake DJ, Nawrotzki RA, and Davies KE.** Genomic organization of the mouse dystrobrevin gene: comparative analysis with the dystrophin gene. *Genomics* 39: 359-369, 1997.
14. **Araishi K, Sasaoka T, Imamura M, Noguchi S, Hama H, Wakabayashi E, Yoshida M, Hori T, and Ozawa E.** Loss of the sarcoglycan complex and sarcospan leads to muscular dystrophy in beta-sarcoglycan-deficient mice. *Hum Mol Genet* 8: 1589-1598, 1999.
15. **Araki E, Nakamura K, Nakao K, Kameya S, Kobayashi O, Nonaka I, Kobayashi T, and Katsuki M.** Targeted disruption of exon 52 in the mouse dystrophin gene induced muscle degeneration similar to that observed in Duchenne muscular dystrophy. *Biochem Biophys Res Commun* 238: 492-497, 1997.
16. **Arthur GD, Booker TS, and Belcastro AN.** Exercise promotes a subcellular redistribution of calcium-stimulated protease activity in striated muscle. *Can J Physiol Pharmacol* 77: 42-47, 1999.



17. **Arthur PG, Grounds MD, and Shavlakadze T.** Oxidative stress as a therapeutic target during muscle wasting: considering the complex interactions. *Curr Opin Clin Nutr Metab Care* 11: 408-416, 2008.
18. **Ashley CC, Mulligan IP, and Lea TJ.** Ca<sup>2+</sup> and activation mechanisms in skeletal muscle. *Q Rev Biophys* 24: 1-73, 1991.
19. **Badalamente MA, and Stracher A.** Delay of muscle degeneration and necrosis in mdx mice by calpain inhibition. *Muscle Nerve* 23: 106-111, 2000.
20. **Barreiro E, and Hussain SN.** Protein carbonylation in skeletal muscles: impact on function. *Antioxid Redox Signal* 12: 417-429, 2010.
21. **Basset O, Boittin FX, Cognard C, Constantin B, and Ruegg UT.** Bcl-2 overexpression prevents calcium overload and subsequent apoptosis in dystrophic myotubes. *Biochem J* 395: 267-276, 2006.
22. **Basset O, Boittin FX, Dorchies OM, Chatton JY, van Breemen C, and Ruegg UT.** Involvement of inositol 1,4,5-trisphosphate in nicotinic calcium responses in dystrophic myotubes assessed by near-plasma membrane calcium measurement. *J Biol Chem* 279: 47092-47100, 2004.
23. **Batchelor CL, and Winder SJ.** Sparks, signals and shock absorbers: how dystrophin loss causes muscular dystrophy. *Trends in Cell Biology* 16: 198-205, 2006.
24. **Baylor SM, and Hollingworth S.** Sarcoplasmic reticulum calcium release compared in slow-twitch and fast-twitch fibres of mouse muscle. *Journal of Physiology-London* 551: 125-138, 2003.
25. **Beard NA, Laver DR, and Dulhunty AF.** Calsequestrin and the calcium release channel of skeletal and cardiac muscle. *Prog Biophys Mol Biol* 85: 33-69, 2004.
26. **Beckman JS, and Koppenol WH.** Nitric oxide, superoxide, and peroxynitrite: the good, the bad, and ugly. *Am J Physiol* 271: C1424-1437, 1996.
27. **Beckmann JS, and Spencer M.** Calpain 3, the "gatekeeper" of proper sarcomere assembly, turnover and maintenance. *Neuromuscul Disord* 18: 913-921, 2008.
28. **Belcastro AN, Shewchuk LD, and Raj DA.** Exercise-induced muscle injury: a calpain hypothesis. *Mol Cell Biochem* 179: 135-145, 1998.
29. **Bellinger AM, Reiken S, Carlson C, Mongillo M, Liu X, Rothman L, Matecki S, Lacampagne A, and Marks AR.** Hypernitrosylated ryanodine receptor calcium release channels are leaky in dystrophic muscle. *Nat Med* 15: 325-330, 2009.
30. **Berridge MJ, Bootman MD, and Roderick HL.** Calcium signalling: dynamics, homeostasis and remodelling. *Nat Rev Mol Cell Biol* 4: 517-529, 2003.
31. **Bezanilla F, Caputo C, Gonzalez-Serratos H, and Venosa RA.** Sodium dependence of the inward spread of activation in isolated twitch muscles of the frog. *Journal of Physiology-London* 223: 507-8, 1972.
32. **Bhupathy P, Babu GJ, and Periasamy M.** Sarcolipin and phospholamban as regulators of cardiac sarcoplasmic reticulum Ca<sup>2+</sup> ATPase. *J Mol Cell Cardiol* 42: 903-911, 2007.
33. **Binder HJ, and Spiro HM.** Tocopherol deficiency in man. *Am J Clin Nutr* 20: 594-603, 1967.
34. **Bischoff R.** Rapid adhesion of nerve cells to muscle fibers from adult rats is mediated by a sialic acid-binding receptor. *J Cell Biol* 102: 2273-2280, 1986.
35. **Bladen CL, Salgado D, Monges S, Foncuberta ME, Kekou K, Kosma K, Dawkins H, Lamont L, Roy AJ, Chamova T, Guergueltcheva V, Chan S, Korngut L, Campbell C, Dai Y, Wang J, Barisic N, Brabec P, Lahdetie J, Walter MC, Schreiber-Katz O, Karcagi V, Garami M, Viswanathan V, Bayat F, Buccella F, Kimura E, Koeks Z, van den Bergen JC, Rodrigues M, Roxburgh R, Lusakowska A, Kostera-Pruszczyk A, Zimowski J, Santos R, Neagu E, Artemieva S, Rasic VM, Vojinovic D, Posada M, Bloetzer C, Jeannet PY, Joncourt F, Diaz-Manera J, Gallardo E, Karaduman AA, Topaloglu H, El Sherif R, Stringer A, Shatillo AV, Martin AS, Peay HL, Bellgard MI, Kirschner J,**

- Flanigan KM, Straub V, Bushby K, Verschuuren J, Aartsma-Rus A, Beroud C, and Lochmuller H.** The TREAT-NMD DMD Global Database: analysis of more than 7,000 Duchenne muscular dystrophy mutations. *Hum Mutat* 36: 395-402, 2015.
36. **Blake DJ.** Dystrobrevin dynamics in muscle-cell signalling: a possible target for therapeutic intervention in Duchenne muscular dystrophy? *Neuromuscul Disord* 12 Suppl 1: S110-117, 2002.
37. **Blake DJ, and Kroger S.** The neurobiology of Duchenne muscular dystrophy: learning lessons from muscle? *Trends Neurosci* 23: 92-99, 2000.
38. **Blake DJ, Nawrotzki R, Peters MF, Froehner SC, and Davies KE.** Isoform diversity of dystrobrevin, the murine 87-kDa postsynaptic protein. *J Biol Chem* 271: 7802-7810, 1996.
39. **Blake DJ, Weir A, Newey SE, and Davies KE.** Function and genetics of dystrophin and dystrophin-related proteins in muscle. *Physiological Reviews* 82: 291-329, 2002.
40. **Blat Y, and Blat S.** Drug Discovery of Therapies for Duchenne Muscular Dystrophy. *J Biomol Screen* 20: 1189-1203, 2015.
41. **Blau HM, Webster C, and Pavlath GK.** Defective myoblasts identified in Duchenne muscular dystrophy. *Proc Natl Acad Sci U S A* 80: 4856-4860, 1983.
42. **Blau HM, Webster C, Pavlath GK, and Chiu CP.** Evidence for defective myoblasts in Duchenne muscular dystrophy. *Adv Exp Med Biol* 182: 85-110, 1985.
43. **Bodensteiner JB, and Engel AG.** Intracellular calcium accumulation in Duchenne dystrophy and other myopathies: a study of 567,000 muscle fibers in 114 biopsies. *Neurology* 28: 439-446, 1978.
44. **Bodine SC, Latres E, Baumhueter S, Lai VK, Nunez L, Clarke BA, Poueymirou WT, Panaro FJ, Na E, Dharmarajan K, Pan ZQ, Valenzuela DM, DeChiara TM, Stitt TN, Yancopoulos GD, and Glass DJ.** Identification of ubiquitin ligases required for skeletal muscle atrophy. In: *Science*. United States: 2001, p. 1704-1708.
45. **Boldrin L, Zammit PS, and Morgan JE.** Satellite cells from dystrophic muscle retain regenerative capacity. *Stem Cell Res* 14: 20-29, 2015.
46. **Bole DG, Hendershot LM, and Kearney JF.** Posttranslational association of immunoglobulin heavy chain binding protein with nascent heavy chains in nonsecreting and secreting hybridomas. *J Cell Biol* 102: 1558-1566, 1986.
47. **Bonaldo P, and Sandri M.** Cellular and molecular mechanisms of muscle atrophy. *Dis Model Mech* 6: 25-39, 2013.
48. **Branca D, Gugliucci A, Bano D, Brini M, and Carafoli E.** Expression, partial purification and functional properties of the muscle-specific calpain isoform p94. *Eur J Biochem* 265: 839-846, 1999.
49. **Brandl CJ, deLeon S, Martin DR, and MacLennan DH.** Adult forms of the Ca<sup>2+</sup>-ATPase of sarcoplasmic reticulum. Expression in developing skeletal muscle. *J Biol Chem* 262: 3768-3774, 1987.
50. **Breckner A, Ganz M, Marcellin D, Richter J, Gerwin N, and Rausch M.** Effect of Calstabin1 depletion on calcium transients and energy utilization in muscle fibers and treatment opportunities with RyR1 stabilizers. *PLoS One* 8: e81277, 2013.
51. **Bredt DS.** Knocking signalling out of the dystrophin complex. *Nat Cell Biol* 1: E89-91, 1999.
52. **Briguet A, Erb M, Courdier-Fruh I, Barzaghi P, Santos G, Herzner H, Lescop C, Siendt H, Henneboehle M, Weyermann P, Magyar JP, Dubach-Powell J, Metz G, and Meier T.** Effect of calpain and proteasome inhibition on Ca<sup>2+</sup>-dependent proteolysis and muscle histopathology in the mdx mouse. *Faseb Journal* 22: 4190-4200, 2008.
53. **Brooke MH, Fenichel GM, Griggs RC, Mendell JR, Moxley R, Florence J, King WM, Pandya S, Robison J, Schierbecker J, and et al.** Duchenne muscular dystrophy: patterns of clinical progression and effects of supportive therapy. *Neurology* 39: 475-481, 1989.

54. **Brookes PS, Yoon YS, Robotham JL, Anders MW, and Sheu SS.** Calcium, ATP, and ROS: a mitochondrial love-hate triangle. *American Journal of Physiology-Cell Physiology* 287: C817-C833, 2004.
55. **Brostrom MA, and Brostrom CO.** Calcium dynamics and endoplasmic reticular function in the regulation of protein synthesis: implications for cell growth and adaptability. *Cell Calcium* 34: 345-363, 2003.
56. **Buckingham M, Bajard L, Chang T, Daubas P, Hadchouel J, Meilhac S, Montarras D, Rocancourt D, and Relaix F.** The formation of skeletal muscle: from somite to limb. *J Anat* 202: 59-68, 2003.
57. **Buetler TM, Renard M, Offord EA, Schneider H, and Ruegg UT.** Green tea extract decreases muscle necrosis in *mdx* mice and protects against reactive oxygen species. *Am J Clin Nutr* 75: 749-753, 2002.
58. **Bulfield G, Siller WG, Wight PA, and Moore KJ.** X chromosome-linked muscular dystrophy (*mdx*) in the mouse. *Proc Natl Acad Sci U S A* 81: 1189-1192, 1984.
59. **Burkin DJ, Wallace GQ, Nicol KJ, Kaufman DJ, and Kaufman SJ.** Enhanced expression of the alpha 7 beta 1 integrin reduces muscular dystrophy and restores viability in dystrophic mice. *J Cell Biol* 152: 1207-1218, 2001.
60. **Burr AR, Millay DP, Goonasekera SA, Park KH, Sargent MA, Collins J, Altamirano F, Philipson KD, Allen PD, Ma J, Lopez JR, and Molkentin JD.** Na<sup>+</sup> dysregulation coupled with Ca<sup>2+</sup> entry through NCX1 promotes muscular dystrophy in mice. *Mol Cell Biol* 34: 1991-2002, 2014.
61. **Burr AR, and Molkentin JD.** Genetic evidence in the mouse solidifies the calcium hypothesis of myofiber death in muscular dystrophy. *Cell Death Differ* 22: 1402-1412, 2015.
62. **Bushby K, Finkel R, Birnkrant DJ, Case LE, Clemens PR, Cripe L, Kaul A, Kinnett K, McDonald C, Pandya S, Poysky J, Shapiro F, Tomezsko J, and Constantin C.** Diagnosis and management of Duchenne muscular dystrophy, part 1: diagnosis, and pharmacological and psychosocial management. *Lancet Neurol* 9: 77-93, 2010.
63. **Bushby K, Finkel R, Birnkrant DJ, Case LE, Clemens PR, Cripe L, Kaul A, Kinnett K, McDonald C, Pandya S, Poysky J, Shapiro F, Tomezsko J, and Constantin C.** Diagnosis and management of Duchenne muscular dystrophy, part 2: implementation of multidisciplinary care. *Lancet Neurol* 9: 177-189, 2010.
64. **Cai D, Frantz JD, Tawa NE, Jr., Melendez PA, Oh BC, Lidov HG, Hasselgren PO, Frontera WR, Lee J, Glass DJ, and Shoelson SE.** IKKbeta/NF-kappaB activation causes severe muscle wasting in mice. In: *Cell*. United States: 2004, p. 285-298.
65. **Call JA, Ervasti JM, and Lowe DA.** TAT- $\mu$ Utrophin mitigates the pathophysiology of dystrophin and utrophin double-knockout mice. *J Appl Physiol (1985)* 111: 200-205, 2011.
66. **Calvo AC, Manzano R, Atencia-Cibreiro G, Oliven S, Munoz MJ, Zaragoza P, Cordero-Vazquez P, Esteban-Perez J, Garcia-Redondo A, and Osta R.** Genetic Biomarkers for ALS Disease in Transgenic SOD1(G93A) Mice. *Plos One* 7: 2012.
67. **Canton M, Menazza S, and Di Lisa F.** Oxidative stress in muscular dystrophy: from generic evidence to specific sources and targets. *J Muscle Res Cell Motil* 35: 23-36, 2014.
68. **Capote J, DiFranco M, and Vergara JL.** Excitation-contraction coupling alterations in *mdx* and utrophin/dystrophin double knockout mice: a comparative study. *American Journal of Physiology-Cell Physiology* 298: C1077-C1086, 2010.
69. **Cardenas C, Juretic N, Bevilacqua JA, Garcia IE, Figueroa R, Hartley R, Taratuto AL, Gejman R, Riveros N, Molgo J, and Jaimovich E.** Abnormal distribution of inositol 1,4,5-trisphosphate receptors in human muscle can be related to altered calcium signals and gene expression in Duchenne dystrophy-derived cells. *Faseb j* 24: 3210-3221, 2010.

70. **Chakkalakal JV, Harrison MA, Carbonetto S, Chin E, Michel RN, and Jasmin BJ.** Stimulation of calcineurin signaling attenuates the dystrophic pathology in *mdx* mice. *Hum Mol Genet* 13: 379-388, 2004.
71. **Chakkalakal JV, Michel SA, Chin ER, Michel RN, and Jasmin BJ.** Targeted inhibition of Ca<sup>2+</sup>/calmodulin signaling exacerbates the dystrophic phenotype in *mdx* mouse muscle. *Hum Mol Genet* 15: 1423-1435, 2006.
72. **Chamberlain JS, Metzger J, Reyes M, Townsend D, and Faulkner JA.** Dystrophin-deficient *mdx* mice display a reduced life span and are susceptible to spontaneous rhabdomyosarcoma. *Faseb j* 21: 2195-2204, 2007.
73. **Chan S, and Head SI.** The role of branched fibres in the pathogenesis of Duchenne muscular dystrophy. *Experimental Physiology* 96: 564-571, 2011.
74. **Chapman VM, Miller DR, Armstrong D, and Caskey CT.** Recovery of induced mutations for X chromosome-linked muscular dystrophy in mice. *Proc Natl Acad Sci U S A* 86: 1292-1296, 1989.
75. **Chaudhary P, Suryakumar G, Prasad R, Singh SN, Ali S, and Ilavazhagan G.** Chronic hypobaric hypoxia mediated skeletal muscle atrophy: role of ubiquitin-proteasome pathway and calpains. *Mol Cell Biochem* 364: 101-113, 2012.
76. **Chevron MP, Echenne B, and Demaille J.** Absence of dystrophin and utrophin in a boy with severe muscular dystrophy. *N Engl J Med* 331: 1162-1163, 1994.
77. **Childers MK, Bogan JR, Bogan DJ, Greiner H, Holder M, Grange RW, and Kornegay JN.** Chronic administration of a leupeptin-derived calpain inhibitor fails to ameliorate severe muscle pathology in a canine model of duchenne muscular dystrophy. *Front Pharmacol* 2: 89, 2011.
78. **Chin ER, and Allen DG.** The contribution of pH-dependent mechanisms to fatigue at different intensities in mammalian single muscle fibres. *Journal of Physiology-London* 512: 831-840, 1998.
79. **Chin ER, and Allen DG.** The role of elevations in intracellular Ca<sup>2+</sup> in the development of low frequency fatigue in mouse single muscle fibres. *Journal of Physiology-London* 491: 813-824, 1996.
80. **Chin ER, Balnave CD, and Allen DG.** Role of intracellular calcium and metabolites in low-frequency fatigue of mouse skeletal muscle. *American Journal of Physiology-Cell Physiology* 272: C550-C559, 1997.
81. **Chin ER, Green HJ, Grange F, Mercer JD, and O'Brien PJ.** Technical considerations for assessing alterations in skeletal muscle sarcoplasmic reticulum Ca<sup>++</sup>-sequestration function *in vitro*. *Mol Cell Biochem* 139: 41-52, 1994.
82. **Chirgwin JM, Przybyla AE, MacDonald RJ, and Rutter WJ.** Isolation of biologically active ribonucleic acid from sources enriched in ribonuclease. *Biochemistry* 18: 5294-5299, 1979.
83. **Collet C, Allard B, Tourneur Y, and Jacquemond V.** Intracellular calcium signals measured with indo-1 in isolated skeletal muscle fibres from control and *mdx* mice. *J Physiol* 520 Pt 2: 417-429, 1999.
84. **Connolly AM, Keeling RM, Mehta S, Pestronk A, and Sanes JR.** Three mouse models of muscular dystrophy: the natural history of strength and fatigue in dystrophin-, dystrophin/utrophin-, and laminin alpha2-deficient mice. *Neuromuscul Disord* 11: 703-712, 2001.
85. **Coral-Vazquez R, Cohn RD, Moore SA, Hill JA, Weiss RM, Davisson RL, Straub V, Barresi R, Bansal D, Hrstka RF, Williamson R, and Campbell KP.** Disruption of the sarcoglycan-sarcospan complex in vascular smooth muscle: a novel mechanism for cardiomyopathy and muscular dystrophy. *Cell* 98: 465-474, 1999.

86. **Coulton GR, Morgan JE, Partridge TA, and Sloper JC.** The mdx mouse skeletal muscle myopathy: I. A histological, morphometric and biochemical investigation. *Neuropathol Appl Neurobiol* 14: 53-70, 1988.
87. **Cros D, Harnden P, Pellissier JF, and Serratrice G.** Muscle hypertrophy in Duchenne muscular dystrophy. A pathological and morphometric study. *J Neurol* 236: 43-47, 1989.
88. **Cullen MJ, Fulthorpe JJ, and Harris JB.** The distribution of desmin and titin in normal and dystrophic human muscle. *Acta Neuropathol* 83: 158-169, 1992.
89. **Culligan K, Banville N, Dowling P, and Ohlendieck K.** Drastic reduction of calsequestrin-like proteins and impaired calcium binding in dystrophic mdx muscle. *J Appl Physiol (1985)* 92: 435-445, 2002.
90. **Dalle-Donne I, Aldini G, Carini M, Colombo R, Rossi R, and Milzani A.** Protein carbonylation, cellular dysfunction, and disease progression. *J Cell Mol Med* 10: 389-406, 2006.
91. **Dandliker WB, and Fox JB, Jr.** Light scattering of D-glyceraldehyde-3-phosphate dehydrogenase. *J Biol Chem* 214: 275-283, 1955.
92. **De Luca A, Pierno S, Liantonio A, Cetrone M, Camerino C, Simonetti S, Papadia F, and Camerino DC.** Alteration of excitation-contraction coupling mechanism in extensor digitorum longus muscle fibres of dystrophic mdx mouse and potential efficacy of taurine. *Br J Pharmacol* 132: 1047-1054, 2001.
93. **De Palma C, Perrotta C, Pellegrino P, Clementi E, and Cervia D.** Skeletal muscle homeostasis in duchenne muscular dystrophy: modulating autophagy as a promising therapeutic strategy. *Front Aging Neurosci* 6: 188, 2014.
94. **Deconinck AE, Potter AC, Tinsley JM, Wood SJ, Vater R, Young C, Metzinger L, Vincent A, Slater CR, and Davies KE.** Postsynaptic abnormalities at the neuromuscular junctions of utrophin-deficient mice. *Journal of Cell Biology* 136: 883-894, 1997.
95. **Deconinck AE, Rafael JA, Skinner JA, Brown SC, Potter AC, Metzinger L, Watt DJ, Dickson JG, Tinsley JM, and Davies KE.** Utrophin-dystrophin-deficient mice as a model for Duchenne muscular dystrophy. *Cell* 90: 717-727, 1997.
96. **Deconinck N, Rafael JA, Beckers-Bleukx G, Kahn D, Deconinck AE, Davies KE, and Gillis JM.** Consequences of the combined deficiency in dystrophin and utrophin on the mechanical properties and myosin composition of some limb and respiratory muscles of the mouse. *Neuromuscul Disord* 8: 362-370, 1998.
97. **Disatnik MH, Dhawan J, Yu Y, Beal MF, Whirl MM, Franco AA, and Rando TA.** Evidence of oxidative stress in mdx mouse muscle: Studies of the pre-necrotic state. *Journal of the Neurological Sciences* 161: 77-84, 1998.
98. **Divet A, and Huchet-Cadiou C.** Sarcoplasmic reticulum function in slow- and fast-twitch skeletal muscles from mdx mice. *Pflug Arch Eur J Phy* 444: 634-643, 2002.
99. **Divet A, Lompre AM, and Huchet-Cadiou C.** Effect of cyclopiazonic acid, an inhibitor of the sarcoplasmic reticulum Ca-ATPase, on skeletal muscles from normal and mdx mice. *Acta Physiologica Scandinavica* 184: 173-186, 2005.
100. **Dominov JA, Kravetz AJ, Ardelt M, Kostek CA, Beermann ML, and Miller JB.** Muscle-specific BCL2 expression ameliorates muscle disease in laminin alpha 2-deficient, but not in dystrophin-deficient, mice. *Hum Mol Genet* 14: 1029-1040, 2005.
101. **Doran P, Donoghue P, O'Connell K, Gannon J, and Ohlendieck K.** Proteomics of skeletal muscle aging. *Proteomics* 9: 989-1003, 2009.
102. **Dorchies OM, Wagner S, Vuadens O, Waldhauser K, Buetler TM, Kucera P, and Ruegg UT.** Green tea extract and its major polyphenol (-)-epigallocatechin gallate improve muscle function in a mouse model for Duchenne muscular dystrophy. *Am J Physiol Cell Physiol* 290: C616-625, 2006.

103. **Duclos F, Straub V, Moore SA, Venzke DP, Hrstka RF, Crosbie RH, Durbeej M, Lebakken CS, Ettinger AJ, van der Meulen J, Holt KH, Lim LE, Sanes JR, Davidson BL, Faulkner JA, Williamson R, and Campbell KP.** Progressive muscular dystrophy in alpha-sarcoglycan-deficient mice. *J Cell Biol* 142: 1461-1471, 1998.
104. **Dudek J, Benedix J, Cappel S, Greiner M, Jalal C, Muller L, and Zimmermann R.** Functions and pathologies of BiP and its interaction partners. *Cell Mol Life Sci* 66: 1556-1569, 2009.
105. **Duguez S, Bartoli M, and Richard I.** Calpain 3: a key regulator of the sarcomere? *Febs Journal* 273: 3427-3436, 2006.
106. **Dupont-Versteegden EE, Kitten AM, Katz MS, and McCarter RJ.** Elevated levels of albumin in soleus and diaphragm muscles of mdx mice. *Proc Soc Exp Biol Med* 213: 281-286, 1996.
107. **Durbeej M, and Campbell KP.** Muscular dystrophies involving the dystrophin-glycoprotein complex: an overview of current mouse models. *Curr Opin Genet Dev* 12: 349-361, 2002.
108. **Durbeej M, Cohn RD, Hrstka RF, Moore SA, Allamand V, Davidson BL, Williamson RA, and Campbell KP.** Disruption of the beta-sarcoglycan gene reveals pathogenetic complexity of limb-girdle muscular dystrophy type 2E. *Mol Cell* 5: 141-151, 2000.
109. **Dwyer TM, and Froehner SC.** Direct binding of Torpedo syntrophin to dystrophin and the 87 kDa dystrophin homologue. *FEBS Lett* 375: 91-94, 1995.
110. **Eagle M, Baudouin SV, Chandler C, Giddings DR, Bullock R, and Bushby K.** Survival in Duchenne muscular dystrophy: improvements in life expectancy since 1967 and the impact of home nocturnal ventilation. *Neuromuscul Disord* 12: 926-929, 2002.
111. **Earnshaw WC, Martins LM, and Kaufmann SH.** Mammalian caspases: structure, activation, substrates, and functions during apoptosis. *Annu Rev Biochem* 68: 383-424, 1999.
112. **Edwards JN, Friedrich O, Cully TR, von Wegner F, Murphy RM, and Launikonis BS.** Upregulation of store-operated  $Ca^{2+}$  entry in dystrophic mdx mouse muscle. *Am J Physiol Cell Physiol* 299: C42-50, 2010.
113. **Emori Y, Kawasaki H, Imajoh S, Imahori K, and Suzuki K.** Endogenous inhibitor for calcium-dependent cysteine protease contains four internal repeats that could be responsible for its multiple reactive sites. *Proc Natl Acad Sci U S A* 84: 3590-3594, 1987.
114. **England SB, Nicholson LV, Johnson MA, Forrest SM, Love DR, Zubrzycka-Gaarn EE, Bulman DE, Harris JB, and Davies KE.** Very mild muscular dystrophy associated with the deletion of 46% of dystrophin. *Nature* 343: 180-182, 1990.
115. **Ermolova N, Kramerova I, and Spencer MJ.** Autolytic Activation of Calpain 3 Proteinase Is Facilitated by Calmodulin Protein. *Journal of Biological Chemistry* 290: 996-1004, 2015.
116. **Ervasti JM.** Dystrophin, its interactions with other proteins, and implications for muscular dystrophy. *Biochimica Et Biophysica Acta-Molecular Basis of Disease* 1772: 108-117, 2007.
117. **Ervasti JM, and Campbell KP.** A role for the dystrophin-glycoprotein complex as a transmembrane linker between laminin and actin. *J Cell Biol* 122: 809-823, 1993.
118. **Esapa CT, Bentham GR, Schroder JE, Kroger S, and Blake DJ.** The effects of post-translational processing on dystroglycan synthesis and trafficking. *FEBS Lett* 555: 209-216, 2003.
119. **Evans NP, Call JA, Bassaganya-Riera J, Robertson JL, and Grange RW.** Green tea extract decreases muscle pathology and NF-kappaB immunostaining in regenerating muscle fibers of mdx mice. *Clin Nutr* 29: 391-398, 2010.
120. **Faber RM, Hall JK, Chamberlain JS, and Banks GB.** Myofiber branching rather than myofiber hyperplasia contributes to muscle hypertrophy in mdx mice. *Skelet Muscle* 4: 10, 2014.
121. **Fajardo VA, Bombardier E, McMillan E, Tran K, Wadsworth BJ, Gamu D, Hopf A, Vigna C, Smith IC, Bellissimo C, Michel RN, Tarnopolsky MA, Quadrilatero J, and Tupling AR.**

Phospholamban overexpression in mice causes a centronuclear myopathy-like phenotype. *Dis Model Mech* 2015.

122. **Fajardo VA, Bombardier E, Vigna C, Devji T, Bloemberg D, Gamu D, Gramolini AO, Quadrilatero J, and Tupling AR.** Co-Expression of SERCA Isoforms, Phospholamban and Sarcolipin in Human Skeletal Muscle Fibers. *PLoS One* 8: e84304, 2013.

123. **Faysoil A, Nardi O, Orlikowski D, and Annane D.** Cardiomyopathy in Duchenne muscular dystrophy: pathogenesis and therapeutics. *Heart Fail Rev* 15: 103-107, 2010.

124. **Fedorova M, Bollineni RC, and Hoffmann R.** Protein carbonylation as a major hallmark of oxidative damage: update of analytical strategies. *Mass Spectrom Rev* 33: 79-97, 2014.

125. **Feissner RF, Skalska J, Gaum WE, and Sheu S-S.** Crosstalk signaling between mitochondrial Ca<sup>2+</sup> and ROS. *Frontiers in Bioscience-Landmark* 14: 1197-1218, 2009.

126. **Fenichel GM, Brooke MH, Griggs RC, Mendell JR, Miller JP, Moxley RT, 3rd, Park JH, Provine MA, Florence J, Kaiser KK, and et al.** Clinical investigation in Duchenne muscular dystrophy: penicillamine and vitamin E. *Muscle Nerve* 11: 1164-1168, 1988.

127. **Ferretti R, Marques MJ, Pertille A, and Santo Neto H.** Sarcoplasmic-endoplasmic-reticulum Ca<sup>2+</sup>-ATPase and calsequestrin are overexpressed in spared intrinsic laryngeal muscles of dystrophin-deficient *mdx* mice. *Muscle Nerve* 39: 609-615, 2009.

128. **Fielding RA, Ralston SH, and Rizzoli R.** Emerging Impact of Skeletal Muscle in Health and Disease. *Calcified Tissue International* 96: 181-182, 2015.

129. **Fornace AJ, Jr., Alamo I, Jr., and Hollander MC.** DNA damage-inducible transcripts in mammalian cells. *Proc Natl Acad Sci U S A* 85: 8800-8804, 1988.

130. **Fougerousse F, Anderson LV, Delezoide AL, Suel L, Durand M, and Beckmann JS.** Calpain3 expression during human cardiogenesis. *Neuromuscul Disord* 10: 251-256, 2000.

131. **Franco-Obregon A, Jr., and Lansman JB.** Mechanosensitive ion channels in skeletal muscle from normal and dystrophic mice. *J Physiol* 481 ( Pt 2): 299-309, 1994.

132. **Gailly P.** New aspects of calcium signaling in skeletal muscle cells: implications in Duchenne muscular dystrophy. *BBA-Proteins Proteom* 1600: 38-44, 2002.

133. **Gailly P, Boland B, Himpens B, Casteels R, and Gillis JM.** Critical evaluation of cytosolic calcium determination in resting muscle fibres from normal and dystrophic (*mdx*) mice. *Cell Calcium* 14: 473-483, 1993.

134. **Gailly P, De Backer F, Van Schoor M, and Gillis JM.** In situ measurements of calpain activity in isolated muscle fibres from normal and dystrophin-lacking *mdx* mice. *Journal of Physiology-London* 582: 1261-1275, 2007.

135. **Gailly P, Hermans E, Octave JN, and Gillis JM.** Specific increase of genetic expression of parvalbumin in fast skeletal muscles of *mdx* mice. *FEBS Lett* 326: 272-274, 1993.

136. **Gehrig SM, van der Poel C, Sayer TA, Schertzer JD, Henstridge DC, Church JE, Lamon S, Russell AP, Davies KE, Febbraio MA, and Lynch GS.** Hsp72 preserves muscle function and slows progression of severe muscular dystrophy. *Nature* 484: 394-398, 2012.

137. **Gervasio OL, Whitehead NP, Yeung EW, Phillips WD, and Allen DG.** TRPC1 binds to caveolin-3 and is regulated by Src kinase - role in Duchenne muscular dystrophy. *Journal of Cell Science* 121: 2246-2255, 2008.

138. **Gervasio OL, Whitehead NP, Yeung EW, Phillips WD, and Allen DG.** TRPC1 binds to caveolin-3 and is regulated by Src kinase - role in Duchenne muscular dystrophy. *J Cell Sci* 121: 2246-2255, 2008.

139. **Gilchrist JS, Wang KK, Katz S, and Belcastro AN.** Calcium-activated neutral protease effects upon skeletal muscle sarcoplasmic reticulum protein structure and calcium release. *J Biol Chem* 267: 20857-20865, 1992.

140. **Golini L, Chouabe C, Berthier C, Cusimano V, Fornaro M, Bonvallet R, Formoso L, Giacomello E, Jacquemond V, and Sorrentino V.** Junctophilin 1 and 2 proteins interact with the L-type Ca<sup>2+</sup> channel dihydropyridine receptors (DHPRs) in skeletal muscle. In: *J Biol Chem*. United States: 2011, p. 43717-43725.
141. **Goll DE, Neti G, Mares SW, and Thompson VF.** Myofibrillar protein turnover: the proteasome and the calpains. *J Anim Sci* 86: E19-35, 2008.
142. **Goll DE, Thompson VF, Li H, Wei W, and Cong J.** The calpain system. *Physiol Rev* 83: 731-801, 2003.
143. **Gomes MD, Lecker SH, Jagoe RT, Navon A, and Goldberg AL.** Atrogin-1, a muscle-specific F-box protein highly expressed during muscle atrophy. In: *Proc Natl Acad Sci U S A*. United States: 2001, p. 14440-14445.
144. **Goonasekera SA, Davis J, Kwong JQ, Accornero F, Wei-Lapierre L, Sargent MA, Dirksen RT, and Molkentin JD.** Enhanced Ca<sup>2+</sup> influx from STIM1-Orai1 induces muscle pathology in mouse models of muscular dystrophy. *Hum Mol Genet* 2014.
145. **Goonasekera SA, Lam CK, Millay DP, Sargent MA, Hajjar RJ, Kranias EG, and Molkentin JD.** Mitigation of muscular dystrophy in mice by SERCA overexpression in skeletal muscle. *J Clin Invest* 121: 1044-1052, 2011.
146. **Goto S, Nakamura A, Radak Z, Nakamoto H, Takahashi R, Yasuda K, Sakurai Y, and Ishii N.** Carbonylated proteins in aging and exercise: immunoblot approaches. *Mech Ageing Dev* 107: 245-253, 1999.
147. **Grady RM, Grange RW, Lau KS, Maimone MM, Nichol MC, Stull JT, and Sanes JR.** Role for alpha-dystrobrevin in the pathogenesis of dystrophin-dependent muscular dystrophies. *Nat Cell Biol* 1: 215-220, 1999.
148. **Grady RM, Teng H, Nichol MC, Cunningham JC, Wilkinson RS, and Sanes JR.** Skeletal and cardiac myopathies in mice lacking utrophin and dystrophin: a model for Duchenne muscular dystrophy. *Cell* 90: 729-738, 1997.
149. **Grady RM, Zhou H, Cunningham JM, Henry MD, Campbell KP, and Sanes JR.** Maturation and maintenance of the neuromuscular synapse: genetic evidence for roles of the dystrophin--glycoprotein complex. *Neuron* 25: 279-293, 2000.
150. **Greenberg B, Yaroshinsky A, Zsebo KM, Butler J, Felker GM, Voors AA, Rudy JJ, Wagner K, and Hajjar RJ.** Design of a phase 2b trial of intracoronary administration of AAV1/SERCA2a in patients with advanced heart failure: the CUPID 2 trial (calcium up-regulation by percutaneous administration of gene therapy in cardiac disease phase 2b). *JACC Heart Fail* 2: 84-92, 2014.
151. **Grijalba MT, Vercesi AE, and Schreier S.** Ca<sup>2+</sup>-induced increased lipid packing and domain formation in submitochondrial particles. A possible early step in the mechanism of Ca<sup>2+</sup>-stimulated generation of reactive oxygen species by the respiratory chain. *Biochemistry* 38: 13279-13287, 1999.
152. **Groschner K, Rosker C, and Lukas M.** Role of TRP channels in oxidative stress. *Novartis Found Symp* 258: 222-230; discussion 231-225, 263-226, 2004.
153. **Grounds MD, Radley HG, Lynch GS, Nagaraju K, and De Luca A.** Towards developing standard operating procedures for pre-clinical testing in the mdx mouse model of Duchenne muscular dystrophy. *Neurobiol Dis* 31: 1-19, 2008.
154. **Guillaume D.** Paralysie musculaire progressive de la langue, du voile du palais et des lèvres. *Arch Gen Med* 1860, p. 283-431.
155. **Guroff G.** A neutral, calcium-activated proteinase from the soluble fraction of the rat brain. *J Biol Chem* 239: 149-155, 1964.



156. **Guyon JR, Kudryashova E, Potts A, Dalkilic I, Brosius MA, Thompson TG, Beckmann JS, Kunkel LM, and Spencer MJ.** Calpain 3 cleaves filamin C and regulates its ability to interact with gamma- and delta-sarcoglycans. *Muscle Nerve* 28: 472-483, 2003.
157. **Haas IG, and Wabl M.** Immunoglobulin heavy chain binding protein. *Nature* 306: 387-389, 1983.
158. **Halliwell B, and Gutteridge JM.** Role of free radicals and catalytic metal ions in human disease: an overview. *Methods Enzymol* 186: 1-85, 1990.
159. **Hauser E, Hoger H, Bittner R, Widhalm K, Herkner K, and Lubec G.** OXYRADICAL DAMAGE AND MITOCHONDRIAL ENZYME-ACTIVITIES IN THE MDX MOUSE. *Neuropediatrics* 26: 260-262, 1995.
160. **Haycock JW, MacNeil S, Jones P, Harris JB, and Mantle D.** Oxidative damage to muscle protein in Duchenne muscular dystrophy. *Neuroreport* 8: 357-361, 1996.
161. **Hayden MS, and Ghosh S.** Signaling to NF-kappaB. In: *Genes Dev.* United States: 2004, p. 2195-2224.
162. **Head SI.** Branched fibres in old dystrophic mdx muscle are associated with mechanical weakening of the sarcolemma, abnormal Ca<sup>2+</sup>transients and a breakdown of Ca<sup>2+</sup>homeostasis during fatigue. *Experimental Physiology* 95: 641-656, 2010.
163. **Head SI.** Membrane potential, resting calcium and calcium transients in isolated muscle fibres from normal and dystrophic mice. *J Physiol* 469: 11-19, 1993.
164. **Hendershot LM.** The ER function BiP is a master regulator of ER function. *Mt Sinai J Med* 71: 289-297, 2004.
165. **Heslop L, Morgan JE, and Partridge TA.** Evidence for a myogenic stem cell that is exhausted in dystrophic muscle. *J Cell Sci* 113 ( Pt 12): 2299-2308, 2000.
166. **Hiramatsu N, Chiang WC, Kurt TD, Sigurdson CJ, and Lin JH.** Multiple Mechanisms of Unfolded Protein Response-Induced Cell Death. *Am J Pathol* 185: 1800-1808, 2015.
167. **Hirata Y, Brotto M, Weisleder N, Chu Y, Lin P, Zhao X, Thornton A, Komazaki S, Takeshima H, Ma J, and Pan Z.** Uncoupling store-operated Ca<sup>2+</sup> entry and altered Ca<sup>2+</sup> release from sarcoplasmic reticulum through silencing of junctophilin genes. *Biophys J* 90: 4418-4427, 2006.
168. **Hoffman EP, Brown RH, Jr., and Kunkel LM.** Dystrophin: the protein product of the Duchenne muscular dystrophy locus. *Cell* 51: 919-928, 1987.
169. **Hoffmann EK, Lambert IH, and Pedersen SF.** Physiology of cell volume regulation in vertebrates. *Physiol Rev* 89: 193-277, 2009.
170. **Hollingworth S, Zeiger U, and Baylor SM.** Comparison of the myoplasmic calcium transient elicited by an action potential in intact fibres of *mdx* and normal mice. *J Physiol* 586: 5063-5075, 2008.
171. **Honda A, Abe S, Hiroki E, Honda H, Iwanuma O, Yanagisawa N, and Ide Y.** Activation of caspase 3, 9, 12, and Bax in masseter muscle of mdx mice during necrosis. *J Muscle Res Cell Motil* 28: 243-247, 2007.
172. **Hopf FW, Turner PR, Denetclaw WF, Jr., Reddy P, and Steinhardt RA.** A critical evaluation of resting intracellular free calcium regulation in dystrophic mdx muscle. *Am J Physiol* 271: C1325-1339, 1996.
173. **Hopf FW, Turner PR, and Steinhardt RA.** Calcium misregulation and the pathogenesis of muscular dystrophy. *Subcell Biochem* 45: 429-464, 2007.
174. **Hunter RB, and Kandarian SC.** Disruption of either the Nfkb1 or the Bcl3 gene inhibits skeletal muscle atrophy. *J Clin Invest* 114: 1504-1511, 2004.

175. **Huxley H, and Hanson J.** CHANGES IN THE CROSS-STRIATIONS OF MUSCLE DURING CONTRACTION AND STRETCH AND THEIR STRUCTURAL INTERPRETATION. *Nature* 173: 973-976, 1954.
176. **Ibraghimov-Beskrovnaya O, Ervasti JM, Leveille CJ, Slaughter CA, Sernett SW, and Campbell KP.** Primary structure of dystrophin-associated glycoproteins linking dystrophin to the extracellular matrix. *Nature* 355: 696-702, 1992.
177. **Ibraghimov-Beskrovnaya O, Milatovich A, Ozcelik T, Yang B, Koepnick K, Francke U, and Campbell KP.** Human dystroglycan: skeletal muscle cDNA, genomic structure, origin of tissue specific isoforms and chromosomal localization. *Hum Mol Genet* 2: 1651-1657, 1993.
178. **Ingalls CP, Warren GL, Williams JH, Ward CW, and Armstrong RB.** E-C coupling failure in mouse EDL muscle after in vivo eccentric contractions. *J Appl Physiol (1985)* 85: 58-67, 1998.
179. **Ito K, Komazaki S, Sasamoto K, Yoshida M, Nishi M, Kitamura K, and Takeshima H.** Deficiency of triad junction and contraction in mutant skeletal muscle lacking junctophilin type 1. *J Cell Biol* 154: 1059-1067, 2001.
180. **Jackson MJ, Jones DA, and Edwards RH.** Measurements of calcium and other elements in muscle biopsy samples from patients with Duchenne muscular dystrophy. *Clin Chim Acta* 147: 215-221, 1985.
181. **Jefferies JL, Eidem BW, Belmont JW, Craigen WJ, Ware SM, Fernbach SD, Neish SR, Smith EO, and Towbin JA.** Genetic predictors and remodeling of dilated cardiomyopathy in muscular dystrophy. *Circulation* 112: 2799-2804, 2005.
182. **Kaczor JJ, Hall JE, Payne E, and Tarnopolsky MA.** Low intensity training decreases markers of oxidative stress in skeletal muscle of mdx mice. *Free Radical Biology and Medicine* 43: 145-154, 2007.
183. **Kameya S, Miyagoe Y, Nonaka I, Ikemoto T, Endo M, Hanaoka K, Nabeshima Y, and Takeda S.** alpha1-syntrophin gene disruption results in the absence of neuronal-type nitric-oxide synthase at the sarcolemma but does not induce muscle degeneration. *J Biol Chem* 274: 2193-2200, 1999.
184. **Kania E, Pajak B, and Orzechowski A.** Calcium homeostasis and ER stress in control of autophagy in cancer cells. *BioMed research international* 2015: 352794-352794, 2015.
185. **Kar NC, and Pearson CM.** A calcium-activated neutral protease in normal and dystrophic human muscle. *Clin Chim Acta* 73: 293-297, 1976.
186. **Kargacin ME, and Kargacin GJ.** The sarcoplasmic reticulum calcium pump is functionally altered in dystrophic muscle. *BBA-GEN Subjects* 1290: 4-8, 1996.
187. **Karpati G, Carpenter S, and Prescott S.** Small-caliber skeletal muscle fibers do not suffer necrosis in mdx mouse dystrophy. *Muscle Nerve* 11: 795-803, 1988.
188. **Khurana TS, Prendergast RA, Alameddine HS, Tome FM, Fardeau M, Arahata K, Sugita H, and Kunkel LM.** Absence of extraocular muscle pathology in Duchenne's muscular dystrophy: role for calcium homeostasis in extraocular muscle sparing. *J Exp Med* 182: 467-475, 1995.
189. **Komazaki S, Ito K, Takeshima H, and Nakamura H.** Deficiency of triad formation in developing skeletal muscle cells lacking junctophilin type 1. *FEBS Lett* 524: 225-229, 2002.
190. **Koopman R, Gehrig SM, Leger B, Trieu J, Walrand S, Murphy KT, and Lynch GS.** Cellular mechanisms underlying temporal changes in skeletal muscle protein synthesis and breakdown during chronic {beta}-adrenoceptor stimulation in mice. *J Physiol* 588: 4811-4823, 2010.
191. **Kornegay JN, Bogan JR, Bogan DJ, Childers MK, Li J, Nghiem P, Detwiler DA, Larsen CA, Grange RW, Bhavaraju-Sanka RK, Tou S, Keene BP, Howard JF, Jr., Wang J, Fan Z, Schatzberg SJ, Styner MA, Flanigan KM, Xiao X, and Hoffman EP.** Canine models of Duchenne muscular dystrophy and their use in therapeutic strategies. *Mamm Genome* 23: 85-108, 2012.

192. **Kramarcy NR, Vidal A, Froehner SC, and Sealock R.** Association of utrophin and multiple dystrophin short forms with the mammalian M(r) 58,000 dystrophin-associated protein (syntrophin). *J Biol Chem* 269: 2870-2876, 1994.
193. **Kramerova I, Kudryashova E, Tidball JG, and Spencer MJ.** Null mutation of calpain 3 (p94) in mice causes abnormal sarcomere formation in vivo and in vitro. *Hum Mol Genet* 13: 1373-1388, 2004.
194. **Krans J.** **The Sliding Filament Theory of Muscle Contraction.** Nature Education: 2010, p. 66.
195. **Kunert-Keil C, Gredes T, Lucke S, Botzenhart U, Dominiak M, and Gedrange T.** DIFFERENTIAL EXPRESSION OF GENES INVOLVED IN THE CALCIUM HOMEOSTASIS IN MASTICATORY MUSCLES OF MDX MICE. *Journal of Physiology and Pharmacology* 65: 317-324, 2014.
196. **Kunert-Keil CH, Gredes T, Lucke S, Botzenhart U, Dominiak M, and Gedrange T.** Differential expression of genes involved in the calcium homeostasis in masticatory muscles of MDX mice. *Journal of physiology and pharmacology : an official journal of the Polish Physiological Society* 65: 317-324, 2014.
197. **Lamb GD, Junankar PR, and Stephenson DG.** Raised intracellular [Ca<sup>2+</sup>] abolishes excitation-contraction coupling in skeletal muscle fibres of rat and toad. *J Physiol* 489 ( Pt 2): 349-362, 1995.
198. **Lang JM, Esser KA, and Dupont-Versteegden EE.** Altered activity of signaling pathways in diaphragm and tibialis anterior muscle of dystrophic mice. *Exp Biol Med (Maywood)* 229: 503-511, 2004.
199. **Laws N, and Hoey A.** Progression of kyphosis in mdx mice. *J Appl Physiol (1985)* 97: 1970-1977, 2004.
200. **Lebakken CS, Venzke DP, Hrstka RF, Consolino CM, Faulkner JA, Williamson RA, and Campbell KP.** Sarcospan-deficient mice maintain normal muscle function. *Mol Cell Biol* 20: 1669-1677, 2000.
201. **Leberer E, Hartner KT, and Pette D.** Postnatal development of Ca<sup>2+</sup>-sequestration by the sarcoplasmic reticulum of fast and slow muscles in normal and dystrophic mice. *Eur J Biochem* 174: 247-253, 1988.
202. **Lee D, and Michalak M.** Membrane associated Ca<sup>2+</sup> buffers in the heart. *Bmb Reports* 43: 151-157, 2010.
203. **Leijendekker WJ, Passaquin AC, Metzinger L, and Ruegg UT.** Regulation of cytosolic calcium in skeletal muscle cells of the *mdx* mouse under conditions of stress. *Brit J Pharmacol* 118: 611-616, 1996.
204. **Letellier G, Mok E, Alberti C, De Luca A, Gottrand F, Cuisset JM, Denjean A, Darmaun D, and Hankard R.** Effect of glutamine on glucose metabolism in children with Duchenne muscular dystrophy. *Clin Nutr* 32: 386-390, 2013.
205. **Li D, Yue Y, and Duan D.** Marginal level dystrophin expression improves clinical outcome in a strain of dystrophin/utrophin double knockout mice. *PLoS One* 5: e15286, 2010.
206. **Liberona JL, Powell JA, Shenoi S, Petherbridge L, Caviedes R, and Jaimovich E.** Differences in both inositol 1,4,5-trisphosphate mass and inositol 1,4,5-trisphosphate receptors between normal and dystrophic skeletal muscle cell lines. *Muscle Nerve* 21: 902-909, 1998.
207. **Lievremont JP, Rizzuto R, Hendershot L, and Meldolesi J.** BiP, a major chaperone protein of the endoplasmic reticulum lumen, plays a direct and important role in the storage of the rapidly exchanging pool of Ca<sup>2+</sup>. *J Biol Chem* 272: 30873-30879, 1997.

208. **Liu N, Bezprozvannaya S, Shelton JM, Frisard MI, Hulver MW, McMillan RP, Wu Y, Voelker KA, Grange RW, Richardson JA, Bassel-Duby R, and Olson EN.** Mice lacking microRNA 133a develop dynamin 2-dependent centronuclear myopathy. *J Clin Invest* 121: 3258-3268, 2011.
209. **Love DR, Flint TJ, Genet SA, Middleton-Price HR, and Davies KE.** Becker muscular dystrophy patient with a large intragenic dystrophin deletion: implications for functional minigenes and gene therapy. *J Med Genet* 28: 860-864, 1991.
210. **Love DR, Flint TJ, Marsden RF, Bloomfield JF, Daniels RJ, Forrest SM, Gabrielli O, Giorgi P, Novelli G, and Davies KE.** Characterization of deletions in the dystrophin gene giving mild phenotypes. *Am J Med Genet* 37: 136-142, 1990.
211. **Lovering RM, Michaelson L, and Ward CW.** Malformed *mdx* myofibers have normal cytoskeletal architecture yet altered EC coupling and stress-induced  $Ca^{2+}$  signaling. *Am J Physiol Cell Physiol* 297: C571-580, 2009.
212. **Luise M, Presotto C, Senter L, Betto R, Ceoldo S, Furlan S, Salvatori S, Sabbadini RA, and Salviati G.** Dystrophin is phosphorylated by endogenous protein kinases. *Biochem J* 293 ( Pt 1): 243-247, 1993.
213. **Lynch GS.** Role of contraction-induced injury in the mechanisms of muscle damage in muscular dystrophy. *Clin Exp Pharmacol P* 31: 557-561, 2004.
214. **Lynch GS, Hinkle RT, Chamberlain JS, Brooks SV, and Faulkner JA.** Force and power output of fast and slow skeletal muscles from *mdx* mice 6-28 months old. *J Physiol-London* 535: 591-600, 2001.
215. **Lynch GS, Rafael JA, Hinkle RT, Cole NM, Chamberlain JS, and Faulkner JA.** Contractile properties of diaphragm muscle segments from old *mdx* and old transgenic *mdx* mice. *Am J Physiol* 272: C2063-2068, 1997.
216. **MacLennan DH, Asahi M, and Tupling AR.** The regulation of SERCA-type pumps by phospholamban and sarcolipin. *Na,K-ATPase and Related Cation Pumps: Structure, Function, and Regulatory Mechanisms* 986: 472-480, 2003.
217. **MacLennan DH, Brandl CJ, Korczak B, and Green NM.** Amino-acid sequence of a  $Ca^{2+}$  +  $Mg^{2+}$ -dependent ATPase from rabbit muscle sarcoplasmic reticulum, deduced from its complementary DNA sequence. *Nature* 316: 696-700, 1985.
218. **Madhavan R, and Jarrett HW.** Calmodulin-activated phosphorylation of dystrophin. *Biochemistry* 33: 5797-5804, 1994.
219. **Madhavan R, and Jarrett HW.** Interactions between dystrophin glycoprotein complex proteins. *Biochemistry* 34: 12204-12209, 1995.
220. **Maki M, Takano E, Mori H, Kannagi R, Murachi T, and Hatanaka M.** Repetitive region of calpastatin is a functional unit of the proteinase inhibitor. *Biochem Biophys Res Commun* 143: 300-308, 1987.
221. **Maki M, Takano E, Mori H, Sato A, Murachi T, and Hatanaka M.** All four internally repetitive domains of pig calpastatin possess inhibitory activities against calpains I and II. *FEBS Lett* 223: 174-180, 1987.
222. **Manzur AY, Kuntzer T, Pike M, and Swan A.** Glucocorticoid corticosteroids for Duchenne muscular dystrophy. *Cochrane Database Syst Rev* Cd003725, 2008.
223. **Maranhao J, de Oliveira Moreira D, Mauricio AF, de Carvalho SC, Ferretti R, Pereira JA, Santo Neto H, and Marques MJ.** Changes in calsequestrin, TNF-alpha, TGF-beta and MyoD levels during the progression of skeletal muscle dystrophy in *mdx* mice: a comparative analysis of the quadriceps, diaphragm and intrinsic laryngeal muscles. *Int J Exp Pathol* 2015.
224. **Marotta M, Ruiz-Roig C, Sarria Y, Peiro JL, Nunez F, Ceron J, Munell F, and Roig-Quilis M.** Muscle genome-wide expression profiling during disease evolution in *mdx* mice. *Physiol Genomics* 37: 119-132, 2009.

225. **Martonosi AN, and Pikula S.** The network of calcium regulation in muscle. *Acta Biochimica Polonica* 50: 1-29, 2003.
226. **Mathur S, Lott DJ, Senesac C, Germain SA, Vohra RS, Sweeney HL, Walter GA, and Vandeborne K.** Age-related differences in lower-limb muscle cross-sectional area and torque production in boys with Duchenne muscular dystrophy. *Arch Phys Med Rehabil* 91: 1051-1058, 2010.
227. **Matsumura CY, Taniguti AP, Pertille A, Santo Neto H, and Marques MJ.** Stretch-activated calcium channel protein TRPC1 is correlated with the different degrees of the dystrophic phenotype in mdx mice. *Am J Physiol Cell Physiol* 301: C1344-1350, 2011.
228. **Matsumura K, Ervasti JM, Ohlendieck K, Kahl SD, and Campbell KP.** Association of dystrophin-related protein with dystrophin-associated proteins in mdx mouse muscle. *Nature* 360: 588-591, 1992.
229. **Maunder-Sewry CA, Gorodetsky R, Yarom R, and Dubowitz V.** Element analysis of skeletal muscle in Duchenne muscular dystrophy using x-ray fluorescence spectrometry. *Muscle Nerve* 3: 502-508, 1980.
230. **McCracken AA, and Brodsky JL.** Assembly of ER-associated protein degradation in vitro: dependence on cytosol, calnexin, and ATP. *J Cell Biol* 132: 291-298, 1996.
231. **Mellgren RL, Miyake K, Kramerova I, Spencer MJ, Bourg N, Bartoli M, Richard I, Greer PA, and McNeil PL.** Calcium-dependent plasma membrane repair requires m- or mu-calpain, but not calpain-3, the proteasome, or caspases. *Biochim Biophys Acta* 1793: 1886-1893, 2009.
232. **Mellgren RL, Zhang W, Miyake K, and McNeil PL.** Calpain is required for the rapid, calcium-dependent repair of wounded plasma membrane. *J Biol Chem* 282: 2567-2575, 2007.
233. **Menazza S, Blaauw B, Tiepolo T, Toniolo L, Braghetta P, Spolaore B, Reggiani C, Di Lisa F, Bonaldo P, and Canton M.** Oxidative stress by monoamine oxidases is causally involved in myofiber damage in muscular dystrophy. *Hum Mol Genet* 19: 4207-4215, 2010.
234. **Messina S, Bitto A, Aguenouz M, Minutoli L, Monici MC, Altavilla D, Squadrito F, and Vita G.** Nuclear factor kappa-B blockade reduces skeletal muscle degeneration and enhances muscle function in Mdx mice. *Exp Neurol* 198: 234-241, 2006.
235. **Michalak M, Fu SY, Milner RE, Busaan JL, and Hance JE.** Phosphorylation of the carboxyl-terminal region of dystrophin. *Biochem Cell Biol* 74: 431-437, 1996.
236. **Millay DP, Goonasekera SA, Sargent MA, Maillet M, Aronow BJ, and Molkentin JD.** Calcium influx is sufficient to induce muscular dystrophy through a TRPC-dependent mechanism. *Proc Natl Acad Sci U S A* 106: 19023-19028, 2009.
237. **Millay DP, Sargent MA, Osinska H, Baines CP, Barton ER, Vuagniaux G, Sweeney HL, Robbins J, and Molkentin JD.** Genetic and pharmacologic inhibition of mitochondrial-dependent necrosis attenuates muscular dystrophy. *Nat Med* 14: 442-447, 2008.
238. **Moens P, Baatsen PH, and Marechal G.** Increased susceptibility of EDL muscles from mdx mice to damage induced by contractions with stretch. *J Muscle Res Cell Motil* 14: 446-451, 1993.
239. **Mongini T, Ghigo D, Doriguzzi C, Bussolino F, Pescarmona G, Pollo B, Schiffer D, and Bosia A.** Free cytoplasmic Ca<sup>++</sup> at rest and after cholinergic stimulus is increased in cultured muscle cells from Duchenne muscular dystrophy patients. *Neurology* 38: 476-480, 1988.
240. **Moore CJ, and Hewitt JE.** Dystroglycan glycosylation and muscular dystrophy. *Glycoconj J* 26: 349-357, 2009.
241. **Moore CJ, and Winder SJ.** The inside and out of dystroglycan post-translational modification. *Neuromuscul Disord* 22: 959-965, 2012.
242. **Moorwood C, and Barton ER.** Caspase-12 ablation preserves muscle function in the mdx mouse. *Human Molecular Genetics* 23: 5325-5341, 2014.

243. **Morine KJ, Sleeper MM, Barton ER, and Sweeney HL.** Overexpression of SERCA1a in the mdx diaphragm reduces susceptibility to contraction-induced damage. *Hum Gene Ther* 21: 1735-1739, 2010.
244. **Mosqueira M, Zeiger U, Forderer M, Brinkmeier H, and Fink RH.** Cardiac and respiratory dysfunction in Duchenne muscular dystrophy and the role of second messengers. *Med Res Rev* 33: 1174-1213, 2013.
245. **Mourkioti F, Kratsios P, Luedde T, Song YH, Delafontaine P, Adami R, Parente V, Bottinelli R, Pasparakis M, and Rosenthal N.** Targeted ablation of IKK2 improves skeletal muscle strength, maintains mass, and promotes regeneration. *J Clin Invest* 116: 2945-2954, 2006.
246. **Muntoni F, Mateddu A, Marchei F, Clerk A, and Serra G.** Muscular weakness in the *mdx* mouse. *J Neurol Sci* 120: 71-77, 1993.
247. **Muntoni F, Torelli S, and Ferlini A.** Dystrophin and mutations: one gene, several proteins, multiple phenotypes. *Lancet Neurol* 2: 731-740, 2003.
248. **Murphy RM.** Calpains, skeletal muscle function and exercise. *Clin Exp Pharmacol Physiol* 37: 385-391, 2010.
249. **Murphy RM, Dutka TL, Horvath D, Bell JR, Delbridge LM, and Lamb GD.** Ca<sup>2+</sup>-dependent proteolysis of junctophilin-1 and junctophilin-2 in skeletal and cardiac muscle. *J Physiol* 591: 719-729, 2013.
250. **Murphy RM, Goodman CA, McKenna MJ, Bennie J, Leikis M, and Lamb GD.** Calpain-3 is autolyzed and hence activated in human skeletal muscle 24 h following a single bout of eccentric exercise. *J Appl Physiol* 103: 926-931, 2007.
251. **Murphy RM, and Lamb GD.** Calpain-3 is activated following eccentric exercise. In: *J Appl Physiol*. United States: 2009, p. 2068; author reply 2069.
252. **Murphy RM, and Lamb GD.** Endogenous calpain-3 activation is primarily governed by small increases in resting cytoplasmic [Ca<sup>2+</sup>] and is not dependent on stretch. *J Biol Chem* 284: 7811-7819, 2009.
253. **Murphy RM, Snow RJ, and Lamb GD.** mu-Calpain and calpain-3 are not autolyzed with exhaustive exercise in humans. *Am J Physiol Cell Physiol* 290: C116-122, 2006.
254. **Murphy RM, Verburg E, and Lamb GD.** Ca<sup>2+</sup> activation of diffusible and bound pools of mu-calpain in rat skeletal muscle. *J Physiol* 576: 595-612, 2006.
255. **Mázala DA, Grange RW, and Chin ER.** The role of proteases in excitation-contraction coupling failure in muscular dystrophy. *Am J Physiol Cell Physiol* ajpcell.00267.02013, 2014.
256. **Mázala DAG, Pratt SJ, Chen D, Molkentin JD, Lovering RM, and Chin ER.** SERCA1 overexpression minimizes skeletal muscle damage in dystrophic mouse models. *Am J Physiol Cell Physiol* ajpcell.00341.02014, 2015.
257. **Nakagawa O, Arnold M, Nakagawa M, Hamada H, Shelton JM, Kusano H, Harris TM, Childs G, Campbell KP, Richardson JA, Nishino I, and Olson EN.** Centronuclear myopathy in mice lacking a novel muscle-specific protein kinase transcriptionally regulated by MEF2. *Genes & Development* 19: 2066-2077, 2005.
258. **Nakagawa T, Zhu H, Morishima N, Li E, Xu J, Yankner BA, and Yuan J.** Caspase-12 mediates endoplasmic-reticulum-specific apoptosis and cytotoxicity by amyloid-beta. *Nature* 403: 98-103, 2000.
259. **Nawrotzki R, Loh NY, Ruegg MA, Davies KE, and Blake DJ.** Characterisation of alpha-dystrobrevin in muscle. *J Cell Sci* 111 ( Pt 17): 2595-2605, 1998.
260. **Newbell BJ, Anderson JT, and Jarrett HW.** Ca<sup>2+</sup>-calmodulin binding to mouse alpha1 syntrophin: syntrophin is also a Ca<sup>2+</sup>-binding protein. *Biochemistry* 36: 1295-1305, 1997.

261. **Niebroj-Dobosz I, Kornguth S, Schutta HS, and Siegel FL.** Elevated calmodulin levels and reduced calmodulin-stimulated calcium-ATPase in Duchenne progressive muscular dystrophy. *Neurology* 39: 1610-1614, 1989.
262. **Niebroj-Dobosz I, and Lukasiuk M.** Immunoblot analysis of sarcoplasmic calcium binding proteins in Duchenne muscular dystrophy. *J Neurol* 242: 82-86, 1995.
263. **Ono Y, Kakinuma K, Torii F, Irie A, Nakagawa K, Labeit S, Abe K, Suzuki K, and Sorimachi H.** Possible regulation of the conventional calpain system by skeletal muscle-specific calpain, p94/calpain 3. *J Biol Chem* 279: 2761-2771, 2004.
264. **Ottenheijm CA, Fong C, Vangheluwe P, Wuytack F, Babu GJ, Periasamy M, Witt CC, Labeit S, and Granzier H.** Sarcoplasmic reticulum calcium uptake and speed of relaxation are depressed in nebulin-free skeletal muscle. *FASEB J* 22: 2912-2919, 2008.
265. **Oyadomari S, Koizumi A, Takeda K, Gotoh T, Akira S, Araki E, and Mori M.** Targeted disruption of the Chop gene delays endoplasmic reticulum stress-mediated diabetes. *J Clin Invest* 109: 525-532, 2002.
266. **Parker MH, Seale P, and Rudnicki MA.** Looking back to the embryo: defining transcriptional networks in adult myogenesis. *Nat Rev Genet* 4: 497-507, 2003.
267. **Pastoret C, and Sebillle A.** *mdx* mice show progressive weakness and muscle deterioration with age. *J Neurol Sci* 129: 97-105, 1995.
268. **Paulin D, and Li Z.** Desmin: a major intermediate filament protein essential for the structural integrity and function of muscle. In: *Exp Cell Res*. United States: 2004, p. 1-7.
269. **Periasamy M, and Kalyanasundaram A.** SERCA pump isoforms: their role in calcium transport and disease. *Muscle Nerve* 35: 430-442, 2007.
270. **Peter AK, Miller G, and Crosbie RH.** Disrupted mechanical stability of the dystrophin-glycoprotein complex causes severe muscular dystrophy in sarcospan transgenic mice. *J Cell Sci* 120: 996-1008, 2007.
271. **Peters MF, Adams ME, and Froehner SC.** Differential association of syntrophin pairs with the dystrophin complex. *J Cell Biol* 138: 81-93, 1997.
272. **Petrof BJ, Shrager JB, Stedman HH, Kelly AM, and Sweeney HL.** Dystrophin protects the sarcolemma from stresses developed during muscle contraction. *Proc Natl Acad Sci U S A* 90: 3710-3714, 1993.
273. **Phimister AJ, Lango J, Lee EH, Ernst-Russell MA, Takeshima H, Ma J, Allen PD, and Pessah IN.** Conformation-dependent stability of junctophilin 1 (JP1) and ryanodine receptor type 1 (RyR1) channel complex is mediated by their hyper-reactive thiols. In: *J Biol Chem*. United States: 2007, p. 8667-8677.
274. **Piluso G, Mirabella M, Ricci E, Belsito A, Abbondanza C, Servidei S, Puca AA, Tonali P, Puca GA, and Nigro V.** Gamma1- and gamma2-syntrophins, two novel dystrophin-binding proteins localized in neuronal cells. *J Biol Chem* 275: 15851-15860, 2000.
275. **Poteser M, Graziani A, Rosker C, Eder P, Derler I, Kahr H, Zhu MX, Romanin C, and Groschner K.** TRPC3 and TRPC4 associate to form a redox-sensitive cation channel. Evidence for expression of native TRPC3-TRPC4 heteromeric channels in endothelial cells. *J Biol Chem* 281: 13588-13595, 2006.
276. **Powers SK, and Howley ET.** *Exercise physiology : theory and application to fitness and performance*. New York: McGraw-Hill, 2012, p. xv, 587, [536] p.
277. **Pratt SJ, Lawlor MW, Shah SB, and Lovering RM.** An in vivo rodent model of contraction-induced injury in the quadriceps muscle. *Injury* 43: 788-793, 2012.
278. **Pratt SJ, Shah SB, Ward CW, Inacio MP, Stains JP, and Lovering RM.** Effects of in vivo injury on the neuromuscular junction in healthy and dystrophic muscles. *J Physiol* 591: 559-570, 2013.

279. **Pratt SJP, and Lovering RM.** A stepwise procedure to test contractility and susceptibility to injury for the rodent quadriceps muscle. *J Biol Methods* 1: 1-10, 2014.
280. **Pressmar J, Brinkmeier H, Seewald MJ, Naumann T, and Rudel R.** Intracellular Ca<sup>2+</sup> concentrations are not elevated in resting cultured muscle from Duchenne (DMD) patients and in MDX mouse muscle fibres. *Pflugers Arch* 426: 499-505, 1994.
281. **Quinlan JG, Johnson SR, McKee MK, and Lyden SP.** Twitch and tetanus in *mdx* mouse muscle. *Muscle & Nerve* 15: 837-842, 1992.
282. **Radley-Crabb H, Terrill J, Shavlakadze T, Tonkin J, Arthur P, and Grounds M.** A single 30 min treadmill exercise session is suitable for 'proof-of concept studies' in adult *mdx* mice: a comparison of the early consequences of two different treadmill protocols. *Neuromuscul Disord* 22: 170-182, 2012.
283. **Radojevic V, Lin S, and Burgunder JM.** Differential expression of dystrophin, utrophin, and dystrophin-associated proteins in human muscle culture. *Cell Tissue Res* 300: 447-457, 2000.
284. **Rafael JA, and Chamberlain JS.** Phenotypic effects of uniform and mosaic expression of a truncated dystrophin transgene in skeletal-muscle of *mdx* mice. *J Cell Biochem* 531-531, 1994.
285. **Rafael JA, Tinsley JM, Potter AC, Deconinck AE, and Davies KE.** Skeletal muscle-specific expression of a utrophin transgene rescues utrophin-dystrophin deficient mice. *Nat Genet* 19: 79-82, 1998.
286. **Ragusa RJ, Chow CK, StClair DK, and Porter JD.** Extraocular, limb and diaphragm muscle group-specific antioxidant enzyme activity patterns in control and *mdx* mice. *Journal of the Neurological Sciences* 139: 180-186, 1996.
287. **Rando TA.** Oxidative stress and the pathogenesis of muscular dystrophies. *American Journal of Physical Medicine & Rehabilitation* 81: S175-S186, 2002.
288. **Rando TA.** The dystrophin-glycoprotein complex, cellular signaling, and the regulation of cell survival in the muscular dystrophies. *Muscle Nerve* 24: 1575-1594, 2001.
289. **Raymackers JM, Debaix H, Colson-Van Schoor M, De Backer F, Tajeddine N, Schwaller B, Gailly P, and Gillis JM.** Consequence of parvalbumin deficiency in the *mdx* mouse: histological, biochemical and mechanical phenotype of a new double mutant. *Neuromuscul Disord* 13: 376-387, 2003.
290. **Reddy PA, Anandavalli TE, and Anandaraj MP.** Calcium activated neutral proteases (milli- and micro-CANP) and endogenous CANP inhibitor of muscle in Duchenne muscular dystrophy (DMD). *Clin Chim Acta* 160: 281-288, 1986.
291. **Reid WD, and Belcastro AN.** Time course of diaphragm injury and calpain activity during resistive loading. *Am J Respir Crit Care Med* 162: 1801-1806, 2000.
292. **Reutenauer J, Dorchies OM, Patthey-Vuadens O, Vuagniaux G, and Ruegg UT.** Investigation of Debio 025, a cyclophilin inhibitor, in the dystrophic *mdx* mouse, a model for Duchenne muscular dystrophy. *Brit J Pharmacol* 155: 574-584, 2008.
293. **Rey MA, and Davies PL.** The protease core of the muscle-specific calpain, p94, undergoes Ca<sup>2+</sup>-dependent intramolecular autolysis. *FEBS Lett* 532: 401-406, 2002.
294. **Richard I, Broux O, Allamand V, Fougousse F, Chiannikulchai N, Bourg N, Brenguier L, Devaud C, Pasturaud P, Roudaut C, and et al.** Mutations in the proteolytic enzyme calpain 3 cause limb-girdle muscular dystrophy type 2A. *Cell* 81: 27-40, 1995.
295. **Richard I, Roudaut C, Marchand S, Baghdiguian S, Herasse M, Stockholm D, Ono Y, Suel L, Bourg N, Sorimachi H, Lefranc G, Fardeau M, Sebille A, and Beckmann JS.** Loss of calpain 3 proteolytic activity leads to muscular dystrophy and to apoptosis-associated I $\kappa$ B $\alpha$ /nuclear factor  $\kappa$ B pathway perturbation in mice. *J Cell Biol* 151: 1583-1590, 2000.



296. **Roberds SL, Anderson RD, Ibraghimov-Beskrovnaya O, and Campbell KP.** Primary structure and muscle-specific expression of the 50-kDa dystrophin-associated glycoprotein (adhalin). *J Biol Chem* 268: 23739-23742, 1993.
297. **Roberds SL, Leturcq F, Allamand V, Piccolo F, Jeanpierre M, Anderson RD, Lim LE, Lee JC, Tome FM, Romero NB, and et al.** Missense mutations in the adhalin gene linked to autosomal recessive muscular dystrophy. *Cell* 78: 625-633, 1994.
298. **Rodriguez MC, and Tarnopolsky MA.** Patients with dystrophinopathy show evidence of increased oxidative stress. *Free Radical Biology and Medicine* 34: 1217-1220, 2003.
299. **Roelofs RI, de Arango GS, Law PK, Kinsman D, Buchanan DC, and Park JH.** Treatment of Duchenne's muscular dystrophy with penicillamine. Results of a double-blind trial. *Arch Neurol* 36: 266-268, 1979.
300. **Ross JJ, Duxson MJ, and Harris AJ.** Formation of primary and secondary myotubes in rat lumbrical muscles. *Development* 100: 383-394, 1987.
301. **Rouger K, Le Cunff M, Steenman M, Potier MC, Gibelin N, Dechesne CA, and Leger JJ.** Global/temporal gene expression in diaphragm and hindlimb muscles of dystrophin-deficient (mdx) mice. *Am J Physiol Cell Physiol* 283: C773-784, 2002.
302. **Ruegg UT, Nicolas-Metral V, Challet C, Bernard-Helary K, Dorchies OM, Wagner S, and Buetler TM.** Pharmacological control of cellular calcium handling in dystrophic skeletal muscle. *Neuromuscular Disord* 12: S155-S161, 2002.
303. **Sadoulet-Puccio HM, and Kunkel LM.** Dystrophin and its isoforms. *Brain Pathol* 6: 25-35, 1996.
304. **Sano M, Yokota T, Endo T, and Tsukagoshi H.** A developmental change in the content of parvalbumin in normal and dystrophic mouse (mdx) muscle. *J Neurol Sci* 97: 261-272, 1990.
305. **Schertzer JD, van der Poel C, Shavlakadze T, Grounds MD, and Lynch GS.** Muscle-specific overexpression of IGF-I improves E-C coupling in skeletal muscle fibers from dystrophic mdx mice. *American Journal of Physiology-Cell Physiology* 294: C161-C168, 2008.
306. **Schneider JS, Shanmugam M, Gonzalez JP, Lopez H, Gordan R, Fraidenaich D, and Babu GJ.** Increased sarcolipin expression and decreased sarco(endo)plasmic reticulum Ca<sup>2+</sup> uptake in skeletal muscles of mouse models of Duchenne muscular dystrophy. *J Muscle Res Cell Motil* 34: 349-356, 2013.
307. **Schneider JS, Shanmugam M, Gonzalez JP, Lopez H, Gordan R, Fraidenaich D, and Babu GJ.** Increased sarcolipin expression and decreased sarco(endo)plasmic reticulum Ca uptake in skeletal muscles of mouse models of Duchenne muscular dystrophy. *J Muscle Res Cell Motil* 2013.
308. **Schneider MF, and Chandler WK.** Voltage dependent charge movement in skeletal muscle: a possible step in excitation-contraction coupling. *Nature* 242: 244-246, 1973.
309. **Selsby J, Pendrak K, Zadel M, Tian Z, Pham J, Carver T, Acosta P, Barton E, and Sweeney HL.** Leupeptin-based inhibitors do not improve the mdx phenotype. *Am J Physiol Regul Integr Comp Physiol* 299: R1192-1201, 2010.
310. **Shao B, Oda MN, Vaisar T, Oram JF, and Heinecke JW.** Pathways for oxidation of high-density lipoprotein in human cardiovascular disease. *Curr Opin Mol Ther* 8: 198-205, 2006.
311. **Shin JH, Hakim CH, Zhang K, and Duan D.** Genotyping mdx, mdx3cv, and mdx4cv mice by primer competition polymerase chain reaction. *Muscle Nerve* 43: 283-286, 2011.
312. **Shkryl VM, Martins AS, Ullrich ND, Nowycky MC, Niggli E, and Shirokova N.** Reciprocal amplification of ROS and Ca<sup>2+</sup> signals in stressed mdx dystrophic skeletal muscle fibers. *Pflugers Arch* 458: 915-928, 2009.

313. **Sicinski P, Geng Y, Ryder-Cook AS, Barnard EA, Darlison MG, and Barnard PJ.** The molecular basis of muscular dystrophy in the mdx mouse: a point mutation. *Science* 244: 1578-1580, 1989.
314. **Simonides WS, and van Hardeveld C.** An assay for sarcoplasmic reticulum Ca<sup>2+</sup>-ATPase activity in muscle homogenates. *Anal Biochem* 191: 321-331, 1990.
315. **Singh J, Itahana Y, Knight-Krajewski S, Kanagawa M, Campbell KP, Bissell MJ, and Muschler J.** Proteolytic enzymes and altered glycosylation modulate dystroglycan function in carcinoma cells. *Cancer Res* 64: 6152-6159, 2004.
316. **Smith IJ, Lecker SH, and Hasselgren PO.** Calpain activity and muscle wasting in sepsis. *Am J Physiol Endocrinol Metab* 295: E762-771, 2008.
317. **Smith J, Fowkes G, and Schofield PN.** Programmed cell-death in dystrophic (*mdx*) muscle is inhibited by IGF-II. *Cell Death Differ* 2: 243-251, 1995.
318. **Sorimachi H, Imajoh-Ohmi S, Emori Y, Kawasaki H, Ohno S, Minami Y, and Suzuki K.** Molecular cloning of a novel mammalian calcium-dependent protease distinct from both m- and mu-types. Specific expression of the mRNA in skeletal muscle. *J Biol Chem* 264: 20106-20111, 1989.
319. **Sorimachi H, and Ono Y.** Regulation and physiological roles of the calpain system in muscular disorders. *Cardiovasc Res* 96: 11-22, 2012.
320. **Spencer MJ, Croall DE, and Tidball JG.** Calpains are activated in necrotic fibers from *mdx* dystrophic mice. *Journal of Biological Chemistry* 270: 10909-10914, 1995.
321. **Spencer MJ, and Mellgren RL.** Overexpression of a calpastatin transgene in *mdx* muscle reduces dystrophic pathology. *Hum Mol Genet* 11: 2645-2655, 2002.
322. **Spencer MJ, and Tidball JG.** Calpain translocation during muscle fiber necrosis and regeneration in dystrophin-deficient mice. *Experimental Cell Research* 226: 264-272, 1996.
323. **Spurney CF, Knoblach S, Pistilli EE, Nagaraju K, Martin GR, and Hoffman EP.** Dystrophin-deficient cardiomyopathy in mouse: expression of Nox4 and Lox are associated with fibrosis and altered functional parameters in the heart. *Neuromuscul Disord* 18: 371-381, 2008.
324. **Stadtman ER, and Levine RL.** Free radical-mediated oxidation of free amino acids and amino acid residues in proteins. *Amino Acids* 25: 207-218, 2003.
325. **Stadtman ER, and Oliver CN.** Metal-catalyzed oxidation of proteins. Physiological consequences. *J Biol Chem* 266: 2005-2008, 1991.
326. **Stedman HH, Sweeney HL, Shrager JB, Maguire HC, Panettieri RA, Petrof B, Narusawa M, Leferovich JM, Sladky JT, and Kelly AM.** The *mdx* mouse diaphragm reproduces the degenerative changes of Duchenne muscular dystrophy. *Nature* 352: 536-539, 1991.
327. **Straub V, and Campbell KP.** Muscular dystrophies and the dystrophin-glycoprotein complex. *Curr Opin Neurol* 10: 168-175, 1997.
328. **Stupka N, Schertzer JD, Bassel-Duby R, Olson EN, and Lynch GS.** Stimulation of calcineurin Aalpha activity attenuates muscle pathophysiology in *mdx* dystrophic mice. *Am J Physiol Regul Integr Comp Physiol* 294: R983-992, 2008.
329. **Suzuki CK, Bonifacino JS, Lin AY, Davis MM, and Klausner RD.** Regulating the retention of T-cell receptor alpha chain variants within the endoplasmic reticulum: Ca(2+)-dependent association with BiP. *J Cell Biol* 114: 189-205, 1991.
330. **Tajbakhsh S, and Buckingham M.** The birth of muscle progenitor cells in the mouse: spatiotemporal considerations. *Curr Top Dev Biol* 48: 225-268, 2000.
331. **Takagi A, Kojima S, Ida M, and Araki M.** Increased leakage of calcium ion from the sarcoplasmic reticulum of the *mdx* mouse. *J Neurol Sci* 110: 160-164, 1992.
332. **Takeshima H, Komazaki S, Nishi M, Iino M, and Kangawa K.** Junctophilins: a novel family of junctional membrane complex proteins. In: *Mol Cell*. United States: 2000, p. 11-22.

333. **Taveau M, Bourg N, Sillon G, Roudaut C, Bartoli M, and Richard I.** Calpain 3 is activated through autolysis within the active site and lyses sarcomeric and sarcolemmal components. *Molecular and Cellular Biology* 23: 9127-9135, 2003.
334. **Tian LJ, Cao JH, Deng XQ, Zhang CL, Qian T, Song XX, and Huang BS.** Gene expression profiling of Duchenne muscular dystrophy reveals characteristics along disease progression. *Genet Mol Res* 13: 1402-1411, 2014.
335. **Tidball JG, and Spencer MJ.** Calpains and muscular dystrophies. *Int J Biochem Cell Biol* 32: 1-5, 2000.
336. **Tidball JG, and Wehling-Henricks M.** Evolving therapeutic strategies for Duchenne muscular dystrophy: Targeting downstream events. *Pediatr Res* 56: 831-841, 2004.
337. **Tinsley J, Deconinck N, Fisher R, Kahn D, Phelps S, Gillis JM, and Davies K.** Expression of full-length utrophin prevents muscular dystrophy in mdx mice. *Nat Med* 4: 1441-1444, 1998.
338. **Tkatchenko AV, Le Cam G, Leger JJ, and Dechesne CA.** Large-scale analysis of differential gene expression in the hindlimb muscles and diaphragm of mdx mouse. *Biochim Biophys Acta* 1500: 17-30, 2000.
339. **Toyoshima C, and Inesi G.** Structural basis of ion pumping by Ca<sup>2+</sup>-ATPase of the sarcoplasmic reticulum. *Annu Rev Biochem* 73: 269-292, 2004.
340. **Tuffery-Giraud S, Beroud C, Leturcq F, Yaou RB, Hamroun D, Michel-Calemard L, Moizard MP, Bernard R, Cossee M, Boisseau P, Blayau M, Creveaux I, Guiochon-Mantel A, de Martinville B, Philippe C, Monnier N, Bieth E, Khau Van Kien P, Desmet FO, Humbertclaude V, Kaplan JC, Chelly J, and Claustres M.** Genotype-phenotype analysis in 2,405 patients with a dystrophinopathy using the UMD-DMD database: a model of nationwide knowledgebase. *Hum Mutat* 30: 934-945, 2009.
341. **Turner PR, Fong PY, Denetclaw WF, and Steinhardt RA.** Increased calcium influx in dystrophic muscle. *J Cell Biol* 115: 1701-1712, 1991.
342. **Turner PR, Schultz R, Ganguly B, and Steinhardt RA.** Proteolysis results in altered leak channel kinetics and elevated free calcium in mdx muscle. *J Membr Biol* 133: 243-251, 1993.
343. **Turner PR, Westwood T, Regen CM, and Steinhardt RA.** Increased protein degradation results from elevated free calcium levels found in muscle from mdx mice. *Nature* 335: 735-738, 1988.
344. **Tutdibi O, Brinkmeier H, Rudel R, and Fohr KJ.** Increased calcium entry into dystrophin-deficient muscle fibres of MDX and ADR-MDX mice is reduced by ion channel blockers. *J Physiol* 515 ( Pt 3): 859-868, 1999.
345. **Valko M, Rhodes CJ, Moncol J, Izakovic M, and Mazur M.** Free radicals, metals and antioxidants in oxidative stress-induced cancer. *Chem Biol Interact* 160: 1-40, 2006.
346. **Vandebrouck A, Ducret T, Basset O, Sebille S, Raymond G, Ruegg U, Gailly P, Cognard C, and Constantin B.** Regulation of store-operated calcium entries and mitochondrial uptake by minidystrophin expression in cultured myotubes. *Faseb J* 19: 136-138, 2005.
347. **Vandebrouck C, Martin D, Colson-Van Schoor M, Debaix H, and Gailly P.** Involvement of TRPC in the abnormal calcium influx observed in dystrophic (mdx) mouse skeletal muscle fibers. *J Cell Biol* 158: 1089-1096, 2002.
348. **Vangheluwe P, Schuermans M, Zador E, Waelkens E, Raeymaekers L, and Wuytack F.** Sarcolipin and phospholamban mRNA and protein expression in cardiac and skeletal muscle of different species. *Biochemical Journal* 389: 151-159, 2005.
349. **Verburg E, Murphy RM, Richard I, and Lamb GD.** Involvement of calpains in Ca<sup>2+</sup>-induced disruption of excitation-contraction coupling in mammalian skeletal muscle fibers. *Am J Physiol Cell Physiol* 296: C1115-1122, 2009.

350. **Verburg E, Murphy RM, Stephenson DG, and Lamb GD.** Disruption of excitation-contraction coupling and titin by endogenous Ca<sup>2+</sup>-activated proteases in toad muscle fibres. *J Physiol* 564: 775-790, 2005.
351. **Wagner KR, Lechtzin N, and Judge DP.** Current treatment of adult Duchenne muscular dystrophy. *Biochim Biophys Acta* 1772: 229-237, 2007.
352. **Walton JN, and Nattrass FJ.** On the classification, natural history and treatment of the myopathies. *Brain* 77: 169-231, 1954.
353. **Wang B, Li J, Fu FH, and Xiao X.** Systemic human minidystrophin gene transfer improves functions and life span of dystrophin and dystrophin/utrophin-deficient mice. *J Orthop Res* 27: 421-426, 2009.
354. **Wang X, Weisleder N, Collet C, Zhou J, Chu Y, Hirata Y, Zhao X, Pan Z, Brotto M, Cheng H, and Ma J.** Uncontrolled calcium sparks act as a dystrophic signal for mammalian skeletal muscle. *Nat Cell Biol* 7: 525-530, 2005.
355. **Warren GL, Ingalls CP, Lowe DA, and Armstrong RB.** What mechanisms contribute to the strength loss that occurs during and in the recovery from skeletal muscle injury? *J Orthop Sports Phys Ther* 32: 58-64, 2002.
356. **Warren GL, Ingalls CP, Shah SJ, and Armstrong RB.** Uncoupling of in vivo torque production from EMG in mouse muscles injured by eccentric contractions. *J Physiol* 515 ( Pt 2): 609-619, 1999.
357. **Weir AP, Burton EA, Harrod G, and Davies KE.** A- and B-utrophin have different expression patterns and are differentially up-regulated in mdx muscle. *J Biol Chem* 277: 45285-45290, 2002.
358. **Westerblad H, and Allen DG.** Changes of myoplasmic calcium concentration during fatigue in single mouse muscle fibers. *J Gen Physiol* 98: 615-635, 1991.
359. **Westerblad H, Duty S, and Allen DG.** Intracellular calcium concentration during low-frequency fatigue in isolated single fibers of mouse skeletal muscle. *J Appl Physiol* 75: 382-388, 1993.
360. **Whitehead NP, Pham C, Gervasio OL, and Allen DG.** N-Acetylcysteine ameliorates skeletal muscle pathophysiology in mdx mice. *J Physiol* 586: 2003-2014, 2008.
361. **Whitehead NP, Streamer M, Lusambili LI, Sachs F, and Allen DG.** Streptomycin reduces stretch-induced membrane permeability in muscles from mdx mice. *Neuromuscul Disord* 16: 845-854, 2006.
362. **Whitehead NP, Yeung EW, and Allen DG.** Muscle damage in *mdx* (dystrophic) mice: role of calcium and reactive oxygen species. *Clin Exp Pharmacol Physiol* 33: 657-662, 2006.
363. **Whitehead NP, Yeung EW, Froehner SC, and Allen DG.** Skeletal muscle NADPH oxidase is increased and triggers stretch-induced damage in the mdx mouse. *PLoS One* 5: e15354, 2010.
364. **Williams IA, and Allen DG.** The role of reactive oxygen species in the hearts of dystrophin-deficient mdx mice. *Am J Physiol Heart Circ Physiol* 293: H1969-1977, 2007.
365. **Williamson RA, Henry MD, Daniels KJ, Hrstka RF, Lee JC, Sunada Y, Ibraghimov-Beskrovnaia O, and Campbell KP.** Dystroglycan is essential for early embryonic development: disruption of Reichert's membrane in *Dag1*-null mice. *Hum Mol Genet* 6: 831-841, 1997.
366. **Willmann R, Possekel S, Dubach-Powell J, Meier T, and Ruegg MA.** Mammalian animal models for Duchenne muscular dystrophy. *Neuromuscul Disord* 19: 241-249, 2009.
367. **Wissing ER, Boyer JG, Kwong JQ, Sargent MA, Karch J, McNally EM, Otsu K, and Molkentin JD.** p38alpha MAPK underlies muscular dystrophy and myofiber death through a Bax-dependent mechanism. In: *Hum Mol Genet*. England: The Author 2014. Published by Oxford University Press For Permissions, please email: journals.permissions@oup.com., 2014, p. 5452-5463.

368. **Wood DS, Sorenson MM, Eastwood AB, Charash WE, and Reuben JP.** Duchenne dystrophy: abnormal generation of tension and Ca<sup>++</sup> regulation in single skinned fibers. *Neurology* 28: 447-457, 1978.
369. **Woods CE, Novo D, DiFranco M, Capote J, and Vergara JL.** Propagation in the transverse tubular system and voltage dependence of calcium release in normal and mdx mouse muscle fibres. *Journal of Physiology-London* 568: 867-880, 2005.
370. **Woods CE, Novo D, DiFranco M, and Vergara JL.** The action potential-evoked sarcoplasmic reticulum calcium release is impaired in mdx mouse muscle fibres. *Journal of Physiology-London* 557: 59-75, 2004.
371. **Wu MM, Buchanan J, Luik RM, and Lewis RS.** Ca<sup>2+</sup> store depletion causes STIM1 to accumulate in ER regions closely associated with the plasma membrane. *J Cell Biol* 174: 803-813, 2006.
372. **Xu CY, Bailly-Maitre B, and Reed JC.** Endoplasmic reticulum stress: cell life and death decisions. *Journal of Clinical Investigation* 115: 2656-2664, 2005.
373. **Yao H, and Rahman I.** Current concepts on oxidative/carbonyl stress, inflammation and epigenetics in pathogenesis of chronic obstructive pulmonary disease. *Toxicol Appl Pharmacol* 254: 72-85, 2011.
374. **Yeung EW, Whitehead NP, Suchyna TM, Gottlieb PA, Sachs F, and Allen DG.** Effects of stretch-activated channel blockers on [Ca<sup>2+</sup>]<sub>i</sub> and muscle damage in the mdx mouse. *J Physiol* 562: 367-380, 2005.
375. **Yokota T, Miyagoe-Suzuki Y, Ikemoto T, Matsuda R, and Takeda S.** alpha1-Syntrophin-deficient mice exhibit impaired muscle force recovery after osmotic shock. *Muscle Nerve* 49: 728-735, 2014.
376. **Youdim MB, Edmondson D, and Tipton KF.** The therapeutic potential of monoamine oxidase inhibitors. *Nat Rev Neurosci* 7: 295-309, 2006.
377. **Zatz M, Rapaport D, Vainzof M, Passos-Bueno MR, Bortolini ER, Pavanello Rde C, and Peres CA.** Serum creatine-kinase (CK) and pyruvate-kinase (PK) activities in Duchenne (DMD) as compared with Becker (BMD) muscular dystrophy. *J Neurol Sci* 102: 190-196, 1991.
378. **Zeiger U, Mitchell CH, and Khurana TS.** Superior calcium homeostasis of extraocular muscles. *Exp Eye Res* 91: 613-622, 2010.
379. **Zhang BT, Whitehead NP, Gervasio OL, Reardon TF, Vale M, Fatkin D, Dietrich A, Yeung EW, and Allen DG.** Pathways of Ca<sup>2+</sup> entry and cytoskeletal damage following eccentric contractions in mouse skeletal muscle. *J Appl Physiol (1985)* 112: 2077-2086, 2012.
380. **Zhang BT, Yeung SS, Allen DG, Qin L, and Yeung EW.** Role of the calcium-calpain pathway in cytoskeletal damage after eccentric contractions. *J Appl Physiol (1985)* 105: 352-357, 2008.
381. **Zhao X, Moloughney JG, Zhang S, Komazaki S, and Weisleder N.** Orai1 mediates exacerbated Ca<sup>(2+)</sup> entry in dystrophic skeletal muscle. *PLoS One* 7: e49862, 2012.
382. **Zinszner H, Kuroda M, Wang X, Batchvarova N, Lightfoot RT, Remotti H, Stevens JL, and Ron D.** CHOP is implicated in programmed cell death in response to impaired function of the endoplasmic reticulum. *Genes Dev* 12: 982-995, 1998.

## Appendices



INSTITUTIONAL ANIMAL CARE AND USE COMMITTEE

1204 Marie Mount Hall  
College Park, MD 20742-5125  
TEL 301.405.4212  
FAX 301.314.1475  
iacuc-office@umd.edu  
www.umresearch.umd.edu/IACUC

DATE: June 11, 2015

TO: Eva Chin, PhD  
FROM: University of Maryland College Park (UMCP) IACUC

PROJECT TITLE: [753305-1] Analysis of skeletal muscle function in mouse models of neuromuscular diseases (Renewal)

IACUC REFERENCE #: R-15-31

SUBMISSION TYPE: New Project

ACTION: APPROVED

APPROVAL DATE: June 11, 2015

EXPIRATION DATE: June 10, 2018

Thank you for your submission of the Animal Study Protocol [R-15-31] Analysis of skeletal muscle function in mouse models of neuromuscular diseases (Renewal). The University of Maryland College Park (UMCP) IACUC has APPROVED your submission. This approval is based on the committee's review of the appropriate use and care of animals within your research goals.

Research must be conducted in accordance with this approved submission. All changes must be submitted to the University of Maryland College Park (UMCP) IACUC as a revision. Conducting research outside the scope of your approved submission is reportable to federal entities and will be investigated by the University of Maryland College Park (UMCP) IACUC and may require interruptions to the research project.

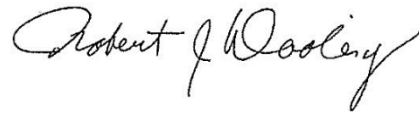
Any revision to previously approved materials must be approved by this committee prior to initiation. Please use the appropriate revision forms for this procedure which are found on the IRBNet Forms and Templates Page.

All UNANTICIPATED PROBLEMS involving UNEXPECTED MORBIDITY or MORTALITY to animals or study personnel must be reported promptly to this office.

This protocol requires continuing review by this committee on an annual basis. Please use the appropriate forms for this procedure. Your documentation for continuing review must be received with sufficient time for review and continued approval before the expiration date of June 10, 2018.

Please note that all research records must be retained for a minimum of three years after the completion of the project.

If you have any questions, please contact Pam Lanford at (301) 405-7295 or planford@umd.edu. Please include your project title and reference number in all correspondence with this committee.

Handwritten signature of Robert J. Dooling in cursive script.

Robert Dooling, IACUC Chair

This letter has been electronically signed in accordance with all applicable regulations, and a copy is retained within University of Maryland College Park (UMCP) IACUC's records.



UNIVERSITY OF  
MARYLAND

DIVISION OF RESEARCH  
*Laboratory Animal Resources*

Central Animal Resources Facility  
College Park, Maryland 20742  
TEL 301.405.4921

May 27, 2015

Davi Mazala  
SPH – Kinesiology

Dear Davi;

This letter is to acknowledge your attendance at the **May 27, 2015** UMD Principal Investigator and Animal User refresher class. You are now in compliance with current Campus regulations that require attendance at an animal-use training program.

The Campus is committed to the humane and appropriate use of animals in research and teaching. We hope that the training session provided you with some insight into the current rules and regulations governing animal care and use. We also hope that it will enable you to work more efficiently and effectively within the UMD Animal Care Program.

The Institutional Animal Care and Use Committee (IACUC) welcomes suggestions on how the campus program can be improved. Any comments or questions concerning the animal care program and/or animal care and use should be directed to me.

Thank you for your participation. Please keep this letter for your records.

Sincerely,

A handwritten signature in cursive script that reads "Douglas A. Powell".

Douglas Powell, DVM, DCLAM  
University Attending Veterinarian